Synthesis of Chromium Carbene Scaffolds for use in Medicinal Chemistry

by

Christopher Carlos Ferreira Rafael

Submitted in fulfillment of the requirements for the degree of

MASTER OF SCIENCE

Supervisor: Dr R. Klein

December 2013

Abstract

This study involves using methyllithium to synthesize Fischer carbene complexes as precursors for metal templated α,β-unsaturated complexes with potential as acceptors in the Baylis Hillman reaction as well as in Dötz benzannulation. Fischer carbene complexes contain low oxidation state metal centers, are electrophilic in nature and are stabilized by π-donating substituents such as alkoxy and amino groups. The increased electron withdrawing nature of the metal carbonyl moiety was expected to improve the rates of reaction compared to organic carbonyls.

Four Fischer carbenes were synthesized via nucleophilic addition of MeLi to chromium and tungsten hexacarbonyl at low temperatures followed by alkylation using either a Meerwein salt (Me_3OBF_4) to give the desired Fischer metal methyl methoxy carbenes or Et_4NBr/alkylhalide to make the corresponding ethoxy and allyloxy carbenes. Characterization was by means of ^{13}C NMR, ^{1}H NMR, and IR. *In silico* studies were carried out looking at the effect of substituents on the carbene bond.

Synthesis of α,β-unsaturated complexes was effected via the aldol condensation route and found to be unfavorable using enolizable aldehydes, although the use of two aryl aldehydes resulted in successful preparation of two α,β-unsaturated complexes. Difficulty in the purification of these complexes hindered their full characterization. Computational studies looked at the effect of substituents on the system as well as variation of the metal from Cr to Mo and W.

Synthesis of Baylis Hillman adducts using α,β-unsaturated complexes as acceptors was unsuccessful due to the ease of product oxidization. One potential product was obtained in its crude form although purification was not possible due to oxidation. Computational studies suggested that the oxygen on the ligand negatively impacts the stability of these Fischer carbene derived Baylis Hillman adducts promoting intramolecular oxidation of the metal.

The α,β-unsaturated complexes and Baylis Hillman adducts were considered to be candidates to undergo Dötz benzannulation methodology. The use of the α,β-unsaturated complexes in this reaction was generally unsuccessful, both in the microwave and in conventional reflux conditions. Computational studies of these compounds were carried out to facilitate understanding of their stability and configuration.

Declaration

I declare that this dissertation, which I hereby submit for the degree MSc (Chemistry) at Rhodes University, is my own work and has not previously been submitted by me for a degree at this or any other tertiary institution.

Signature:

Date:

Table of Contents

List of Figures

List of Schemes

List of Tables

List of Abbreviations

^{13}C NMR	Carbon Nuclear Magnetic Resonance
^{1}H NMR	Proton Nuclear Magnetic Resonance
Å	Angstrom
B3LYP	Becke 93-parameter, Lee, Yang, Parr functional
BDE	Bond Dissociation Energy
Bu	Butyl
C_6D_6	Deuterated benzene
CDA	Charge Decomposition Analysis
d	Doublet
DCD	Dewar-Chatt-Duncanson
DCM	Dichloromethane
dd	Doublet of doublets
DFT	Density Functional Theory
EDA	Energy Decomposition Analysis
Et	Ethyl
Et_2O	Ether
HF	Hartree–Fock
HAL	Halogen
HOMO	Highest Occupied Molecular Orbital
IR	Infrared spectroscopy
J	Coupling constant
LUMO	Lowest Unoccupied Molecular Orbital
Me	Methyl
MLCT	Metal to Ligand Charge Transfer
MsCl	Methane sulfonylchloride
NBO	Natural Bond Orbital analysis
n.o.	Not observed
NMR	Nuclear Magnetic Resonance spectroscopy
Ph	Phenyl
PPh_3	Triphenylphosphine
ppm	Parts Per Million
R	Alkyl group
RT	Room Temperature
s	Singlet (NMR)
THF	Tetrahydrofuran
TM	Transition Metal
UV	Ultraviolet

Acknowledgements

My gratitude goes first to my supervisor Dr Rosa Klein. Thanks to her I learnt just what it means to be a practicing organic chemist. More than a supervisor she helped me a lot with constant support and friendship in my personal life. “Thank you for everything” and always having my back over the last four years.

My thanks and appreciation to the chemistry department:
-Dr Lobb, for being available for questions regarding computational chemistry, proof that patience goes a long way.
-Alicia, for your help and constant friendship.
-My interns, Kerry and Kelvin for making some reactions work by accident - proof that some mistakes in chemistry are more fortunate than others.

I would like also to thank my family, for their unconditional support whatever I decided. They have been waiting for my first ‘book’ so here it is - enjoy all the pictures of the chicken wire :)

To Candice “*o amor da minha vida*” with whom I have shared the last 8 years of my life with, life keeps changing but we keep getting better. I dedicate this to you

“Whoever said nothing is impossible
obviously never tried
to staple water to a tree”
Anonymous

1 Introduction

> On a commuter train to London there were two passengers who always caught the train at the same time, and who often sat across from one another. One of the passengers had a pad of paper and kept throwing a sheet out the window during the ride. After some days of seeing this, the other passenger asked, “Why are you doing this?” His answer was “To keep the lions away.” The questioner said, “But there are no lions in England,” and the response was, “Yes, so you see it works.”[1]

1.1 Carbene complexes – overview of the metal carbon double bond

A direct bond between carbon and a metal comprises the basis of an organometallic complex. Metal carbene complexes are made with transition metals such as chromium, tungsten and molybdenum and the reactivity and stability of the various carbenes have been well documented over the years with a number of reviews being published on this topic.[2-4] The wide range of chemical applications and discoveries involving these complexes has been fueled by advances in industry especially in the area of catalysis. As well as being good stereo- and regio-selective agents or important intermediates in olefin metathesis, organometallic complexes form a bridge between organic and inorganic chemistry bringing with them new techniques and reactions to each field.[2]

The discovery of the first metal carbene was recorded by Chugaev and co-workers in 1915. Due to a lack of spectroscopic techniques available to accurately reveal the structure, the discovery was not confirmed until much later. In 1973 the structure of the hydrazine-bridged platinum complex that Chugaev’s group

synthesized was elucidated by X-ray crystal diffraction and NMR techniques.[3,5] In the meantime, the first carbene complex to be characterized had been reported by Fischer and Maasböl in 1964.[6] These metal carbene complexes have opened new opportunities for the metal-carbon double bond and numerous examples have been documented with different transition metals,[7] allowing for diversity in the organometallic complexes that are able to be synthesized. At the same time that Fischer and Maasböl were looking into their carbenes, Wanzlick was working on diaminocarbenes which he thought were stabilized due to the presence of the amino substituents, although he had been unsuccessful in isolating the carbene.[8] He later reported an NHC-metal complex[9] more than 20 years before the first NHC was isolated and described by Arduengo.[10] All these carbene complexes, incorporating the metal-to-carbon double bond system and having unique properties, have stimulated the field of organometallic research.

Since the discovery of organometallic carbene complexes, first formally described by Fischer in his Nobel Prize lecture,[11] these derivatives have become widely used as organic synthons. It was observed that transition metals had the ability to stabilize these carbene systems by coordination, yielding two types of complexes with contrasting reactivities. These are named 'Fischer-type' carbenes, where the carbene carbon is electrophilic and 'Schrock-type' carbene complexes where the polarity is reversed.[11,12] Typical Fischer carbene complexes are said to contain a low valent Group VI to VIII transition metal which is stabilized by π-acceptor ligands. Schrock type carbenes are usually identified as having an early transition metal in a high oxidation state.

1.1.1 Schrock carbene complexes

The Schrock carbenes are named after Richard R. Schrock who first synthesized them in 1974.[12,13] They are nucleophilic at the carbene carbon centre since they don't have a heteroatom to stabilize the complex like Fischer carbenes do (Figure 1). They are poorly stabilized, having a small gap between their singlet and triplet states, with strong donor and weak acceptor ligands. The most common examples of nucleophilic Schrock carbenes are represented in Figure 2.

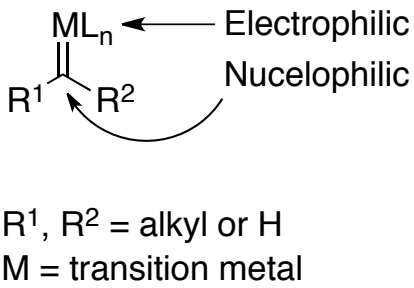

Figure 1: Structure of a Schrock carbene[13]

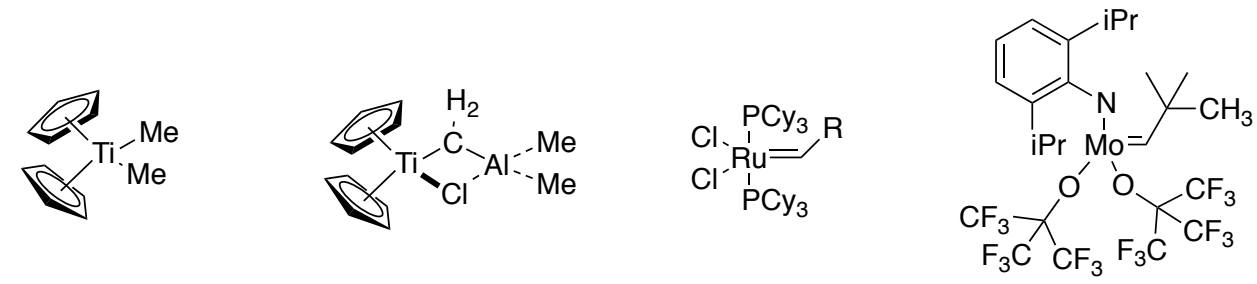

Figure 2: Common Schrock carbenes[13-16]

In organic synthesis, Schrock carbene complexes play an important role as both reagents and catalysts. Schrock carbenes are considered to be dinegative ligands and are said to donate four electrons.[3] The Schrock carbene is most commonly viewed as an ylide type structure. The metals used to form these complexes are said to have oxophilicity and as a result the complexes can then be used as synthetic equivalents in the Wittig reaction where the by product becomes a stable metal oxo species. Besides having Wittig-like reactivity, these complexes can also form metallacycles with olefins.[2] Olefination[2] (Scheme 2), and alkene metathesis (Scheme 4) are two good examples of reactions where Schrock carbenes play an important role in synthetic chemistry.

A classic example, the Tebbe reagent, is prepared by reacting titanocene dichloride with triethylaluminum (Scheme 1a),[17] and has been very well studied due to its importance in olefination. The Tebbe reagent is compatible with a wide range of functional groups, although the aluminum moiety is a problem for more sensitive groups. In these instances the Petasis reagent can be employed. This reagent is more air stable and easier to handle than the Tebbe and gives the desired carbene on heating in THF (Scheme 1b). These active carbenes can olefinate a wide range of substrates including ketones (hindered and enolizible types, difficult reagents in the Wittig reaction), aldehydes, esters and amides (Scheme 2). The major limitation with these reagents is, they can only transfer a methylene group. As with the Wittig-like reaction, a key step is the formation of a betaine-like four centered intermediate (**1**) by [2+2] cycloaddition. This decomposes by cycloreversion to give the titanium oxide(**3**) and alkene (**2**) (Scheme 2).

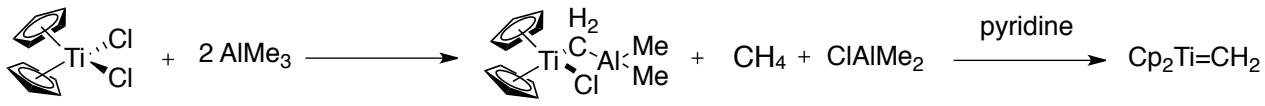

A

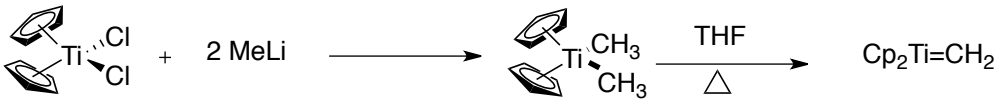

B

Scheme 1 A: Preparation of Petasis reagent[18], B: Preparation of Tebbe reagent[16]

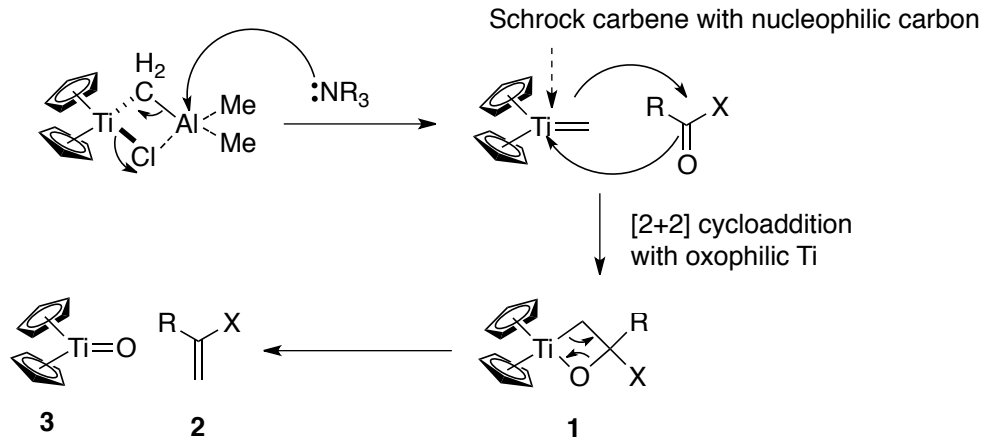

Scheme 2: Mechanism of Carbonyl Olefination using Schrock carbenes

In alkene metathesis, Schrock carbenes are used as catalysts in the process where two alkenes exchange their alkylidene fragments (Scheme 3). This reaction has been extensively studied and has been used on an industrial scale. There are two main variations of the reaction, namely Ring-Opening Metathesis Polymerization (ROMP) and Ring-Closing Metathesis (RCM). The general mechanism associated with alkene metathesis is seen in Scheme 3.

One of the most common catalysts used in alkene metathesis is the molybdenum based Schrock catalyst which has good efficiency with terminal and internal alkenes and is stable under inert conditions away from oxygen and protic solvents.[15] The other common family of catalysts is the ruthenium based Grubb's catalyst which is said to be less reactive, and is only effective with terminal alkenes. It is observed that internal alkenes result in little or no reaction. The benefit of Grubb's catalyst is that it requires less stringent control over the reaction conditions.[15]

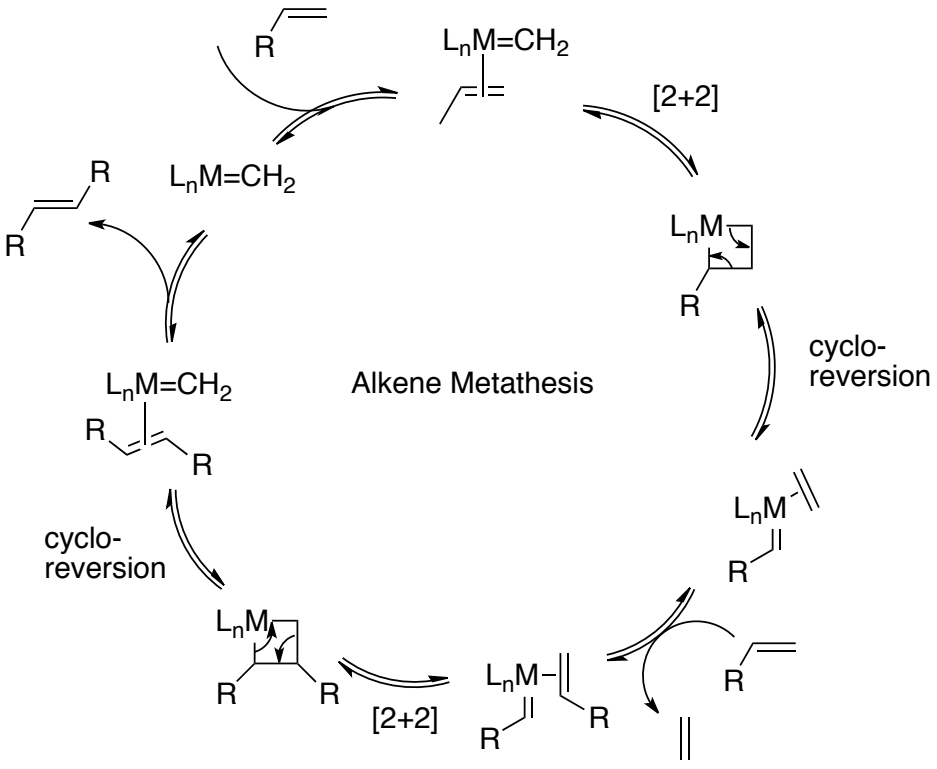

Scheme 3 : General Mechanism of Alkene Metathesis

1.1.2 Fischer carbene complexes

Several reviews have explored the development of these carbene systems, especially as tools in organic synthesis involving organometallic transformations.[19,20,21,23] It has been noted that the strong electron withdrawing pentacarbonyl moiety gives these complexes a general reactivity profile similar to that of an activated carboxylic acid derivative. Fischer carbenes, and specifically α,β-unsaturated carbene systems, show exceptional versatility. These carbenes are analogous to α,β-unsaturated esters and it has been shown that reactions such as substitution[22], and the Diels Alder reaction readily occur under similar conditions to those used for esters. Scheme 4 highlights the versatility of these systems and include nucleophilic addition (**A**)[24], ligand replacement (**B**), oxidation (**C**), photolysis (**D**)[29], deprotonation (**E**) and cycloadditions (**F**), including Diels-Alder[26], cyclopropanation[27], and benzannulation.[30]

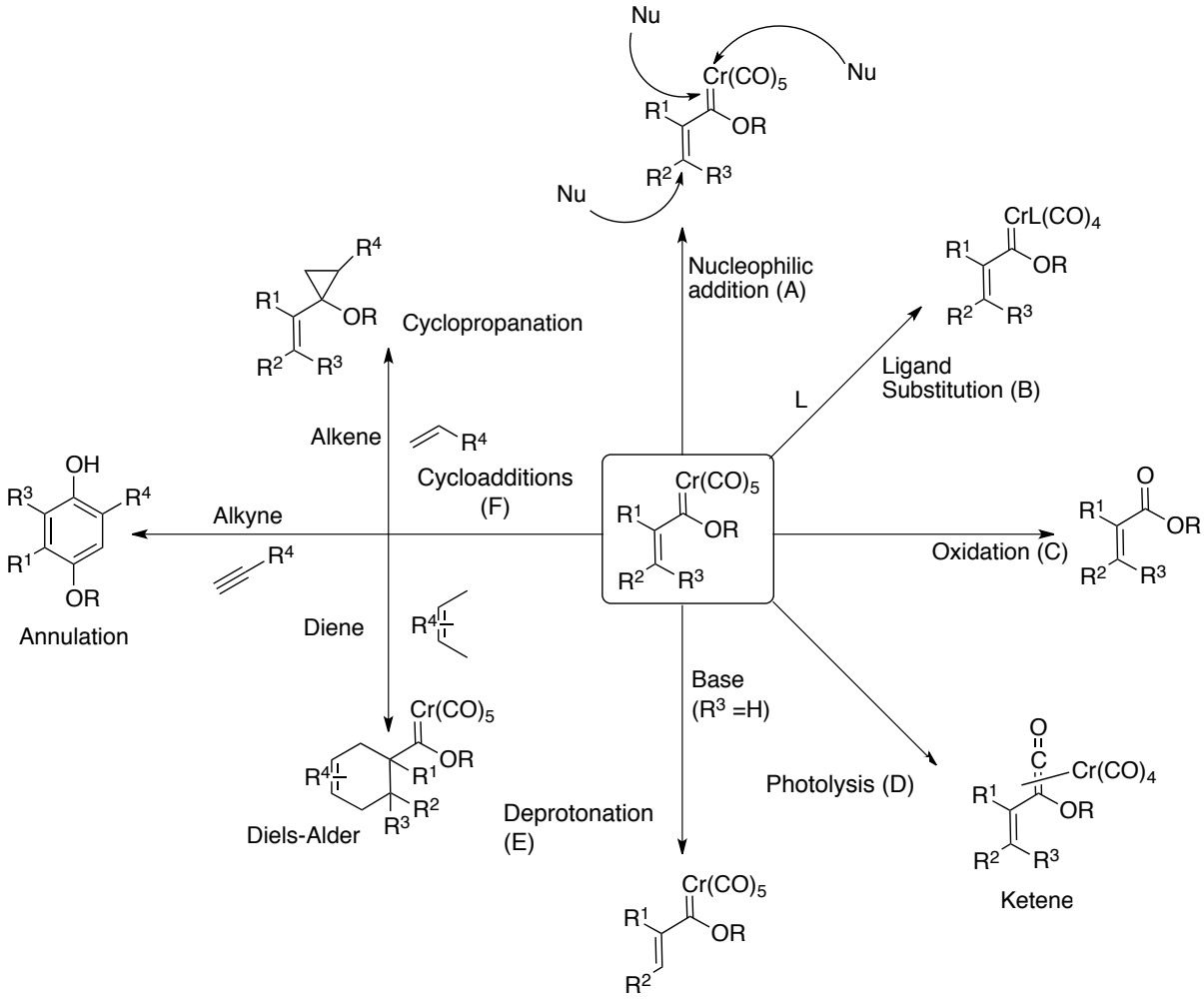

Scheme 4: Range of reactions possible with unsaturated carbenes [28]

Significant advances in the scope of reactions involving Fischer carbene complexes have been demonstrated in the area of nucleophilic additions, especially the Michael addition, and in asymmetric synthesis.[28] Barluenga discussed how a series of ketone-derived lithium enolates (**5**) reacted with chiral alkenylcarbene complexes (**4**) in a Michael fashion. This reaction led to the formation of the corresponding functionalized adducts **6** as single diastereomers in most cases. Scheme 5 illustrates the sequential Michael

addition, direct addition and subsequent 4,5,6-dihydropyran (**8**) formation as explained by Barluenga.[28]

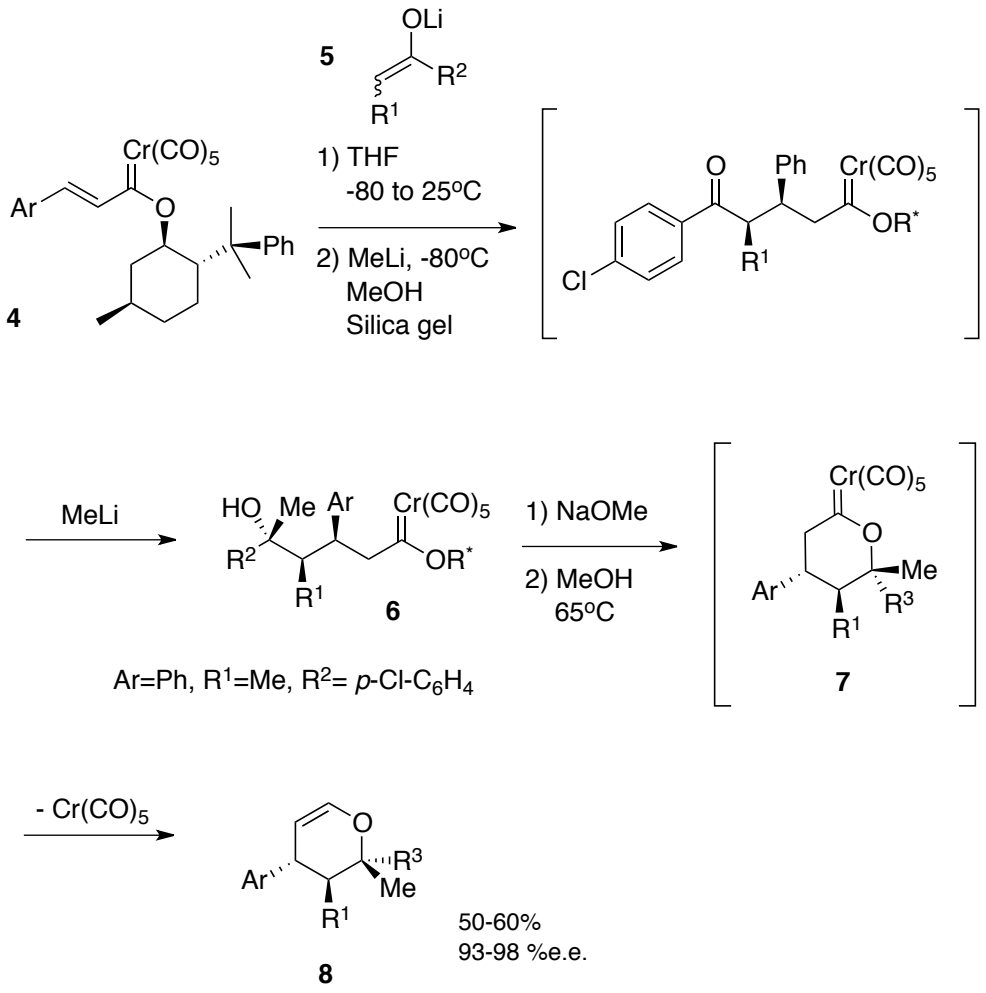

Scheme 5: Application of Michael addition in Fischer carbene complexes [28]

One reaction in particular, benzannulation (discussed later in 1.2.1 p14) of α,β-unsaturated carbene complexes, has become the most flexible and widely used carbene transformation.[30-28] This reaction was first discovered in the 1970's by Dötz and is a formal [3+2+1] cycloaddition of Fischer carbene complexes to alkynes incorporating a CO insertion. The scope and limitations of this reaction have been studied at length, looking at both the inter- and intramolecular versions using a diverse range of highly functionalized alkynes and carbene complexes.[30-28]

The wide range of complex compounds that can be achieved using carbene complexes is significant, and one feature that is often used in synthetic strategies employing carbenes is the fact that the metal-carbon bond can be retained in the product while a ligand is modified. Thus, otherwise difficult transformations are made possible by attaching the ligand to the metal. This moiety can then be modified and later cleaved from the metal to give the compound of interest. [30-28]

1.1.3 Theoretical bonding model

Most carbene complexes can be classified in the conventional method as either Fischer or Schrock-type carbenes, but there are species that are difficult to assign to these traditional classes. For example, dihalocarbene complexes may exhibit characteristics of a carbene but are unique in that they can be both nucleophilic (like Shrock carbenes) or electrophilic (like Fischer carbenes) in their behavior.[29,30] With advances in the power of computational chemistry for theoretical studies, it has been possible to gain new insight into the nature of the chemical bond in these transition metal carbene compounds as shown by Frenking and Frölich. [29,30]

Fischer-type carbene complexes are generally characterized by the formula $(CO)_5M=C(X)R$ (where M=Cr, Mo or W; X=π-donor substituent; and R=alkyl, aryl, alkenyl or alkynyl). Fischer-type carbene complexes are characterized by a formal metal-carbon double bond to a low-valent transition metal which is usually stabilized by π-acceptor substituents. The electronic structure of the metal–carbene bond determines the reactivity of the complex.[32-34] Several theoretical studies have been conducted using semiempirical,[35] Hartree–Fock (HF)[36,37] and density functional theory (DFT) calculations.[38-40] Many of these studies have compared Fischer- and Schrock-type carbenes[33,36,37,41] and the consensus from both experimental and computational studies is that Fischer-type carbene complexes are formed by the coordination of a singlet carbene ligand to a transition metal fragment in the singlet state. There is a significant carbene to metal σ donation and metal to carbene π back-donation (Figure 3A).[33,36,37,41] Schrock-type carbenes can be characterized by the interaction of a triplet carbene ligand with a transition metal fragment in the triplet state (Figure 3B).

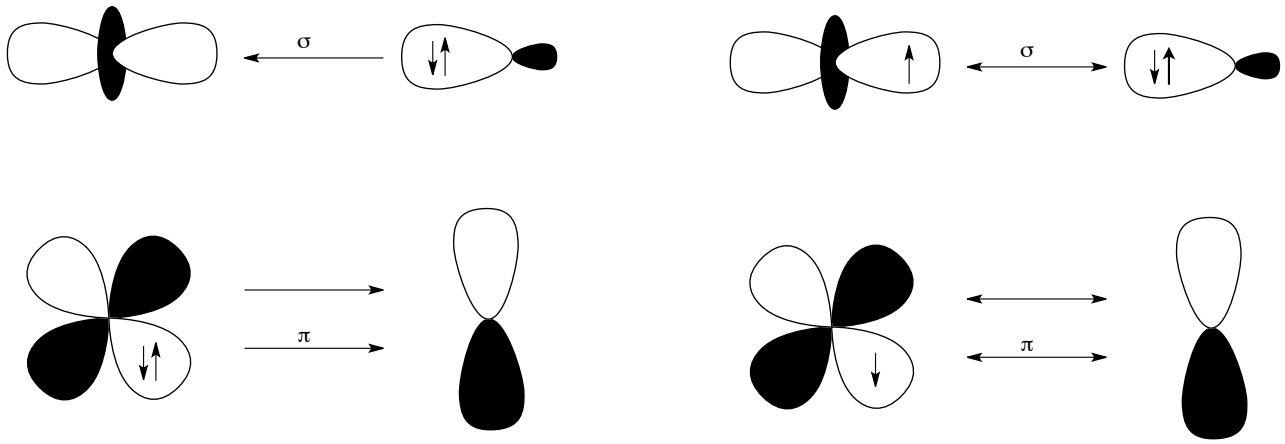

A Fischer-type carbene complexes

B Schrock-type carbene complexes

Figure 3 : Dominant orbital interactions in (A) Fischer and (B) Schrock carbene complexes [33,41]

A study by Frenking[38] looked at the influence of the carbene substituents on a pentacarbonyl-chromium Fischer-type complex. Frenking found that the electronic characteristics of the substituents control the reactivity of these complexes. The study investigated 25 different chromium carbene complexes having different σ- and π-donor strengths effected by combining different ligands. BP86 calculations together with a

basis set of triple-z quality were used to reproduce the geometries of experimentally known structures of the pentacarbonyl chromium series very well, underestimating the $Cr–C_{carbene}$ bond length by only 0.048 Å with the variance for the Cr–CO and C–O bond lengths even smaller. According to Ziegler and co-workers, the BP86 functional is especially well suited for $Cr(CO)_6$ and its accuracy is comparable to that of CCSD(T) calculations.[42] The shortest $Cr–C_{carbene}$ bond lengths for any given substituent R always correspond to the complex where X=H, the weakest π-electron donor. Increasing the π donation, by changing to R=OH or $R=NH_2$, leads to a significant lengthening of the $Cr–C_{carbene}$ bond length - about 0.05 Å.

This can be interpreted in terms of the Dewar–Chatt–Duncanson (DCD) model[43,44] as regular behavior where larger $Cr–C_{carbene}$ bond lengths correlate with shorter $Cr–CO_{trans}$ and $C–O_{trans}$ bond distances. In general a larger $Cr–C_{carbene}$ bond length relates to a smaller BDE (Bond dissociation energy). The π-electron-donating character does play a major role; for any substituent X the complex with R=H always shows the largest BDE while the larger π donation of the amino group reduces the back-donation to the carbene.

Charge decomposition analysis (CDA) looks at chemical systems which are described as donor-acceptor complexes. The electronic and energetic charges associated with the formation of the complex consisting of two fragments namely A and B are partitioned in terms of the Dewar-Chatt-Duncanson model.[43,44] The energy analysis is then feasible within the HF (Hartree-Fock approximation) while the CDA can also be carried out at correlated levels such as DFT as looked at in this study. Frenking showed that CDA studies pointed out a clear dependence of the electrophilicity of the carbene on the π-donor substituents. Strong donors reduce the electrophilicity because the acceptor orbital of the carbene becomes occupied by π donation from the heteroatom substituent. For a given substituent R, back-donation from the metal decreased in the order $H>OH>OCH_3>NH_2>NHCH_3$, becoming less with increasing π-donor character of the group X.[41,43,44,54]

Unlike the Fischer carbenes, Schrock carbenes do not have a stabilizing π-donating substituent at the carbene ligand. The different chemical behaviour is attributed to a different bonding situation in these complexes, where higher covalent double bond character was dominant. The nature of this bond was the subject of several theoretical studies[45-49] using different levels of theory. In a pioneering study, Hall suggested that the difference in the chemical behaviour results from changes in the electronic configuration of the transition metal.[50] Frenking[41] reported accurate *ab initio* calculations on several low-valent carbene complexes of the type $[(CO)_5WCX_2]$ and high-valent alkylidenes of the type $[(Hal)_4WCX_2]$, the bonding situation being examined by using the Bader,[50,51] NBO[53] and CDA[54] analyses.

Bader analysis can be considered as a way to divide molecules into atoms and can be called Bader's Quantum Theory of Atoms in Molecules (QTAIM). His definition of an atom is based purely on the electronic charge density and uses what he describes as zero flux surfaces to divide these atoms.[50,51] A zero flux surface can be better interpreted as a 2D surface where the charge density is a minimum perpendicular to the surface. In most molecular systems the charge density reaches a minimum between the atoms and this is a neutral place to separate atoms from each other. Bader's QTAIM theory is a useful tool used in charge

analysis as the charge enclosed within the Bader volume is a good approximation to the total electronic charge of an atom. Bader's analysis can be used to define the hardness of atoms, quantifying the cost of removing charge from an atom. The theory also provides a definition for chemical bonding that assigns numerical values for bond strength.[50,51]

While QTAIM is used to to approximate the total charge of an atom, the concept of Non Bonding Orbitals (NBO) is used to describe the unique set of orthonormal 1 electron functions that are intrinsic to the N-electron wave function. NBO is therefore a calculated bonding orbital with maximum electron density. NBO's form part of a sequence of natural localized orbital sets including natural atomic orbitals (NAO), natural hybrid orbitals (NHO) and natural semi-localized molecular orbitals (NLMO).[53] These sets form the basis atomic orbitals (AO) and molecular orbitals (MO). NLMO's are used in computational chemistry to calculate the distribution of electron density in atoms and bonds. They have the "maximum occupancy character" in localized 1 and 2 center regions of the molecule. NBO's include the highest possible percentage of electron density providing the most accurate possible natural Lewis structure of the wave function. A high percentage of electron density therefore corresponds to an accurate natural Lewis structure.[53]

Using the Bader, NBO and CDA analyses Frenking[41] reported that the bonding situation in the neutral low-valent and high-valent complexes is significantly different. The Schrock-type carbene complexes have a much shorter W-$C_{carbene}$ bond than the low-valent Fischer complexes, which is in agreement with experimentally reported geometries.[29] This can be explained by the smaller radius of the metal atom in a higher oxidation state or a different type of metal–carbene bonding interaction, which was found to be the case in the complexes studied. Topological analysis of the electron density distribution (Bader analysis) clearly shows the differences between Fischer-type and Schrock-type carbene complexes.[52,52]

The Laplacian distributions show that the charge distribution around the carbene carbon atom, i.e. the lone-pair electrons of the carbene, are independent of the metal fragment in both types of complexes, while the Laplacian distribution in the p plane of the carbene ligand shows significant differences.[92] Fischer complexes show an area of charge depletion in the direction of the π(p) orbitals, leading to holes in the electron concentration and therefore possible sites of nucleophilic attack, while the Schrock complexes are shielded by continuous areas of charge concentration. It was found that the Laplacian distribution in Fischer carbenes is similar to the situation in a singlet ($1A^1$) methylene group, while the Laplacian distribution in Schrock complexes agrees well with a triplet ($3B^1$) methylene group.[41]

Another measure of the double bond character is the calculated ellipticities, which demonstrate that the Schrock-type complexes show a much higher double bond character.[41] This is in agreement with the results of the NBO calculations, where Fischer-type complexes show a tungsten–carbene bond which is polarized towards the metal, while the Schrock-type complexes show σ and π bonds that are both polarized towards the carbon end. The carbene ligands carry a significant negative partial charge and the population of the π(p) carbene orbital is higher in the Schrock-type complexes. The results of the NBO analysis, which focuses on the orbital structure, are in good agreement with the Bader analysis, which is based on the total electron

density. The CDA results clearly show that the Schrock carbene complexes should be interpreted as an interaction between a triplet metal moiety and a ($^3B_1$) triplet carbene.[41]

The UV-vis spectra of the carbene complexes exhibit three absorption bands; a spin-forbidden metal-ligand charge transfer (MLCT) absorption around 500 nm, a spin-allowed ligand-field (LF) absorption with a moderate intensity between 350-450 nm, followed by a more intense LF absorption in the range of 300-350 nm.[122] Previously, the MLCT band had been assigned to the promotion of an electron from the non-bonding metal-centered HOMO orbital to the carbene carbon p-orbital centered LUMO (Figure 4).[122] The ligand field band has been attributed to the promotion of an electron to the more energetic population of the metal-centered LUMO+1.[122,123] However, recent DFT calculations suggest that the MLCT band results from the promotion of an electron characteristic of the metal-centered HOMO-1 → LUMO transition. This involves a p-orbital of the carbene carbon. The LF band is characteristic of the HOMO-3 → LUMO which involves the π-system of the carbene ligand, in this case an aryl group, hence it is a π-π* transition (Figure 4).[121]

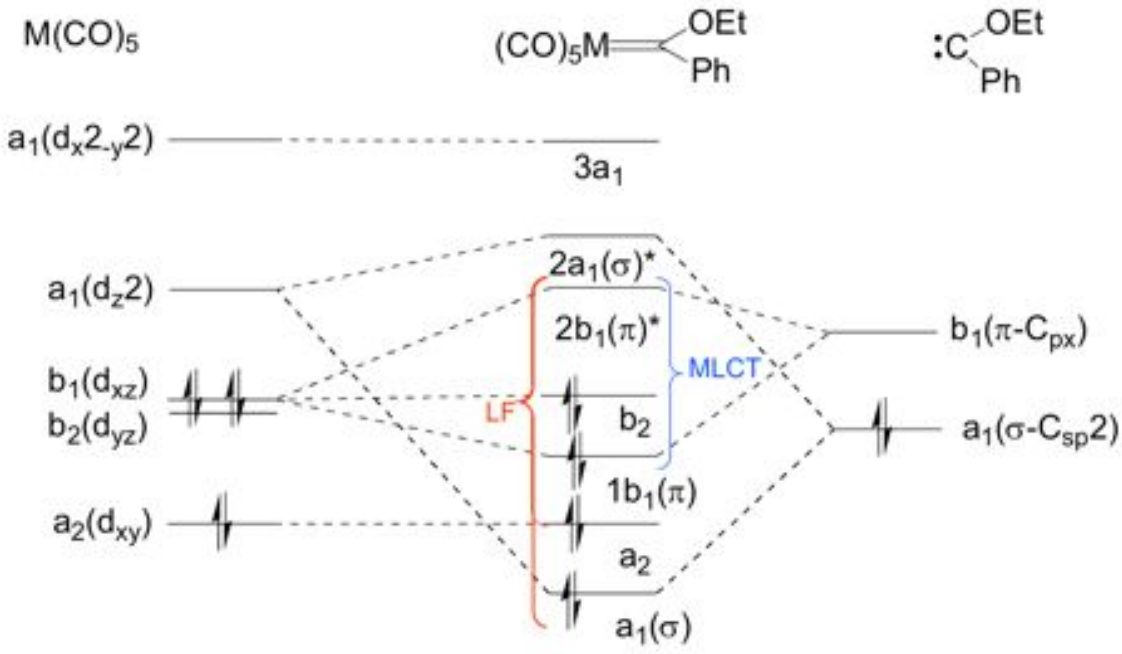

Figure 4: Electron promotion leading to MLCT and LF bands in the UV-vis spectrum

Taylor and Hall[124] examined the theoretical aspects of the bonding found in Fischer carbenes. The use of several techniques including dissociation energies, molecular orbital diagrams and fragment analysis of molecular orbitals enabled them to determine the difference in bonding between Fischer carbenes and Schrock carbenes. This work greatly influenced the theoretical work that followed as they originally suggested that heteroatom substituents stabilize the singlet Fischer carbene.[124,125] Many groups, including Ziegler [109] and co-workers, and Sierra[28,25,121] and co-workers have continued to use theoretical studies to achieve a better understanding of the electronic properties of Fischer carbenes and how they influence the reaction mechanisms Fischer carbenes undergo.

1.1.4 Typical synthesis routes for Fischer carbenes

In 1964 the first example of a transition metal carbene was prepared by E.O Fischer.[6] He accomplished this by adding an organolithium to hexacarbonyl chromium. Subsequently, this has become a trusted method for the synthesis of heteroatom stabilized metal carbene complexes. Studies of chromium carbene complexes within transition metal chemistry have allowed this simple method discovered by Fischer to be extended to apply to many of the other transition metals.

Two types of Fischer carbenes are synthetically accessible: the alkoxy carbenes and amino carbenes. This classification of carbenes refers to the stabilizing substituents connected to the carbene carbon. The synthesis of amino carbenes will be discussed briefly but the primary focus will be on the Fischer synthetic approach to alkoxy carbenes.

The first method by which carbenes have been synthesized is through the well-known Fischer route.[111] This method leads to the formation of alkoxycarbenes, *via* organolithium compounds reacting with a metal carbonyl such as chromium hexacarbonyl (Scheme 6). The resultant product, an acyl metalate **9**, then undergoes alkylation to form the alkoxy carbene complex **10**.[111,114] This alkoxy carbene **10** can subsequently be converted into the amino carbene by reaction with an amine nucleophile, to afford the amino carbene complex **11** (Scheme 7).[114] This method, although tried and tested and giving a wide variety of complexes, is limited by the availability of the organolithium compound. Many alkylating agents have been used in the alkylation step of the Fischer synthesis route. These include trialkyloxonium tetrafluoroborates, alkyl fluorosulfonates and alkyl trifluoromethanesulfonates.[96,114] Another method of alkylation was described by Matsuyama *et al.*[115] where alkyldiphenylsulfonium salts were used to deliver a variety of functionalized alkyl groups.

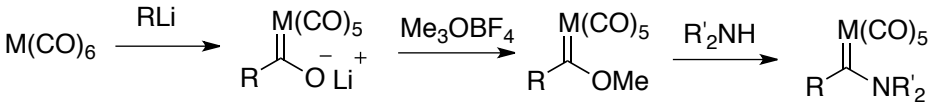

9 **10** **11**

M= Cr, Mo, W

R= alkyl, aryl, vinyl

R'= H, alkyl

Scheme 6 : Fischer route to carbenes

The second route to carbenes was developed by Semmelhack and Hegedus (Scheme 7) and involves the reaction of a pentacarbonylchromate dianion (**12**) with acyl chlorides or amides. This dianion can be formed by the reduction of chromium hexacarbonyl with sodium naphthalenide. The reaction with acyl chlorides led to the formation of alkoxy carbenes (**14**) following the addition of an alkylating agent to the acyl metalate (**13**). Similarly, the tetrahedral intermediate (**15**) derived from the amide was reacted with TMSCl to afford the aminocarbene complex (**16**).[112,114]

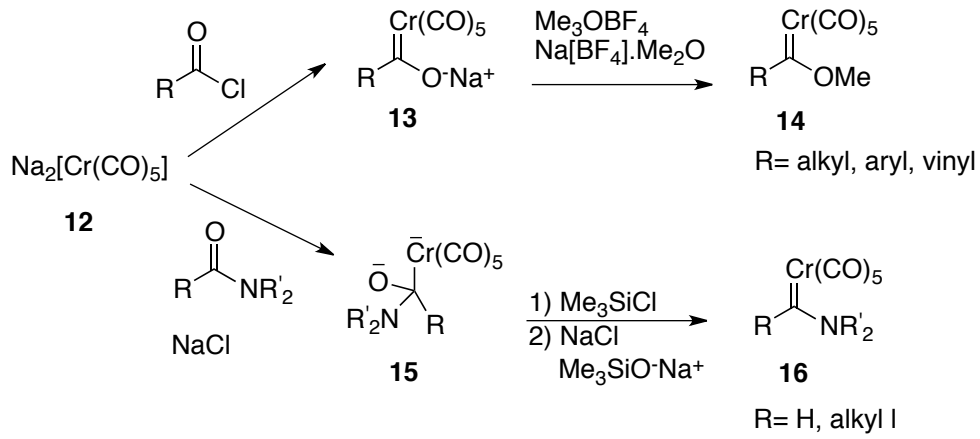

Scheme 7 : The Semmelhack-Hegedus method to alkoxy and amino carbenes[21]

Other methods used to synthesize aminocarbenes include the use of Vilsmeier salts in the presence of a tertiary amine, leading to the deprotonation of the iminium salt to form unstable amino carbenes. A stabilized amino carbene is formed when the Vilsmeier salt is reacted with a metal such as platinum(IV).[117]

Carbenes can also be formed from diazirines[118] or by transmetallation and carbene transfer. Transfer of a carbene ligand was first reported in 1970.[119] Thus Group IV metal complexes have been converted to late transition metal complexes such as rhodium, palladium, copper and gold carbene complexes.[59] A tungsten Fischer dimethylaminocarbene **17** was reacted with gold(V) tetrachloride hydride with the possible reaction pathway proceeding *via* a chloride-bridged dinuclear species **18** (Scheme 8). The formation of the gold(I) carbene **19** occurs at low temperature (0°C) and it is stable at room temperature.[120]

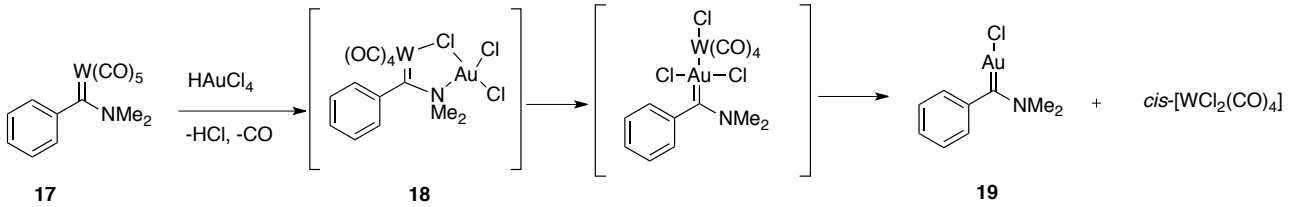

Scheme 8 : Formation of gold(I) carbenes from tungsten carbenes via transmetallation

Carbene complexes have varied reactivity which is dependent on the substituents - alkoxy and amino groups - as well as on the metal center involved.[121,122] The electronic characteristics of Fischer carbenes allow for application of photochemical methods in the preparation of organic compounds.[122] Fischer chromium carbenes are generally brightly colored, ranging from pale yellow to dark red due to the different substituents and the associated electronic characteristics of each substituent.[121] Amino groups are strong π-donors and give rise to pale yellow complexes, while alkoxy groups are weaker π-donors, resulting in a darker yellow color. Alkyl groups which are π-donors cause a blue shift in the electromagnetic spectrum and π-acceptor substituents such as phenyl groups cause a red shift in the electromagnetic spectrum and so yield dark red (or brown) compounds.[121]

1.2 Application of carbenes

The reactions of Fischer carbene complexes are multifaceted and consequently a wide range of products is accessible. One feature often utilized in synthetic strategies is the fact that, in these reactions, either the metal-carbon bond is retained in the product whilst a ligand is modified, or the bond undergoes reaction and the metal is lost. Bearing this in mind, the organic framework attached to the metal through a carbene carbon, allows this moiety to be modified and then cleaved from the metal to yield the desired product in the end.[3]

Many important reactions involving Fischer carbene complexes have been studied and documented, of which nucleophilic attack on the carbene carbon, carbyne synthesis and modification of carbene substituents are the most common. Since Fischer-type carbene complexes are characterized by an electrophilic carbene carbon atom, these carbene complexes show some behavior analogous to that of organic carbonyl compounds.

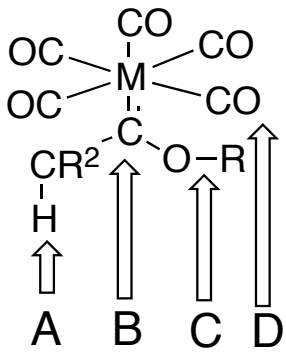

Figure 5 : Reaction sites on Fischer carbenes.[93]

Alkylcarbene complexes can be deprotonated by bases to form metal carbene anions **(A)** and nucleophilic attack can occur at the electrophilic carbene carbon **(B)**. Electrophiles such as Lewis acids can coordinate to the alkoxy substituent **(C)**, resulting in elimination, leading to the formation of metal-coordinated carbyne complexes, while carbonyl substitution by other ligands can occur at **(D)**.[93] Figure 5 illustrates the high degree of versatility possible in reactions. They are also highly compatible with a host of different functional groups in synthetic routes.

Strong nucleophiles, such as organolithiums can react with an electrophilic carbene **20**, (without α-protons) (Scheme 9a) resulting in a tetrahedral intermediate **21** which collapses to a diphenyl carbene **22** upon exposure to aqueous acid. Similarly the enhanced acidity of the α-protons facilitates the preparation of lithium enolate analogs (**24**) (Scheme 9b). These can be used in aldol type reactions to give β-hydroxy carbenes (**25**).

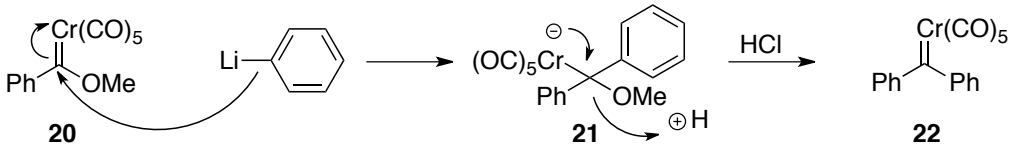

20 **21** **22**

A: Nucleophilic Substitution [28]

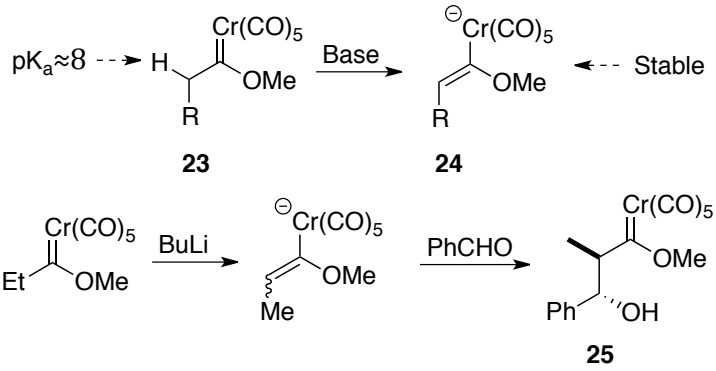

23 **24** **25**

B: Aldol-like Reaction [31]

Scheme 9: Reactions of Fischer Carbenes

The wide range of synthetic routes available makes reactions involving carbenes valuable. Not only are they compatible with a wide variety of functional groups, Fischer carbenes have also been seen to accelerate a reaction in comparison with that of the related carbonyl.[129] This was mainly attributed to the high electronegatively of the carbene making it more reactive. In order to create synthetically useful compounds the metal needs to be readily removed from the complex. Heteroatom stabilized Fischer carbenes show a high degree of stability although demetallation can be achieved by oxidation (Scheme 10).[78]

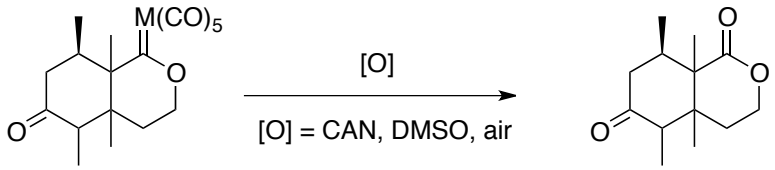

Scheme 10 : Demetallation of carbenes via oxidation[78]

Over the decades Fischer carbene complexes have been used as selective reagents in organic synthesis.[130] This is mainly due to the electron acceptor nature of these complexes but also due to the the non-classical cycloaddition reactions that these complexes undergo as a result of the metal carbonyl fragment. The most useful and well-established of these reactions is the chromium templated benzannulation reaction which allows for a one pot reaction giving densely functionalized oxygenated arenes with a coordinated $Cr(CO)_3$.[130] The reaction is considered superior because it is compatible with a host of different functional groups and occurs under mild conditions with high chemo-, regio- and diastereoselectivity.[131]

1.2.1 Chromium-templated Dötz benzannulation reactions

The Dötz benzannulation reaction (also called Wulff-Dötz reaction) was first reported in 1975 by Karl Heinz Dötz.[61] The thermal [3+2+1]-benzannulation reaction of α,β-unsaturated Fischer carbene complexes with alkynes opened up the potential for an organometallic template allowing a stereo-controlled reaction using different ligands as well as being able to create C–C bonds using a low-valent metal centre, which had previously not been possible. This reaction has now proved to be one of the most powerful methods to generate densely substituted benzenoid compounds - often as a one pot process.[74]

Since this reaction can quickly generate complex phenolic compounds, the Wulff-Dötz reaction has been used often in the synthesis of natural products, especially Vitamins E and K.[77] The first example of a thermal [3+2+1] benzannulation reaction involving an α,β-unsaturated carbene complex with an alkyne[78] was reported by Dötz in 1975. It was also the first example of a three part coupling involving different ligands (Scheme 11). This then opened up further research into a potential organometallic template that allowed stereo-controlled assembly of different ligands around a low valent metal center.

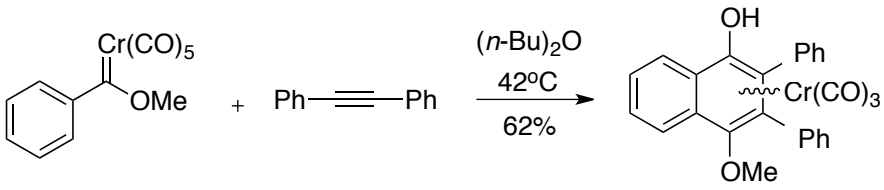

Scheme 11 : First example of a metal templated benzannulation reaction with three ligands[78]

In a typical reaction, an aryl pentacarbonyl complex **26** produced a host of different organic molecules, depending on the reaction conditions (Scheme 12). It was observed that the major product was the 4-methoxy-1-naphthol derivative (**27**), although indene products (**28**) occured as well.[62-64]

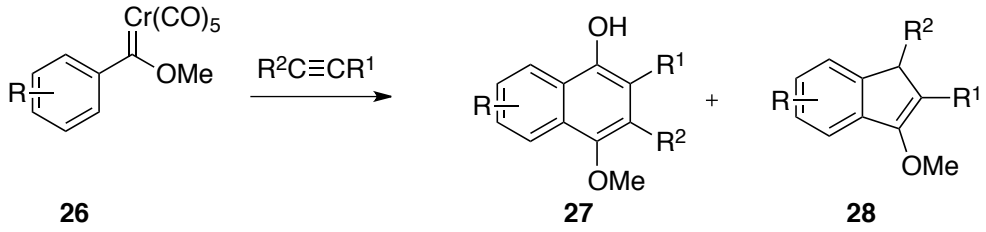

Scheme 12 : General benzannulation using chromium carbene

The benzannulation reaction is one of the most powerful strategies in creating functionalized and polycyclic aromatics. The first reported synthesis using this type of reaction was aromatic annulation incorporating acetylene in 1866 by Berthelot.[74] This reaction used a thermal [2+2+2] cyclotrimerization. Chromium-mediated benzannulation reactions have, over time, demonstrated the potential for transition metals in novel reaction pathways. Metals are able to coordinate a variety of organic substrates in a predictable manner determined by their nature and oxidation state, providing versatile and powerful reaction pathways. They act as templates which activate and fix ligands in specific orientations and thus allow regio-specific inter-ligand

coupling.[76] This also allowed very high atom economy in a one pot synthesis. Scheme 13 highlights the atom connectivity, high atom economy and stereo-control.

Several reviews have been published looking at the applications and mechanism of the reaction. The consensus is that the Dötz benzannulation can be described as the reaction of an aromatic or vinylic alkoxy pentacarbonyl chromium carbene complex **29** with an alkyne and carbon monoxide to give a $Cr(CO)_3$-coordinated substituted phenol **30,** (Scheme 13).[55] The position of substituents in the product is highly predictable with the largest alkyne substituent (R_L) neighboring the phenol and the smallest alkyne substituent (R_S) next to **X** as described in Scheme 13.[79]

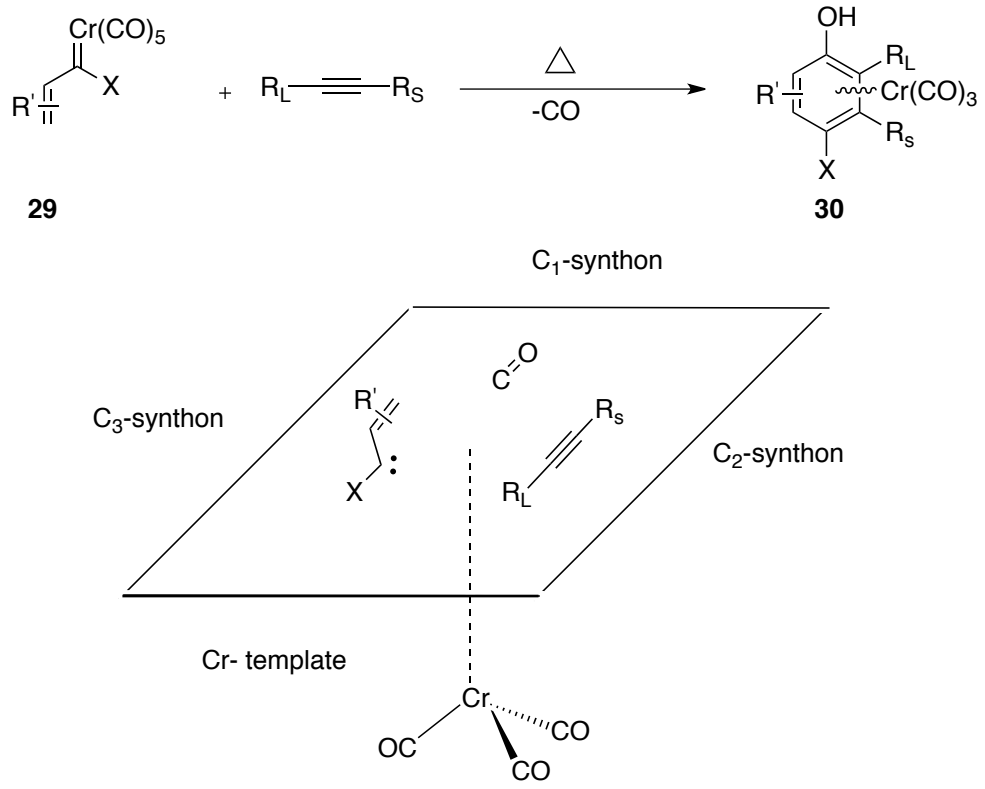

Scheme 13 : Basic ligand connectivity in the thermal [3+2+1]-benzannulation reaction

Chromium is a good choice as a metal template in that it allows for good chemo- and regio-selectivity under relatively mild reaction conditions. Studies have investigated the use of other metals in the reaction, but almost all have have poor to moderate chemoselectivity using harsh conditions.[67-69] Chromium has also been chosen to be the most suitable metal due to the extensive knowledge concerning the benzannulation reaction conditions, solvent and temperature.[70,71] Chromium Fischer carbenes of the amino type have been recognized as giving higher yielding reactions compared to their alkoxy counterparts.

In the study which follows (Scheme 14) amino carbenes were not chosen since in the benzannulation it has been noted that amino(aryl)carbene complexes and amino(alkenyl)carbene complexes react preferentially to give cyclopentannulation products with very low or non-existent yields of benzannulation product. The reaction pathway to the benzannulation product was preferred here and therefore alkoxy carbenes were

chosen. In natural product synthesis it has been observed that the 4-methoxy-1-naphthol products are attractive since they can be converted to naphthoquinones via an oxidative step. These are precursor subunits in several natural product synthetic pathways.[65,66]

Mechanism of Phenol Formation

The benzannulation reaction has been theoretically and experimentally elucidated in detail and a general consensus has now been reached regarding the mechanism[80] of the reaction. Scheme 14 shows that the first step involves CO dissociation from the initial pentacarbonyl complex **31** to give a coordinatively unsaturated tetracarbonyl complex **32**. This first step has been identified as being the rate determining step of the reaction. Experimental studies have shown that this step may be induced thermally, photochemically, sonochemically or via microwave irradiation.

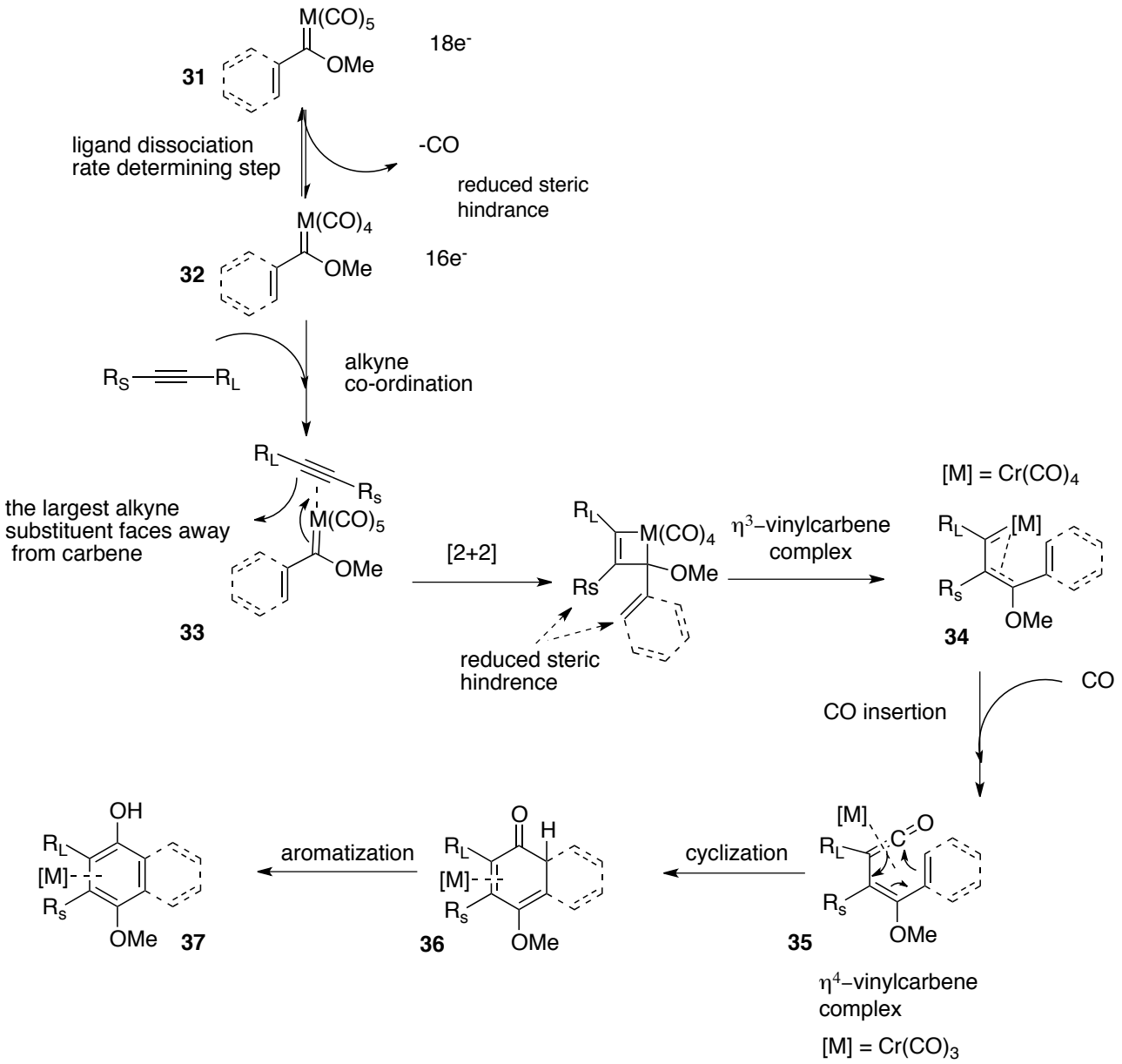

Scheme 14 : Mechanism of the benzannulation reaction

Following the rate determining step, the trapping of the coordinatively unsaturated 16e complex by the alkyne gives complex **33**. This is then immediately followed by the insertion of the alkyne into the metal-carbene bond to give the (η_1:η_3)-vinylcarbene complex **34** which may have either a *Z* or *E* configured metallatriene. It has been suggested by Minatti and Dötz[81] that this is a branching point in the reaction mechanism. Different routes are theoretically possible although no consensus has been reached as to exactly what happens in the last step due to the fact that in order to validate mechanistic details one would need a benzannulation reaction where each step can be established by characterization of all the relevant intermediates. This goal has not been reported so far in literature although Barluenga did come close when investigating what he called "the first stepwise benzannulation reaction". Unfortunately he didn't get the exact phenol product expected.[82]

It is generally accepted that the η_3-vinylcarbene complex **34** forms an η_4-vinylketene **35** by inserting CO into the chromium-carbene bond. This is followed by electrocyclization to give the η_4-cyclohexadienone **36**. The last step of the reaction is the tautomerism of the η_4-cyclohexadienone **36** to give the phenol product **37**. The intermediate was cleverly validated by Wulff who managed to synthesize an η_4-cyclohexadienone analogue starting from a molybdenum carbene complex and 3-hexyne. He established that the complex tautomerises in THF at 70°C to yield the expected phenol product (Scheme 15).[80-82]

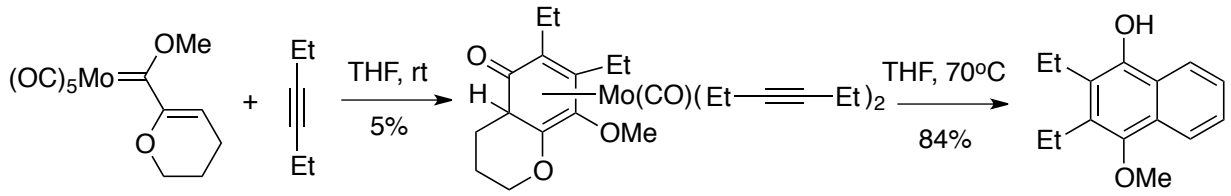

Scheme 15 : Intermediate validation by Wulff showing tautomerism in THF at 70 °C [80-82]

Patterns, trends and general observations

In his 2004 review on the benzannulation reaction, Dötz reported that the reaction can be influenced by a number of factors, one of which is the allochemical effect.[83] This describes how the distribution of products is influenced by the concentration of the alkyne in the reaction. Dötz reported that, in strongly coordinating solvents, the ratio of the phenolic benzannulation product (**27**) increases as opposed to the five membered ring cyclization (Scheme 13). This so-called allochemical effect has been explained by the increased rate at which the CO insertion takes place as a result of coordination of the alkyne (Scheme 16). During the CO insertion it has been noted that the alkyne can act as either a 2e or a 4e donor resulting in saturation of the metal center in the intermediate (**40**). When the benzannulation takes place in a non-coordinating solvent the allochemical effect is greatly reduced or in some cases doesn't occur at all. The allochemical effect is predictable and thus useful in selective production of the desired product, either the phenol or cyclopentadiene derivative. In general, ethereal solvents are the solvents of choice due to the fact that they give cleaner reactions, giving the desired $Cr(CO)_3$ coordinated benzannulation products.[83]

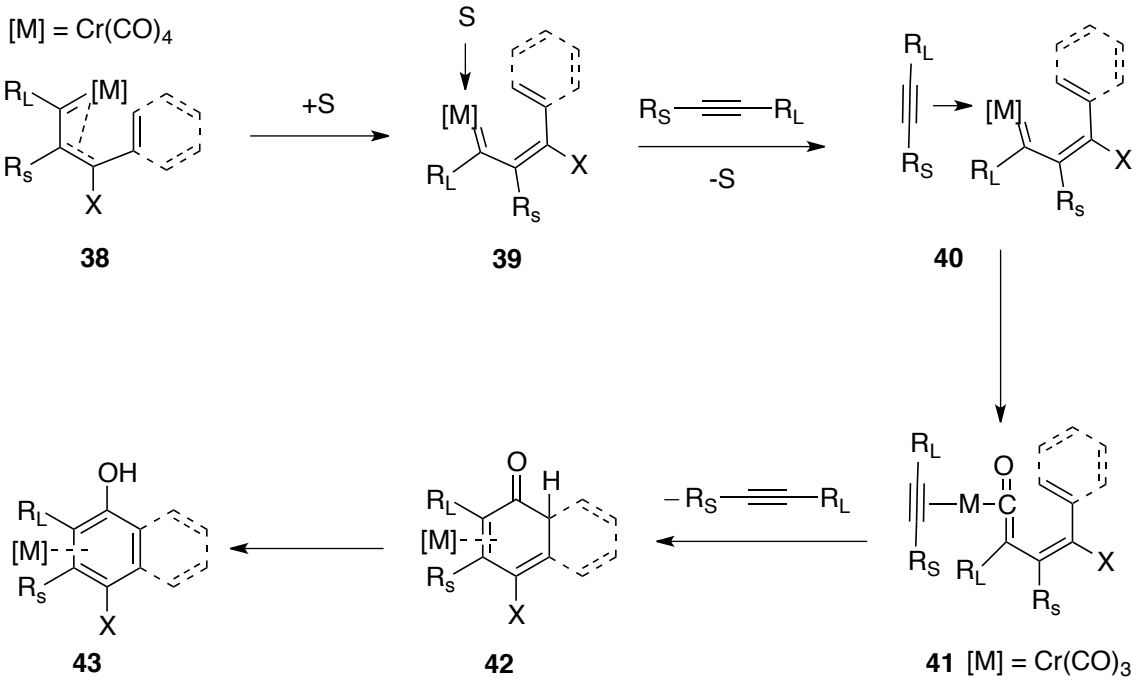

Scheme 16 : The allochemical effect

Another interesting characteristic of the benzannulation reaction is that the chemoselectivity changes depending on the substrate used.[84] In his 2004 review, Dötz showed that the chemoselectivity of phenol formation is much higher for alkoxy(alkenyl)carbenes than for alkoxy(aryl)carbene complexes.[79] Dötz described this particular trend in his review as being because the formation of the η_6-vinylketene complex **35** (Scheme 14) is favored when starting from alkenylcarbene complexes. In the case of the aryl complexes this transformation doesn't occur readily since this would require dearomatisation of the complex which isn't favored.[84]

In the case of amino(aryl)carbene complexes and their alkenyl carbene counterparts, it has been observed that the aryl complexes prefer to undergo a cyclopentannulation reaction rather than benzannulation.[85] The alkenyl complexes can undergo the cyclopentannulation but with some difficulty. This reactivity is said to be due to the high electron density that results at the metal center due to the donor nature of the amino groups compared to the alkoxy substituents, resulting in an increased M-CO bond strength in the aminocarbene complexes. In the benzannulation reaction this means the that the initial decarboxylation step would require harsher conditions.

Regioselectivity in benzannulation is mainly attributed to the steric bulk of the alkyne substituents. When the benzannulation is carried out using unsymmetrical alkynes the major regioisomer will generally bear the larger alkyne substituent next to the phenolic group. A complete reversal of this regioselectivity is achieved by either an intramolecular benzannulation or by using stannyl actylenes or alkynyl boronates (Scheme 17). [86] The inverse regioselectivity has been debated and two reasons for this have been postulated: firstly that the electron rich metal centers (Sn or B) are positioned far away from the electrophilic carbene center; and secondly that there could be a Lewis acid/base interaction leading to stabilization of the η_3-metallatriene (Scheme 17).

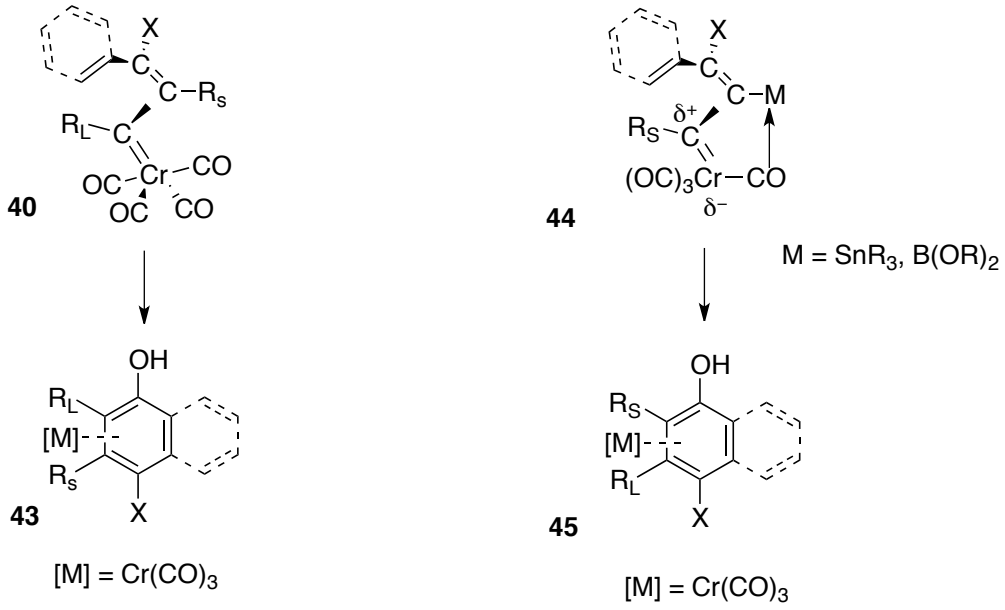

Scheme 17 : Normal and inverse regioselectivity

1.3 Baylis Hillman Reaction

The Baylis-Hillman reaction is best described as a three component reaction involving the coupling of an activated alkene with a carbon electrophile in the presence of a tertiary amine catalyst to produce a highly functionalized system **46**[88] (Scheme 18). The high atom economy and highly functionalized products characteristic of the Baylis-Hillman reaction are favored as a 'green' process in synthetic chemistry. The reaction was first discovered in the 1960's by Morita, who described the reaction of an aldehyde with an acrylic compound catalyzed by a phosphine catalyst.[89] The reaction was formalized in the 1970's by A. Baylis and M. Hillman. Since then it has become a popular method with diverse synthetic applications.[90]

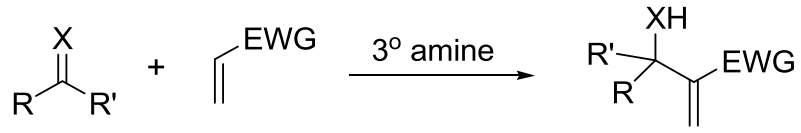

R = aryl, alkyl, heteroaryl
R' = H, COOR, alkyl
EWG = COR, CHO, CN,
COOR, $PO(OEt)_2$
SO_2Ph, SO_3Ph, SOPh
X = O, NCOOR, NTs, NSO_2Ph

Scheme 18 : The Baylis Hillman reaction

A deeper understanding of the mechanism has proved an ongoing challenge. Kaye and co-workers have made a significant contribution to the methodology and understanding of this reaction.[91] The generally

accepted mechanism for this reaction is shown in Scheme 19 where the reaction is illustrated between methyl vinyl ketone (MVK), as the activated alkene, and benzaldehyde as the electrophilic carbon center, catalyzed by DABCO (1,4-diazabicyclo[2.2.2]octane). Step one involves a Michael type nucleophilic addition of the tertiary amine to the activated alkene to give a zwitterionic enolate intermediate **47**. This facilitates the aldol-like nucleophilic attack onto the aldehyde center to generate the second zwitterionic species **48**. The reaction is complete after proton migration and elimination of the catalyst has occurred, giving **50**.

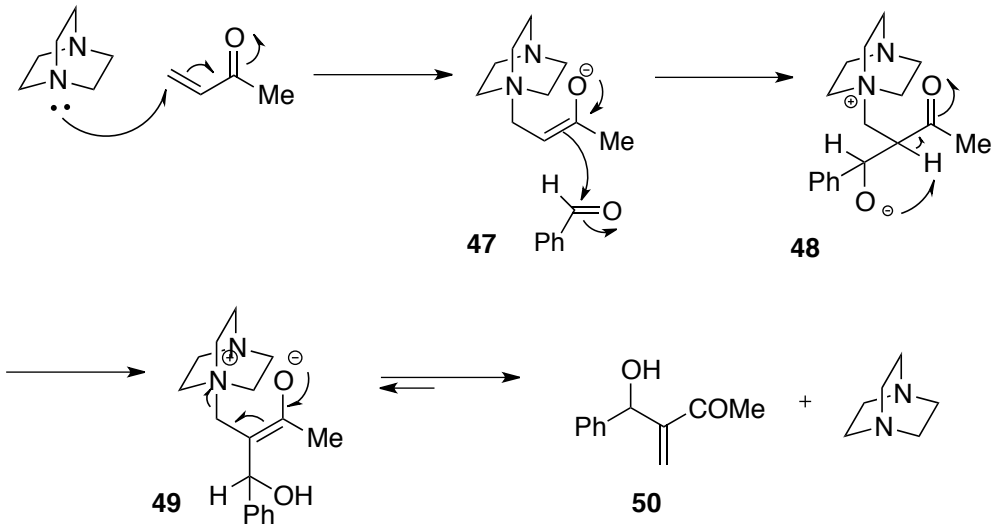

Scheme 19 : The Baylis Hillman reaction mechanism

Aumann and coworkers investigated the application of the Baylis Hillman reaction using Fischer carbenes instead of the organic carbonyls as electrophiles with great success (Scheme 20).[60] In that case a tungsten carbene **51** was added to the Baylis Hillman zwitterion **52**. The resulting intermediate **53** decomposed with loss of $W(CO)_4$ to give the substituted amide **54**.

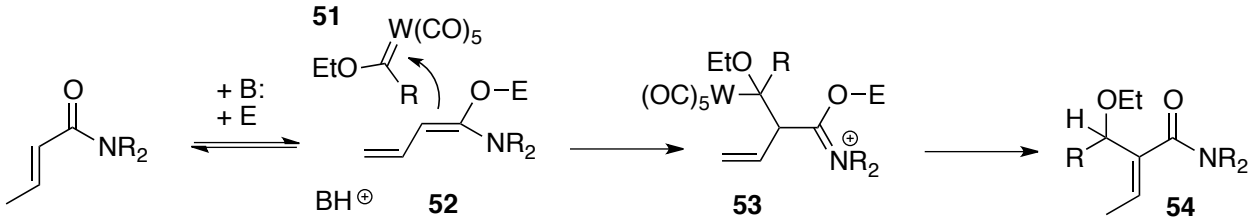

Scheme 20 : Baylis Hillman type addition of a Fischer carbene complex to a α,β-unsaturated amide. [60]

Variation of the starting reagents allows for a variety of highly functionalized products to be prepared which can be useful in further synthetic transformations and contain structural elements (such as β-hydroxy carbonyl) that are widely present in products of biological and medicinal interest. One of the most significant challenges of the Baylis Hillman reactions is its slow reaction rate. Typically it can take a few days up to a few weeks for the reaction to reach completion. Due to the valuable products obtained there has been a substantial amount of research into improving the reaction rates. Much of this research looked into varying the three components of the reaction as well as the use of different conditions including ultra sound, microwave irradiation, pressure and temperature control.[87]

1.4 Aim

The aim of this project was to synthesize novel scaffolds based on chromium carbene templates for use in the ongoing medicinal chemistry research in our research group. The Fischer method was to be used to synthesize carbene complexes with a range of substituents. These would then be subjected to an aldol type condensation reaction giving the desired α,β-unsaturated carbene systems which would then undergo a benzannulation reaction to form substituted ring systems, or, through the well studied Baylis Hillman pathway give different ring systems as seen below in Scheme 21.

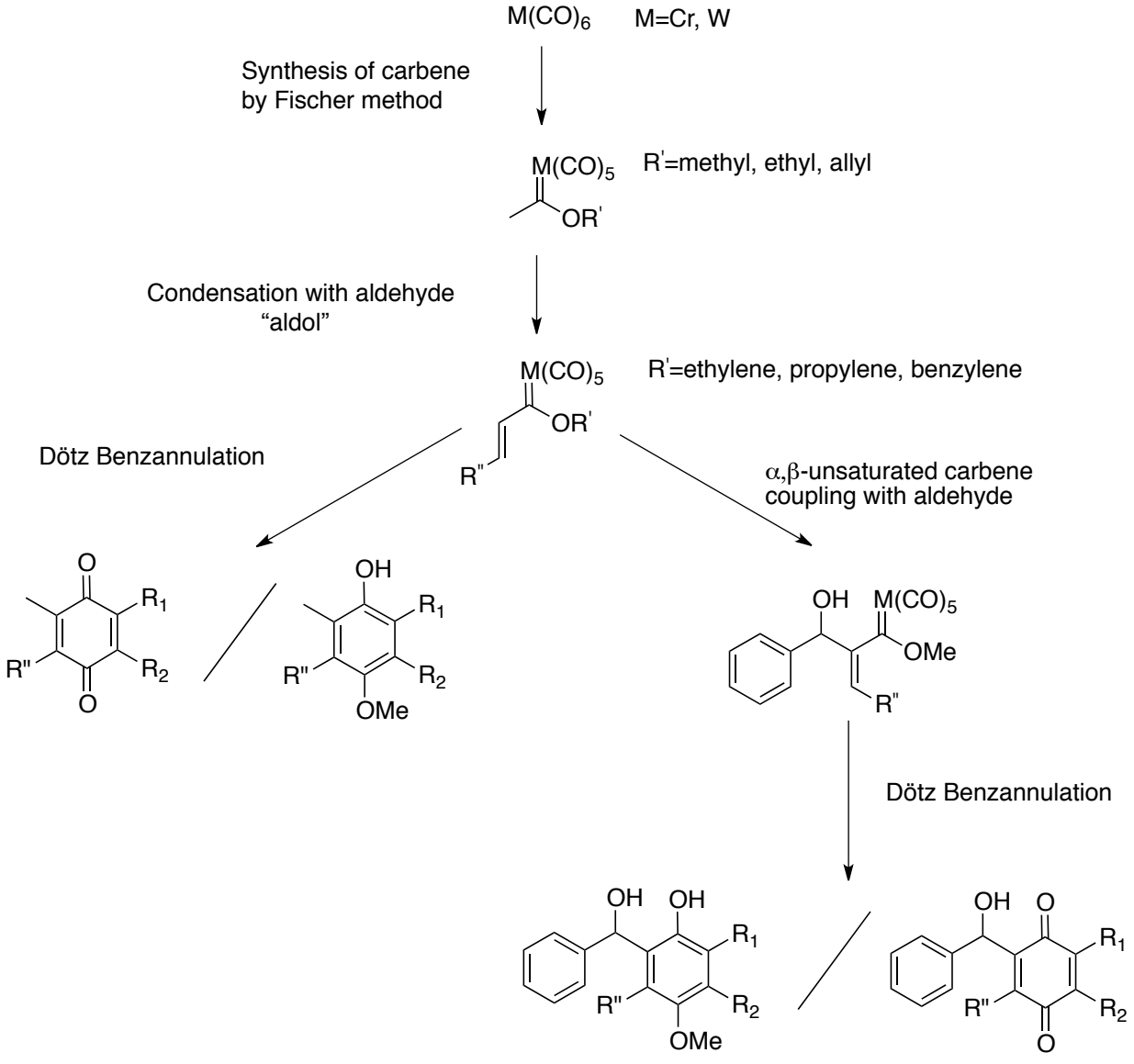

Scheme 21 : Proposed synthetic route

2 Results and Discussion

> "Unlike history or philosophy, chemistry cannot profitably be read chapter by chapter but must be vigorously attacked with a dozen sharp pencils and a ream of inexpensive paper close at hand. When information is used to solve problems, it rapidly becomes part of your knowledge." -- Rodger W. Griffin,
>
> "Griffin was right, but add an eraser to your organic chemistry study equipment. An eraser is essential because you will explore, and exploring means taking wrong turns and making mistakes. Mistakes lead to a deeper understanding of what is right, what is wrong, why some things work and other don't. Don't be afraid to make mistakes, and wear out an eraser or two." --Dr Hardinger.

This discussion is focused on the application of chromium and tungsten Fischer carbenes in the synthesis of α,β-unsaturated carbenes towards acceptors in the Dötz benzannulation and Baylis-Hillman reactions.

2.1 Synthesis of Carbene complexes

From a review of the relevant literature, it became evident that carbenes are very useful in organic synthesis. This is primarily due to the good balance between reactivity and relative stability which has enabled a wide variety of applications involving Fischer carbenes to be exploited.[19] Extensive research has been carried out on these metal complexes revealing some of the associated challenges, such as the sensitivity to light and oxygen.[114] Despite the challenges faced with using carbenes, there are, however, many advantages to using Fischer carbenes in alkylation,[58] aldol and Michael-type reactions, [110] and pericyclic reactions such as the Dötz benzannulation reaction.[117]

2.1.1 Methyl carbene synthesis and NMR characterization

A review of the literature showed that the preferred method of synthesis for Fischer carbenes is the Semmelhack-Hegedus method[105,105] because it is more versatile and does not have the limiting factor of finding a suitable organolithium. Nonetheless, the original Fischer method is simpler.[105-108] In order to synthesize the methyl carbene substrate required for this study, a simple variation of this variation devised by Hoye and co-workers[107] was used, since it allowed variation of the *O*-alkyl moiety.

Chromium hexacarbonyl was reacted with methyllithium in ether under argon at room temperature, to yield an acyl metalate which was alkylated by either Me_3OBF_4 or Et_4NBr/alkylhalide to form the expected bright yellow carbene complexes (Scheme 22). The reaction was then repeated with tungsten hexacarbonyl to give the corresponding tungsten carbenes.

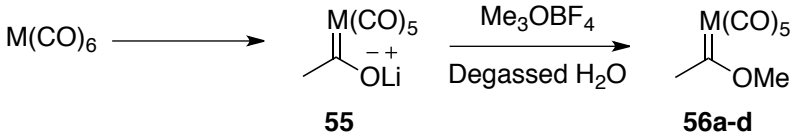

55 **56a-d**

Scheme 22: Synthesis of a simple Fischer carbene

Due to the facile oxidation of these complexes[114] and the sensitivity to moisture of the reagents, it was very important to use Schlenk techniques to eliminate air from the reaction system. In order to achieve the addition of methyl carbanion to the carbonyl carbon to form an acylpentacarbonyl-chromate salt, the methyllithium was added drop-wise to a suspension of the hexacarbonyl complexes in dry Et_2O.[72] The mixture turned from a pale yellow to dark brown within 30 minutes and so the alkylation step followed using a range of alkylating agents and degassed water (in order to avoid any accidental oxidation). The yellow Fischer carbenes **56a-c**, (Table 1) were extracted into dry Et_2O which turned bright yellow, while the aqueous layer became pale yellow and then almost colorless in a second extraction. The solvent was removed under reduced pressure to give the crude carbene product as a yellow solid residue in *ca* 65% yield. The corresponding methoxy stabilized tungsten Fischer carbene was synthesized following the same route giving the carbene **56d** as bright yellow crystals in a slightly higher yield (78%).

Table 1 : Carbenes synthesized using chromium and tungsten

56	M	R	Alkylating agent	Experimental yield (%)	Structure
a	**Cr**	Me	Me	68	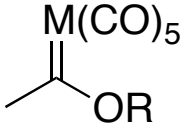
b	**Cr**	Et	Et_4	65	
c	**Cr**	Allyl	Et_4	62	
d	**W**	Me	Me	78	

In the synthesis of these carbenes general observations were made. Some of the chromium or tungsten hexacarbonyl did not dissolve and a small quantity of white solid observed at the bottom of the Schlenk flask

was later found by NMR to be the corresponding hexacarbonyl complex. Additional methyllithium was added to compensate. It was also noted that, in most instances, when the crude mixture was left in the cold room overnight (0-4^{o}C) a green solid formed at the bottom of the flask in the case of chromium and blue in the case of tungsten. Since Fischer carbenes are readily oxidized to give carbonyl analogs it was suspected that the green and blue solids were in fact the metallated fragments of the oxidized analogs of the corresponding carbenes. Confirmation of the oxidized analogs was attempted using a method adapted from Perdicchia *et al.*[60] using a sodium hypochlorite solution (NaOCl) with tetrabutylammonium bromide (Bu_4NBr) in an ethyl acetate/water mixture. Although the mixture turned green indicating the change in the oxidation state of the chromium, the oxidized organic product could not be isolated or observed.

In an effort to obtain the carbenes in high yield and high purity various purification techniques, including sublimation and chromatography, were attempted to remove the impurities without decomposition of the product. Although higher purity compounds were obtained, the overall yield decreased substantially. It was observed that even immediately after an initial purification, decomposition was already taking place. Consequently, it was necessary to forego standard purification methods. Instead, the product mixture was filtered through a column of molecular sieves, anhydrous $MgSO_4$ and celite under Ar pressure. The column was washed with a column volume of dry pentane. This ensured that the carbene was dry, and that decomposition products and residual starting material were trapped on the celite.

1-D NMR analysis of the methyl carbene **56a** was comparable to that found by Nandi *et al.* (Table 2).[75] The ^{1}H spectrum of the carbene **56a** (Figure 6) shows the distinctive methoxy resonance at 3.89 ppm and the methyl resonance at 2.41 ppm. The methoxy signal is further downfield because of the electronegative effect of the oxygen, and appears very broad. The broadness of the signal is due to the stabilizing effect of the methoxy group on the carbene carbon, resulting from delocalization of electrons over the two bonds causing a partial loss of double bond character in the M-C bond and allowing more free rotation, (Scheme 23). The broadness of the peaks can possibly be attributed to the relatively slow rotation about the bond, causing the substituents to occupy changing chemical environments, either eclipsed or staggered with the carbonyls. There is however a difference in chemical shift observed in the experimental values [400 MHz (9.4 Tesla)], [600 MHZ (14.1 Tesla)] and values found in literature [500 MHz (11.7 Tesla)] this suggests that CSA (Chemical Shift Anisotropy) is a possible relaxation mechanism for these centers.

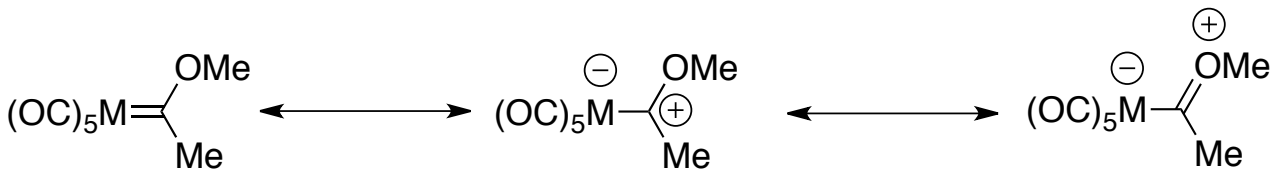

Scheme 23 : Bonding in Fischer carbene complexes

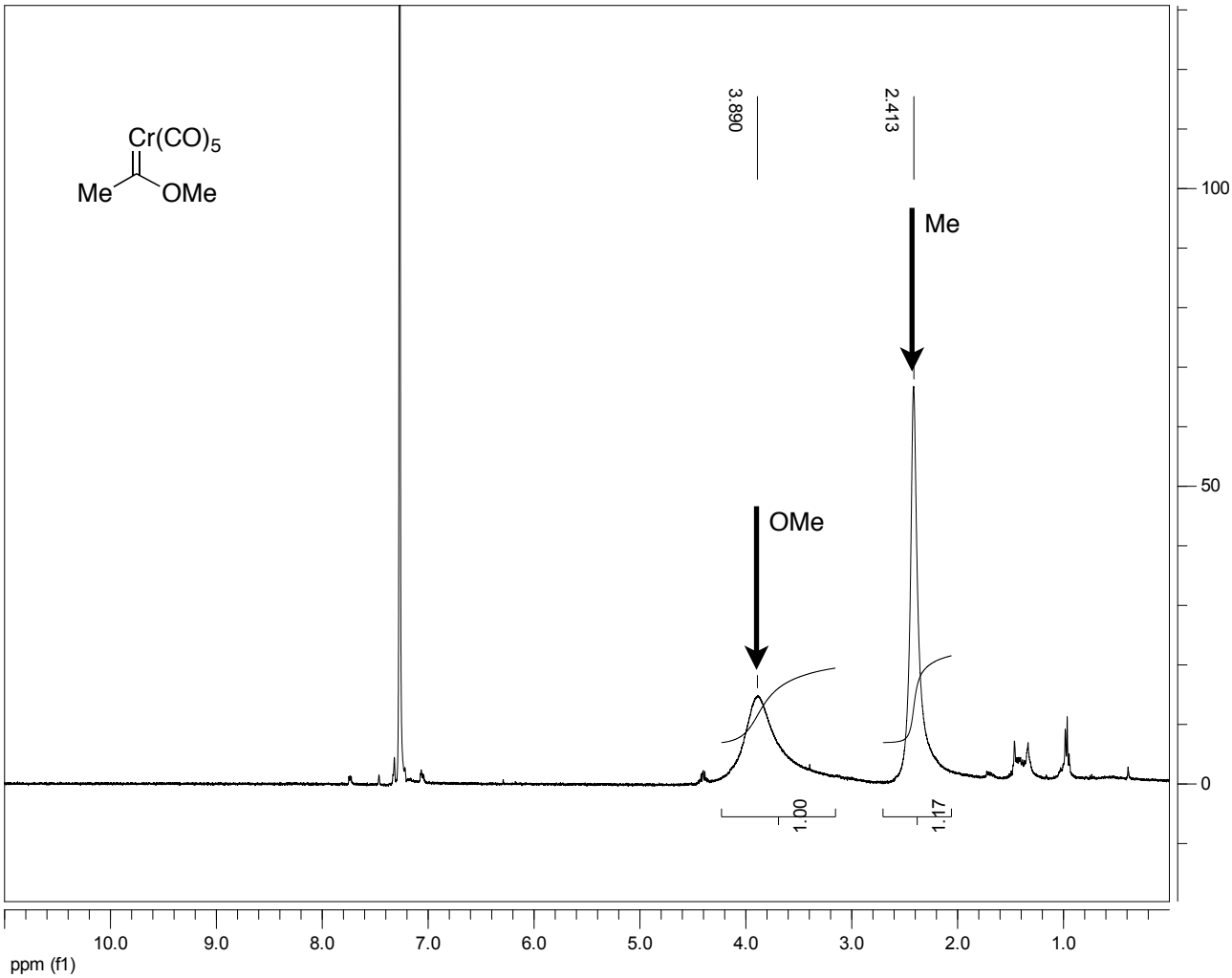

Figure 6 : ^{1}H NMR spectrum (400 MHz $CDCl_3$) of carbene 56a

Table 2 : Comparison of experimental and literature ^{1}H chemical shifts of carbene 56a

	Experimental (400 MHz chemical shifts)	Literature (500 MHz chemical shifts)	Experimental (600 MHz chemical shifts)
O-CH	3.89	4.70	5.11
Cr=C-CH	2.41	2.94	3.92

The ^{13}C spectrum of the synthesized Fischer carbenes (Figure 7) clearly shows the expected resonances of the five unique carbons. The electron deficient nature of the carbene carbon results in a low field resonance in ^{13}C NMR which, from literature, is in the range of 350 – 400 ppm. In the case of the chromium carbene, the resonance at 359.8 ppm confirmed the presence of the carbene carbon and the carbonyl in the *trans* position was observed at 223.6 ppm while the remaining four *cis* carbonyls are coincident at 216.8 ppm. The broad, low intensity signals at 66.9 ppm and 49.3 ppm correspond to the OCH_3 and CH_3 respectively.

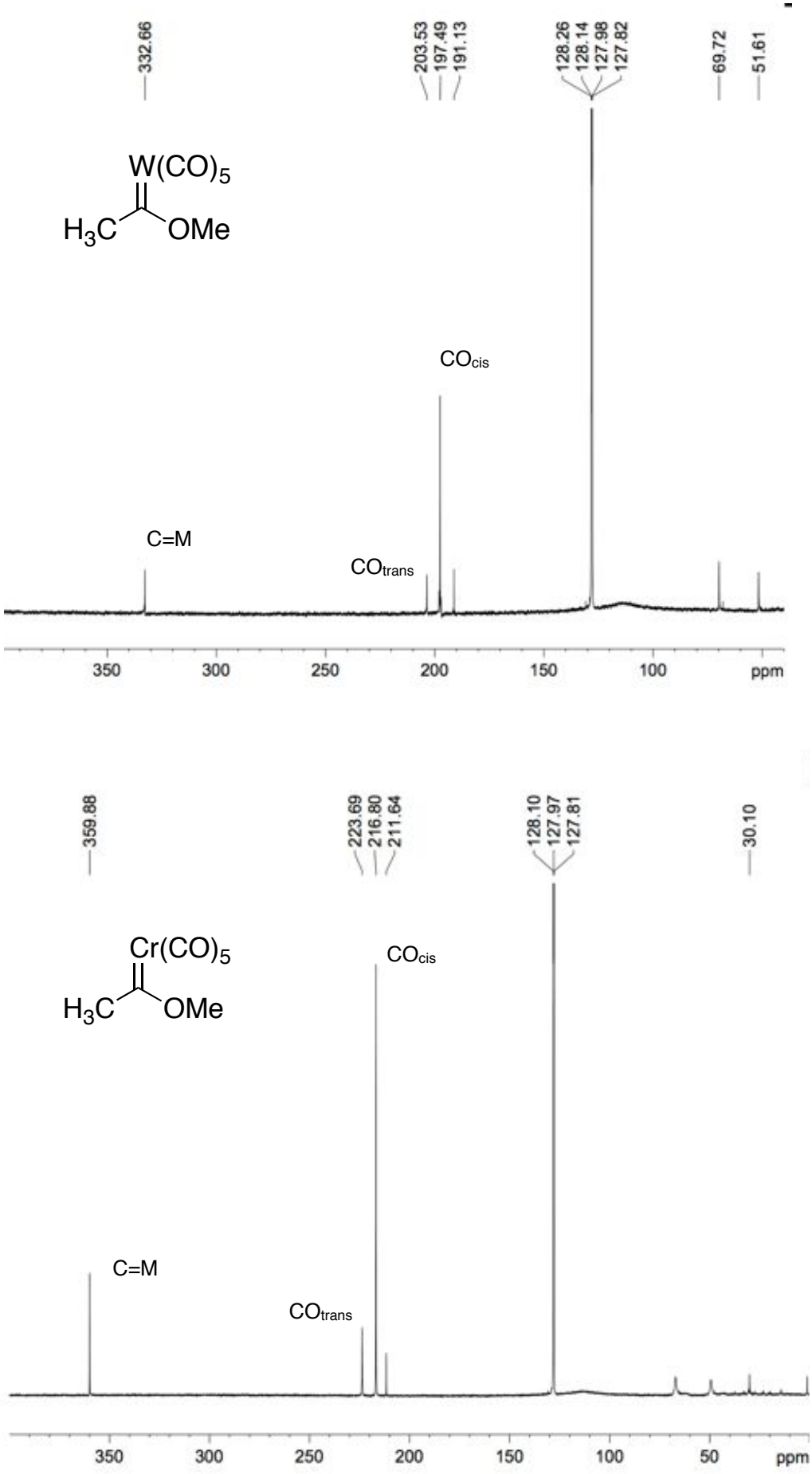

Figure 7: ^{13}C NMR spectra (150MHz, C_6D_6) of tungsten and chromium methoxy methyl carbenes (56a,d)

The ^{13}C NMR spectrum of the tungsten complex showed a similar distribution of signals, although all the metallated carbon signals were shifted upfield. The chemical shift of the carbene carbon was at 332.7 ppm while the *cis* and *trans* carbonyls were observed at 197.9 and 203.5 ppm respectively. The two methyl groups were found at 69.7 ppm (OCH_3) and 51.6 ppm (CH_3). The chemical shifts associated with **56d** also correlate with those available in literature (Table 3) confirming that the product was successfully synthesized.

Table 3: Experimental and literature ^{13}C chemical shifts of 56a,d

Metal	Carbon	Experimental	Literature
Chromium	Cr=C	359.8	360.5
	trans CO	223.6	223.5
	cis CO's	216.8	216.5
	-OCH	66.9	67.3
	-CH	49.3	49.6
Tungsten	W=C	332.7	333.3
	trans CO	203.5	203.5
	cis CO's	197.9	197.2
	-OCH	69.7	70.3
	-CH	51.6	52.1

The instability of these simple carbenes can best be seen at room temperature with decomposition occurring after a short period of time (as little as 6 hours). The decomposition is attributed to the loss of a carbonyl which then promotes further fragmentation of the complex at the carbene carbon as described by Lotz *et al*.[73] This can be seen experimentally by the apparent decrease in size of the *trans* carbonyl signal around 225.0 ppm and the appearance of an ester signal around 167 ppm (Figure 8) corresponding to the decomposition product. Meyer[70] observed that adding an oxidizing agent to the carbene products resulted in the appearance of a similar ester carbonyl signal around 167 ppm. Experimentally it was seen that this process could be slowed down by storing the carbene under argon in the cold room (< 5°C). There was, however, always a small amount of green solid precipitate, depending on storage conditions, which was a clear indicator of decomposition through oxidation as the chromium changes from colorless chromium(0) to green chromium(III).

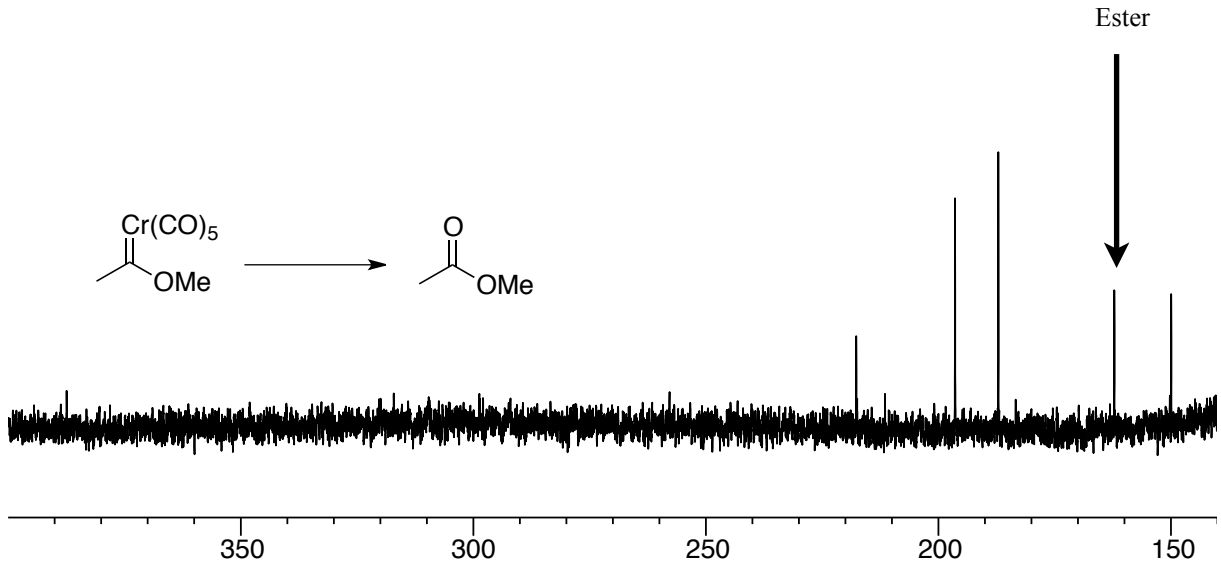

Figure 8: 150MHz ^{13}C NMR spectrum of chromium carbene solution (C_6D_6) with evidence of ester decomposition product

Although there were many synthetic challenges, it was possible to generate the carbenes, albeit in lower yields than expected (65-70%). The main cause for the mediocre in yield was the unreacted metal hexacarbonyl present due to the low concentration of the MeLi solution we received (6 month shipping). Precautions were taken to exclude water and trace amounts of oxygen from all solvents since these could also affect the organolithium and reduce its ability to participate in the reaction.

The carbenes generated decomposed much more slowly over time when stored in dark, air free conditions in a cold room, although oxidized products still formed if not used within a week. This proved a challenge as a clean product could never be ensured for use in subsequent reaction steps. In order to avoid this problem the crude product was dissolved in dichloromethane and rinsed through a column of celite, molecular sieves and anhydrous magnesium sulfate immediately prior to a subsequent reaction.

2.2 Condensation of carbenes with aldehydes

2.2.1 The aldol reaction

Due to the ester-like nature of the Fischer carbenes, the preparation of the α,β-unsaturated carbene complexes could be effected *via* a condensation reaction. Aldol condensation methodology was the chosen means of synthesizing α,β-unsaturated products retaining the metal-carbon double bond. The conditions required include either a strong or mild base, and an appropriate aldehyde. The reaction, even with esters, is known to generate a β-hydroxy carbonyl compound as an intermediate which may subsequently undergo facile dehydration.[64]

2.2.2 Synthesis of α,β-unsaturated complexes and NMR characterization

The methyl carbene complexes **56a-c** were reacted with aldehydes in the presence of a tertiary amine base following the method by Barluenga *et al.*[24] Methane sulfonylchloride (MsCl) was added to the system to enhance the leaving group potential of the resultant hydroxyl group, and so facilitate elimination to give the desired complexes **57** (Scheme 24).

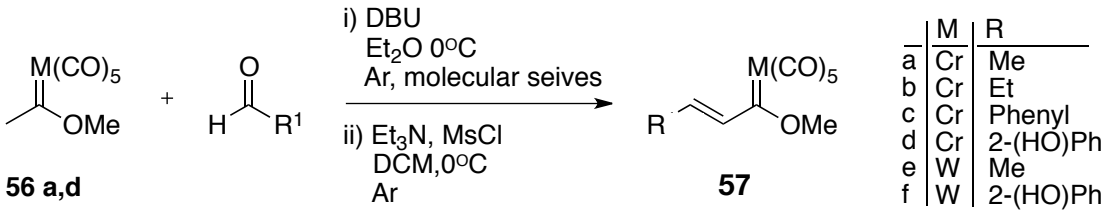

Scheme 24: Aldol condensation with Fischer carbenes

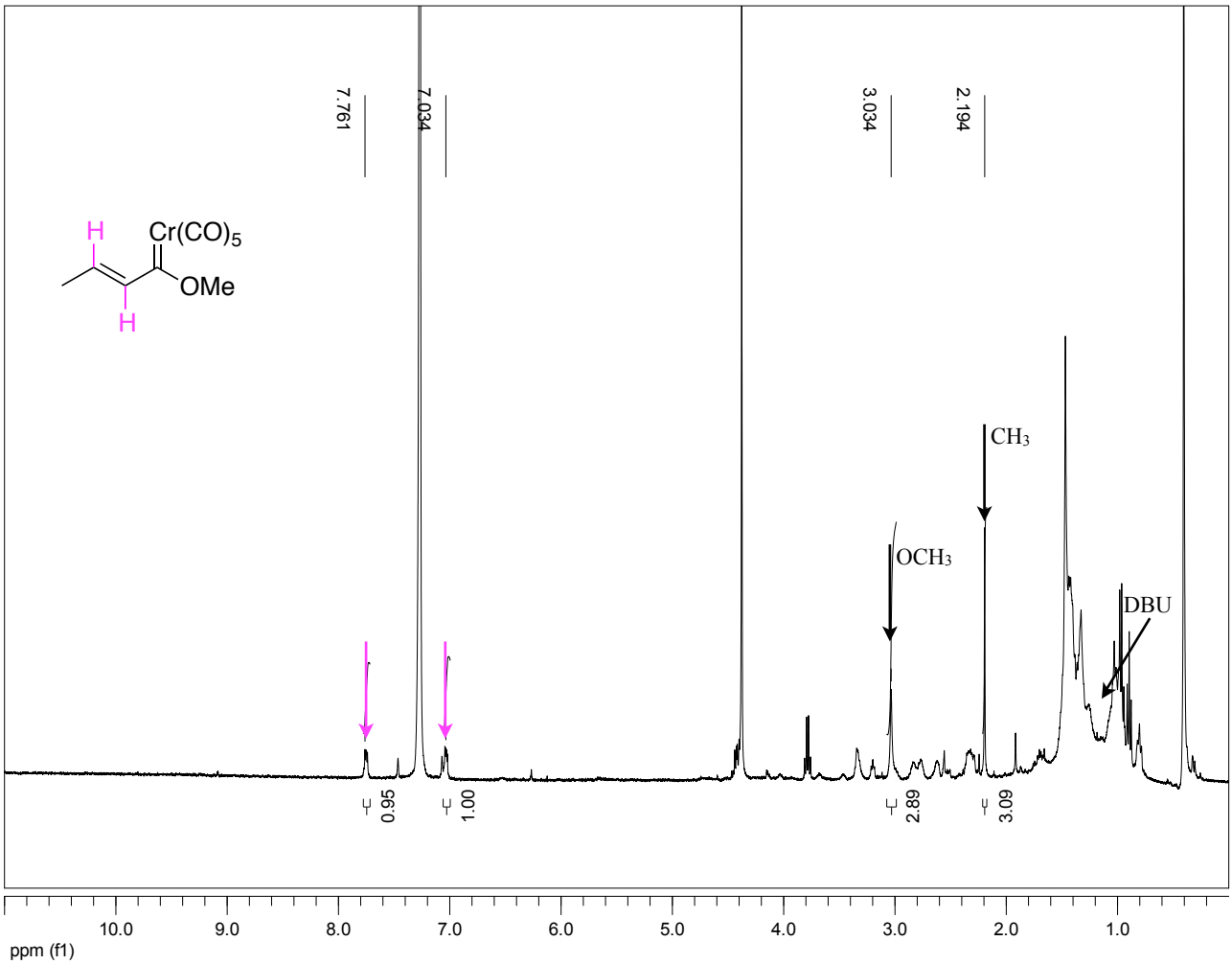

Figure 9: ^{1}H NMR spectrum (600 MHz, C_6D_6) of 57a

^{1}H NMR (Figure 9) was used to confirm the synthesis of **57a**. The signals at 7.76 and 7.03 ppm were attributed to the protons on either end of the double bond. The signal at 3.03 ppm is due to the methoxy hydrogens. The remaining terminal methyl protons resonate as the signal at 2.19 ppm. The NMR is of a

crude reaction mixture since attempts at purification resulted in the rapid oxidation of the the compound. It was difficult to isolate a pure fraction even *via* air free silica column chromatography or re-crystallization.

Formaldehyde would have been a good candidate due to its small size, and because it contains no enolizible protons. Although formaldehyde was not used it was thought that acetaldehyde and propionaldehyde had a sufficiently small size suitable for our proposed application of these complexes in the Baylis Hillman reaction (Section 2.3). Previous research done in our research group, where enolizible acetaldehyde and propionaldehyde were used to synthesize the same α,β-unsaturated carbene complexes in "good yields (55-70%)" suggested that our choice of aldehydes would be suitable.[74] Unfortunately, we were not able to replicate these reactions using propionaldehyde.

After limited success, further investigation of the literature was carried out in order to understand why this simple reaction didn't yield the products as expected. Although it is well-known that the aldol reaction is less efficient with enolizable aldehydes, it was hoped that the use of the relatively weak amine base would circumvent enolization. The aldol reaction of alkyl carbenes has been investigated by Wulff and coworkers and others [66,67,111,116,117,118] and found to have predictable chemistry mirroring the aldol reaction in general. This reaction was first looked into by Casey[129] and it was discovered that generally the carbene anion would not add to a carbonyl compound. Addition products were obtained only when elimination occurred. The forced elimination drives the equilibrium towards the formation of the unsaturated products. This was as expected and the reason for adding DBU in the first step was to accelerate the elimination. More interestingly, it was noted by Wulff[103,104] that the formation of products via this 'aldol condensation method' was limited to aryl aldehydes and non-enolizable aldehydes as with esters.[122]

Since the mixed results of the above reactions can be accounted for by the choice of aldehyde, the same method was used going forward using benzaldehyde and salicylaldehyde, neither of which contained α-hydrogens. In reaction with benzaldehyde, the product was not easily observed. However, an approximate yield of 10% was obtained with salicylaldehyde following reaction with both chromium and tungsten carbenes. Figure 10 shows the ^{1}H NMR spectrum of **57d**. The six multiplets between 6 and 8 ppm correspond to the four aromatic protons and the two alkene protons - confirming the formation of the condensed complex. These have been tentatively assigned based on **57a**. It was not possible to acquire the necessary 2D spectra due to the relatively short life times of these complexes. The methoxy group was shifted downfield to 4.32 ppm, possibly as a result of the now extended conjugation. This was further illustrated by a substantial color change from yellow to deep purple suggesting the formation of a highly conjugated system. These results are summarized in Table 4. The presence of a very large signal for the aldehyde (10.14 ppm) suggests that there is still a significant proportion of unused aldehyde in the system. Overlap in signals at 7.62 and 7,08 ppm correspond to the alkene protons of **57d** and overlap at signals 6.80, 6,72 and 6.46 ppm correspond to aryl protons of complex **57d.** No signals corresponding to carbene starting material (**57a**) were seen, indicating it was completely consumed in the reaction. This indicates that product **57d** was formed albeit in a small quantity.

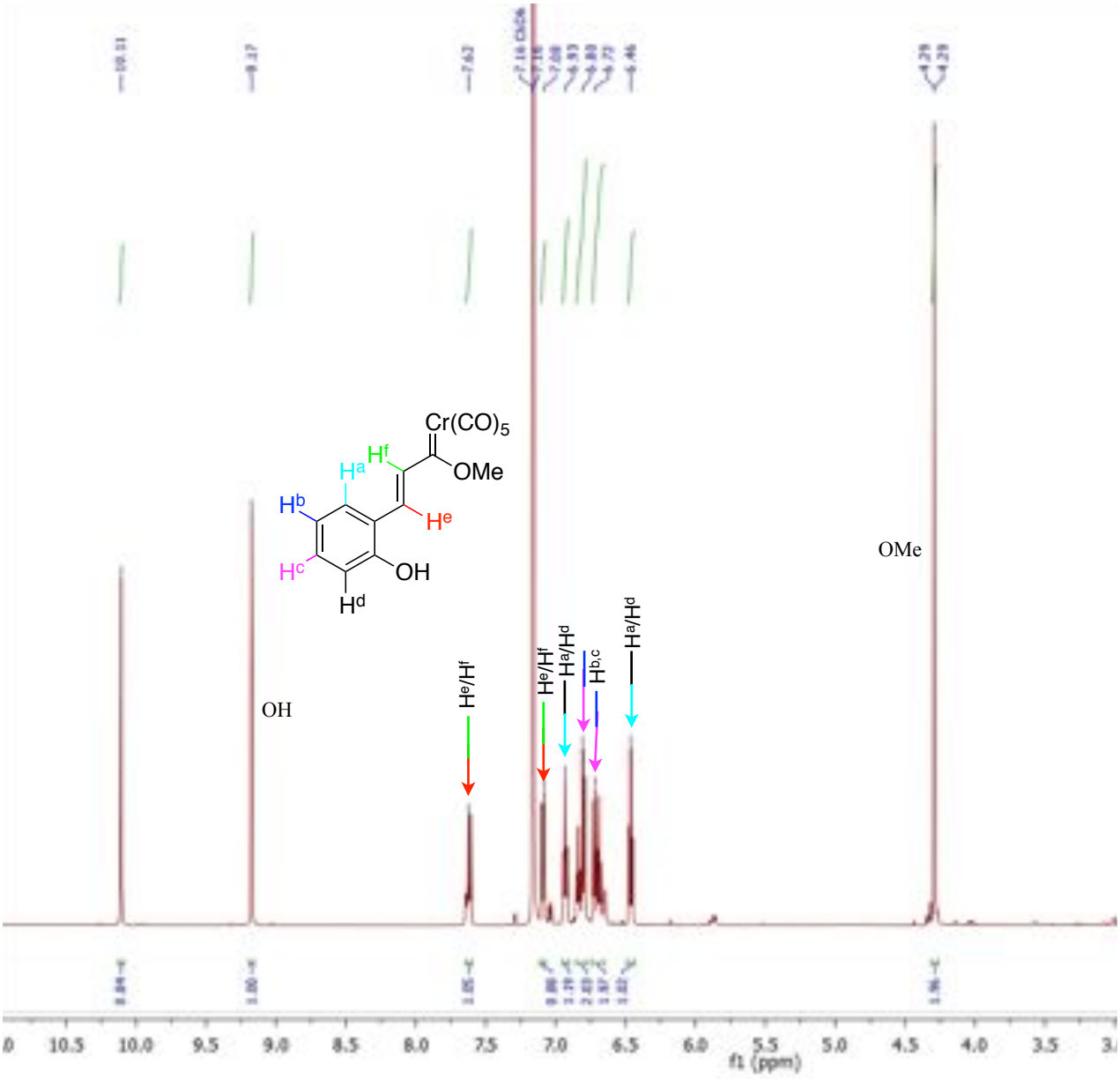

Figure 10: ^{1}H NMR spectrum (600MHz, C_6D_6) of 57d (chromium Fischer carbene 56a condensed with salicylaldehyde).

Table 4: Summary of W and Cr condensation products synthesized

57	M	R	R	Yield (%) Experimental	Structure
a	Cr	Me	Me	60%*	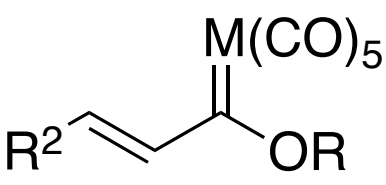
b	Cr	Me	Et	-	
c	Cr	Me	Phenyl	30%*	
d	Cr	Me	2-(HO)Ph	10%*	
e	W	Me	Me	-	
f	W	Me	2-(HO)Ph	17%*	

- reaction did not yield product
** based on crude mass (calculated from NMR) **

Inspection of the ^{13}C NMR spectrum **57f** (Figure 11A) clearly showed that the distinguishing carbene signal was not observed around 360 ppm but rather 395 ppm. This substantial shift could be due to the highly conjugated system which results from this condensation reaction. This would suggest that the product has been formed, albeit in low quantities. There are no signals corresponding to the methyl carbene suggesting that it has been completely transformed into the unsaturated carbene. Again, due the unstable nature of the product, separation proved difficult and resulted in the disappearance of the carbene carbon signal at 395 ppm after work up.

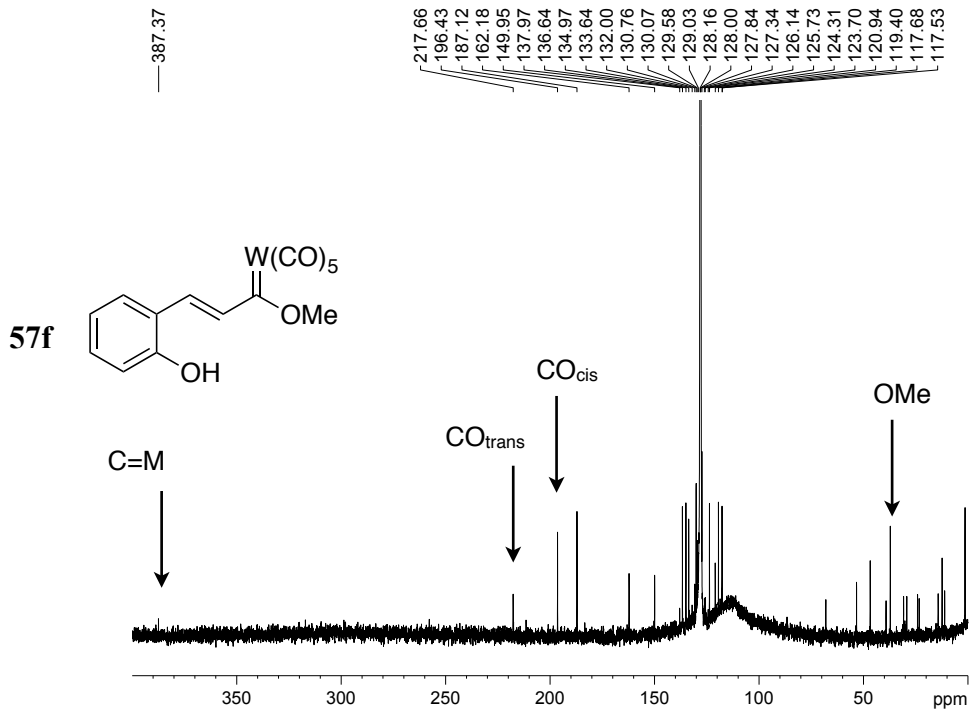

Figure 11A: ^{13}C NMR spectrum (150MHz, C_6D_6) of 57f

The ^{13}C NMR spectrum of **57f** (Figure 11B) also showed a substantial shift of the carbene signal from around 360 ppm to around 390 ppm in relation to the corresponding chromium Fischer carbene starting material. The change in chemical shift can be attributed to the extension in the conjugated system however the magnitude of this change is dependent on the metal. When using chromium as the metal the change in chemical shift observed was about 35 ppm while the use of tungsten resulted in a 55 ppm change in chemical shift.

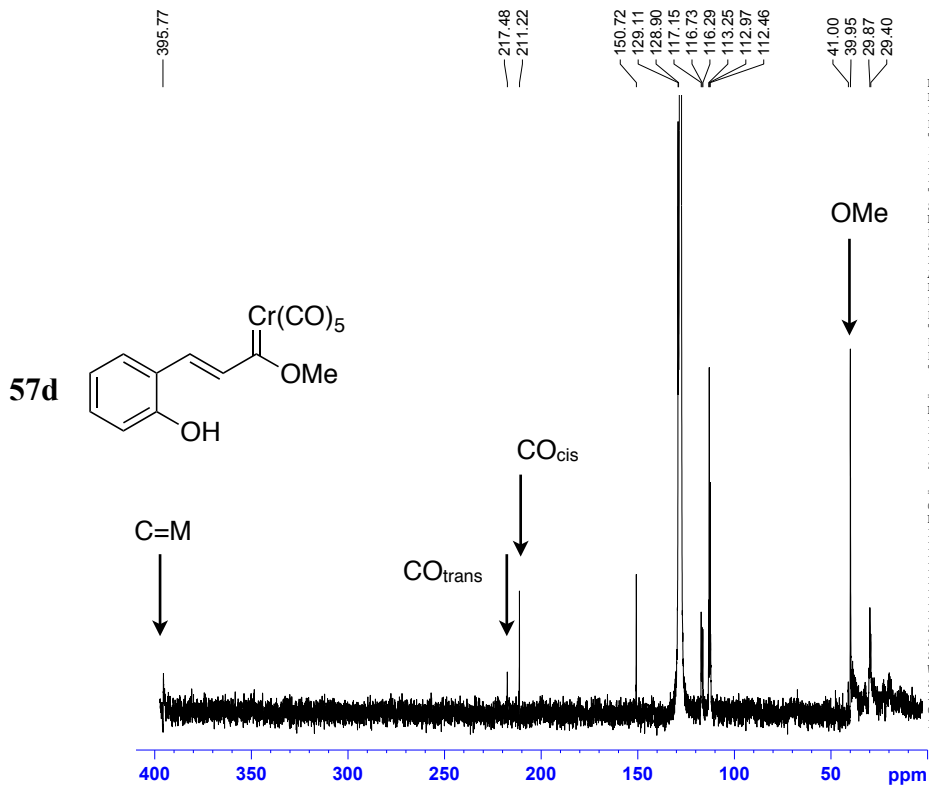

Figure 11B: ^{13}C NMR spectrum (150MHz, C_6D_6) of 57d

General stability of the α,β-unsaturated complexes was low, often resulting in complete decomposition of the products within a few hours. Storage of these systems was often not possible even after following the same precautions as the Fischer carbenes discussed in Section 2.1. Oxidized product was still formed, as in the case of the methyl carbenes, and all attempts at isolation of the product resulted in a high degree of oxidation. In order to alleviate this problem, the crude product was stored immediately under argon in the cold room (<5°C) after evaporating the solvent under reduced pressure. Just before using the product in further reactions it was rinsed through a column of celite, molecular sieves and anhydrous magnesium sulfate.

Thus, the synthesis of α,β-unsaturated carbenes proved to be a challenge as it was not possible to purify the condensation products of type **57d** and **57f** in sufficient quantities for detailed further studies and subsequent reactions were carried out on the crude condensation products.

2.3 Baylis Hillman type reaction

2.3.1 Synthesis of Baylis Hillman adducts using α,β-unsaturated carbene complexes as acceptors

The Baylis Hillman (BH) reaction is a slow C-C bond forming reaction, often taking several days to complete. The major benefit of this reaction is the highly functionalized system that results. It was hoped that using the metal-carbene moiety instead of the organic carbonyl would improve the reaction rate of the BH reaction and subsequent reactions due to the metal-pentacarbonyl fragment being more electron withdrawing than a

simple carbonyl. This is due to the chromium metal being directly attached to five carbonyls bearing electron deficient oxygen atoms. These groups tend to attract electron density away from the carbene double bond, resulting in a more reactive carbene carbon and consequently, a faster reaction should be possible.

The BH reactions under investigation here were carried out according to the procedure following Kaye *et al.* [109,128] Three different aldehydes were reacted with each of the α,β-unsaturated carbene complexes **57a** and **57f** (crude mixtures) in the presence of DBU using DCM as a solvent (Scheme 25)b. Although DABCO is the most commonly used catalyst, in this reaction we chose DBU which has been used previously and also proved effective.[109,128] DBU was preferred for this study because, as a liquid, it was easier to introduce to the reaction flask without oxygen being introduced. The other reason why DBU was preferred is due to ease of purification because it evaporates under reduced pressure along with the solvent.

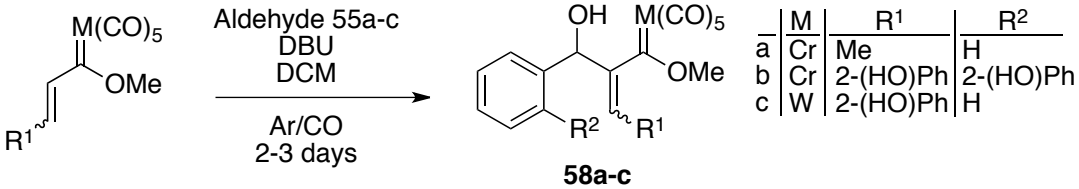

	M	R^1	R^2
a	Cr	Me	H
b	Cr	2-(HO)Ph	2-(HO)Ph
c	W	2-(HO)Ph	H

58a-c

57a R^1 = Me, M = Cr
57d R^1 = 2-(HO)Ph, M = Cr
57f R^1 = 2-(HO)Ph, M = W

Scheme 25: Baylis Hillman reaction using α,β-unsaturated carbene complexes as acceptors

It was noted by Kaye *et al.* that acrylate precursors with no substitution at R_2 (Scheme 18) gave the best results in the Baylis Hillman reaction. In order to use the metal carbonyl condensation products as Michael acceptors in the Baylis Hillman reaction it would have been ideal to synthesize systems where R^2=H.This raised the concern of the effect of using a large R_2 fragment which would possibly slow down or even inhibit the Baylis Hillman reaction by obstructing the attack by the tertiary amines such as DABCO (Figure 12).

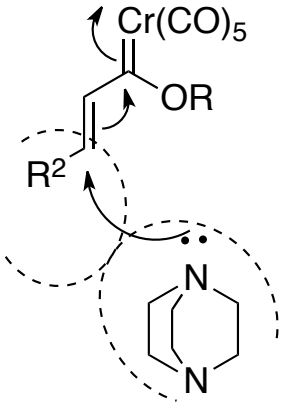

Figure 12: Steric effects in aryl substituted aldol products as Baylis Hillman acceptors

Synthesis of the Baylis Hillman adducts proved very difficult (Table 5). In almost all cases no product could be obtained in any reasonable quantity. A large amount of green oxidized chromium III was obtained when using the chromium based α,β-unsaturated adduct **57d**. In the case of **57a,** which was carried out under a reducing atmosphere of CO instead of argon and with 4Å molecular sieves, some success was achieved, albeit only on a very small scale. A tiny amount of product was detected.

A microwave assisted version of the Baylis Hillman reaction has been reported to give slightly higher yields with significantly reduced reaction time.[64] It was therefore decided to attempt a microwave synthesis on two of the condensation products (**57a** and **57d)** using the method as described: microwave irradiation at 25°C with continuous cooling in 15 min intervals for up to 8 cycles. These attempts were unsuccessful since after 3 cycles most of the reaction mixture appeared to be a green oxidation product, as seen before. It was decided not to pursue attempts using the microwave reactor as this appeared to accelerate the rate of decomposition, rather than facilitating the desired reaction.

Table 5: Baylis Hillman adducts synthesis and attempts

From	58	M	R	R	R	Atmosphere	Yield (%) Conventional	Yield (%) Microwave	Structure
57a	**a**	Cr	Me	Me	H	CO	8%	n.o	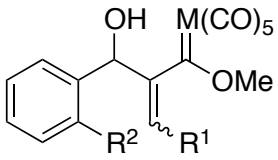
57d	**b**	Cr	Me	2-(HO)Ph	OH	Ar	n.o	n.a	
57f	**c**	W	Me	2-(HO)Ph	H	Ar	n.o	n.a	

n.o - not observed
n.a - not attempted

Even though the reactions in both the conventional and microwave methods were under an inert atmosphere it appeared that, as the reaction continued, the product was in fact being oxidized. Although no Baylis Hillman product was isolated, ^{1}H NMR of **58a** did show some indication of the diagnostic signals for the expected internal double bond protons, shifted ~1 ppm downfield relative to the analogous methyl acrylate product (6.05 and 6.65 ppm).102-104 This substantial shift is due to the effect of the electron withdrawing nature of the chromium pentacarbonyl (Figure 13)

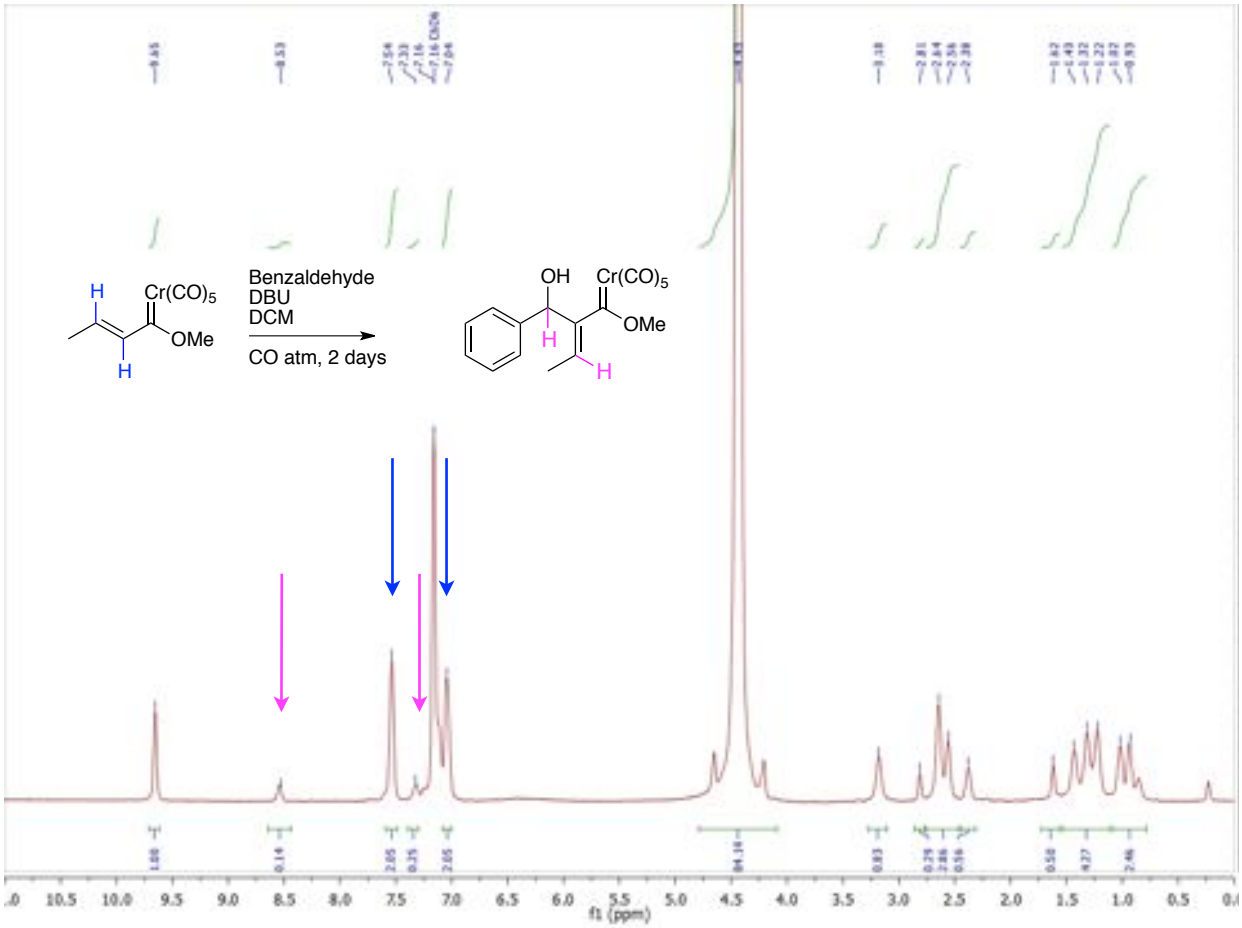

Figure 13: ^{1}H NMR spectrum of (600MHz, C_6D_6) 58a

Similarly, a ^{1}H NMR spectrum of **58b** showed significant changes from the corresponding spectrum of **57d**. Although all signals are shifted relative to the starting material, since the product was no longer soluble in deuterated benzene, it was assumed that the most likely origin of the additional signals was the appearance of the corresponding ester. ChemDraw® was used to predict the ^{1}H NMR spectrum of the ester (Scheme 14, black). To our surprise it showed no correspondence with the experimentally observed spectrum, suggesting the likelihood of an alternative decomposition pathway.

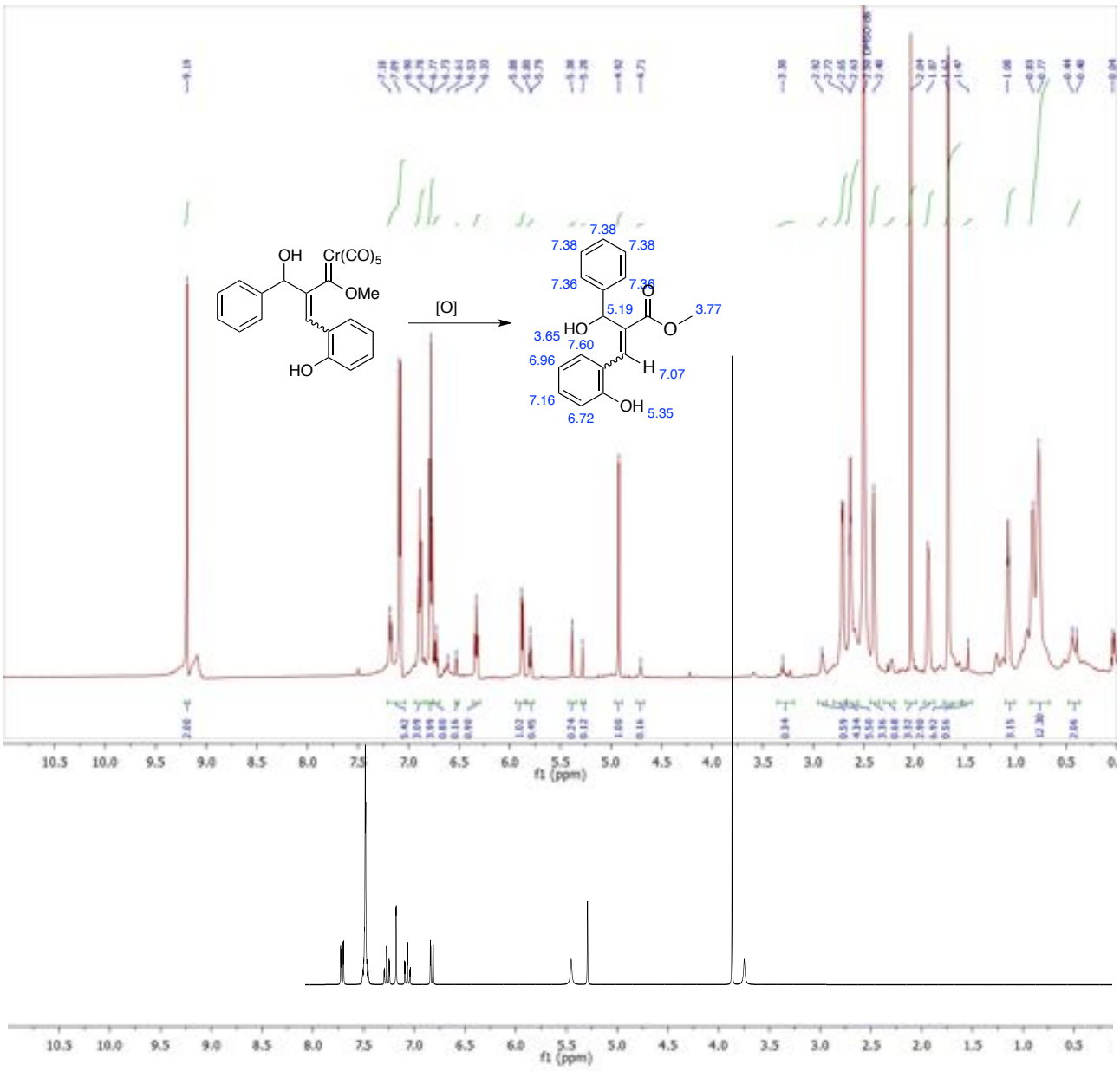

Figure 14: ^{1}H NMR (600MHz, C_6D_6) spectrum of 58b (red) and ChemDraw® prediction of possible oxidized product (black)

Purification was difficult since any attempts to separate the mixture resulted in further oxidation. The addition of molecular sieves to the reaction did help in decreasing the amount of oxidized product being formed, allowing for storage of the compounds for up to a week. We then decided to investigate these complexes through computational chemistry in order to understand the susceptibility to oxidation. This is discussed in Section 2.5.3

2.4 The Dötz Benzannulation Reaction

Traditionally the Dötz benzannulation has been carried out under thermal conditions in a donor solvent. This has been accompanied by the inconvenience of long reaction times with low yields depending on the alkyne being used. Following work by Hutchinson[63] and co workers it was decided in this study to use a microwave reactor, because this approach was expected to be highly efficient. Benzannulated products were to have been achieved by using either α,β-unsaturated carbene complexes as acceptors or the Baylis Hillman adducts derived from these complexes (Scheme 26).

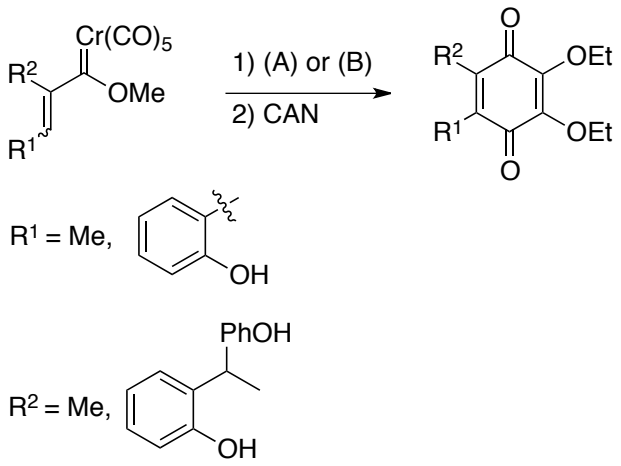

Scheme 26: Routes to proposed benzannulated product

The approach suggested by Hutchinson[63] was to add 0.15 mmol of the metal complex to 0.3 mmol of an (unsymmetrical) alkyne (optimal ratio), resulting in yields as high as 91%. The solvent of choice was nBu_2O but for this study Et_2O was used as it also gave favorable yields according to Hutchinson and coworkers.[124] The reaction was to be carried out in a sealed vessel at a set temperature of 130°C for 300 seconds followed by an oxidative work up using ceric ammonium nitrate (CAN).

Due to safety concerns it was decided not to use a sealed vessel for this reaction due our microwave not being a high pressure controlled microwave. It was decided to conduct the reaction under a positive pressure of carbon monoxide attached to a reflux condenser over a round bottomed flask within the microwave reactor cavity. Due to the limited success in preparing the Baylis Hillman precursors needed for this reaction it was decided to use only the aryl derived α,β-unsaturated carbene complexes as substrates since they proved more stable with regards to storage and purification in addition to being easier to prepare.

The reaction set-up did not allow for efficient temperature modulation to 130°C due to the low boiling point of the solvent. It was then decided to try a range of higher boiling solvents in an attempt to raise the temperature high enough for the reaction to take place (Table 6). In all cases where microwave heating was used the temperature of the solution could not be raised above 80°C and even after increasing the reaction time four-fold in the microwave reactor, no product was obtained. Using conventional methods

benzannulation takes place at reflux at 66°C.[63] Even though it was possible to raise the temperature sufficiently high (around 66°C), again none of the desired product was isolated (Table 7).

Table 6: Solvents used in Dötz Benzannulation reaction reported in literature

Solvent	Boiling Point/	Temperature achieved/
Et_2	**34**	34
THF	**66**	66
Toluene	**110**	80
Ethylene glycol monoethylether	**134**	80

It was decided that due to the system not being a closed vessel reaction, no product would be obtainable using the microwave as suggested by the Hutchinson.[63] So the microwave heating was replaced by conventional heating and the reaction was repeated using toluene at 100°C. The reaction still yielded a quantitative amount of reduced ceric ammonium nitrate (Table7), but no quinones.

Table 7: Dötz Benzannulation using condensation products

59	α,β-unsaturated system	Yield (%) Conventional	R	Expected Product
a	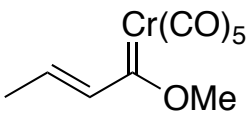 **57a**	trace	CH	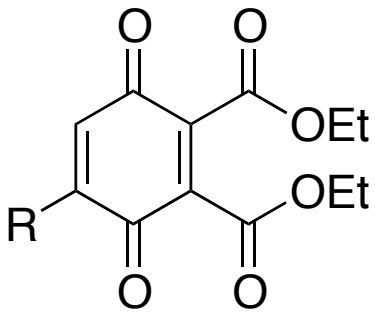
c	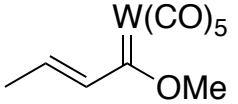 **57f**	-	CH	

**based on crude mass*
- no product observed

It was thought that the large symmetrical alkyne used and the bulky aryl side groups of the α,β-unsaturated complex may cause sufficient steric hindrance to prevent the formation of the benzannulated product. The low availability of CO to the reaction was also suggested as a possible cause for the reaction not proceeding. CO was supplied via three balloons after flushing the system out with CO. Figure 15 shows the result of benzannulation using conventional heating. In both cases there is a marked absence of any aromatic systems as well as no signals to indicate the formation of the expected benzannulation product. There is also no evidence for the formation the possible decomposition product expected (hydroquinone). This suggested that due to over heating the reaction most likely did not occur.

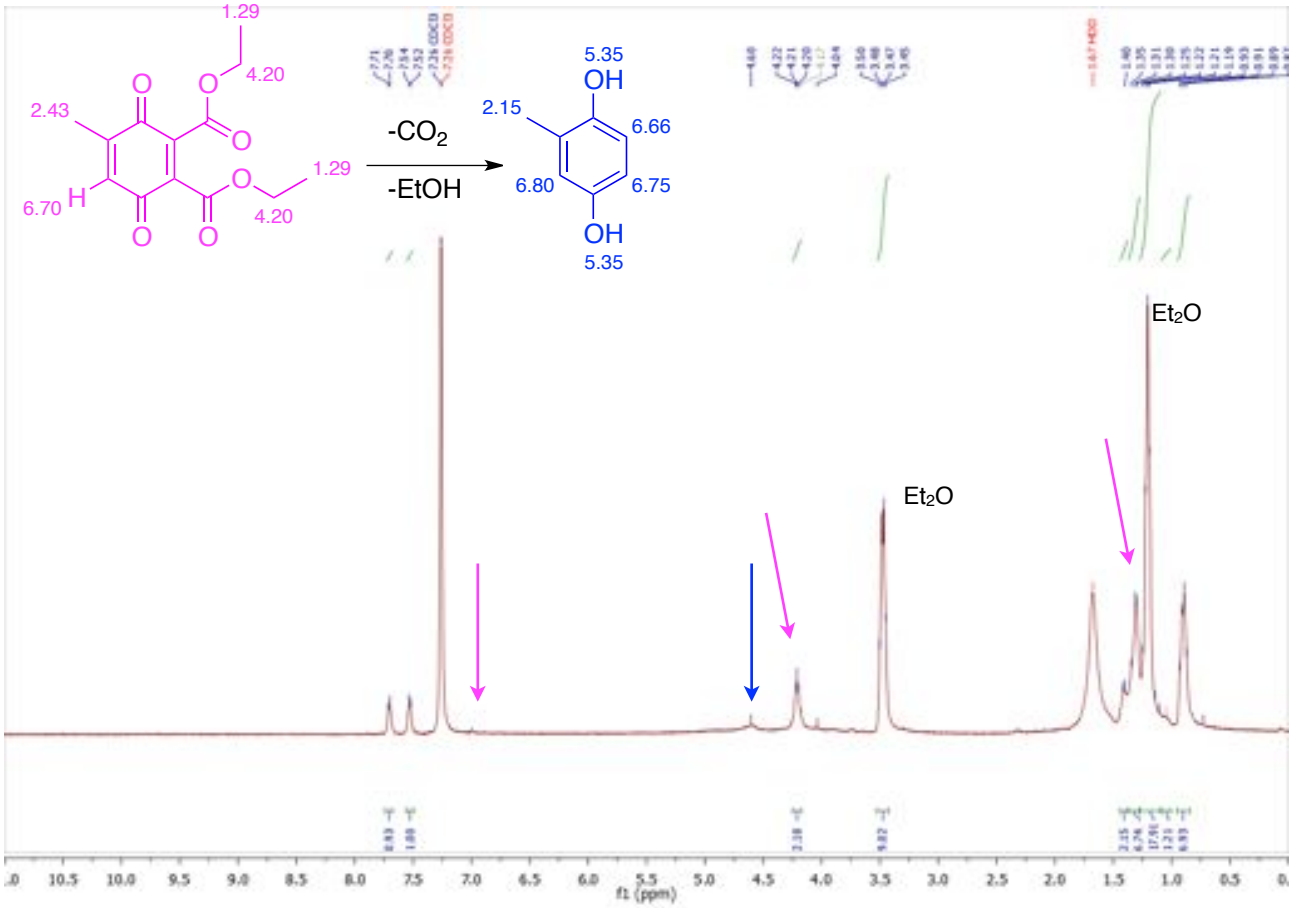

Figure 15: ^{1}H NMR spectrum (600MHz, C_6D_6) of 59a (magenta) indicating possible quinone formation (blue)

2.5 Exploring spectroscopic data of selected carbenes as a function of electron density

2.5.1 T_1 relaxation times of selected carbenes

Signals in the region of 300-400 ppm in the ^{13}C NMR spectrum are considered diagnostic of the successful synthesis of a Fischer carbene. Typically, when running a standard ^{13}C acquisition, these carbenes yielded spectra with poor signal strength including occasionally inverted signals (Figure 16). Due to carbene complexes being brightly colored, observation of a color change was also used to confirm the success of the reaction when the ^{13}C NMR spectra were inconclusive. In order to improve the quality of spectra we decided to increase the relaxation delay interval between transients (D1 on Bruker Topspin software) in order to allow the system to relax completely to equilibrium since slow relaxation was thought to be the cause of the initial poor spectra.

The default D1 used in our lab for a ^{13}C experiment is 2 seconds. We guessed that 3 seconds might be enough time to allow for relaxation of the nuclei following a 30^o pulse. This was increased to 5 seconds and then 9 seconds. In all cases the best resolution was seen with 3 seconds as the longer delays didn't have significant improvement in signal-to-noise to warrant the extra time needed to run the ^{13}C experiments. Changing D1 to 3 seconds significantly improved the signals around the 200-240 ppm range and the

diagnostic carbene signal at around 360 ppm could then be easily identified (Figure 16). The absence of the carbons associated with the methyl and methoxy moieties remained a concern. If present these signals were broad and had very low intensity.

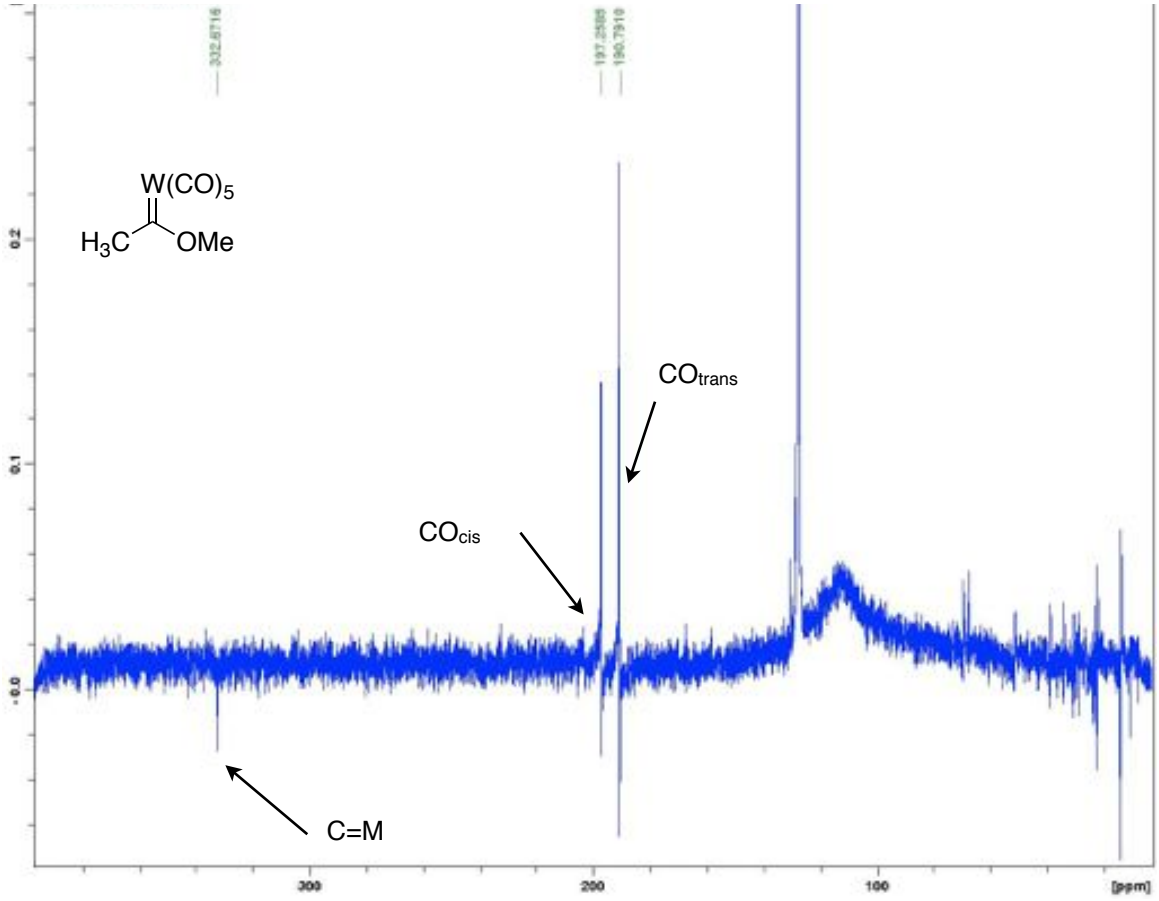

Figure 16: 100MHz ^{13}C NMR spectrum of simple tungsten carbene showing poorly phased carbonyl signals and inverted carbene signals due to inappropriate relaxation delays

In order to gain valuable information from our NMR experiments and begin to understand the dynamics causing the low resolution and inverted signals observed in our spectra, T_1 measurements were considered necessary.

Spin lattice relaxation time T_1 represents the "lifetime" of the process that returns the magnetization back to the Boltzman equilibrium distribution along the +Z axis. The most common T_1 relaxation techniques to measure this parameter include Inversion Recovery (IRFT), Progressive Saturation (PSFT) and Saturating Comb.[130] After a delay of $1xT_1$, about 60% of the magnetization is recovered along the +Z axis. This means that in order to recover 99% of the magnetization, a longer delay of $5xT_1$ is necessary. Nuclei with spin ½ and low magnetogyric ratio have relatively long relaxation times compared to nuclei with spin > ½ that have short relaxation times.

The spin lattice relaxation time governs the optimum time interval between two transients. Intervals shorter than $5xT_1$ decrease the accuracy of the experiment. When using an interval shorter than $5xT_1$ the pulse width must be adjusted to accommodate the reduced duration of the relaxation process to obtain the best

sensitivity for each nucleus in the NMR experiment based on the Ernst angle (Table 8). Since we were using a 30^{o} pulse, it should have been adequate to use a relaxation delay of 1xT_1, assuming our T_1 values were short (4-10sec).

Table 8: Optimised Pulse angles for different relaxation times.[95]

Relaxation time (sec)	Ernst Angle (in degrees)
100 (very slow T	8
10	25
4	33
2	53
1	68
0.4	86
0.1 (rapid T	90

In a typical inversion recovery sequence a spin in equilibrium is subjected to a 180° pulse, the sum magnetization M_o is inverted with respect to the direction of the external field - becoming antiparallel to the main magnetic field. Following the inversion, the magnetization starts to recover towards its equilibrium state, the rate of recovery being inversely proportional to T_1. If, after a certain delay time, the inversion time T*i*, we subject the system to a 90° pulse, the actual magnetization M_z(T*i*) will become observable in the x'-y' plane as an FID. By applying a range of different delay times, the time dependence of magnetization can be studied in detail. After a delay time T*i* of approximately 5 × T_1, the magnetization is fully restored to its equilibrium state.

This 180°-90° pulse sequence is called an inversion-recovery sequence (Figure 17). The return to equilibrium can be expressed mathematically as $M_z(T_i) = M_z(0)\ [1 - 2 \times \exp(-T_i / T_1)]$.[64]

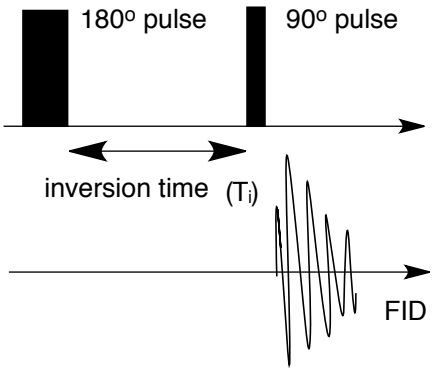

Figure 17: Inversion recovery sequence.

Due to the fact that carbenes decompose relatively quickly, T_1 experiments did give some cause for concern especially since the optimal relaxation delay is 5xT_1. It can been seen just how long these experiments can

run for if you were to assume values over 50 seconds (5x50 per scan)! At least 100 scans are required to obtain reasonable signal to noise ratio. A long delay time results in a predicament in that the compound would slowly decompose in the NMR tube even after precautions such as filling an air tight NMR tube with Ar. Consequently, abridged inversion recovery NMR experiments were carried out on the ^{13}C nuclei of both **56a** and **56d** carbenes in an attempt to establish the parameters needed to acquire an optimal ^{13}C NMR. The procedure for the inversion recovery method was obtained following guidelines found in the Bruker Avance NMR User's Manual. The results of these experiments are seen in Table 9.

Table 9: Longitudinal relaxation time

Metal	δ (ppm)	T_1 (sec)*
Chromium	359	2.1
	223	2.8
	216	2.3
	68	10
	50	9
Tungsten	333	2.9
	204	8.0
	198	3.1
	70	-
	52	-

**calculations according to Topspin software*

The initial estimate of a three second interval for the relaxation delay was close to the Topspin estimate for T*i* for the signals above 200 ppm. The signals below 100 ppm couldn't be detected when using a D1=3sec and this was confirmed by the calculated estimates of the relaxation delay being much longer. These delays do not make sense when thinking about the time delay needed to relax a metal bound carbon nucleus in comparison to a simple proton bound nucleus which according to our calculations has a longer delay time.

There are several relaxation mechanisms that govern the return to equilibrium (Table 10). With the exception of scalar coupling, all of the mechanisms involve the magnetogyric ratio of the nucleus. Relaxation mechanisms are distinguished by various factors including: strength of interaction, isotopic variation (in identifying a dipolar mechanism), field dependence (CSA and quadrupole mechanisms) and temperature dependence.

Table 10: Spin relaxation time (T_1) relaxation mechanisms

Interaction	Range of interaction (Hz)	Parameters which affect this interaction
Dipolar coupling	10^4	abundance of magnetically active nuclei size of the magnetogyric ratio
Quadrupolar coupling	10^6	size of quadrupolar coupling constant electric field gradient at the nucleus
Paramagnetic	10^7	concentration of paramagnetic species
Scalar coupling	10 - 10	size of the scalar coupling constants
Chemical Shift Anisotropy (CSA)	10 - 10	size of the chemical shift anisotropy symmetry at the nuclear site

Dipole-dipole interactions are seen as a through-space relaxation mechanism, and are particularly important for molecules containing protons, since protons are abundant nuclei with a large magnetogyric ratio. Dipolar coupling depends on the orientation/distance between the interacting nuclei, and on molecular motion. This results in protonated carbons relaxing more rapidly compared to quaternary carbons.[131] This mechanism seems less likely to dominate in the system in question.

Proton relaxation is dominated by dipolar relaxation. Relaxation of X-H (hetero-nuclei directly attached to proton) is also usually dominated by dipolar relaxation due to the short distance between the nuclei and due to the fact that proton has a large magnetogyric-ratio. If a proton is replaced by deuterium, resulting in an X-D bond, the X-nuclei relax more slowly than in the corresponding X-H compound due to the reduced dipole-dipole relaxation. Studying these relaxation times can tell us whether a given chemical environment is in a rigid portion of the molecule or in a flexible part of the molecule. There is also dipole relaxation resulting from the electron magnetic moment, as well as transfer of unpaired electron density to a relaxing nucleus. This is probably more relevant in our case.[131]

Chemical Shift Anisotropy occurs as a result of the chemical shift being dependent on the orientation of the molecule in the magnetic field. This effect is very well known in solid state NMR where it is responsible for the wide line widths observed in these samples. However, in solution, CSA is normally averaged out by molecular tumbling. The modulation of the shielding as a result of molecular motion can provide a relaxation mechanism in the absence of any other mechanisms. This mechanism is highly field dependent and can be an important relaxation mechanism for nuclei with large chemical shift scale such as the chromium and tungsten based carbenes we are working with.[131]

Paramagnetic Relaxation is a result of molecular motion in the electric field due to an unpaired electron spin. Cr(0) is not paramagnetic but a Cr(VI) decomposition product may lead to the presence of paramagnetic species.

The main relaxation mechanisms likely in systems such as the Fischer carbenes in this study would be due to CSA, dipolar coupling and paramagnetic relaxation with the decomposition product providing

paramagnetic species. Chemical shift of a nucleus is a function of the orientation of the molecule in the magnetic field.[131] The CSA effect is most apparent in the ^{1}H NMR and clearly observed in the methyl Fischer carbene **56a** where a substantial downfield shift of 1.22 ppm was observed for the OMe and a 1.55 ppm downfield shift for the Cr=C-Me protons where these differences were recorded at 600 MHz (14.1 Tesla) and compared to readings at 400 MHz (9.4 Tesla). This is strong evidence to support CSA as a predominant relaxation mechanism due to the relationship between increasing magnetic field strength and the corresponding downfield proton shift. This trend is also seen in the ^{13}C NMR of **56d** showing a downfield shift of the carbene carbon from 387 ppm (100 MHz) to 395 (150 MHz).

A simple first-order treatment of the inversion recovery data (Figure 18) suggested that there was a single major mechanism for relaxation. There seemed to be a linear relationship in the low value estimates for T_1 (15 seconds and below). The outlier, where D1 was estimated at 50 seconds, skewed the data and makes the most sense if additional relaxation mechanisms are considered. Due to the vast increase in time needed to run a T_1 experiment where the estimates for D1 are over 100 seconds, this would mean that these sensitive carbenes would have already decomposed by the time inversion recovery experiments finished. A different method for resolving this issue needs to be looked at if future work is to be done in this area.

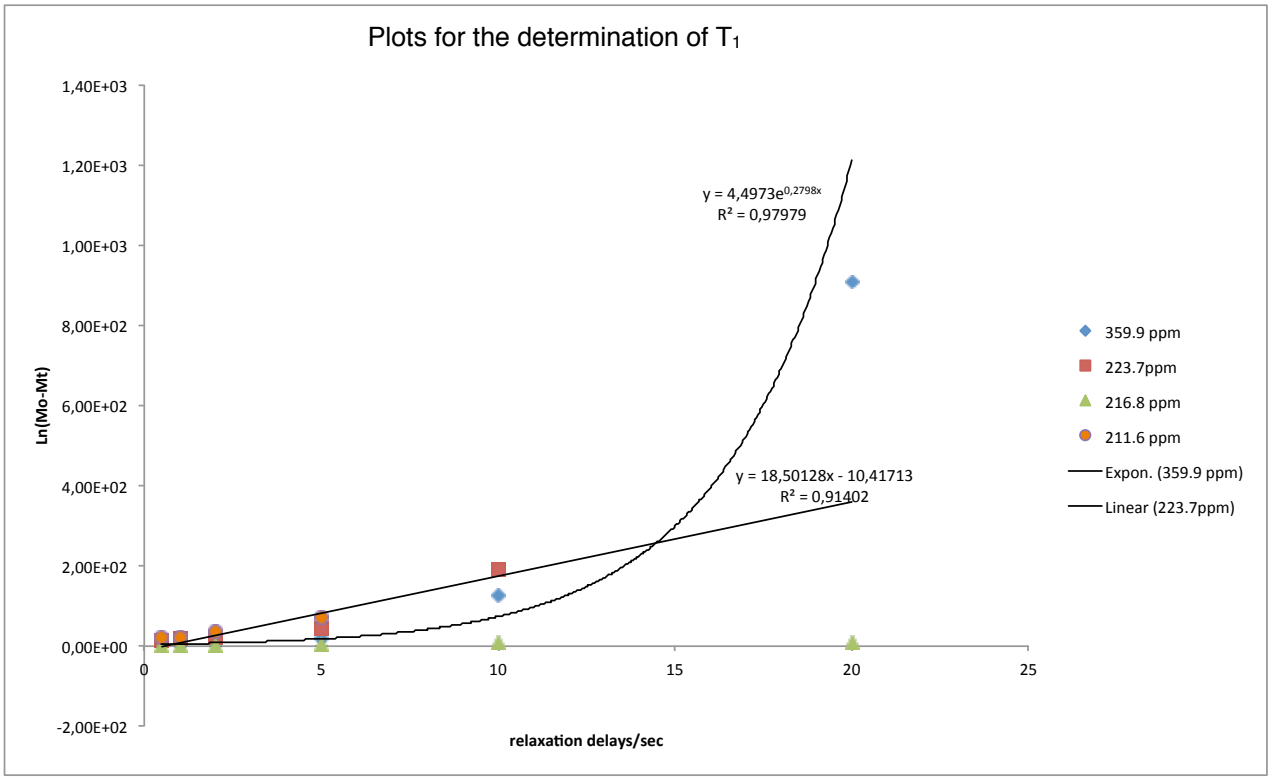

Figure 18: Inversion recovery experiments of Fischer carbenes (56a, 56d) to determine T_1

2.5.2 Exploring chemical shifts and IR correlation of carbene complexes

In work carried out in 1973, George Bonder demonstrated a linear correlation between chemical shifts and carbonyl stretching frequencies in the pentacarbonylchromium and pentacarbonyltungsten carbene complexes.[112] Work done by Vergamini and Matwiyoff[113] showed the same relationship in rhodium-carbonyl complexes. This sparked a need for a more complete understanding of the implications of this correlation.

Bonder explained that the carbonyl force constant increases with an increase in the carbonyl σ-donor ability, based on molecular orbital calculations done by Fenske and coworkers.[38] The results showed that the carbonyl σ-orbital involved in dative bonding to the transition metal had a negative overlap population such that the dominant electron density from the orbital strengthens the C-O σ-bond. Fenske also found that a decrease in transition metal to carbonyl π back-donation also decreases the electron density in the carbonyl π* orbital. Because the molecular orbital is said to be predominantly carbon in character this means that there is a decrease in the electron density on the carbon resulting in an increase in the strength of the C-O bond strength in the carbene moiety, (C_7-O_{14} in Table 11).

Darensbourg[130], Fenske[38] and Bonder's[112] explanations are consistent with several experimental observations leading to the idea that the ^{13}C NMR carbonyl chemical shifts are dominated by dependence on electron density at the carbonyl carbon. A net de-shielding of the carbonyl resonance should be observed with increasing stretching force constants within a series of closely related derivatives. This statement is borne out in the case of the simple Cr and W carbenes prepared in this study. The asymmetric C≡O stretching frequencies (at 1900 and 1872 cm^{-1}) correspond to ^{13}C chemical shifts at 223 ppm and 204 ppm respectively for the *cis* carbonyls.

Chemical shift data alone can also reveal some further features of the Fischer carbenes. One of these features is the relationship between electron density and the chemical shift data and the consequences this has for chemical reactions. The most important factors influencing chemical shifts in NMR are electron density, electronegativity of neighboring groups and anisotropically induced magnetic field effects. In the case of electron density, electrons "shield" the carbon nucleus from the applied magnetic field and this means that less energy is necessary to excite the carbon nucleus from one spin state to another and therefore its chemical shift comes at a lower frequency than it would otherwise. For example, the carbon atom in a carbonyl group has a relatively low electron density around it, and thus is relatively "de-shielded" and consequently has a higher chemical shift than most other types of carbons.

When comparing the actual NMR chemical shifts found for two simple chromium and tungsten carbenes with their calculated electron density using NBO (natural bond orbital) calculations a correlation could be observed. Appendix 3A(i)-(iii) shows graphically the electron density results of the simple methylmethoxy carbenes with metal centers Cr, Mo, W, while Table 11 compares this data to chemical shifts found experimentally. Mo carbenes were not synthesized in this project and therefore experimental chemical shift data is only seen for Cr and W. From the data it is clear that the reason why chromium carbenes have higher chemical shifts is due to the total electron density, as calculated by the NBO studies, as having a lower overall electron density at the carbene carbon center when compared to that of tungsten. For the carbene carbon the change is almost 0.15 units, (with a difference in chemical shift of 30 ppm) while for the carbonyl carbons it is only 0.07 units (with a related change in chemical shift of 20 ppm)

Table 11: Calculated NBO and chemical shift data for Cr, Mo and W carbenes

Metal	Atom	R^1		R^1		R^1		Structure
		NBO	δ_C	NBO	δ_C	NBO	δ_C	
Cr	$C_{7(carbene)}$	0.253	359.8	0.254	360	0.226	358.5	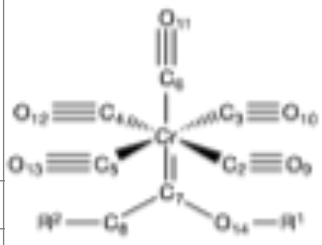
	$C_{2(cis)}$	0.336	216.8	0.378	216.0	0.368	217.0	
	$C_{3(cis)}$	0.383		0.388		0.324		
	$C_{4(cis)}$	0.425		0.375		0.294		
	$C_{5(cis)}$	0.388		0.329		0.326		
	$C_{6(trans)}$	0.344	223.6	0.342	223.0	0.294	223.9	
	CH	-0.490	49.3	-0.489	*a*	0.488	48.5	
	O-CH	-0.211	66.9	‡	‡	‡	‡	
Mo	$C_{7(carbene)}$	0.402	352.2	0.403	*c*	0.404	*c*	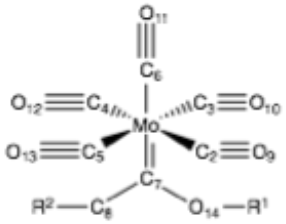
	$C_{2(cis)}$	0.721	213.3	0.721	*c*	0.720	*c*	
	$C_{3(cis)}$	0.727		0.727	*c*	0.686	*c*	
	$C_{4(cis)}$	0.724		0.724	*c*	0.731	*c*	
	$C_{5(cis)}$	0.676		0.676	*c*	0.730	*c*	
	$C_{6(trans)}$	0.657	205.7	0.656	*c*	0.657	*c*	
	CH	-0.731	50.1	-0.730	*c*	-0.728	*c*	
	O-CH	-0.350	69.4	‡	‡	‡	‡	
W	$C_{7(carbene)}$	0.107	332.7	0.046	*c*	0.003	*c*	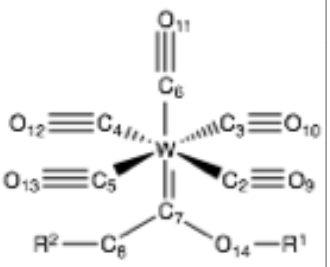
	$C_{2(cis)}$	0.263	197.9	0.234	*c*	0.231	*c*	
	$C_{3(cis)}$	0.212		0.221	*c*	0.282	*c*	
	$C_{4(cis)}$	0.256		0.228	*c*	0.258	*c*	
	$C_{5(cis)}$	0.293		0.208	*c*	0.204	*c*	
	$C_{6(trans)}$	0.266	203.5	0.257	*c*	0.249	*c*	
	CH	-0.477	51.6	-0.479	*c*	-0.474	*c*	
	O-CH	-0.207	69.7	‡	‡	‡	‡	

‡ not applicable to the molecule
a not detected in spectrum possibly due to poor signal to noise ratio
b literature value available (not synthesized in this study)[122]
c No literature value available (not synthesized in this study)

When considering this, based on only the NBO calculations done on the Mo carbene and the periodic trend of Mo, one would expect the corresponding carbene carbon shift for the Mo based complex to be in the region of 345 ppm, due to the small difference in electron occupancy between the NBO calculations of tungsten and chromium carbenes (0.146 units). Even though the Mo carbene carbon has a higher overall electron occupancy compared to both the Cr and W carbene carbons and does not fit the periodic trend in this regard.

From our data, there is a relationship seen between shielding and its effects on the chemical shift of the carbene. Further computational work was then carried out looking at substituents on the carbene and how they affect the electron density on the carbene carbon and hence its chemical shift. Figure 19 shows a

graphical representation of Cr and W carbenes with various side chains. It can be concluded that the electron density around the carbene carbon is significantly affected by the nature of the transition metal bound to the carbene carbon with Cr having the lowest electron density on the carbene carbon followed by Mo and then W.

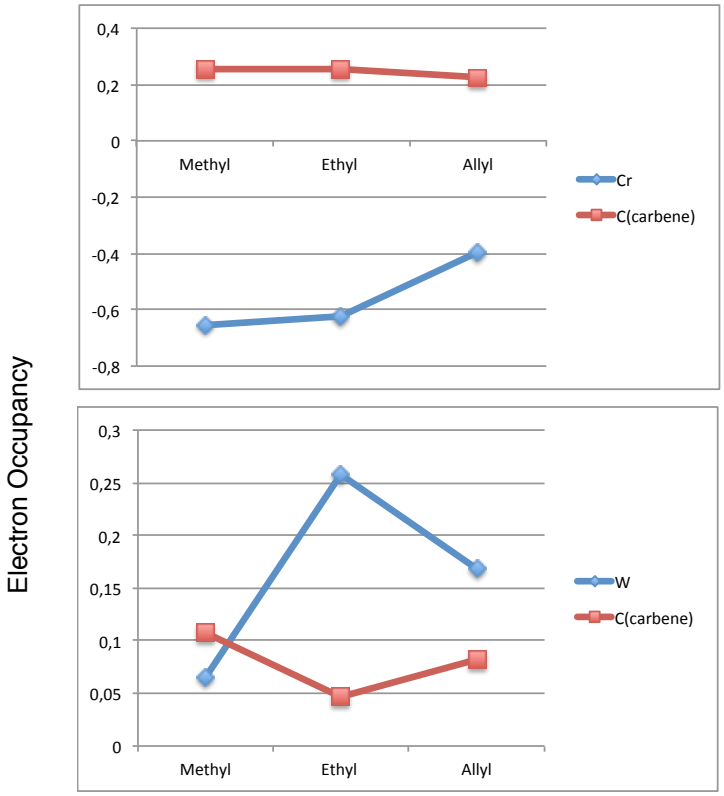

Figure 19: NBO calculations showing how electron occupancy on Cr and W carbene carbons changes with increase in side chain length.

In the case of the chromium carbenes there isn't a substantial difference in the calculated electron density (NBO) but there are indications that a growing side chain on the O-R^1 moiety seems to cause a slight increase in the electron density on the carbene carbon (Figure 19). This relationship is not as evident in the W or Mo carbenes though. It can also be seen that different side chains don't affect electron density around the carbonyls attached to the metal (Table 11). The *trans* carbonyl does, however, seem to have slightly higher overall electron occupancy compared to the *cis* carbonyls. This is corroborated by an upfield change in chemical shift of 5 ppm for the *trans* CO. Figure 20 highlights the electron occupancy difference in two methylmethoxy chromium and tungsten Fischer carbenes. There is a large difference in electronegativity between the chromium and the tungsten metal centers (0.71 units). The chromium methylmethoxy carbene has a highly electronegative metal center and a maximum electron occupancy of 0.253 at the carbene carbon as calculated by NBO calculations. This is double that of the corresponding tungsten methylmethoxy carbene (0.107) and accounts for the chemical shift difference seen experimentally, with the chromium carbene resonating around 359 ppm and the tungsten carbene almost 30 ppm upfield at 332 ppm. The lower electron occupancy of the chromium carbene in comparison to the tungsten carbene has the effect of a lower shielding effect resulting in the downfield change in chemical shift.

Molecular modeling studies were carried out on a set of chromium, molybdenum and tungsten Fischer carbenes (Appendix 3Ai-iii). Calculations were carried out using density functional theory (DFT) by using the Becke's three-parameter exchange functional in conjunction with the Lee-Yang-Parr correlation functional (B3LYP)[68, 123] level of theory as implemented in GAUSSIAN 03 suite of programs.[71] The basis set 6-31G(d)[115,116] was assigned for the atoms C, H and O, while the effective core potentials basis set was assigned by LANL2DZ[70,124] for the metals. A summary of the bond lengths obtained from the optimized chromium Fischer carbene is shown in Table 12 (the complete data set for Cr, Mo and W carbenes can be found in Appendix 1A).

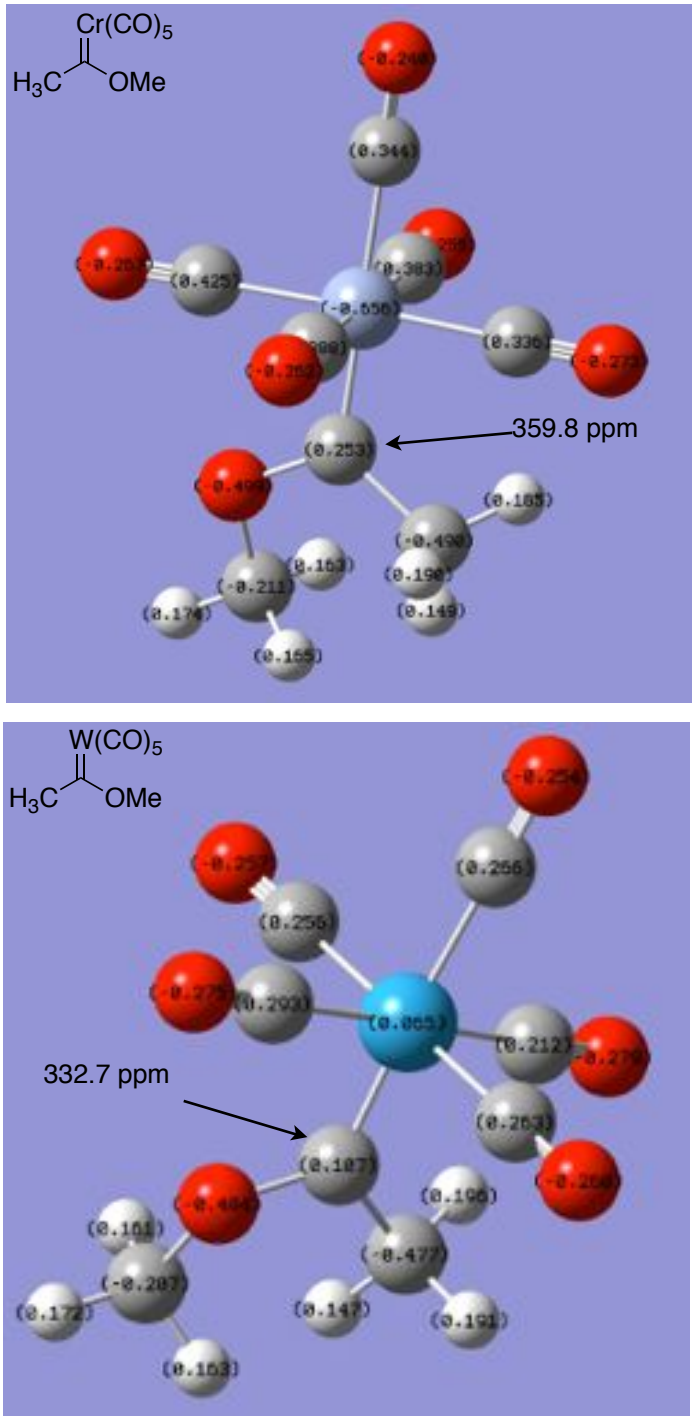

Figure 20: Electron occupancy comparison (NBO) between Cr and W methylmethoxy carbene complexes

Table 12: Theoretical bond lengths (NBO) in selected chromium Fischer carbenes

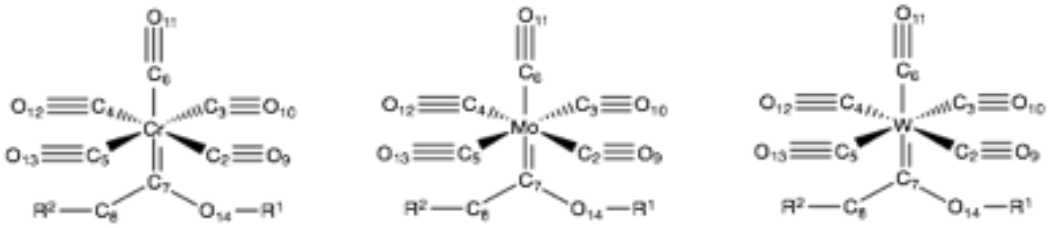

Chromium Fischer carbenes					Molybdenum Fischer carbenes				Tungsten Fischer carbenes			
Bond	Bond Length (Å)				Bond Length (Å)				Bond Length (Å)			
	R^2=Me											
#	R^1	R^1	R^1	Δr	R^1	R^1	R^1	Δr	R^1	R^1	R^1	Δr
M - $C_{7(carbene)}$	2.01006	2.01452	2.01478	0.00472	2.14826	2.15781	2.15222	0.00396	2.15592	2.16801	2.16089	0.00497
M - C	1.8914	1.89073	1.89099		2.0469	2.04697	2.04646		2.55525	2.05517	2.05477	
M - C	1.89129	1.89003	1.88982	-0.00147	2.05270	2.04966	2.05115	-0.00155	2.06389	2.05934	2.06192	-0.00197
C_7	1.51037	1.51099	1.51112		1.50989	1.51073	1.51073		1.50998	1.15110	1.51078	
C_7	1.35137	1.34783	1.34770	-0.00367	1.35480	1.35110	1.35156	-0.00324	1.35167	1.34730	1.34812	-0.00355
$C_{2\ ave}$	1.17246	1.17270	1.17472		1.17465	1.17497	1.17484		1.17304	1.17246	1.1727	
C_5 $O_{13(trans)}$	1.17313	1.17341	1.17344		1.17556	1.17601	1.17584		1.17356	1.17406	1.17387	

Δr calculated as bond length(Allyl)- bond length(Me) for selected bonds

It was observed that the C_7-O_{14} bond is shorter by at least 0.35 Å in the presence of a metal $M(CO)_5$ compared to that of an ester (with oxygen replacing the metal hexacarbonyl moiety) which has a calculated bond length of 1.43. This indicates that this bond becomes stronger in carbenes. The carbene is a strong σ-donor but the metal is a weak π-donor (back donor). As a result, C_7 becomes electron deficient and the charge compensation comes from the alkoxy oxygen lone pairs as a π-bond, which consequently decreases the C_7-O_{14} bond length. This pattern observed is in agreement with previous DFT studies and crystallographic data obtained for known Fischer carbenes.[125,126]

There is little to no change for the Cr=C carbene bond length in all the compounds modeled when changing the methoxy group as the π-donor to other alkoxy groups (Appendix 1A). This is similar to the effect observed in the ^{13}C NMR with the chemical shift showing only a slight difference between the compounds.

By understanding bond lengths of the calculated carbenes it was thought that it would be possible to estimate the effect of the various substituents on the carbene carbon as well as the level of back donation that these substituents provide. Studies by Sola *et al.* have concluded that for a Fischer carbene system the general trend is that back donation from the carbene center is proportional to the Cr-CO_{trans} distance and inversely proportional to the Cr=$C_{carbene}$ and C-O_{trans} distances.[112] Back donation is an important factor in the stabilization of the electron deficient carbene carbon center. In order to assess the average back donation in

the carbenes studied, the difference between the largest values (allyl) and the lowest values (methyl) in each metal series for the bond lengths M-CO_{trans} and M=$C_{carbene}$ were calculated as Δr and summarised in Table 12. A positive value for Δr shows that there has been an overall lengthening in the bond as is evident for the the values of M-CO_{trans}. A negative value would show the corresponding shortening of the bond as is evident for the M=$C_{carbene}$ bond length difference increasing slightly from Cr to Mo and then W having the largest positive difference. It can then be concluded that there is an inverse relationship between Cr=$C_{carbene}$ and C-O_{trans} bond length distances, as expected. The positive Δr for the Cr=C bond corresponds to an increase in back donation. In all the carbenes modelled the greatest amount of back donation can therefore be seen in tungsten carbenes followed by chromium then molybdenum carbenes. Since back donation is key to the stabilization of the carbene carbon it can be better understood why tungsten carbenes have a better bench top stability and higher yield than that of chromium, and in the case of molybdenum it can understood why additional ligands are needed to increase stability.

2.5.3 IR spectra

Calculated vibrational spectra were obtained from the computational analysis of a set of standard chromium and tungsten carbenes (**56a**, **56d** Figure 21, 22). Computed IR frequency data were visualized using IR Plotter 1.0, which removed lines with intensities (Int) equal to zero. The frequencies were rounded and the intensities were then normalized. This gives a realistic IR spectrum correlating with what would be seen experimentally. The calculated IR frequencies, recalculated frequencies and experimental IR frequencies (where synthesized) are recorded in Appendix 2A. In both cases, for the tungsten and chromium carbenes, calculated IR matched very closely to the experimental IR frequencies. Figures 21-22 show the mid IR region with the broad carbonyl vibrations of the pentacarbonyl moiety in the region 2032-1893 cm^{-1} as well as a carbene carbon metal (C=Cr) bend near 650 cm^{-1}. The far IR spectrum was not measured experimentally but calculated as having the Cr-C stretches of the carbonyls around 489 cm^{-1}. Work done by Meyer[70] showed these to be found experimentally at 471 cm^{-1}, a close match to what we calculated. The Cr-C bend was calculated as being at 166 cm^{-1} and observed experimentally by Meyer as being at 175 cm^{-1}.

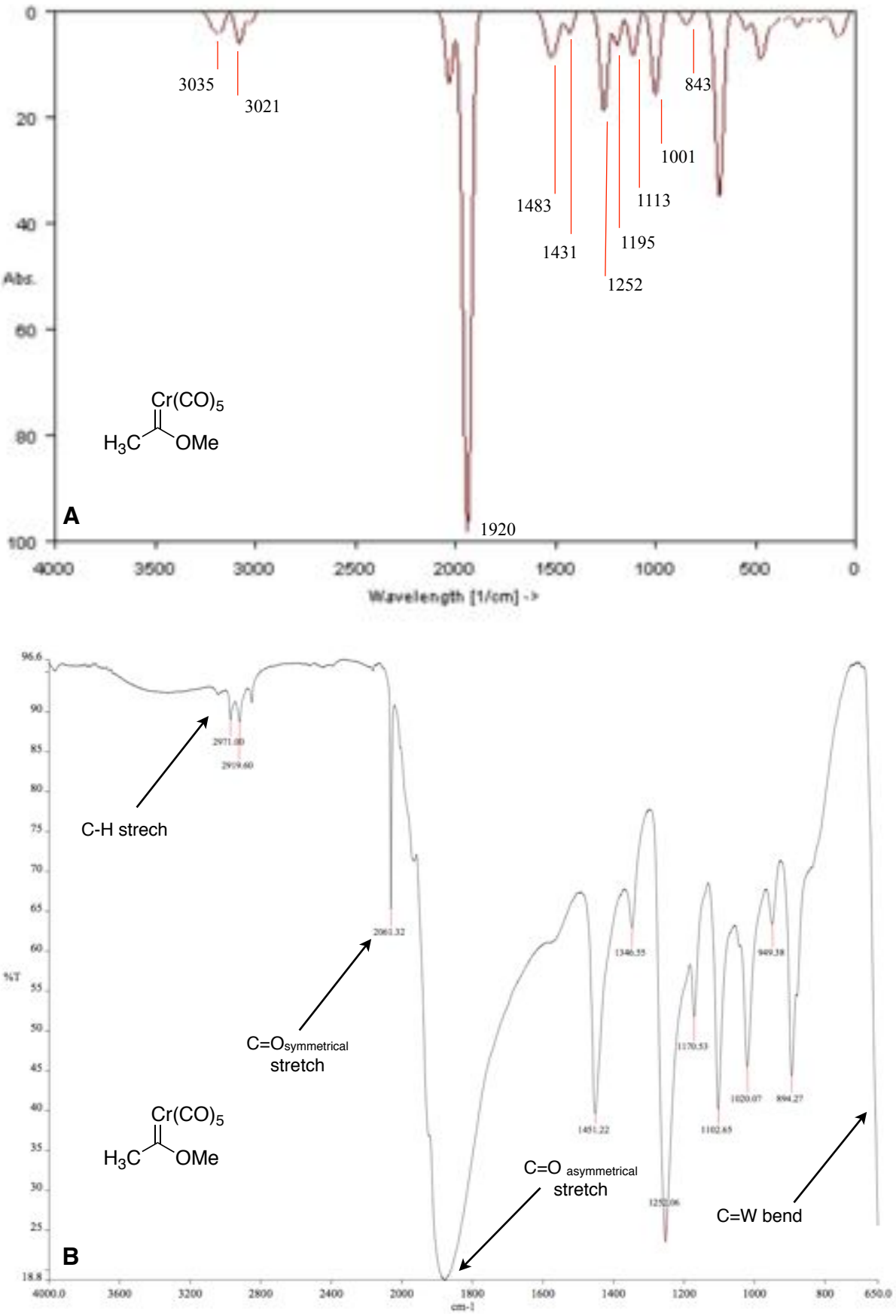

Figure 21: Comparison of theoretical (A) and experimental IR (B) frequencies for 56a

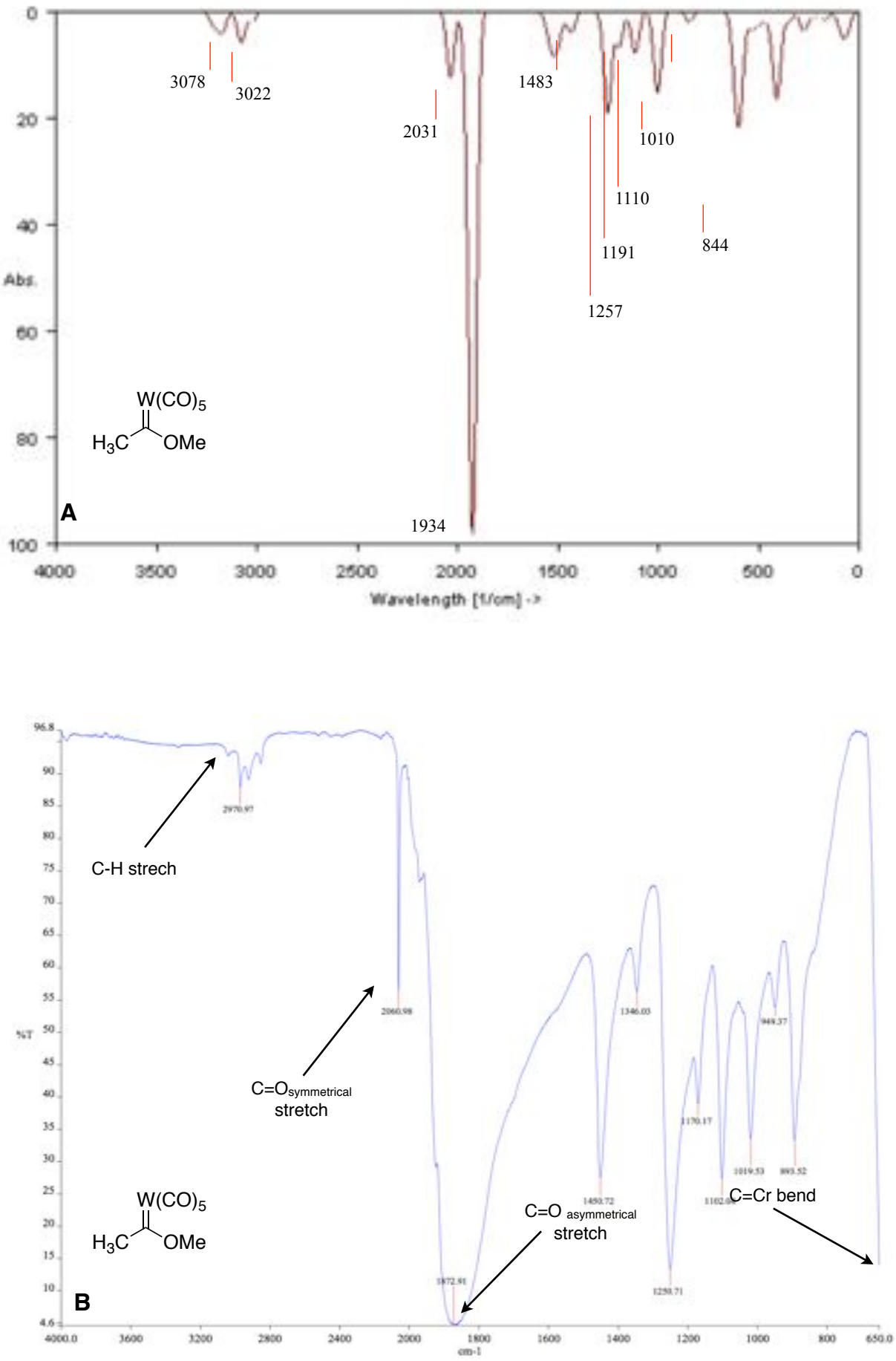

Figure 22: Comparison of theoretical (A) and experimental (B) IR frequencies for 56d

Figure 22B shows the mid IR region with the broad carbonyl vibrations of the pentacarbonyl moiety in the region 2032-1893 cm^{-1} as well as a carbene carbon to metal (C=Cr) bend near 650 cm^{-1}. The far-IR spectrum was not measured experimentally but was calculated as having Cr-C stretches of the metal carbonyls around 489 cm^{-1}. The Cr-C bend of all Cr-C≡O was calculated as being at 166 cm^{-1}. Calculated values for IR were consistently slightly higher than the expected values and this difference can be attributed to the calculations been done in the gas phase, not taking intermolecular effects into account.[71]

2.6 Computational studies carried out on α,β-unsaturated complexes and the effect of substituents on the carbene center

Molecular modeling studies were carried out on a set of chromium, molybdenum and tungsten Fischer carbenes condensed with acetaldehyde, propionaldehyde, benzaldehyde and salicylaldehyde (Table 13). As with the methyl carbenes, calculations were carried out using density functional theory (DFT) by using Becke's three-parameter exchange functional in conjunction with the Lee-Yang-Parr correlation functional (B3LYP)[68,123] level of theory as implemented in GAUSSIAN 03[71] suite of programs. The basis set 6-31G(d)[123] was assigned for the atoms C, H and O, while the effective core potentials basis set was assigned by LANL2DZ[70,124] for the metals. This allowed for accurate calculations and an appropriate level of approximation of the metal orbitals to maximize computer resources for this study. A list of the optimised structures for all complexes modelled are summarised in Table 13 and the results of the modeling for each specific compound and can be seen in detail in Appendix 3B. NBO analysis was used in order to better understand the electron distribution within the complexes to explore the bonding in these complexes, in particular how varying side chains affect bond strength as well as bench top stability. The specific bond lengths for each compound modelled are summarized in Appendix 3B. The frequencies for each compound were calculated using GAUSSIAN 03 and are summarized in Appendix 2B (i)-(iii).

Table 13: Summary of α,β-unsaturated complexes modelled

Metal (M)	Cr	Mo	W	Structure
R_1	R_2			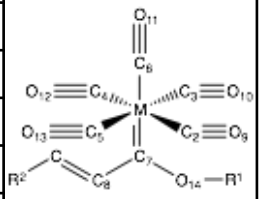
	R_2			
	R_2			
	R_2			
R_1	R_2			
	R_2			
	R_2			
	R_2			
R_1	R_2			
	R_2			
	R_2			
	R_2			

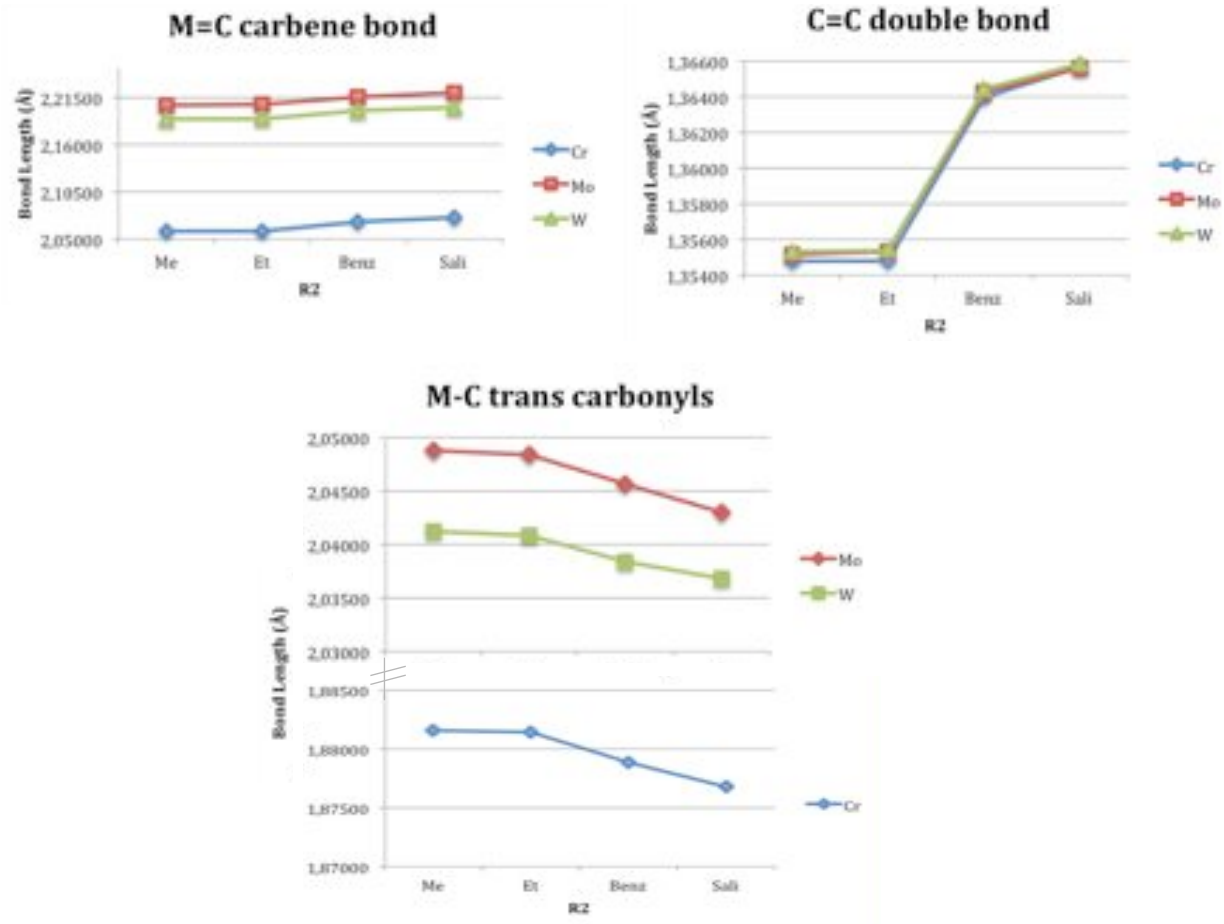

Figure 23: Bond trends in condensation products

In all optimized structures the M=$C_{carbene}$ bond length increases when moving from an alkyl side chain to a larger aryl group (Figure 23) regardless of M. There seems to be a correlation between this increase in bond length and benchtop stability where the alkyl substituted condensation reactions failed to produce products in most cases compared to the aryl substituted products. The chemistry suggests that this may be due to the increased conjugation rather than simple steric constraints, so that extended conjugation results in a more stable complex. The *trans* carbonyl (M-C) seems to shorten with an increase in substituent aromaticity indicating a movement of electrons towards the M-$C_{carbene}$ bond which correlates well with the increase in the M-C bond lengths of the *trans* carbonyls. There is also a marked difference in the C=C bond length between the aryl and alkyl substituents, where the bond length seems to increase suggesting a movement of electrons out of the bond, as the aromaticity of the substituent increases. All bond lengths correlate to behavior corresponding to highly conjugated systems, even more so when adding an aryl group as the delocalization is extended allowing for movement of electrons throughout the conjugated systems as described.

The *cis* carbonyls are the only ones that seem to remain unchanged with variation of the substituents. There is also a small change in bond length between carbenes on different metals with Cr having the longest overall M-$C_{carbene}$ bond length followed by Mo and then W in periodic order.

2.7 Computational studies - investigating the structure of Baylis Hillman Adducts

The Baylis Hillman reaction is known best for allowing highly substituted products to be synthesized in a one pot reaction in relatively good yields. A Baylis Hillman reaction incorporating Fischer carbenes into the substrates would theoretically help speed up the Baylis Hillman reaction due to the highly electrophilic carbon centre created and also supply favourable highly substituted products as candidates for a benzannulation reaction. Experimentally, this proved very difficult. In one reaction attempt **57a** distinguishing Baylis Hillman signals were detected but isolation was not possible due to ease of oxidation.

We therefore considered three of the prospective compounds (Table 14) and modeled them to see if their conformations and connectivity were stable by comparing calculated bond lengths and literature - or whether they might be prone to facile decomposition. We also expected to see the steric factors involved in using bulkier aldehydes for the reaction. Calculations were carried out as before. All optimized models can be found in Appendix 3B.

Table 14: Theoretical bond length of Cr=C bond

BH Adduct	Bond Length
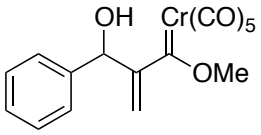	2.03582
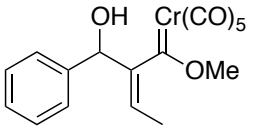	2.04277
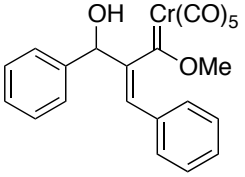	2.04277

In a study by Makanjee,[124] molecular bonding orbitals in a chromium Baylis Hillman system were calculated. It was found that the carbonyl group closest to the the hydroxyl is able to donate electrons from its HOMO to a suitably vacant LUMO. As noted in section 2.3.1 oxidation of these compounds readily took place even under a reducing atmosphere and thus Makanjee's calculation supports our argument that the Baylis Hillman products could be experiencing intramolecular oxidation due to the formation of a six membered cyclic ester system following abstraction of the proton on the hydroxyl (Scheme 26).

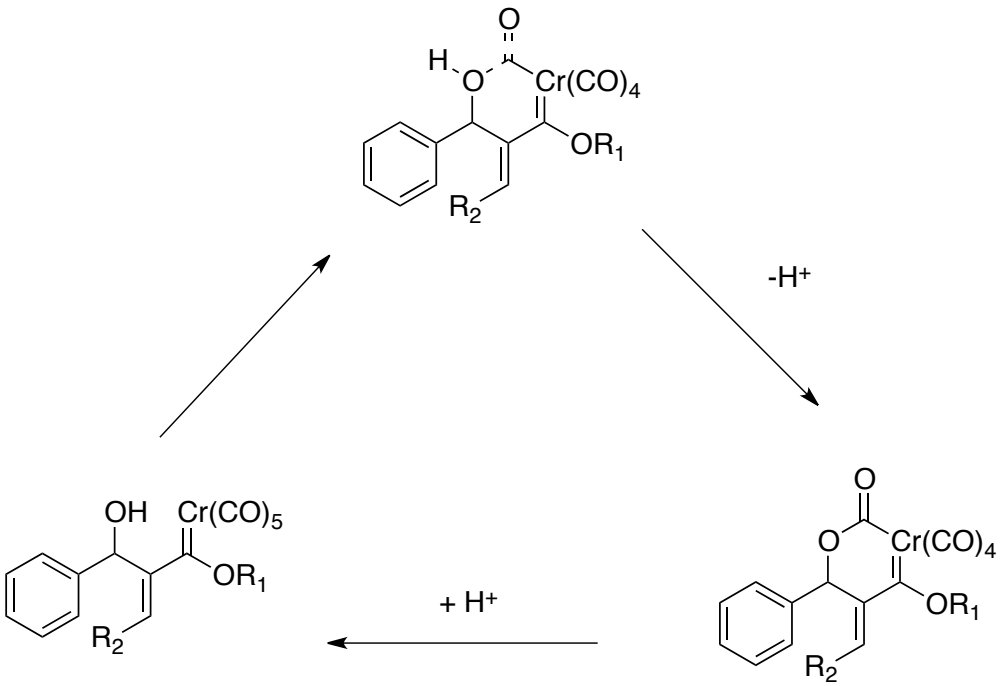

Scheme 26: Formation of cyclic ester upon deprotonation

It was thought that if the modeling showed an increase in the bond length between the metal fragment and the carbene carbon then this suggested a tendency for the metals to be easily removed from the complex thereby promoting oxidation. Although it can be seen that there is an increase in the bond length, a literature search indicated that extended bond lengths are common in Fischer carbene systems because a delocalized system is set up from the Cr=C to the OMe group and the bond lengths calculated in our study are similar to various carbene systems.[116] It was thought that this understanding could apply to all our unsaturated Fischer derived compounds as they haven't yet been reported in literature discussing modeling.

Since the synthesis of Baylis Hillman adducts could not be achieved it was decided to explore these compounds using computer based studies. NBO studies were completed for the compounds listed in Table 15, and presented in their entirety in Appendix 3C including the stabilities and conformations of these Baylis Hillman adducts.

Table 15: Summary of Baylis Hillman adducts studied (NBO)

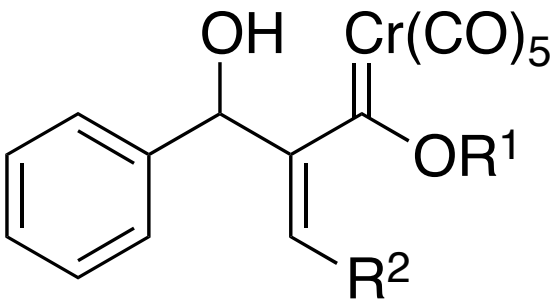

R^1	R^2
OMe	Me
	Phenyl
	2-(HO)Ph
OEt	Me
	Phenyl
	2-(HO)Ph
OAllyl	Me
	Phenyl
	2-(HO)Ph

The results of the computational studies indicated the need to examine the reaction route from the preliminary chromium Fischer carbene to the aldol condensation product and viability of the pathway ending with the Baylis Hillman adduct to evaluate the stability of these complexes. It became apparent that electron density is redistributed somewhat in forming the condensation product from the initial carbene in order to increase overall stability. This increase in stability is also seen by the increased electron density around the carbene carbon indicating a strengthening of the carbene bond. Bench top stability was noted as being higher in the case of the carbene precursor and decreasing when moving to the condensation product and then the Baylis Hillman product. The *cis* carbonyls seem to be the least affected but do show an overall increase in electron occupancy when moving through the process, indicating a slight strengthening of the bond to the metal. This could be primarily due to the geometry of these carbonyls not being directly affected by the changes in conjugation of the system as it is extended through the molecule from the initial carbene to the condensation adduct and finally the Baylis Hillman products. The *trans* carbonyls experience an opposite effect to that of their *cis* counterparts with a slight decrease in the electron occupancy suggesting a weakening of the metal bond and therefore a slight increase in bond length. This could be due to electrons delocalizing into the conjugated system.

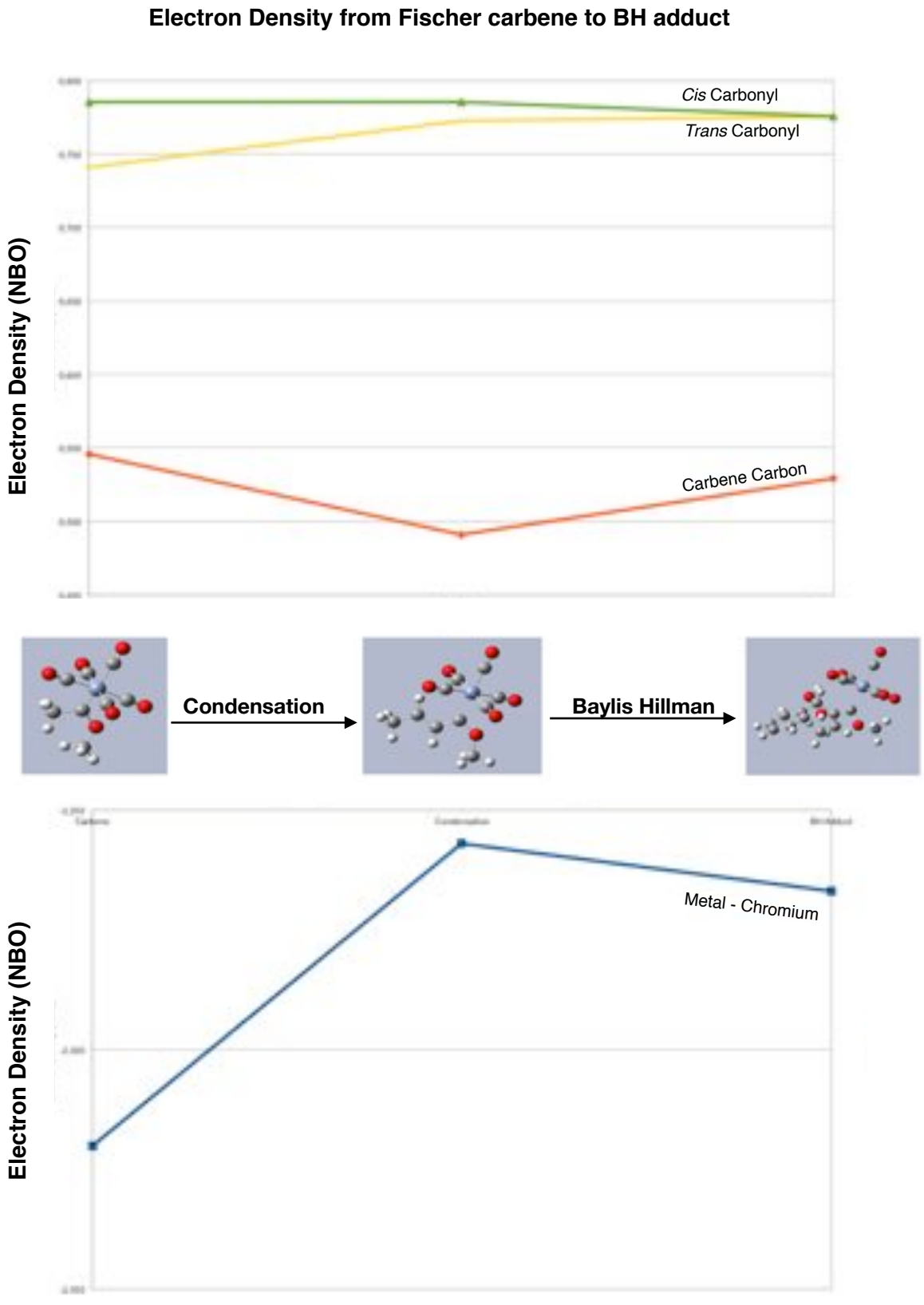

Figure 24: Reaction scheme based on NBO electron density calculations

2.8 Investigating the structure of Benzannulated Products

Molecular models of benzannulated products were calculated using Gaussian with the same parameters as described in the previous section. All optimized models can be found in Appendix 4A. Figure 25 shows two of the modeled Dötz benzannulation products before and after CAN oxidation. Before oxidation there is strong hydrogen bonding that takes place between the hydroxyl groups which results in the phenyl ring being rotated out of the plane to compensate for the steric factors present. This behavior was observed in all the models computed.

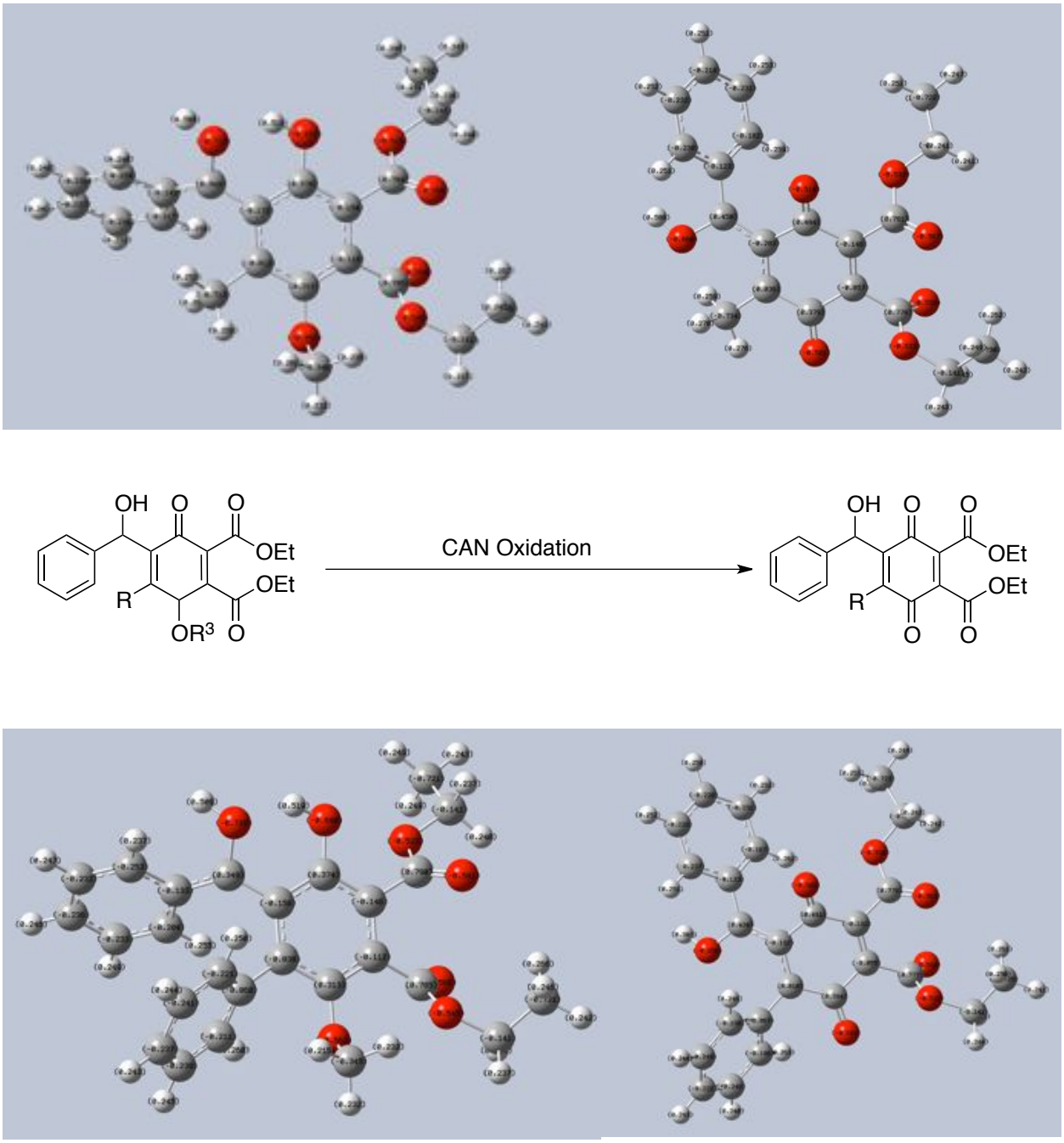

Figure 28: Benzannulated products before and after CAN oxidation based on NBO electron density

A summary of the compounds that were modelled are listed in the Table 16 and seen in detail in Appendix 4A. After CAN oxidation there is no hydrogen bonding interaction observed and the phenyl ring rotates out away from the quinone to alleviate the strain and a new conjugation is set up through the molecule. It was also observed that lengthening the side chain at R^2 did not have a substantial effect on the electron density distribution in these molecules.

Table 16: Summary of Benzannulated Baylis Hillman products modelled

Entry	R^1	R^2	Structure	Oxidized
1	H	Me	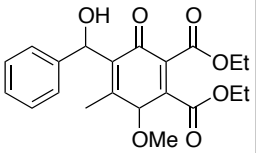	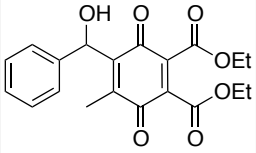
2	Ph	Me	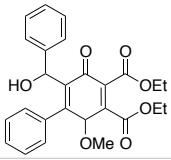	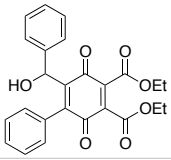
3	2-HO-Ph	Me	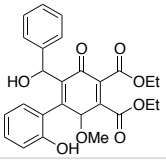	
4	H	OEt	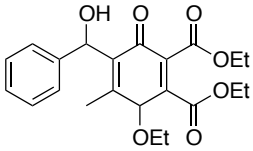	
5	Ph	OEt	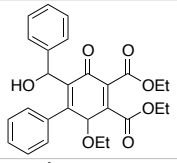	
6	2-HO-Ph	OEt	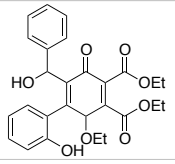	
7	H	OAllyl	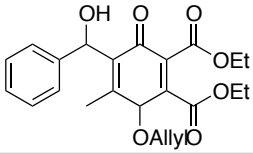	
8	Ph	OAllyl	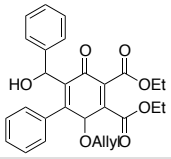	
9	2-HO-Ph	OAllyl	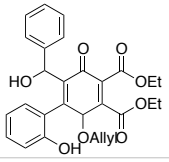	

2.9 Conclusions

Four Fischer carbenes were synthesized via nucleophilic addition of MeLi to chromium and tungsten hexacarbonyl at low temperatures followed by alkylation to give the desired Fischer chromium and tungsten methyl alkoxy carbenes. Derivatives of the chromium Fischer carbenes were explored using different substituents at the α-alkoxy fragment. Characterization of these complexes was by means of ^{13}C NMR, ^{1}H NMR, and IR and by comparison with literature precedent. *In silico* studies were carried out looking at the effect of substituents on the carbene bond.

Synthesis of α,β-unsaturated complexes was achieved via the aldol condensation route and proved challenging when using enolizable aldehydes, although the use of two aryl aldehydes resulted in the successful preparation of two α,β-unsaturated complexes. Difficulty in the purification of these complexes hindered their full characterization. Computational studies looked at the effect of substituents on the system as well as variation of the metal from Cr, to Mo and W. Molecular modelling identified that tungsten had the highest degree of back donation followed by chromium and then molybdenum. The higher stability of the tungsten carbenes vs chromium was evident in the higher yields and bench top stability for the tungsten Fischer carbenes in relation to their chromium counterparts.

T_1 calculations indicated that longer relaxation delays must be beneficial. However, these would result in longer acquisition times for carbene complexes with short lifetimes!

Synthesis of Baylis Hillman adducts using α,β-unsaturated complexes as acceptors was unsuccessful due to the ease of product (and substrate) oxidation. One potential product was obtained in its crude form although purification was not possible due to oxidation. Computational studies suggested that the oxygen negatively impacts the stability of these Fischer carbene derived Baylis Hillman adducts promoting intramolecular oxidation of the metal due to interaction of the Baylis Hillman OH and the metal carbonyl moiety.

Both the α,β-unsaturated complexes and Baylis Hillman adducts were considered to be candidates to undergo Dötz benzannulation methodology. The use of the α,β-unsaturated complexes in this reaction was tested in wide range of solvents both in the microwave and in conventional heating conditions. These methods proved ineffective and computational studies on these compounds were an attempt to understand their stability and configuration. It was found that the ligands surrounding the metal moiety attached to the carbene carbon had an influence on both the stability and reactivity of these Fischer carbene derived organometallic complexes. The comparison of the relative bond lengths showed that the M=C bond length is related to back donation which relates directly to the stability of the complexes *in silico* and on the bench top.

Future work will include an

a) Optimized T_1 experiment in order to gain valuable information regarding the nature of the relaxation processes which are occurring.This experiment should also focus on methods and techniques that will

reduce the acquisition time to ensure that decomposition of the product is limited.

b) Additional work needs to be done in synthetic methods to promote the formation of the Baylis Hillman adducts. The development of B-H methodology remains an important goal in exploring novel scaffolds that can be used in the development of heterocyclic and carbocyclic species with medicinal potential. This could include the use of various protecting groups on the hydroxyl group to prevent possible intramolecular oxidation.

3 Experimental

A student wished to make some potassium hydroxide solution (aqueous) and decided to throw a large lump of potassium into a bucket of water. The professor observed what was about to happen, out of the corner of his eye and hurried towards the student. After confirming this was what the student was intending to do, asked first to stir the water in the bucket for five minutes before adding the potassium. The student was puzzled and ran after the professor to ask the purpose of this action. 'It will give me time to get away' said the professor --V. Rogers

3.1 General

All reagents were supplied by Aldrich® and used without further purification unless stated otherwise. Dry solvents were prepared using methods described by Perrin and Armarego.[99] Thus, THF and toluene were distilled from Na/benzophenone and collected over molecular sieves (4 Å) under N_2; DCM and pentane were refluxed with CaH_2 and distilled over molecular sieves (4 Å) under N_2. All dry solvents were stored over

molecular sieves under N_2 or Ar and handled under the same conditions; N_2 and Ar gas was supplied by Afrox and passed through Drierite® prior to use.

Normal phase thin layer chromatography (TLC) was performed on Merck silica gel 60 PF254 plates. Visualization on silica was achieved using either iodine vapor or UV light at 254 nm. Normal phase flash chromatography was performed using Merck silica gel 60 (particle size 0.040 – 0.063 mm).
NMR data was obtained using Bruker 400 MHz Avance and 600 MHz Avance II spectrometers at 303 K in the specified deuterated solvent. NMR spectra were generated and optimized using MestReC, MestReNova and Bruker Topspin software. All chemical shifts are given in ppm and coupling constants in Hz and spectra were calibrated on residual protonated solvent signals ($CDCl_3$: ^1H – 7.26 ppm; ^{13}C – 77.00 ppm; DMSO–d_6: ^1H – 2.50 ppm; ^{13}C – 39.51 ppm; D_2O: ^1H – 4.80 ppm; MeOH–d_4: ^1H – 3.35 ppm; ^{13}C – 49.15 ppm). Infrared spectral data was obtained on a Perkin–Elmer Spectrum 100 FT–IR and manipulated using Perkin–Elmer Spectrum v6.35 and Essential FTIR v1.50.252 software.

All reactions were conducted in oven-dried glassware under an atmosphere of Ar using standard Schlenk and vacuum techniques on a double manifold connected directly to the Ar source and a vacuum pump. Liquids were transferred using Ar–flushed disposable Norm–ject® syringes (without rubber plunger insert) and stainless steel needles.

General Procedure for the Filtration of Suspended Solids under Inert Gas
A Schlenk tube was connected to a scintered glass funnel (complete with Quickfit© joint below the scintered glass) and filled with molecular sieves (4 Å), celite and anhydrous magnesium sulphate then flushed through with Ar. The reaction mixture was transferred to the scintered funnel, either by connecting the reaction Schlenk tube to the Quickfit© joint above the scintered glass or simply by transfer with a syringe and needle.

General procedure for the removal of solvents under vacuum
Reaction mixtures were concentrated *in vacuo* by removing solvents via evaporation into one of the solvent traps, which was immersed in liquid N_2. Reaction vessels were evacuated under vigorous stirring and the tap was opened very slowly and carefully to avoid bumping.

General procedure for degassing solvents
Due to the possible sensitivity of the metal complexes to oxygen and/or moisture, deuterated solvents were degassed to avoid decomposition during NMR experiments. Activated molecular sieves (4Å) were added to a Schlenk tube/flask (no more than a quarter–filled) and deuterated solvent added to *ca* 2/3 above the level of the sieves. The flask was stoppered and connected to the manifold, then immersed to above the solvent line in liquid nitrogen. When the solvent was completely frozen, the flask was removed and placed under vacuum until the solvent started to thaw. The flask was then flushed with Ar until all of the solvent had thawed. The procedure was repeated twice before the solvent was stored under Ar in the dark.

General procedure for microwave reactions

Microwave assisted reactions were performed in a CEM Discover single–mode microwave apparatus, producing controlled irradiation at 2450 MHz, using standard 10 mL septum sealed glass pressure vials. All reaction times described refer to hold times at the indicated temperature and not total irradiation times.

3.2 Synthesis of Alkyl-carbene complexes using chromium hexacarbonyl

3.2.1 Pentacarbonyl[methoxy(methyl)carbene]chromium(0) 56a[59]

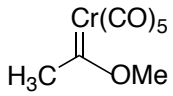

MeLi (12.00 ml) was added slowly to a solution of $Cr(CO)_6$ (4.10 g, 0.18 mol) in dry Et_2O (20 ml). The color changed from colorless to bright yellow to brown yellow when left to react for 15 min under argon at room temperature. The solvent was removed under reduced pressure and the residue taken up in degassed H_2O. The Meerwein salt Me_3OBF_4 (5.40 g, 0.077 mol) was then added to the solution and left to stir overnight at room temperature under argon. The reaction was complete when the color changed from yellow-brown to dull yellow. Work up was done by extracting the product in 3 x 15ml of degassed pentane. The pentane layers were combined and dried using $MgSO_4$ (anhydrous), filtered and the solvent evaporated *in vacuo* to give the product *pentacarbonyl[methoxy(methyl)carbene]chromium(0)* **56a**, as a yellow solid in a 68% yield. δ_H (600MHz, C_6D_6): 4.75 (3H, s, OCH_3), 2.99 (3H, s, $-CH_3$); δ_C (100MHz, C_6D_6): 359.1 (s, $C=Cr(CO)_5$), 216.8 and 211.6 (s, $Cr(CO)_5$), 69.7 (q, OCH_3), and 30.1 (q, CH_3) IR ν_{max}/cm^{-1} 2061, 1900, 1451 1252

3.2.2 Pentacarbonyl[ethoxy(methyl)carbene]chromium(0) 56b

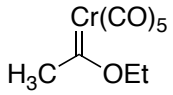

MeLi (12.00 ml) was added slowly to a solution of $Cr(CO)_6$ (4.00 g, 0.18 mol) in dry Et_2O (20 ml). The color changed from colorless to bright yellow to brown yellow when left to react for 15 min under argon at room temperature. The solvent was removed under reduced pressure and the residue taken up in degassed H_2O and DCM (20ml). Et_4NBr (0.40 g, 1.9 mol) was then added to the solution and the color changed from yellow-brown to dull yellow. Ethylbromide (2.7 ml, 0.036 mmol) was then added to the solution and left to stir overnight at room temperature under argon. The product was extracted into 3 x 15ml of dry DCM. The DCM layers were combined and dried using $MgSO_4$ (anhydrous), filtered and the solvent evaporated *in vacuo* to give the product *pentacarbonyl[ethoxy(methyl)carbene]chromium(0)* **56b**, as a yellow solid in a 65% yield. δ_H (400MHz, C_6D_6): 4.98 (2H, s, OCH_2), 2.91 (3H, s, $-CH_3$), 1.56 (3H, t, $-CH_3$) ; δ_C (100MHz, C_6D_6): 223.0 (s, CO_{trans}), 216.0 (s, CO_{cis}), 66.0 (t, OCH_2), 28.5 (q, $Cr=C-CH_3$), and 19.5 (q, $O-CH_2-\underline{CH_3}$)

3.2.3 Pentacarbonyl[allyloxy(methyl)carbene]chromium(0) 56c

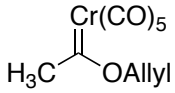

MeLi (12.00 ml) was added slowly to a solution of $Cr(CO)_6$ (4.00 g, 0.18 mol) in dry Et_2O (20 ml). The color changed from colorless to bright yellow to brown yellow when left to react for 15 min under argon at room temperature. The solvent was removed under reduced pressure and the residue taken up in degassed H_2O and DCM (20ml). Et_4NBr (0.3 g, 0.18 mmol) was then added to the solution and the color changed from yellow-brown to dull yellow. Allyliodide (3.0 ml, 0.04 mmol) was then added to the solution and left to stir overnight at room temperature under argon. Work up was done by extracting the product in 3 x 15ml of dry DCM. The DCM layers were combined and dried using $MgSO_4$ (anhydrous), filtered and the solvent evaporated *in vacuo* to give the product *pentacarbonyl[allyloxy(methyl)carbene]chromium(0)* **56c**, as a yellow solid in a 62% yield. δH (400MHz, C_6D_6): 5.51 (1H, m, CH), 4.94 (2H, d, OCH_2), 4.29 (2H, d, CH_2) and 2.33 (3H, s, CH_3) ; δC (100MHz, C_6D_6): 358.5 (s, Cr=C), 223.0 (s, CO_{trans}), 216.9 (s, CO_{cis}), 130.9 (d, CH), 119.8 (t, CH_2CH), 53.7 (t, OCH_2) and 30.4 (q, CH_3)

3.2.4 Pentacarbonyl[methoxy(methyl)carbene]tungsten(0) 56d

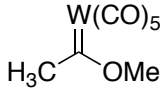

MeLi (0.01 ml) was added slowly to a solution of $W(CO)_6$ (0.18 g, 0.5 mmol) in dry Et_2O (5 ml). The color changed from colorless to bright yellow to brown yellow when left to react for 15 min under argon at room temperature. The solvent was removed under reduced pressure and the residue taken up in degassed H_2O. The Meerwein salt $MeOBF_4$ (0.044 g, 0.06 mmol) was then added to the solution and left to stir overnight at room temperature under argon. The reaction was complete when the color changed from yellow-brown to dull yellow. Work up was done by extracting the product in 3 x 15ml of degassed pentane. The pentane layers were combined and dried using $MgSO_4$ (anhydrous), filtered and the solvent evaporated in vacuo to give the product *pentacarbonyl[methoxy(methyl)carbene]tungsten(0)* **56d**, as a yellow solid in a 78% yield. δ_C (100MHz, C_6D_6): 332.6 (s, C=$Cr(CO)_5$), 203.5 and 197.4 (s, $Cr(CO)_5$), 69.7 (q,OCH_3), and 51.6 (q,CH_3). IR ν_{max}/cm^{-1} 2060, 1872, 1450, 1250

3.3 Condensation of Aldehydes with chromium carbene complexes

3.3.1 Pentacarbonyl[methoxy(ethylene)carbene]chromium(0) 57a

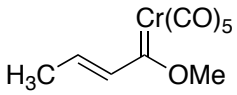

Acetaldehyde (0.4ml, 6.7 mmol) was added to a stirred solution of carbene **56a** (0.40g, 1.5mol) in dry Et_2O (20 ml), and then cooled to 0°C. DBU (0.1 ml) was added to the solution and the reaction left to stir for 1 hour at 0°C under argon. The color changed from yellow to brown yellow. The solvent was removed under reduced pressure and the residue taken up in degassed DCM (20 ml) and cooled again to 0°C. Methane sulfonylchloride (MsCl) (0.3 ml, 3.6 mmol) and triethyl amine (Et_3N) (0.5 ml, 3.6 mmol) were added to the solution and left to stir for 30 min under Ar, after which it was left to warm to room temperature overnight under argon. Removing the DCM under reduced pressure gave the product *pentacarbonyl-[ethylene(methyl)carbene]chromium(0)* **57a**, as a red-brown oil 60% yield. δ_H (400MHz, C_6D_6): 7.76 (1H, d, CH-CH_3), 7.03 (1H, d, CH-C=Cr), 2.19 (3H, s,CH_3); δ_C (100MHz, C_6D_6): 359.1 (s, C=Cr), 223.1 (CO_{trans}), 132.5 (d, CHC=Cr), 129.4 (d, CH_3CH), 67.5 (q, OCH_3) and 30.2 (q, CH_3CH)

3.3.2 Pentacarbonyl[methoxy(benzylene)carbene]chromium(0) 57c

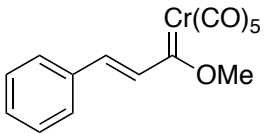

Benzaldehyde (5ml, 1.3 mmol) was added to a solution of **56a** (0.3 g, 1.2 mmol) in Et_2O. DBU (0.5 ml) was added and the reaction left to stir at 0°C for 2 h. The color changed from yellow to dark brown. The solvent was removed under reduced pressure and the residue taken up into degassed DCM. Et_3N (1ml, 1.2 mmol). and MsCl (0.4 ml, 5.6 mmol) were added to the solution and left to react at 0°C for 15 min under Ar. The solvent was evaporated under reduced pressure to yield a crude yellow-brown oil *pentacarbonyl-[methoxy(benzylene)carbene]chromium(0)* in a 30% yield. **57c**. δ_H (400MHz, C_6D_6): 7.93 - 7.58 (Ar-Hs), 6.50 (1H, s, CH-Ar), 6.46 (1H, s, CHC=Cr), 4.51 (3H, s, OCH_3); δ_C (100MHz, C_6D_6): 360.0 (s, C=Cr), 223.5 (s, CO_{trans}), 216.7 (s, CO_{cis}) 138.2 (s, CHC=Cr), 130.5 (s, CHAr), 129.0 - 127.0 (s, ArCs), and 60.5 (s, OCH_3)

3.3.3 Pentacarbonyl[methoxy(benzylene)carbene]chromium(0) 57d

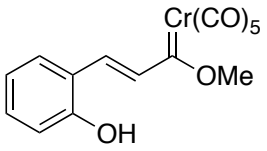

Salicylaldehyde (2-hydroxybenzaldehyde) (1.4 ml, 1.3 mmol) was added to a solution of **56a** (0.3 g, 1.18 mmol) in Et_2O. DBU (0.5ml) was added and the reaction left to stir at 0°C for 2 h. The color changed from yellow to dark brown. The solvent was removed under reduced pressure and the residue was taken up into degassed DCM. Et_3N (1 ml, 1182 mmol) and MsCl (0.4 ml, 5.6mmol) were added to the solution and left to react at 0°C for 15 min under Ar, solution turned deep purple. The solvent was evaporated under reduced pressure to yield a deep purple oil 10% yield **57d**.

Attempted Condensation of Aldehydes with chromium carbene complexes

3.3.4 Pentacarbonyl[methoxy(propylene)carbene]chromium(0) 57b

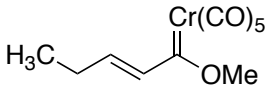

Propionaldehyde (0.08 ml, 11 mmol) was added to a stirred solution of carbene **56a** (0.19 g, 7.8 mmol) in dry Et_2O (5ml), and then cooled to 0°C. DBU (0.15 ml) was added to the solution and the reaction left to stir for 1 hour at 0°C under Ar. The color changed from yellow to brown yellow. The solvent was removed under reduced pressure and the residue picked up in degassed DCM (20 ml) and cooled again to 0°C. Methane sulfonylchloride (MsCl) (0.08 ml, 9.4 mmol) and triethyl amine (Et_3N) (0.13 ml, 9.4 mmol) were added to the solution and left to stir for 30min under Ar, after which if was left to warm to room temperature overnight under argon. Removing the DCM under reduced pressure gave a impure brown oil **57b**. δ_C (100MHz, C_6D_6): 361.0 (s, C=Cr), 216.6 (s, CO_{trans}), 211.7 (CO_{cis}), 132.2 (d, CHC=Cr), 53.0 (q, OCH_3) and 30.5 (CH_3CH_2)

3.3.5 Pentacarbonyl[methoxy(ethylene)carbene]tungsten(0) 57e

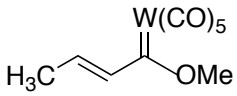

Acetaldehyde (0.4ml, 6.7 mmol) was added to a stirred solution of carbene **56d** (0.40 g, 1.5 mol) in dry Et_2O (20 ml), and then cooled to 0°C. DBU (0.1 ml) was added to the solution and the reaction left to stir for 1 h at 0°C under argon. The color changed from yellow to brown yellow. The solvent was removed under reduced pressure and the residue picked up in degassed DCM (20 ml) and cooled again to 0°C Methane sulfonylchloride (MsCl) (0.3 ml, 3.6 mmol) and triethyl amine (Et_3N) (0.5 ml, 3.6 mmol) were added to the solution and left to stir for 30min under Ar, after which it was left to warm to room temperature overnight under argon. Removing DCM under reduced pressure gave the product *pentacarbonyl-[ethylene(methyl)carbene]chromium(0)* **57e**, as a impure red-brown oil δ_C (100MHz, C_6D_6): 332.0 (s, C=Cr), 203.5 (CO_{trans}), 197.49 (CO_{trans}), 128.1(d, CH_3CH), 67.5 (q, OCH_3) and 30.0 (q, CH_3CH)

3.3.6 Pentacarbonyl[methoxy(benzylene)carbene]tungsten(0) 57f

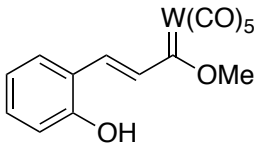

Salicylaldehyde (1.4 ml, 1.3 mmol) was added to a solution of **56d** (0.3 g, 1.2 mmol) in Et_2O. DBU (0.5ml) was added and the reaction left to stir at 0°C for 2 hours. The color changed from yellow to dark brown. The solvent was removed under reduced pressure and the residue taken up into degassed DCM. Et_3N (1 ml, 1.2 mmol). MsCl (0.5 ml, 5.6 mmol) was added to the solution and left to react at 0°C for 15 min under Ar. The solvent was evaporated under reducded pressure to yeild a deep purple oil *Pentacarbonyl-[methoxy(benzylene)carbene] tungsten(0)* **57f** 17%yield.. δ_H (400MHz, C_6D_6): 9.17 (1H, s, OH), 7.62 (1H, d, CH), 7.08 (1H, d, ArH), 6.93 (1H, t, ArH), 6.80 (1H, q, ArH), 6.43 (1H, t, CH); δ_C (100MHz, C_6D_6): 387.3 (s, $C=Cr(CO)_5$, 217.1 (CO_{trans}), 196.0 (CO_{cis}), 38.5 (q, OCH_3)

3.4 Coupling of α,β-unsaturated carbene complexes with aldehydes

3.4.1 (2-(hydroxy(phenyl)methyl)-1-methoxybut-2-en-1-ylidene) chromium hexacarbonyl 58a

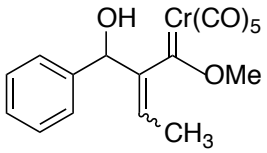

Conventional method

Benzaldehyde (0.4 ml, 3,7 mmol) was added to a stirred solution of **57a** (0.35 g, 1.2 mmol) in dry DCM (5ml). DBU (0.15 ml) was added to the solution and the reaction left to stir overnight, after which it was monitored by TLC for 3 days. The solvent was removed under reduced pressure and gave a crude yield of 8% as an impure dark brown oil. Crude NMR suggested the possible presence of the product but rapid decomposition hindered further analysis.

Microwave method

Benzaldehyde (0.4 ml, 3,7 mmol) was added to a stirred solution of **57a** (0.35g, 1.2mmol) in dry DCM (2 ml). DBU (0.15 ml) was added to the solution and irradiated at 25°C in 30 minute cycles. After four cycles the solvent was removed under reduced pressure and the residue was a dark brown oil. Crude NMR did not indicate the presence of the desired compound.

3.5 Benzannulation of α,β-unsaturated carbene complexes

3.5.1 Diethyl 4-methyl-3,6-dioxocyclohexa-1,4-diene-1,2-dicarboxylate 59a

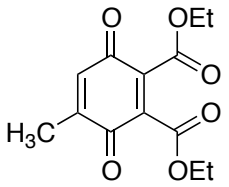

Condensation product **57a** (0.05 g, 0.18 mmol) was added to a solution of diethyl but-2-ynedioate (0.30 mmol) in Et_2O (3 ml). The reaction vessel was placed in a microwave reactor and a reflux condenser fitted with a rubber septum was attached. CO filled balloons provided a reducing atmosphere via the septum of the condenser. The reaction was irradiated for 300s. After automatic cooling the reaction mixture was poured into a solution of CAN (0.6 g, 1.1 mmol) in water (3 ml). The mixtures were then stirred for a further 20 minutes and extracted with diethyl ether (3x20 ml). The organic extracts were combined and the solvent removed via reduced pressure. ^1H NMR of the crude mixture was inconclusive.

4 References

1. Story attributed to Joseph Chatt by Basolo, F. “Mechanisms of Platinum Reactions.” In *Modern Coordination Chemistry*: The Legacy of Joseph Chatt. Leigh, G. J., Winterton, N., Eds. Royal Society of Chemistry: Cambridge, **2002**, pp. 326.

2. Herndon, J. W., *Coord. Chem. Rev.*, **2010**, *254:* 103-194.

3. de Frémont, P.; Marion, N.; Nolan, S. P., *Coord. Chem. Rev.*, **2009**, *253:* 862-892.

4. Dötz, K. H.; Stendel Jr., *J. Chem. Rev.*, **2009**, *109:* 3227-3274.

5. Butler, W. M.; Enemark, J. H.; Parks, J.; Balch, A. L., *Inorg. Chem.,* **1973**, *12:* 451-457.

6. Fischer, E. O.; Maasböl A., *Angew. Chem., Int. Ed,* **1964**, *3:* 580.

7. Special edition dedicated to carbene and carbyne complexes and their applications, *J. Organomet. Chem.*, **2001**, 617-618.

8. Bourissou, D.; Guerret, O.; Gabbai, F. P.; Bertrand, G., *Chem. Rev.,* **2000**, *100:* 39-92.

9. Wanzlick, H. W.; Schönherr, H. J., *Angew. Chem., Int. Ed***, 1968**, *7:* 141-142.

10. Arduengo, A. J.; Harlow, R. L.; Kline, M., *J. Am. Chem. Soc.,* **1991**, *113:* 361-363.

11. Fischer, E. O., *Angew. Chem.,* **1974,** *86:* 651.

12. Whittal, I.R.; McDonagh, A.M.; Humphrey, M.G.; Samoc, M., *Adv. Organomet. Chem.***, 1998**, 291.

13. Schrock, R. R., *J. Am. Chem. Soc.,* **1974**, *96:* 6796-6797.

14. Herndon, J.W., *Coord. Chem. Rev.,* **2000**, *237:* 206-207.

15. Schrock, R. R., *Chem. Rev.*, **2002**, *102:* 145-180.

16. Truscott, B. J.; Klein, R.; Kaye, P. T., *Tetrahedron Lett.,* **2010**, *51:* 5041-5043.

17. Tebbe, F. N.; Parshall, G. W.; Reddy, G. S., *J. Am. Chem Soc.*, **1978**, *100:* 3611-3613.

18. Petasis, N. A.; Bzowej, E. I., *J. Am. Chem. Soc.,* **1990**, *112:* 6392-6394.

19. Fischer, E. O.; Maasböl, A., Angew*. Chem. Int. Ed. Engl.,* **1964**, *645*.

20. Herndon, J. W*., Coord. Chem. Rev.,* **2000,** *237:* 206 – 207.

21. Hegedus, L.S., Transition Metals in the Synthesis of Complex Organic Molecules, University Science Books, Mill Valley, California **1994**.

23. de Meijere, H.; Schirmer, M.; Duetsch., *Angew. Chem. Int. Ed.,* **2000**, *39:* 22.

24. Barluenga, J; Florez, J; Fananas, J., *J. Organomet. Chem.*, **2001**, *5*, 624

25. Sierra, M.A; Hegedus, L.S., *J. Am. Chem. Soc.*, **1989**, *111:* 2335-2336

26. Wulff, W. D.; Bauta, W. E.; Kaesler, R. W.; Lankford, P. J.; Miller, R. A.; Murray, C. K.; Yang, D. C., *J. Am. Chem. Soc.*, **1990**, *112:* 3642.

27. Barluenga, J; Fernandez-Acebes, A.A; Trabanco, J; Florez, J., *J. Am. Chem. Soc.*, **1997**, *119:* 7591

28. Wulff, W.D., *Organometallics,* **1998,** *3116*.

29. Barluenga, J., *Pure Appl. Chem.,* **2002**, *8:* 1317-1325.

30. Dötz, K.H; Tomuschat, P., *Chem. Soc. Res.*, **1999**, *28:* 187.

31. Wulff, W. D. in Comprehensive Organic Synthesis, Trost, B. M.; Fleming, I., Eds . Pergamon: Oxford, **1991,** *5:* 1065.

32. Schrock, R.R., *Acc. Chem. Res.,* **1979**, *12:* 98.

33. Frenking, G.; Fröhlich, N., *Chem. Rev.,* **2000**, *100:* 717.

34. Frohlich, N.; Frenking G., *Phys. Organomet. Chem.,* **1999**, *2:* 173 .

35. Frenking, G.; Froehlich N., *Chem. Rev.,* **2000**, *100:* 717 .

36. Frenking, G.; Pidun U, *J., Chem. Soc. Dalton. Trans.*, **1997**, 1653 .

37. Jiang, W.; Fuertes, M. J.; Wulff, W. D*., Tetrahedron*, **2000**, *56:* 2183 .

38. Block, T. F.; Fenske R. F., *J. Organomet. Chem.*, **1977,** *139:* 235 .

39. Nakatsuji, H.; Ushio, J; Han, S; Yonezawa, T., *J. Am. Chem. Soc.,* **1983**, *105:* 426 .

40. Ushio, J.; Nakatsuji, H.; Yonezawa,T., *J. Am. Chem. Soc.,* **1984**, *106:* 5892.

41. Cases, M.; Frenking, G.; Duran, M.; Sola, M., *Organometallics,* **2002,** *21:* 4182.

42. Jacobsen, H.; Ziegler, T., *Organometallics,* **1995**, *14:* 224 .

43. Beste, A,.; Kramer, O.; Gerhard, A.; Frenking, G,. *Eur. J. Inorg. Chem.,* **1999**, 2037.

44. Vyboishchikov, S.F.; Frenking, G., *Chem. Eur. J.,* **1998**, *4:* 1428 .

45. Li, J.; Schreckenbach, G.; Ziegler, T., *J. Phys. Chem.,* **1994**, *98:* 4838 .

46. Dewar,M,J,S., *Bull. Soc. Chim. France*, **1951,** 71.

47. Chatt, J.; Duncanson, L. A., J. Chem. Soc., **1953**, 2939.

48. Spangler, D.; Wendoloski, J. J.; Dupuis, M.; Chen, M. M. L.; Schaefer, H. F., *J. Am. Chem. Soc.,* **1981**, *103:* 3985.

49. Amin, S. R.; Sarkar, A., *Organometallics,* **1995**, *14:* 547-550.

50. Fox, H. H.; Schofield, M. H.; Schrock, R. R., *Organometallics,* **1994**, *13:* 2804.

51. Schoeller, W. W.; Rozhenko, A. J. B.; Alijah, A., *J. Organomet. Chem.,* **2001**, *435:* 617-618.

52. Bernardi, F.; Bottoni, A.; Miscione, G. P*., Organometallics*, **2000**, *19:* 529.

53. Marquez, A.; Fernandez Sanz, J., *J. Am. Chem. Soc.,* **1992**, *114:* 1019.

54. Taylor, T. E.; Hall, M. B., *J. Am. Chem. Soc.,* **1984**, *106:* 1576.

55. Bader, R. F. W.; Laidig, K. E., *THEOCHEM.,* **1991**, *80:* 75.

56. Bader, R. F. W., *Acc. Chem. Res.,* **1985**, *18:* 9.

57. Dapprich, S.; Frenking, G., *J Phys Chem.*, **1995**, *99:* 9352.

58. Dötz, K. H.; Stendel Jr., *J., Chem. Rev.,* **2009,** *109:* 3227-3274.

59. Reed, A. E.; Curtiss, L. A.; Weinhold, F., *Chem. Rev.*, **1988**, *88:* 899.

60. Perdicchia, D.; Licandro, E.; Maiorana, S.; Vandoni, B.; Baldoli, C., *Org. Lett.,* **2002,** *4*: 827-830.

61. Aravind, A; George, S; Kumar,S., *Cem Cent J.*, **2012**, 1186-1752

62. Clayden, J.; Greeves, N.; Warren, St.; Wothers, P., Organic Chemistry., Oxford University Press, **2001**, p. 691. ISBN 978-0-19-850346-0.

63. Hutchinson, E.J; Kerr, W.J; Magennis, E.J., *Chem. Commun.*, **2002**, 2262-2263

64. Webb, S.; Flower, M. A., *Webb's Physics of Medicinal Imaging.*, Taylor & Francis Group, LLC. **2012,** p. 509. ISBN 978-0-7503-0573-0

65 Fürstner, A.; Mathes, C.; Lehmann, C. W., *J. Am. Chem. Soc.*, **1999**, 9453–9454

66. Lee, C. T; Yang, W. T.; Parr, R. G.,*Phys. Rev. B,* **1998**, *37:* 785

67. Petersson G.A.; Al-Laham M.A., *J. Chem. Phys.,* **1991**, *94:* 6081-90.

68. Dunning Jr. T.H.*, J. Chem. Phys.*, **1989**, *90*: 1007-23.

69. R.F, Fenske, *Pure Appl. Chem.,* **1971**, *27*: 61.

70. Meyer, A., Masters Thesis, Rhodes University, Department of Chemistry, **2011**

71. Frisch, M. J.; Frisch, G. W., *Gaussian 03 User's Reference*, Gaussian Inc., Wallingford, CT 06492, U.S.A. (info@gaussian.com).

72. Matsuyama, H.; Nakamura, T.; Masahiko, I., *J.Org.Chem.,* **2000**, *65*: 16

73. Lotz, S; Crause, C; Olivier, A.J; Liles, D.C; Gorls, H; Landman, M; Brzuidenhout, D.I., *Dalton Trans.*, **2009**, 697-710

74. Hutchinson, E.J; Kerr, W.J; Magennis, E.J., *Chem. Commun.*, **2002**, 2262-2263

75. Nandi, B.; Sinha, S., *Tetrahedron*, **2011**, *67:* 106-113.

76. Barroso,C., Doctor of Philosophy, The University Manchester The University Manchester, Faculty of Engineering and Physical Sciences, **2010**

77. Bakhmutov, V. I*., Practical Nuclear Magnetic Resonance Relaxation for Chemists* ., **2005**,

78. Minatti, A.; Dötz, K. H.,*Tetrahedron: Asymmetry*, **2005**, *16:* 3256-3267.

79. Dorawld F.Z., *Metal Carbenes in Organic Synthesis*,. Wiley, **1999,** p. 1-10. ISBN 3-527-29625-5

80. Barluenga, J.; Vicente, R.; López, L.A.; Tomás, M., *J. Am. Chem. Soc.*, **2006,** *128:* 7050-7054

81. Dötz, K. H., *Angew. Chem. Int. Ed. Engl.,* **1975**, *14:* 644-645.

82. Makabe, V., unpublished work., Rhodes University., **2010**

83. Basavaiah, D. et al. *Tetrahydron,* **1996**, *52:* 8001.

84. Dötz, K.H.; Dietz, R.; von Imhof, A.; Lorenz, H.; Huttner, G., *Chem. Ber.,* **1976,** *109:* 2033.

85. Timko, J.M.; Yamashita, A., *Org. Synth.,* **1998,** *9:* 1.

86. Rawat, M.; Wulff, W. D., *Org. Lett.*, **2004**, *6:* 329-332.

87. Basavaiah, D.; Veeraraghavaiah, G., *Chem. Soc. Rev.*, **2012**, *41:* 68-78

88. Minatti A.; Dötz K. H., *Topics Organomet. Chem.,* **2004**, *13:* 123 - 156

89. Bull, J.A.; Lujan, C.; Hutchings, M. G., *Tetrahedron Letters.,* **2009**, *50:* 3617-3620

90. Rubin, M.; Sromek, A.W.; Gevorgyan, V., *Synlett,* **2003**, *15:* 2265-2291

91. Waters, M. L.; Bos, M. E.; Wulff, W. D., *J. Am. Chem. Soc.*, **1999**, *121:* 6403.

92. Chamberlin, S.; Wulff, W. D.; Bax, B., *Tetrahedron*, **1993**, *49:* 5531.

93. Dötz, K. H*., Angew. Chem. Int. Ed. Engl.,* **1975**, *14:* 644–645.

94. White, J.D.; Smits, H., *Org. Lett.,* **2005,** *2:* 235-238.

95. Spyroudis, S., *Molecules* **, 2000**, 5: 1291-1330

96. Bos, M.E.; Wulff W.D.; Miller R.A.; Chamberlin S.; Brandvold T.A., *J. Am. Chem. Soc.,* **1991**, *24:* 9293

97. Ballard, C. E., *J. Chem. Ed.*, **2010**, *87:* 190–193.

98. Barluenga J. A.; Lopez L. A.; Martõnez S.,*Tetrahedron*, **2000**, *56*: 4967-4975

99. Armarego, W. L. F.; Perrin, D. D., *Purification of Laboratory Chemicals; 4th* Ed Butterworth-Heinemann, **1997**

100. Kim J.N.; Kim J.M.; Lee K.Y.; Gowrisankar S., *Bull. Korean Chem. Soc.*, **2004**, *25*: 1733

101. Wei Y.; Shi M., *Acc. Chem. Res.,* **2010**, *43*: 1005–1018

102. Strassner, T., *Topics Organomet Chem.*, **2004**, 1-20

103. Wulff, W.D., *Comprehensive Organometallic Chemistry II,* Pergamon Press, **1995**

104. Wulff, W.D., *Organometallics,* **1998,** *17:* 3116.

105. Semmelhack, M.F.; Lee, G.R., *Organometallics,* **1987,** *6:* 1839-1844.

106. Imwinkelried, R.; Hegedus, L.S., *Organometallics,* **1988**, *7:* 702-706.

107. Hoye, T. R.; Suriano, J. A., *Organometallics,* **1992,** *11*: 2044 - 2050.

108. Aumann, R; Fu, X; Holst, C; Frohlich, R., *Organometallics*, **2002**, *21:* 4356-4368

109. Kaye, P. T., *South African Journal of Science*, **2004**, *100:* 545-548

110. Dötz, K. H.; Tomuschat, P., *Chem. Soc. Rev.,* **1999**, *28:* 187-198.

111. Zheng, Z.; Chen, J.; Yu, Z.; Han, X., J. *Organomet. Chem.,* **2006**, *691:* 3679-3692.

112. Bonder, G.; Todd, L., *Inorganic Chemistry.***1974,** *13*: 1335-1337

113. P.J, Vergamini,: N.A,Matwiyoff, abstracts of the Rocky Mountain Regional Meeting of the American Chemical Society, **1972**

114. Gawley, R. E.; Narayan, S.; Vicic, D. A., *J. Org. Chem.*, **2005**, *70:* 328-329.

115. Huan, W.; Hsung, R.P.; Wulff, W.D., *Tetrahedron LeH.,* **1998**, *39:* 1849-1852

116. Sola, M.; Poater, J.; Cases, M.; Ftadera, X.; Duran, M., *Chem. Phys.,* **2003**, *294:* 192-139.

117. Becke, A. D. *J.Chem. Phys.,* **1993,** *98:* 5648

118. Petersson G. A.; Bennett A.; Tensfeldt T. G.; Al-Laham M.A.; Shirley W.A.; and Mantzaris J., *J. Chem. Phys.,* **1988**, *89:* 2193-218.

119. Frenking, G.; Sola`, M.; Vyboishchikov, S.F*., J. Organomet. Chem.,* **2005**, *690*: 6178.

120. Wang, C. C.; Wang, Y.; Liu, H. J.; Lin, K. J.; Chou, L. K.; Chan, K. S., *J. Phys. Chem.,***1997,** *101:* 8887-8901.

121. Reinheimer, E. W.; Kantardjieff, K. A.; Ouyang, X.; Herron, S. R.; Lu, T.; Casalnuovo, J. A., J. *Chem.Cryst.,* **2007**, *37:* 507-515

122. Bernasconi, C. F.; Leyes, A. E.; Ragains, M. L.; Shi, Y.; Wang, H.; Wulff, W. D., *J. Am. Chem. Soc.,***1998,** *120:* 8632.

123. T. H. Dunning Jr.; P. J. Hay., *Modern Theoretical Chemistry,* Ed. H. F. Schaefer III, Vol. 3 (Plenum, New York, **1976**) 1-28.

124. Makanjee C., Masters Thesis, Rhodes University, Department of Chemistry, **2012**

125. Wang, H.; Hsung, R. P.; Wulff, W. D., *Tetrahedron Lett.,* **1998,** *39*: 1849.

126. Powers, T. S.; Shi, Y.; Wilson, K. J.; Wulff, W. D*., J. Org. Chem.,* **1994,** *59:* 6882.

127. Berthelot, M. C. R. *Acad. Sci.,* **1866,** *62:* 905

128. Kaye, P. T; Robinson, R. S., *Synth. Commun*., **1996**, *26:* 2085-2097

129. Casey, C. P.; Boggs, R. A.; Anderson, R. L., *J. Am. Chem. Soc*., **1972**, *94*: 8947.

130. D.J, Darensbourg.; M.Y, Darensbourg., *Inorg. Chem.,* **1970,** I: 1691.

131 D.C. Look and I.J. Lowe, "Nuclear Magnetic Dipole-Dipole Relaxation Along the Static and Rotating Magnetic Fields: Application to Gypsum," J. Chem. Phys. 44, 2995 (1966).

5 Appendices

Appendix -1A:

Bond lengths (NBO) of selected carbenes

Theoretical bond lengths (NBO) in selected Molybdenum Fischer carbenes

Molybdenum Fischer carbenes			
Bond	Bond Length (Å)		
	R^2		
#	R	R	R
M - C	2.14826	2.15781	2.15222
M - C	2.05096	2.05172	2.05137
M - C	2.05102	2.05103	2.04980
M - C	2.04276	2.04982	2.04265
M - C	2.04284	2.03531	2.04202
M - C	2.05270	2.04966	2.05115
C_7	1.50989	1.51073	1.51073
C_7	1.35480	1.35110	1.35156
C_2	1.17306	1.17380	1.17301
C_3	1.17307	1.17328	1.17347
C_4	1.17625	1.17466	1.17638
C_5	1.17622	1.17813	1.17649
C_5	1.17556	1.17601	1.17584

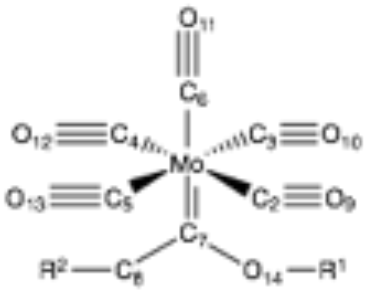

Table 6: Theoretical bond lengths (NBO) in selected Tungsten Fischer carbenes

Tungsten Fischer carbenes			
	Bond Length (Å)		
Bond	R^2		
#	R^1	R^1	R^1
M - C	2.15592	2.16801	2.16089
M - C	2.05963	2.05969	2.06013
M - C	2.05964	2.06034	2.05849
M - C	0.05085	2.05740	2.05048
M - C	2.05086	2.04324	2.04999
M - C	2.06389	2.05934	2.06192
C_7	1.50998	1.15110	1.51078
C_7	1.35167	1.34730	1.34812
C_2	1.17153	1.17240	1.17146
C_3	1.17153	1.17153	1.17190
C_4	1.17455	1.17324	1.17469
C_5	1.17455	1.17618	1.17477
C_5	1.17356	1.17406	1.17387

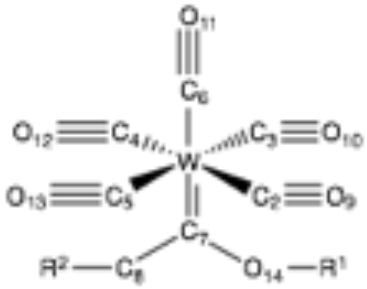

Appendix -**1B:**

Bond lengths (NBO) of selected condensation products

Chromium Carbenes Condensation products				
Bond	Bond Length (Å)			
	R^1=Me			
#	R	R	R^2	R^2
M - C	2.05895	2.05904	2.07041	2.07506
M - C	1.89651	1.89598	1.89718	1.89644
M - C	1.89825	1.89885	1.18972	1.89465
M - C	1.88213	1.88217	1.88025	1.87949
M - C	1.87989	1.87949	1.88023	1.87945
M - C	1.88158	1.88143	1.87887	1.87681
C_7	1.46046	1.46010	1.45048	1.45043
C_7	1.36200	1.36198	1.36683	1.36628
C_8	1.35477	1.35478	1.36399	1.36570
C_{15}	1.49396	1.49809	1.45627	1.45172
C_2	1.17133	1.17148	1.17120	1.17154
C_3	1.17078	1.17070	1.17121	1.17153
C_4	1.17575	1.17573	1.17607	1.17650
C_5	1.17576	1.17593	1.17609	1.17652
C_5	1.17472	1.17478	1.17539	1.17602
#	R^1=Et			
	R	R	R^2	R^2
M - C	2.06367	2.06558	2.07449	2.07985
M - C	1.89549	1.89558	1.89554	1.89529
M - C	1.89695	1.89667	1.89655	1.89529
M - C	1.88176	1.88105	1.88092	1.87985
M - C	1.88016	1.88014	1.88033	1.87985
M - C	1.88032	1.88004	1.87786	1.87578
C_7	1.46144	1.46099	1.45196	1.45181
C_7	1.35864	1.35884	1.36316	1.36281
C_8	1.35455	1.35487	1.36334	1.36494
C_{15}	1.49416	1.49811	1.45666	1.45187
C_2	1.17164	1.17159	1.17171	1.17189
C_3	1.17124	1.17134	1.17146	1.17189
C_4	1.17582	1.17585	1.17616	1.17654
C_5	1.17588	1.17604	1.17606	1.17654
C_5	1.17497	1.17506	1.17558	1.17622

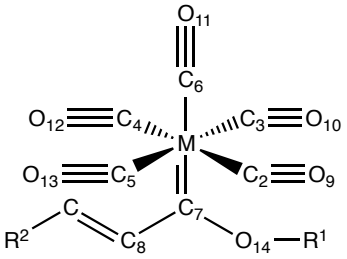

#	R1=Allyl			
	R	R	R^2	R^2
M - C	2.06161	2.06355	2.07367	2.07780
M - C	1.89681	1.89491	1.89699	1.89640
M - C	1.89779	1.89951	1.89723	1.89629
M - C	1.88193	1.88203	1.87979	1.87936
M - C	1.87962	1.87912	1.88068	1.88011
M - C	1.8808	1.88016	1.87802	1.87611
C_7	1.46171	1.46121	1.45193	1.45180
C_7	1.35869	1.35874	1.36348	1.36309
C_8	1.35432	1.35457	1.36345	1.36483
C_{15}	1.49431	1.49825	1.45660	1.45200
C_2	1.17128	1.17188	1.17144	1.17169
C_3	1.17111	1.17054	1.17121	1.17158
C_4	1.17593	1.17583	1.17612	1.17645
C_5	1.17583	1.17612	1.17623	1.17660
C_5	1.1749	1.17504	1.17555	1.17615

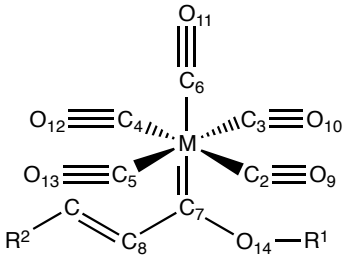

Molybdenum Carbenes Condensation products				
Bond	Bond Length (Å)			
	R^1=Me			
#	R	R	R^2	R^2
M - C	2.20599	2.20693	2.21612	2.22065
M - C	2.06137	2.06124	2.06128	2.06085
M - C	2.06134	2.06170	2.06129	2.06085
M - C	0.04377	2.04400	2.04253	2.04189
M - C	2.04235	2.04170	2.04251	2.04188
M - C	2.04878	2.04840	2.04563	2.04378
C_7	1.45855	1.45806	1.44874	1.44857
C_7	1.36219	1.36221	1.36656	1.36607
C_8	1.35515	1.35532	1.36427	1.36565
C_{15}	1.49361	1.49756	1.45547	1.45096
C_2	1.17169	1.17176	1.17176	1.17205
C_3	1.17158	1.17153	1.17175	1.17205
C_4	1.17630	1.17629	1.17673	1.17713
C_5	1.17652	1.17677	1.17673	1.17713
C_5	1.17542	1.17549	1.17608	1.1767
#	R^1=Et			
	R	R	R^2	R^2
M - C	2.04733	2.01096	2.21895	2.22389
M - C	2.66032	2.06026	2.06016	2.05973

M - C	2.06022	2.06043	2.06016	2.05973
M - C	2.04323	2.04432	2.04275	2.04216
M - C	2.04348	2.04189	2.04275	2.04213
M - C	0.04733	2.04723	2.04487	2.04300
C_7	1.45957	1.45932	1.45000	1.44993
C_7	1.35863	1.35881	1.36343	1.36297
C_8	1.45957	1.145932	1.36387	1.36535
C_{15}	1.35497	1.35499	1.45595	1.45126
C_2	1.17199	1.17210	1.17211	1.17238
C_3	1.17202	1.17194	1.17211	1.17238
C_4	1.17651	1.17634	1.17675	1.17715
C_5	1.17645	1.17681	1.76750	1.17715
C_5	1.17567	1.17572	1.17626	1.17687
#	R1=Allyl			
	R	R	R^2	R^2
M - C	2.20868	2.21137	2.21788	2.22286
M - C	2.06218	2.05974	2.06037	2.05982
M - C	2.06048	2.06247	2.06203	2.06151
M - C	2.04439	2.04341	2.04187	2.04142
M - C	2.04161	2.04220	2.04286	2.04220
M - C	2.04785	2.04695	2.04484	2.04302
C_7	1.45970	1.45920	1.44993	1.44969
C_7	1.35880	1.35894	1.36375	1.36330
C_8	1.35472	1.35510	1.36383	1.35546
C_{15}	1.49385	1.49765	1.45605	1.45117
C_2	1.17157	1.17211	1.17211	1.17238
C_3	1.17193	1.17143	1.17159	1.17188
C_4	1.17638	1.17648	1.17684	1.17724
C_5	1.17667	1.17676	1.17678	1.17717
C_5	1.1756	1.17574	1.17625	1.17685

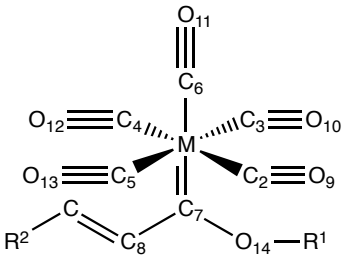

Tungsten Carbenes Condensation products				
Bond	Bond Length (Å)			
	R^1=Me			
#	R	R	R^2	R^2
M - C	2.18985	2.19085	2.19988	
M - C	2.05242	2.05223	2.05210	
M - C	2.05217	2.05227	2.05211	
M - C	2.03687	2.03729	2.03543	
M - C	2.03461	2.03427	2.03539	
M - C	2.04128	2.04085	2.03842	
C_7	1.45864	1.45240	1.44861	

C_7	1.36598	1.36582	1.37028	
C_8	1.35530	1.35542	1.36449	
C_{15}	1.49390	1.49782	1.45539	
C_2	1.17324	1.17330	1.17332	
C_3	1.17308	1.17310	1.17332	
C_4	1.17801	1.17797	1.17849	
C_5	1.17835	1.17856	1.17850	
C_5	1.17726	1.17734	1.17795	
#	R^1=Et			
	R	R	R^2	R^2
M - C	2.19378	2.19425	2.20275	
M - C	2.05140	2.05147	2.05105	
M - C	2.05108	2.05091	2.05104	
M - C	2.03698	2.0379	2.03564	
M - C	2.03510	2.0345	2.03570	
M - C	2.04014	2.03996	2.03769	
C_7	1.14597	1.45951	1.44986	
C_7	1.36246	1.35503	1.36708	
C_8	1.35506	1.49792	1.36413	
C_{15}	1.49407	1548	1.45582	
C_2	1.17359	1.17364	1.17368	
C_3	1.17352	1.17352	1.17369	
C_4	1.17810	1.17804	1.17852	
C_5	1.17836	1.17856	1.17850	
C_5	1.17749	1.17757	1.17814	
#	R1=Allyl			
	R	R	R^2	R^2
M - C	2.19232	2.19345	2.20129	
M - C	2.05309	2.05188	2.05093	
M - C	2.05940	2.05252	2.05283	
M - C	2.03741	2.03717	2.03487	
M - C	2.03434	2.03413	2.03593	
M - C	2.04044	2.04013	2.03786	
C_7	1.45989	1.45961	1.44975	
C_7	1.36268	1.36251	1.36759	
C_8	1.35486	1.35516	1.36414	
C_{15}	1.49408	1.49791	1.45594	
C_2	1.17307	1.17371	1.17371	
C_3	1.17354	1.17300	1.17314	
C_4	1.17808	1.17816	1.17858	
C_5	1.17841	1.17861	1.17854	
C_5	1.17744	1.17758	1.17811	

Appendix -**1C:**

Bond lengths (NBO) of selected Baylis Hillman products

Cr Baylis Hillman			
Bond	Bond Length (Å)		
	R2=Me		
#	R1=Me	R1=Et	R1=Allyl
M – C1(carbene)		2.06958	
C1 – O2		1.35680	
C1 – C3		1.44366	
C3 – C4		1.32573	
C3 – C5		1.50856	
Bond	Bond Length (Å)		
	R2=Ph		
#	R1=Me	R1=Et	R1=Allyl
M – C1(carbene)	2.06158	2.06578	2.08103
C1 – O2	1.36477	1.36092	1.36624
C1 – C3	1.43572	1.43726	1.43245
C3 – C4	1.34112	1.34078	1.33709
C3 – C5	1.51364	1.51310	1.50681
Bond	Bond Length (Å)		
	R2=Benz		
#	R1=Me	R1=Et	R1=Allyl
M – C1(carbene)	2.06811	2.06881	
C1 – O2	1.35821	1.35530	
C1 – C3	1.43780	1.43908	
C3 – C4	1.33806	1.33895	
C3 – C5	1.50167	1.50410	

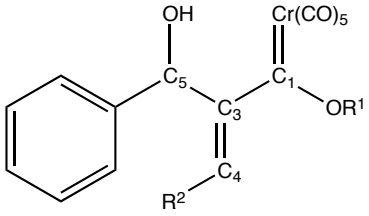

Appendix -**2A:**

Predicted IR of carbene products

Computational and experimental IR frequencies for Cr based carbenes

Chromium Carbenes

CrCO5OMe						CrCO5SiH						CrCO5OMe					
Calculated (Original)			Experimental			Calculated (Original)		Calculated (IR Printer)		Calculated (Original)		Calculated (IR Printer)			
Frequency (1/cm)	IR Intensity (a.u.)	IR Intensity (a.u.)	Observed Frequencies	Difference		Frequency (1/cm)	IR Intensity (a.u.)	Frequency (1/cm)	IR Intensity (a.u.)	Frequency (1/cm)	IR Intensity (a.u.)	Frequency (1/cm)	IR Intensity (a.u.)		
25,3972	0,0608	0,02				20,7380	0,1091	21	0,83	20,0753	0,1291	20	0,96		
62,6412	1,4283					49,8510	1,1240	50	2,65	49,9694	0,3477	41	0,38		
63,125	1,545	61				57,843	0,792	58	2,24	48,566	0,649	49	2,13		
70,0277	1,5262	70				65,8771	0,5653	66	1,98	61,1566	0,6685	61	2,64		
86,9806	1,6566	87				69,2975	0,8967	69	2,39	69,5693	0,2133	70	1,18		
92,628	0,397	93				85,336	0,093	85	2,52	72,294	0,471	72	1,75		
97,4861	0,5321	97				86,6247	0,1485	87	0,97	84,2043	0,8222	86	2,12		
103,5016	2,1186	104				97,5573	0,0859	96	0,74	91,8604	0,5726	92	1,93		
105,794	0,163	106				99,041	1,922	99	3,18	97,759	0,033	98	0,46		
109,4661	0,8467	109				105,0689	0,2076	105	1,40	100,0799	2,7198	100	3,72		
113,6116	0,2808	114				107,4396	1,8728	107	3,45	106,6868	1,8483	107	3,47		
173,644	0,046	174				145,673	0,131	146	0,91	107,697	0,535	108	1,87		
223,4886	0,231	223				156,4497	1,6033	156	3,39	154,0662	0,0975	154	0,86		
231,2947	1,0743	231				165,5691	0,0403	166	0,51	160,5292	0,8283	161	2,33		
288,448	0,1518	288				251,152	1,207	251	2,77	185,584	1,827	186	3,45		
348,4686	2,8849	349				275,6708	9,9496	275	7,71	251,4815	5,4830	251	5,97		
353,7017	0					311,8705	1,0091	311	2,53	301,9559	5,9108	302	6,21		
390,619	0,0397	391				348,405	0,1069			344,525	0,751	342	7,56		
402,388	3,5537	403				376,6548	9,2701	379	5,26	356,7385	0,0001	357	0,03		
408,7034	0,415	408				392,4952	0,0734	392	0,82	391,8669	0,1708	392	1,36		
453,3444	0,2703	453				408,795	0,2853	404	4,95	403,446	3,7911	403	4,96		
472,5097	13,4413	473				466,7537	11,2527	435	11,53	466,4455	0,3743	466	1,65		
474,8302	17,7648	475				470,1051	1,5108	430	11,23	474,0629	0,8219	474	2,31		
482,707	17,587	483				473,751	19,585	454	11,16	468,947	3,968	469	5,06		
521,2595	0,0364	521				475,4849	17,7998	475	10,40	475,1306	18,2102	475	16,80		
527,2961	0,4584	527				483,8342	16,2892	484	10,18	476,3976	17,4653	475	10,68		
545,071	2,22	545				524,047	0,012	523	0,28	484,261	16,994	485	10,52		
547,2546	0,5941	547				527,7455	0,4878	528	1,75	522,7985	0,0154	523	0,82		
549,4257	1,2238	549				545,7416	2,1836	546	5,40	528,1351	0,5534	528	1,96		
613,151	0,37	613				584,638	0,443	551	2,76	545,371	1,681	546	5,83		
675,1088	175,6297	676				650,6423	1,2154			548,8549	0,3698	551	2,95		
675,4397	171,5823	674				654,8541	3,7778	635	4,87	550,9399	1,3286				
689,091	123,026	689				676,146	173,746	676	33,25	615,966	2,859	620	4,32		
843,5416	7,7036	844				677,2594	108,1598	677	32,71	651,1682	22,5434	651	12,13		
996,672	263,9295	957	894,27	962,73	62,73	691,2852	236,3129	691	38,78	676,3736	174,8967	676	33,71		
1010,913	15,953	1010	948,38	16,07		790,329	1,409	790	2,99	680,102	158,946	680	31,69		
1110,4472	81,7395	1110	1020,07	15,35		847,9556	9,4061	848	4,72	691,6006	265,8153	682	40,71		
1133,808	0,7028	1134	1100,65			894,1571	241,0167	894	30,23	828,3013	40,3851	828	16,52		
1190,768	49,072	1191	1170,53	-20,47	-34	1008,068	13,339	1008	9,71	963,591	93,809	964	12,47		
1257,3121	458,3899	1257	1229,06	-8,94		1022,6299	868,5505	1023	17,58	994,2944	288,6497	984	43,41		
1425,3182	20,3235	1428	1396,59	-31,41		1110,8192	43,6861	1111	16,66	992,2987	2,8739	992	4,33		
1482,825	8,941	1483	1453,22	-33,78		1165,398	5,993	1166	27,27	1007,303	69,865	1007	18,01		
1508,7827	28,7685	1509				1166,0993	89,9679			1035,6081	8,5731	1017	7,48		
1519,3418	0,553	1519				1257,2344	560,8338	1257	59,74	1045,7920	7,1615	1036	6,84		
1526,77	5,338	1527				1314,008	0,315	1314	1,42	1157,936	86,990	1126	23,83		
1543,1157	16,0628	1543				1408,6312	1,2647	1410	2,84	1182,7889	22,4656	1184	12,11		
1934,1362	1487,7938	1934				1428,1748	21,5552	1428	11,71	1248,5859	590,0004	1249	62,07		
1934,949	1563,196	1935				1469,960	11,936	1470	8,71	1264,146	9,549	1264	7,30		
1946,3394	955,5552	1945				1510,0417	23,6950	1510	12,24	1352,9443	1,0218	1353	2,56		
1962,6754	210,0978	1962				1523,0531	1,5230	1523	3,41	1384,7221	1,1902	1385	2,76		
2031,098	223,745	2031				1529,371	13,983	1530	9,41	1428,431	22,295	1428	13,06		
3021,7718	5,2531	3022	2061,32	80,32		1538,3886	2,0673	1535	5,64	1498,3531	6,7066	1498	6,62		
3077,5267	21,4223	3078	2941,6	-220,4		1543,9047	7,8466	1548	7,07	1510,2042	23,8714	1510	12,48		
3079,071	4,381	3079		-337		1633,346	10,10,210	1633	10,03	1524,786	2,466	1525	4,01		
3170,0563	13,4426	3170				1933,9373	1974,6495	1934	100,00	1530,5831	0,9762	1531	4,41		
3194,1239	2,8089	3194				1946,8767	923,9608	1947	76,67	1731,7145	1,1456	1732	2,73		
3216,462	5,178	3217				1959,992	166,923	1960	32,59	1732,548	1466,518	1933	100,00		
						2023,9295	222,2584	2030	37,61	1933,8042	3531,5563	1954	78,93		
						3021,7490	5,0882	3023	5,02	1947,0854	953,4787	1947	78,93		
						3065,059	14,943	3063	9,55	2861,1359	201,329	1961	36,31		
						3071,4262	10,2296	3071	10,16	2029,9587	240,4015	2030	39,82		
						3080,2238	4,0749	3080	5,69	3021,7381	6,8338	3022	6,08		
						3127,765	6,672	3128	6,53	3022,949	15,822	3023	10,16		
						3161,8048	16,9207	3163	10,38	3029,6645	4,2653	3060	5,04		
						3161,8048	30,0710	3163	11,53	3111,1232	9,8715	3111	6,03		
						3373,422	8,647	3153	9,82	3158,1459	6,417	3158	6,49		
										3159,7134	6,8695	3159	5,23		
										3196,1385	3,1975	3196	4,57		
										3251,748	12,846	3262	9,16		

Computational a IR frequencies for molybdenum based carbenes

Molybdenum Carbenes																			
MoCOSOMe				MoCOSOEt						MoCOSOAllyl									
Calculated (Original)		Calculated (IR Plotter)		Calculated (Original)		Calculated (IR Plotter)				Calculated (Original)		Calculated (IR Plotter)							
Frequency (1/cm)	IR Intensity (a.u.)	Frequency (1/cm)	IR Intensity (a.u.)	Frequency (1/cm)	IR Intensity (a.u.)	Frequency (1/cm)	IR Intensity (a.u.)			Frequency (1/cm)	IR Intensity (a.u.)	Frequency (1/cm)	IR Intensity (a.u.)						
25.1647	0.0155	25	0.29	**8.4659**	0.1876	**8**	1.00			**15.2291**	0.1293	**15**	0.85						
53.3436	0.8620	53	2.18	**44.8826**	2.1370	**45**	3.38			**40.1525**	0.0434	**40**	0.50						
56.183	1.773	56	3.12	**54.107**	0.766	**54**	2.02			**44.878**	0.920	**45**	2.28						
56.5166	1.3936	57	2.77	**55.5828**	0.1831	**56**	0.99			**53.6280**	1.1727	**54**	2.57						
74.1674	1.1460	74	2.51	**61.4554**	0.0397	**61**	0.46			**55.8573**	0.1753	**56**	0.99						
77.536	0.276	78	1.23	**73.563**	0.124	**74**	0.81			**65.045**	0.131	**65**	0.86						
83.8688	1.8050	84	3.15	**75.5089**	0.2453	**76**	1.14			**73.6825**	0.4402	**74**	1.58						
84.9848	0.0751	85	0.64	**84.8720**	0.0155	**85**	0.29			**79.6977**	0.4017	**80**	1.51						
86.137	0.274	86	1.23	**86.012**	0.717	**86**	1.96			**83.523**	1.946	**84**	3.31						
88.4188	0.3910	88	1.47	**86.9984**	0.3705	**87**	1.41			**85.3312**	0.1524	**85**	0.93						
112.8316	0.0030	113	0.13	**88.4199**	1.6144	**88**	2.93			**86.3504**	0.5951	**86**	1.83						
165.393	4.001	165	4.69	**118.290**	0.944	**118**	2.24			**88.887**	0.586	**89**	1.82						
213.2891	1.2240	213	2.60	**145.4510**	1.0009	**145**	2.31			**140.2511**	0.4659	**140**	1.62						
221.0832	0.3766	221	1.44	**152.2387**	0.4894	**152**	1.62			**149.6982**	1.2225	**150**	2.63						
268.925	16.289	269	9.47	**248.127**	1.710	**248**	3.02			**180.116**	1.513	**180**	2.92						
341.4911	0.0014	341	0.09	**256.8372**	13.4689	**257**	8.60			**237.1965**	9.7791	**237**	7.24						
343.5482	4.1217	344	4.76	**302.4072**	1.3627	**302**	2.70			**283.2563**	7.6206	**283**	6.56						
370.932	0.214	371	1.09	**341.354**	0.022	**341**	0.34			**337.852**	9.526	**338**	7.33						
391.2949	20.9987	391	10.75	**367.4447**	0.8114	**367**	2.08			**342.3415**	0.0052	**342**	0.17						
392.6845	32.1541	393	24.40	**373.1583**	9.0771	**373**	6.96			**371.5725**	0.0430	**372**	0.49						
392.905	22.363			**389.962**	29.619	**390**	12.57			**392.652**	26.668	**393**	25.29						
405.6413	6.4087	406	5.94	**396.6497**	23.5389	**397**	11.20			**393.3487**	29.9936	**394**	11.77						
410.3033	13.8349	410	8.73	**398.0807**	32.6584	**398**	13.20			**394.1939**	24.5249								
417.330	8.263	417	6.75	**405.582**	3.705	**406**	4.44			**406.591**	6.843	**407**	6.22						
479.7398	1.8278	480	3.17	**413.3375**	3.1411	**413**	4.09			**409.4315**	9.0336	**409**	7.14						
483.5139	1.7979	484	3.15	**419.9037**	7.9797	**420**	6.52			**418.4694**	7.7031	**418**	6.60						
514.977	5.655	515	5.58	**480.307**	3.920	**480**	4.57			**448.899**	1.706	**449**	3.10						
524.5481	0.0200	525	0.33	**482.9420**	0.5257	**483**	1.67			**481.1540**	1.9993	**481**	3.36						
530.4415	1.6641	530	3.03	**512.4919**	1.4223	**512**	2.75			**484.2057**	1.7629	**484**	3.16						
594.027	82.913	594	21.37	**525.962**	7.621	**526**	6.37			**516.439**	5.895	**516**	5.77						
599.6835	101.0913	600	23.59	**533.3339**	0.3763	**533**	1.42			**525.4413**	0.1344	**525**	0.87						
609.1109	30.6234	609	12.99	**593.4992**	95.4830	**593**	22.56			**529.1701**	1.1599	**529**	2.56						
620.288	106.530	620	24.27	**599.909**	95.940	**600**	22.62			**595.231**	89.869	**595**	22.53						
836.7131	3.9889	837	4.69	616.3808	91.9825	616	22.14			**599.2758**	99.6393	**599**	23.72						
994.7873	224.1997	995	35.14	635.9064	34.2044	636	13.50			**613.1226**	72.8380	**613**	20.28						
1005.738	9.567	1006	7.26	781.902	3.122	782	4.08			623.083	59.817	**623**	18.38						
1107.5214	75.4270	1108	20.38	846.6908	3.0758	847	4.05			652.4417	15.3041	652	9.30						
1132.1003	0.5913	1132	1.80	989.3233	235.3691	989	35.42			823.1101	51.4875	823	17.05						
1190.648	51.094	1191	16.77	1004.112	28.743	1004	12.38			962.480	26.025	962	12.12						
1254.9822	461.3238	1255	50.40	1022.0761	43.5402	1022	15.24			980.4754	301.7717	980	41.28						
1428.3513	21.1391	1428	10.79	1109.0806	38.6941	1109	14.36			990.6454	2.4397	991	3.71						
1481.550	7.485	1482	6.42	1162.957	16.004	1163	9.24			1006.858	48.241	1007	16.50						
1507.7454	30.3534	1508	12.93	1166.8478	56.0628	1167	17.29			1013.9739	6.2172	1014	5.93						
1519.8665	0.7536	1520	2.04	1255.0584	572.4290	1255	55.24			1046.0480	7.1277	1046	6.34						
1526.134	5.765	1526	5.63	1312.515	0.740	1313	1.99			1126.114	81.028	1126	21.39						
1543.0578	15.0289	1543	9.10	1407.2892	2.4503	1407	3.61			1183.2326	24.7363	1183	11.82						
1920.8392	1747.8804	1921	98.11	1428.0647	20.8747	1428	10.55			1245.4648	611.3517	1245	58.75						
1921.580	1815.970	1922	100.00	1470.802	11.518	1471	7.84			1263.287	10.258	1263	7.61						
1936.0096	953.8406	1936	72.47	1506.7379	25.8384	1507	11.74			1352.8390	1.2078	1353	2.61						
1954.0796	129.6978	1954	26.72	1524.8637	8.4173	1525	6.70			1383.3530	1.5864	1383	2.99						
2029.757	203.915	2030	33.51	1530.077	13.359	1530	8.44			1428.035	23.423	1428	11.50						
3018.6785	6.0021	3019	5.75	1535.8965	3.4091	1536	4.26			1498.1095	6.5686	1498	6.09						
3075.9603	4.1419	3076	4.78	1546.9888	7.6256	1547	6.38			1507.7465	25.3274	1508	11.96						
3077.208	22.607	3077	11.16	1912.112	1693.026	1912	95.01			1523.910	2.250	1524	3.56						
3169.6774	13.0845	3170	8.49	1926.2233	1875.6654	1926	100.00			1530.2702	2.3793	1530	4.24						
3193.0056	3.0851	3193	4.12	1933.7523	957.0562	1934	71.43			1731.6556	1.1800	1732	2.58						
3217.448	5.248	3217	5.38	1953.776	101.596	1954	23.77			1919.641	1757.313	1920	99.61						
				2028.6852	208.1323	2029	33.31			1920.8713	1770.9579	1921	100.00						
				3020.5582	6.4848	3021	5.88			1934.7058	979.8216	1935	74.38						
				3065.328	13.946	3065	8.62			1953.328	121.558	1953	26.20						
				3072.6406	15.0614	3073	8.96			2028.8121	220.1225	2029	35.26						
				3079.1864	6.7557	3079	6.00			3018.5294	7.4146	3019	6.47						
				3129.392	5.917	3129	5.62			3063.084	15.741	3063	9.43						
				3143.4030	17.1103	3143	9.55			3076.5290	4.1155	3077	4.82						
				3163.7045	20.8297	3164	10.54			3131.3275	9.5403	3131	7.34						
				3198.473	3.080	3198	4.05			3168.599	6.488	3169	6.05						
										3189.8191	4.1435	3190	4.84						
										3196.0609	3.3128	3196	4.33						
										3261.688	12.804	3262	8.50						

Computational and experimental IR frequencies for tungsten based carbenes

Tungsten Carbenes																							
WCOSOMe							WCOSOEt							WCOSOAllyl									
Calculated (Original)		Calculated (IR Plotter)		Experimental			Calculated (Original)		Calculated (IR Plotter)					Calculated (Original)		Calculated (IR Plotter)							
Frequency (1/cm)	IR intensity (a.u.)	Frequency (1/cm)	IR intensity (a.u.)	Observed Frequencies	Difference		Frequency (1/cm)	IR intensity (a.u.)	Frequency (1/cm)	IR intensity (a.u.)				Frequency (1/cm)	IR intensity (a.u.)	Frequency (1/cm)	IR intensity (a.u.)						
27.3673	0.0081	27	0.21				10.8565	0.2227	20	1.07				16.0863	0.1356	16	0.86						
55.6421	0.5926	56	1.77				45.4068	1.9686	45	3.18				41.1739	0.0612	41	0.58						
57.852	1.697	[redacted]					53.333	0.237	53	1.10				46.808	0.836	47	2.13						
57.9368	1.8731	58	6.15				56.1144	0.6013	56	1.76				55.0080	1.3047	55	2.66						
75.8949	0.7668	76	2.02				57.6268	0.0985	58	0.71				57.3865	0.0293	57	0.40						
79.680	0.291	80	1.24				75.485	0.255	75	1.14				67.017	0.141	67	0.87						
84.0499	1.2510	84	2.57				77.1780	0.0687	77	0.59				75.8435	0.4039	76	1.48						
87.3700	0.5497	87	1.71				87.3559	0.8966	87	2.15				82.1614	0.3755	82	1.43						
88.200	0.281	88	1.22				87.897	0.297	88	1.24				83.575	1.392	84	2.75						
89.4776	0.2326	89	1.11				89.3761	0.1468	89	0.87				87.7246	0.5107	88	1.66						
114.8098	0.0110	115	0.24				90.6859	0.9469	91	2.21				88.5232	0.6455	89	1.87						
166.498	3.355	166	4.22				118.037	0.881	118	2.13				89.936	0.197	90	1.03						
218.9685	0.7721	219	2.02				143.6044	1.0652	144	2.34				139.3240	1.0008	139	2.33						
225.1885	0.4040	225	1.04				150.2334	0.4890	150	1.58				155.9075	1.0975	156	2.44						
273.296	18.445	273	9.89				248.673	0.961	249	2.24				178.684	1.214	179	2.57						
347.7050	4.4341	348	4.85				298.1918	16.3076	299	9.15				291.9532	11.7061	292	6.08						
363.9430	0.0017	364	0.09				311.1586	1.5324	311	2.81				291.9532	6.8092	292	6.08						
390.410	1.163	390	2.48				364.085	0.017	364	0.30				340.744	9.490	341	7.17						
404.3822	38.6684	405	14.31				378.0846	10.3383	378	7.29				364.9245	0.0066	365	0.19						
407.4965	41.5507	407	14.84				386.8539	0.8150	387	2.05				390.8062	1.6790	391	3.02						
416.447	21.477	417	10.67				405.606	37.545	405	13.89				405.723	37.408	406	14.24						
419.9464	2.7686	420	3.83				407.6983	33.7639	408	14.11				408.2272	40.3459	408	14.79						
445.6442	0.7577	446	2.00				418.6667	0.0062	418	0.63				446.6048	0.1638	447	1.32						
446.633	1.4201	447	2.71				435.555	1.6701	435	1.75				421.1328	2.2177	421	3.54						
488.3002	1.5451	489	2.86				453.4610	1.6151	453	2.88				434.3831	0.8868	434	2.19						
491.3308	2.1953	492	3.41				488.0399	1.7338	448	2.98				446.7741	2.8467	447	3.93						
528.696	7.541	529	6.23				488.550	2.721	489	3.74				451.740	0.501	452	1.65						
535.6016	0.0870	536	0.68				492.0967	1.1584	492	2.44				490.4530	1.7438	490	3.08						
542.0444	0.7083	542	1.94				524.1118	1.8408	524	3.07				492.7319	2.2139	493	3.47						
589.443	58.149	589	17.55				539.660	8.785	540	6.72				529.922	7.994	530	6.58						
592.5389	76.4772	593	20.13				543.0355	1.4686	543	2.55				535.1895	0.1165	535	0.79						
610.5819	78.2023	611	20.36				588.3921	68.0640	588	18.70				542.5193	0.5408	543	1.73						
617.080	26.075	617	11.74				592.850	70.158	593	18.98				590.371	60.873	590	18.17						
842.8800	5.2367	843	5.27	893.52	50.64		613.9942	86.2570	614	21.05				592.7478	74.9344	593	20.16						
1000.9280	237.2040	1001	35.45	949.37	51.56		638.4078	10.3404	638	7.29				612.1365	98.3389	612	23.09						
1015.886	8.700	1016	6.79	1019.53	3.64		788.782	2.281	789	3.42				622.450	7.016	622	6.17						
1113.4620	74.0784	1113	19.81	1102.04	11.42		846.6436	2.8442	847	3.82				656.1996	10.6257	656	7.59						
1133.9261	0.5287	1134	1.67				995.1872	264.3750	995	36.85				831.1979	47.0993	831	15.98						
1194.853	60.797	1195	17.95	1170.17	24.68		1013.402	8.897	1013	6.76				963.754	21.890	964	10.90						
1251.8224	498.4245	1252	51.39	1250.71	1.11		1023.4239	58.7219	1023	17.37				985.5425	348.6490	986	43.48						
1431.3026	20.7301	1431	10.48	1346.03	85.27		1113.2808	36.2078	1113	13.64				993.8294	2.0051	994	3.30						
1483.363	6.508	1483	5.91	1450.72	32.64		1164.841	9.664	1165	7.05				1007.479	44.597	1007	15.55						
1509.2533	31.2089	1509	12.86				1168.9569	68.5955	1169	18.77				1020.1009	6.0889	1020	5.75						
1520.1399	0.9365	1520	2.23				1248.7214	613.1114	1249	56.11				1046.2550	6.6109	1046	5.99						
1527.467	5.617	1527	5.46				1312.566	0.371	1313	1.38				1132.838	80.567	1133	20.90						
1543.6678	14.2651	1544	8.69				1408.2283	3.3990	1408	4.18				1185.0125	28.1466	1185	12.36						
1919.8235	1829.3711	1920	98.46	1872.91	46.91		1431.2252	20.5759	1431	10.28				1241.1920	661.3191	1241	59.89						
1920.505	1887.095	1921	100.00				1470.616	11.895	1471	7.82				1263.935	8.972	1264	6.98						
1933.7574	1000.9517	1934	72.83				1508.9294	28.9136	1509	12.19				1352.8084	1.2054	1353	2.56						
1954.1946	120.7701	1954	25.30				1523.7132	7.9013	1524	6.37				1385.1622	2.3381	1385	3.56						
2034.863	206.960	2035	33.12	2060.98	26.12		1529.898	13.817	1530	8.42				1431.146	23.004	1431	11.17						
3020.8541	5.5514	3021	5.42	2970.97	49.88		1535.5128	2.9396	1536	3.89				1498.3610	7.1213	1498	6.21						
3076.0580	24.3979	3076	11.37				1547.2054	7.2012	1547	6.08				1509.9309	25.8359	1510	11.84						
3077.857	3.750	3078	4.46				1909.583	1766.324	1910	95.24				1524.225	2.122	1524	3.39						
3167.7194	13.3752	3168	8.42				1926.0437	1947.1224	1926	100.00				1530.8506	3.0015	1531	4.03						
3191.6102	3.0485	3192	4.02				1931.5397	1012.0830	1932	72.10				1731.5767	1.1547	1732	2.50						
3216.240	5.340	3216	5.32				1954.185	86.411	1954	21.11				1918.494	1919.419	1918	49.79						
[redacted]							2033.5325	213.7216	2034	33.13				1919.7946	1843.8263	1920	100.00						
							3020.8861	6.2039	3021	5.69				1952.6878	1024.0143	1953	74.52						
							3065.8951	1.1477	3065	4.53				1955.8407	1.1553	1955	2.83						
							3070.2898	16.9805	3070	9.34				2033.8628	224.4304	2034	34.89						
							3078.0685	4.2372	3078	4.72				3020.6999	6.9554	3021	6.14						
							3126.316	6.893	3126	5.95				3061.194	16.378	3061	9.42						
							3143.3349	4.3272	3143	9.43				3078.3040	9.8687	3078	4.47						
							3162.8233	20.3005	3163	10.21				3139.1036	9.8687	3129	7.32						
							3198.178	2.889	3198	3.85				3168.822	6.504	3169	5.94						
														3188.3611	4.1168	3189	4.73						
														3196.3602	3.1848	3196	4.16						
														3261.674	12.744	3262	8.31						

Appendix -**2B(i):**

Predicted IR of condensation products

Chromium Condensation products

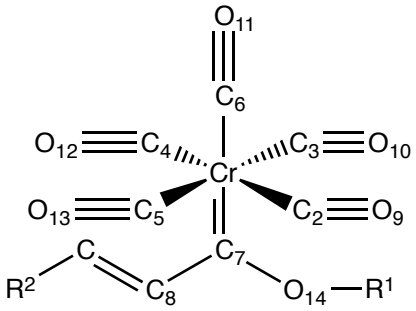

R^1 = Me, Et, Allyl
R^2 = Me, Et, Benz, Sali

Cromium Carbene Condensation

R^1=Me

R^2=Me				R^2=Et				R^2=Benz				R^2=Sali			
Calculated (Original)		Calculated (IR Plotter)		Calculated (Original)		Calculated (IR Plotter)		Calculated (Original)		Calculated (IR Plotter)		Calculated (Original)		Calculated (IR Plotter)	
Frequency (1/cm)	IR Intensity (a.u.)	Frequency (1/cm)	IR Intensity (a.u.)	**Frequency (1/cm)**	IR Intensity (a.u.)	**Frequency (1/cm)**	IR Intensity (a.u.)	**Frequency (1/cm)**	IR Intensity (a.u.)	**Frequency (1/cm)**	IR Intensity (a.u.)	**Frequency (1/cm)**	IR Intensity (a.u.)	**Frequency (1/cm)**	IR Intensity (a.u.)
17,7105	0,0153	18	0,33	**11,6115**	0,0595	**12**	0,32	**7,5401**	0,1729	**8**	1,11	**11,6899**	0,0114	**12**	0,29
55,5242	0,8849	56	2,52	**38,5274**	0,2783	**39**	0,68	**18,9592**	0,0074	**19**	0,23	**24,353**	0,0882	**24**	0,79
57,7678	0,7619	58	2,34	**50,903**	0,177	**51**	0,54	**45,2667**	0,0748	**45**	0,73	**46,3395**	0,1339	**46**	0,97
64,828	1,1867	65	2,92	**62,3484**	1,1871	**62**	1,41	**50,728**	0,8417	**51**	2,46	**52,036**	1,4516	**52**	3,22
83,7692	0,4519	84	1,8	**66,281**	0,1455	**66**	0,49	**65,6168**	0,6438	**66**	2,15	**65,8429**	0,4825	**66**	1,86
94,5796	0,2034	95	1,21	**75,974**	1,191	**76**	1,41	**69,5868**	1,2953	**70**	3,05	**71,5295**	1,0444	**72**	2,73
96,196	0,0405	96	0,54	**84,7928**	0,1446	**85**	0,49	**79,6318**	0,0262	**80**	0,43	**80,1338**	0,2371	**80**	1,3
98,8808	0,3121	99	1,5	**97,2457**	0,0145	**97**	0,16	**95,1807**	0,3283	**95**	1,53	**94,5878**	0,005		
105,5535	0,929	106	2,59	**99,544**	1,95	**100**	1,8	**97,0371**	0,3179	**97**	1,51	**94,9693**	0,3479	**95**	1,76
106,6437	3,2944	107	4,87	**100,8**	2,3126	**101**	1,97	**97,8775**	0,3761	**98**	1,64	**96,5433**	0,4038	**97**	1,7
112,6895	0,5961	113	2,07	**106,4534**	0,5706	**106**	0,98	**104,4775**	3,1413	**104**	4,75	**103,6074**	2,6256	**104**	4,33
143,7451	0,299	144	1,47	**110,542**	0,055	**111**	0,3	**104,6187**	0,2707	**105**	1,39	**106,7803**	0,44	**107**	1,77
166,8727	3,0334	167	4,67	**145,4208**	2,2661	**145**	1,95	**111,2201**	0,3778	**111**	1,65	**111,0178**	0,2017	**111**	1,2
187,4774	0,2611	187	1,37	**161,6974**	2,2549	**162**	1,94	**123,5629**	0,0009	**124**	0,08	**143,2607**	0,0059	**143**	0,21
200,7865	1,591	201	3,38	**177,896**	2,389	**178**	2	**154,082**	0,4147	**154**	1,72	**149,2148**	0,2174	**149**	1,24
213,0453	1,1634	213	2,89	**197,6863**	0,7025	**198**	1,08	**167,5547**	3,9787	**168**	5,34	**169,2321**	3,8603	**169**	5,25
242,7598	1,4003	243	3,17	**227,4833**	2,3635	**227**	1,99	**212,8749**	4,1594	**213**	5,46	**205,8982**	4,3398	**206**	5,56
259,3669	10,1781	259	8,56	**251,986**	0,664	**252**	1,05	**229,8933**	0,1633	**230**	1,08	**210,4874**	0,0433	**210**	0,55
356,9863	0,0053	357	0,2	**262,8132**	1,2345	**263**	1,44	**274,7025**	0,0307	**275**	0,47	**246,2322**	0,2274	**246**	1,27
364,8693	1,6804	365	3,48	**317,4908**	7,9409	**317**	3,64	**285,8323**	6,456	**286**	6,8	**281,2668**	8,2599	**281**	7,68
401,1404	0,0893	401	0,8	**357,011**	0	**393**	2,31	**356,9924**	0,0057	**357**	0,19	**309,3956**	6,1424	**309**	6,62
404,3983	4,283	404	5,55	**392,811**	3,2048	**401**	1,73	**365,4029**	22,0029	**365**	12,56	**357,9595**	0,0114	**358**	0,29
409,7249	1,2785	410	3,03	**400,7882**	1,7995			**400,4564**	0,1102	400	0,89	**360,8766**	25,1584	**361**	13,4
413,4927	1,1762	413	2,91	**402,791**	3,664	**403**	2,47	**404,5917**	6,2182	**405**	6,68	**394,0881**	0,4081	394	1,71
459,0073	19,5678	459	11,87	**409,8377**	2,7454	**410**	2,14	**410,0258**	1,0796	**410**	2,78	**403,2364**	0,0049	**403**	0,19
477,7735	18,9408	478	11,68	**424,3458**	1,2834	**424**	1,46	**418,2792**	0,0165	**418**	0,34	**405,8759**	6,6106	**406**	6,87
480,6675	17,1713	481	11,12	**442,786**	1,518	**443**	1,59	**428,5838**	1,4287	**429**	3,2	**410,8996**	0,846	**411**	2,46
508,2705	9,7296	508	8,37	**455,9189**	22,3607	**456**	6,11	**435,3216**	6,0092	**435**	6,56	**421,8448**	133,4904	**422**	30,86
522,2349	0,3414	522	1,57	**476,4386**	21,1689	**476**	5,95	**461,2948**	20,5258	**461**	12,13	**428,9044**	2,0621	**429**	3,84
536,5786	0,558	537	2	**483,48**	12,886	**483**	4,64	**475,8661**	8,332	**476**	7,73	**463,2244**	21,669	**463**	12,43
545,8263	1,641	546	3,44	**523,2822**	1,7259	**523**	1,7	**481,9239**	14,6169	**482**	10,24	**472,6726**	0,2218	**473**	1,26
555,2422	1,5353	555	3,32	**532,0037**	1,0149	**532**	1,3	**494,5557**	12,626	**495**	9,51	**473,7109**	14,6595	**474**	10,23
588,9367	8,9081	589	8,01	**545,536**	2,288	**546**	1,95	**522,5168**	0,0476	**523**	0,58	**484,4047**	18,3084	**484**	11,43
630,7561	3,5351	631	5,04	**550,1705**	1,8571	**550**	1,76	**538,1716**	1,1129	**538**	2,82	**486,2336**	9,9125	**486**	8,41
679,3659	148,0994	679	32,65	**601,406**	23,0487	**601**	6,2	**545,8881**	2,5228	**546**	4,25	**522,9411**	0,0348	**523**	0,5
689,1367	226,4706	689	40,37	**672,99**	151,978	**673**	15,93	**555,0073**	2,0225	**555**	3,01	**539,3003**	1,7206	**539**	3,5
690,8132	182,0795	691	36,2	**686,0569**	237,3294	**686**	19,91	**603,9003**	27,9458	**604**	14,15	**546,5267**	2,2426	**547**	4
862,1321	8,7446	862	7,93	**694,8052**	157,4978	**695**	16,22	**632,5415**	40,7876	**633**	17,1	**556,2652**	1,7151	**556**	3,5
868,2437	10,8138	868	8,82	**775,572**	43,739	**776**	8,55	**648,9535**	0,5275	**649**	1,94	**556,74**	5,6435	**557**	6,35
976,5437	54,5068	977	19,81	**816,5788**	24,2042	**817**	6,36	**667,3778**	13,615	**667**	9,88	**566,7935**	10,8198	**567**	8,79
1010,0536	25,1796	1010	13,46	**837,0698**	36,1324	**837**	7,77	**683,1925**	108,1783	**683**	27,85	**608,8174**	19,8189	**609**	11,89
1094,3629	245,4196	1094	42,03	**895,456**	13,96	**895**	4,83	**689,601**	312,9168	**690**	47,36	**647,2898**	38,0958	**647**	16,49
1108,1441	6,0168	1108	6,58	**943,8941**	17,4181	**944**	5,39	**690,9886**	152,2817	**691**	33,04	**673,3934**	55,738	**673**	19,94
1131,4001	1,0165	1131	2,7	**1002,2937**	124,6648	**1002**	14,43	**713,7327**	5,0218	**714**	6	**685,8836**	91,1766	**686**	25,5
1166,2302	17,6282	1166	11,26	**1028,766**	64,821	**1029**	10,4	**793,4797**	66,5237	**793**	21,84	**692,0149**	297,1697	**692**	46,05
1200,3906	175,2824	1200	35,52	**1068,1143**	167,5407	**1068**	16,73	**848,7666**	0,7334	**849**	2,29	**693,8893**	136,7711	**694**	31,24
1232,6802	212,9379	1233	39,15	**1118,4904**	2,9674	**1118**	2,23	**869,2293**	0,7229	**869**	2,28	**763,8581**	4,4134	**764**	5,61
1352,664	20,223	1353	12,06	**1139,393**	7,906	**1139**	3,63	**892,479**	10,0574	**892**	8,49	**782,924**	1,1557	**783**	2,87
1408,8942	28,9712	1409	14,44	**1165,8693**	20,1911	**1166**	5,81	**923,6057**	19,0981	**924**	11,7	**785,1768**	91,8429	**785**	25,6
1458,714	16,0111	1459	10,73	**1186,9088**	8,0073	**1187**	3,66	**959,3985**	1,5929	**959**	3,38	**865,7701**	1,1728	**866**	2,89
1480,4307	1,4807	1480	3,26	**1264,95**	239,878	**1265**	20,01	**1005,2049**	1,0636	**1005**	2,76	**881,3089**	0,0042	**881**	0,17
1516,2797	13,0384	1516	9,69	**1300,36**	7,719	**1300**	3,59	**1021,4107**	12,4711	**1021**	9,45	**919,3586**	40,8306	**919**	17,07
1523,7488	64,3703	1524	21,52	**1345,4142**	4,6336	**1345**	2,78	**1035,0413**	11,3028	**1035**	9	**946,4624**	17,7306	**946**	11,25
1529,5481	1,0199	1530	2,71	**1367,011**	7,08	**1367**	3,44	**1044,1522**	1,0253	**1044**	2,71	**981,2507**	2,1049	**981**	3,87
1538,644	9,4835	1539	8,26	**1396,5894**	24,7956	**1397**	6,43	**1064,2991**	1,4732	**1064**	3,25	**1020,3863**	7,4527	**1020**	7,29
1687,2238	116,0981	1687	28,91	**1458,5944**	2,0288	**1459**	1,84	**1112,8919**	266,8585	**1113**	43,74	**1034,9972**	14,5852	**1035**	10,2
1923,4802	1389,547	1923	100	**1485,259**	8,693	**1485**	3,81	**1131,1054**	21,6961	**1131**	13,65	**1082,5022**	3,82	**1083**	5,22
1925,1322	1386,1464	1925	99,88	**1522,4154**	11,5553	**1522**	4,39	**1131,399**	0,1927			**1115,7511**	319,3803	**1116**	47,73
1941,2878	997,5701	1941	84,73	**1526,3205**	11,1408	**1526**	4,31	**1177,1325**	254,6563	**1177**	42,72	**1133,0719**	0,1368	**1133**	0,99
1959,4538	315,8107	1959	47,67	**1538,732**	18,079	**1539**	5,49	**1219,5126**	514,4877	**1220**	60,73	**1137,3194**	37,6953	**1137**	16,4
2023,7532	356,35	2024	50,64	**1544,2016**	11,2703	**1544**	4,34	**1226,9133**	10,493	**1227**	8,67	**1178,4138**	250,2606	**1178**	42,25
3034,5273	6,9098	3035	7,05	**1549,1565**	4,79	**1549**	2,83	**1243,2554**	1,6796	**1243**	3,47	**1214,2036**	195,5406	**1214**	37,35
3070,9945	23,7751	3071	13,08	**1670,41**	119,686	**1670**	14,14	**1286,3567**	23,2568	**1286**	12,91	**1218,8258**	340,6106	**1219**	49,3
3087,5077	5,8565	3088	6,49	**1931,5269**	1437,4471	**1932**	100	**1342,1305**	15,3162	**1342**	10,48	**1227,1634**	13,3643	**1227**	9,76
3137,8308	14,6156	3138	10,26	**1932,2366**	1557,9725			**1386,3565**	22,6854	**1386**	12,75	**1285,9139**	32,7879	**1286**	15,29
3164,3949	18,2652	3164	11,46	**1944,139**	960,195	**1944**	40,04	**1401,2101**	45,3499	**1401**	18,03	**1299,0863**	28,2496	**1299**	14,2
3166,1392	25,8986	3166	13,65	**1959,072**	189,8674	**1959**	17,81	**1414,0227**	38,7823	**1414**	16,67	**1332,1206**	96,2599	**1332**	26,21
3208,7097	6,6838	3209	6,94	**2025,6923**	388,1459	**2026**	25,46	**1479,9126**	3,0898	**1480**	4,71	**1392,8413**	42,7377	**1393**	17,46
3227,7444	7,6082	3228	7,4	**3022,23**	12,019	**3022**	4,48	**1509,9387**	33,5926	**1510**	15,52	**1402,5257**	25,0751	**1403**	13,38
				3047,3477	36,3398	**3047**	7,79	**1527,3341**	35,1585	**1527**	15,87	**1417,2629**	26,7834	**1417**	13,82
				3082,6122	6,1306	**3083**	3,2	**1537,3295**	9,6721	**1537**	8,33	**1480,7025**	3,2278	**1481**	4,8
				3084,821	18,994	**3085**	5,63	**1554,8808**	4,9344	**1555**	5,95	**1505,6588**	34,7619	**1506**	15,75
				3123,5117	33,2751	**3124**	7,45	**1628,2438**	49,3367	**1628**	18,81	**1528,2417**	39,644	**1528**	16,82
				3133,3099	30,0478	**3133**	7,08	**1652,5363**	237,2329	**1653**	41,24	**1536,1959**	8,8251	**1536**	7,93
				3158,469	14,708	**3158**	4,96	**1667,6503**	145,8742	**1668**	32,34	**1559,2417**	14,0398	**1559**	10,01
				3183,8916	2,6637	**3184**	2,11	**1921,6424**	1395,1288	**1922**	100	**1633,2333**	162,8927	**1633**	34,09
				3185,2335	12,77	**3185**	4,62	**1922,7666**	1336,6262	**1923**	97,88	**1657,4399**	282,2606	**1657**	44,88
				3204,367	5,005	**3204**	2,89	**1938,0202**	1035,9848	**1938**	86,17	**1668,1101**	72,7283	**1668**	22,78
								1958,331	324,3951	**1958**	48,22	**1919,3862**	1401,6412	**1919**	100
								2020,1313	597,6746	**2020**	65,45	**1920,3028**	1336,2319	**1920**	97,64
								3066,0344	23,6548	**3066**	13,02	**1935,0587**	1058,6045	**1935**	86,91
								3157,6328	17,1481	**3158**	11,09	**1956,463**	329,4397	**1956**	48,48
								3183,8896	22,3669	**3184**	12,66	**2018,8747**	574,1633	**2019**	64
								3199,7048	2,3702	**3200**	4,12	**3069,1018**	24,6344	**3069**	13,26
								3203,6635	0,8355	**3204**	2,45	**3160,8406**	16,1726	**3161**	10,74
								3205,8397	9,3091	**3206**	8,17	**3186,6507**	13,7407	**3187**	9,9
								3213,5541	3,1606	**3214**	4,76	**3204,6538**	10,5196	**3205**	8,66
								3223,1392	25,2376	**3223**	13,45	**3208,4902**	0,3783	**3208**	1,64
								3231,4039	13,4502	**3231**	9,82	**3218,6254**	7,0354	**3219**	7,08
								3233,7693	24,8829	**3234**	13,35	**3223,1129**	8,5062	**3223**	7,79
												3237,9247	19,5233	**3238**	11,8
												3258,3403	0,5635	**3258**	2,01
												3659,7343	44,0514	**3660**	17,73

K^2=Me				K^2=H	
Calculated (Original)		Calculated (IR Plotter)		Calculated (Original)	
Frequency (1/cm)	IR Intensity (a.u.)	Frequency (1/cm)	IR Intensity (a.u.)	Frequency (1/cm)	IR Intensity (a.u.)
12,4203	0,0453	12	0,57	8,4378	0,1514
45,6829	0,5342	45	2,14	32,595	0,0357
49,4472	0,1063	48	0,88	42,8040	0,5367
54,2802	0,7050	54	2,26	51,2484	0,2777
64,5761	0,5642	65	3,5	57,1580	0,4011
73,5059	0,0784	74	0,75	61,47	0,1919
84,9989	0,2845	85	1,45	73,335	0,2574
90,5863	0,3473	91	1,58	86,558	0,6071
95,4184	0,3606	95	1,59	86,7593	0,3796
100,4373	2,2128	100	1,97	94,2577	0,1493

Appendix -**2B(ii):**

Predicted IR of condensation products

Molybedenum Condensation products

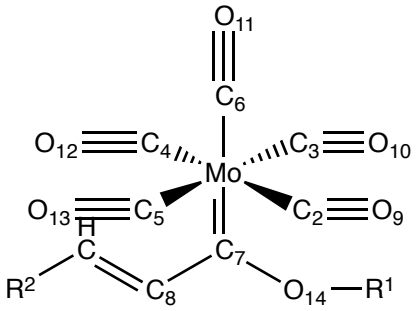

R^1 = Me, Et, Allyl
R^2 = Me, Et, Benz, Sali

Molybdeum Carbene Condensation

R^1=Me

R^2=Me				R^2=Et				R^2=Benz				R^2=Sali			
Calculated (Original)		Calculated (IR Plotter)		Calculated (Original)		Calculated (IR Plotter)		Calculated (Original)		Calculated (IR Plotter)		Calculated (Original)		Calculated (IR Plotter)	
Frequency (1/cm)	IR Intensity (a.u.)	Frequency (1/cm)	IR Intensity (a.u.)	**Frequency (1/cm)**	IR Intensity (a.u.)	**Frequency (1/cm)**	IR Intensity (a.u.)	**Frequency (1/cm)**	IR Intensity (a.u.)	**Frequency (1/cm)**	IR Intensity (a.u.)	**Frequency (1/cm)**	IR Intensity (a.u.)	**Frequency (1/cm)**	IR Intensity (a.u.)
13,1356	0,0036	13	0,15	**10,9282**	0	[redacted]		**15,1587**	0,1327	**15**	0,45	**14,8696**	0,0107	**15**	0,13
41,3682	0,6376	41	1,97	**45,1674**	0,3415	**45**	0,72	**19,4043**	0,0113	**19**	0,13	**21,3364**	0,1693	**21**	0,51
51,7695	1,1124	52	2,6	**48,1568**	0,9882	**48**	1,23	**41,8322**	0,078	**42**	0,35	**42,0187**	0,171	**42**	0,52
53,2976	1,0287	53	2,51	**48,8597**	0,6369	**49**	0,98	**46,5446**	1,1665	**47**	1,35	**47,8452**	1,5012	**48**	1,53
72,0319	0,237	72	1,2	**67,229**	0,0043	**67**	0,08	**55,7578**	0,2997	**56**	0,68	**55,762**	0,1709	**56**	0,52
78,7142	0,1003	79	0,78	**75,1489**	0,2998	**75**	0,67	**65,0154**	1,3515	**65**	1,45	**64,3583**	1,1498	**64**	1,34
81,7536	0,6306	82	1,96	**76,0991**	0,1257	**76**	0,44	**69,7506**	0,0537	**70**	0,29	**69,3073**	0,2051	**69**	0,57
82,8296	1,1543	83	2,65	**82,5065**	1,2376	**83**	1,37	**80,7137**	0,4674	**81**	0,85	**80,2099**	0,6208	**80**	0,98
85,8536	0,8888	86	2,33	**85,0492**	0,629	**85**	0,98	**83,7945**	1,1527	**84**	1,34	**83,0224**	0,871	**83**	1,16
87,8504	0,7972	88	2,21	**87,959**	1,752	**88**	1,63	**86,4269**	1,4473	**86**	1,5	**85,1642**	0,0704	**85**	0,33
92,2794	0,5895	92	1,9	**90,5039**	0,2935	**91**	0,67	**87,2316**	0,4026	**87**	0,79	**86,3109**	1,2685	**86**	1,41
129,188	0,2801	129	1,31	**120,9657**	0,1903	**121**	0,54	**89,8531**	0,0039	**90**	0,07	**88,2191**	0,4957	**88**	0,88
160,8189	2,9641	161	4,25	**123,5979**	0,2792	**124**	0,65	**93,3657**	0,368	**93**	0,76	**92,8529**	0,243	**93**	0,62
178,9481	0,1964	179	1,09	**139,377**	0,0354	**139**	0,23	**122,1216**	0,0022	**122**	0,06	**136,0441**	0,1836	**136**	0,53
193,4122	1,4349	193	2,96	**142,4268**	1,132	**142**	1,31	**143,3083**	0,6596	**143**	1,01	**139,8657**	0,0297	**140**	0,21
198,5539	1,2702	199	2,78	**184,9919**	0,5497	**185**	0,91	**161,6432**	3,5916	**162**	2,37	**163,211**	3,2484	**163**	2,25
237,2061	1,089	237	2,58	**212,7264**	1,4292	**213**	1,47	**197,903**	5,014	**198**	2,8	**191,3007**	4,5363	**191**	2,66
244,0364	15,2879	244	9,66	**234,4356**	13,7323	**234**	4,57	**226,8766**	0,2027	**227**	0,56	**208,2573**	0,0308	**208**	0,22
342,3393	0,024	342	0,38	**248,0449**	1,0389	**248**	1,26	**272,8692**	0	[redacted]		**243,8423**	0,2876	**244**	0,67
360,4076	0,6093	360	1,93	**310,5184**	0,7423	**311**	1,06	**279,387**	8,1262	**279**	3,56	**274,1297**	9,771	**274**	3,9
381,7484	1,6215	382	3,14	**342,9963**	0,0434	**343**	0,26	**343,5048**	0,06	**344**	0,31	**307,3475**	4,9719	**307**	2,78
390,9843	15,0441	391	9,58	**351,4638**	2,6279	**351**	2	**355,4448**	30,0492	**355**	6,84	**343,5937**	0,0026	**344**	0,06
392,1769	22,3183	392	11,67	**383,6115**	2,3643	**384**	1,9	**383,5426**	1,4754	**384**	1,52	**351,5954**	32,6192	**352**	7,13
399,9941	29,2926	400	13,37	**392,3394**	8,2187	**392**	3,54	**392,128**	27,5135	**392**	6,55	**385,4895**	1,9102	**385**	1,73
406,4335	23,1752	406	11,89	**393,1941**	25,6669	**393**	6,25	**395,464**	25,3979	**395**	6,29	**391,922**	8,1977	**392**	3,57
412,0614	11,1	412	8,23	**400,7119**	28,8481	**401**	6,62	**408,7062**	29,8883	**409**	6,83	**393,1069**	25,1427	**393**	6,26
419,4593	4,1093	419	5,01	**407,7878**	21,8133	**408**	5,76	**412,8156**	10,0269	**413**	3,95	**397,7761**	18,5431	**398**	5,37
483,8472	3,4369	484	4,58	**412,7479**	11,0684	**413**	4,1	**413,6369**	2,2744	**414**	1,88	**410,5143**	29,1181	**411**	6,74
494,0792	1,8486	494	3,36	**420,4635**	4,6788	**420**	2,67	**418,8504**	0,256	**419**	0,63	**412,0186**	0,3281	**412**	0,71
501,7564	10,3205	502	7,93	**484,6756**	2,527	**485**	1,96	**423,6987**	1,5087	**424**	1,53	**413,2354**	3,8031	**413**	2,43
522,254	3,8294	522	4,83	**495,0889**	1,885	**495**	1,69	**435,6059**	4,6995	**436**	2,71	**421,3421**	149,3803	**421**	15,26
527,6369	0,1181	528	0,85	**518,3356**	8,789	**518**	3,66	**483,7567**	1,2778	**484**	1,41	**423,422**	2,0132	**423**	1,77
563,8577	25,0728	564	12,37	**528,7238**	0,0627	**529**	0,31	**484,9747**	1,8273	**485**	1,69	**473,1666**	6,7415	**473**	3,24
597,6144	71,8931	598	20,94	**533,3509**	15,3959	**533**	4,84	**501,9076**	5,2445	**502**	2,86	**475,8018**	1,2455	**476**	1,39
618,6045	96,9477	619	24,32	**564,7766**	26,2234	**565**	6,32	**522,9366**	5,4616	**523**	2,92	**485,8482**	1,0611	**486**	1,29
625,7797	78,0728	626	21,82	**600,9983**	76,9045	**601**	10,82	**528,8591**	0,0523	**529**	0,28	**499,74**	2,142	**500**	1,83
631,0031	53,5769	631	18,08	**621,1104**	130,157	**621**	14,07	**573,2345**	55,4357	**573**	9,3	**523,6829**	5,4545	**524**	2,92
856,2537	6,3761	856	6,24	**626,91**	77,4926	**627**	10,86	**597,2163**	82,8165	**597**	11,36	**529,2218**	0,0411	**529**	0,25
864,9661	8,441	865	7,18	**654,0335**	10,5372	**654**	4	**620,3656**	144,7268	**620**	15,02	**553,0126**	14,8128	**553**	4,8
974,927	49,7851	975	17,43	**795,5164**	16,3053	**796**	4,98	**633,5537**	12,8586	**634**	4,48	**566,4504**	11,4592	**566**	4,23
1007,4099	22,2786	1007	11,66	**850,0493**	8,4349	**850**	3,58	**636,5734**	44,3473	**637**	8,31	**579,2001**	36,884	**579**	7,58
1093,364	263,3716	1093	40,08	**873,0091**	1,9798	**873**	1,74	**649,1495**	1,4628	**649**	1,51	**598,3594**	78,633	**598**	11,07
1107,6073	1,9922	1108	3,49	**978,3197**	50,1975	**978**	8,74	**672,0861**	34,3146	**672**	7,31	**621,1366**	149,5062	**621**	15,26
1130,6233	0,4015	1131	1,57	**1010,1529**	20,0472	**1010**	5,52	**712,8738**	21,8044	**713**	5,83	**639,7079**	46,6669	**640**	8,53
1165,7952	14,333	1166	9,35	**1021,0202**	44,7032	**1021**	8,25	**793,372**	55,1215	**793**	9,27	**647,4512**	21,1061	**647**	5,73
1201,461	190,385	1201	34,08	**1103,0351**	310,5078	**1103**	21,73	**845,1723**	0,1253	**845**	0,44	**679,7601**	29,9513	**680**	6,83
1235,2052	202,1857	1235	35,12	**1108,5977**	1,1687	**1109**	1,33	**870,2256**	0,3915	**870**	0,78	**763,3846**	1,3812	**763**	1,47
1345,5626	19,124	1346	10,8	**1144,2801**	5,394	**1144**	2,86	**888,6483**	14,2688	**889**	4,72	**782,4369**	1,3791	**782**	1,47
1407,3485	30,8535	1407	13,72	**1164,0705**	5,0173	**1164**	2,76	**926,7098**	16,4102	**927**	5,06	**785,1238**	83,1749	**785**	11,38
1458,4135	16,4863	1458	10,03	**1197,6107**	221,3069	**1198**	18,35	**960,3534**	1,3112	**960**	1,43	**859,7445**	0,0649	**860**	0,32
1479,9912	0,871	1480	2,31	**1231,838**	247,2469	**1232**	19,39	**1005,9513**	0,6762	**1006**	1,03	**881,5161**	0,0923	**882**	0,38
1515,8881	13,0438	1516	8,92	**1313,7756**	0,017	**1314**	0,16	**1025,6111**	9,5321	**1026**	3,85	**917,857**	46,8189	**918**	8,54
1522,8224	60,794	1523	19,26	**1349,6406**	26,8122	**1350**	6,39	**1035,2216**	10,9162	**1035**	4,13	**948,7128**	16,0549	**949**	5
1529,4246	2,1549	1529	3,62	**1399,6151**	3,0123	**1400**	2,14	**1045,044**	1,1339	**1045**	1,33	**981,4497**	1,9628	**981**	1,75
1538,5197	8,9958	1539	7,41	**1414,0315**	35,2978	**1414**	7,33	**1064,3667**	1,7469	**1064**	1,65	**1020,8814**	5,7062	**1021**	2,98
1686,1371	119,666	1686	27,02	**1459,8543**	15,6259	**1460**	4,88	**1112,7959**	271,7115	**1113**	20,58	**1036,1133**	11,884	**1036**	4,3
1910,3686	1639,2643	1910	100	**1467,1455**	15,9657	**1467**	4,93	**1130,3965**	0,2149	**1130**	0,58	**1082,2181**	2,9981	**1082**	2,16
1911,8874	1626,8206	1912	99,62	**1516,6663**	12,0907	**1517**	4,29	**1130,9863**	18,7028	**1131**	5,4	**1115,3285**	320,2009	**1115**	22,34
1928,5466	1063,5883	1929	80,55	**1524,777**	42,6508	**1525**	8,05	**1178,4559**	253,2263	**1178**	19,89	**1132,2929**	0,1583	**1132**	0,5
1951,699	242,5922	1952	38,47	**1528,5985**	12,4808	**1529**	4,36	**1221,69**	505,7474	**1222**	28,08	**1136,8133**	40,2144	**1137**	7,92
2023,3503	317,5997	2023	44,02	**1540,2976**	7,0183	**1540**	3,27	**1227,0209**	25,0079	**1227**	6,24	**1179,8423**	241,0988	**1180**	19,38
3033,9615	6,9776	3034	6,52	**1549,9797**	2,938	**1550**	2,11	**1243,6516**	2,1888	**1244**	1,85	**1213,6587**	121,9967	**1214**	13,79
3071,3949	25,1309	3071	12,38	**1686,6445**	120,827	**1687**	13,56	**1285,319**	29,468	**1285**	6,78	**1219,6078**	432,6329	**1220**	25,96
3086,8262	5,5659	3087	5,83	**1909,5919**	1664,0264	**1910**	100	**1344,1231**	13,7407	**1344**	4,63	**1227,0421**	13,9981	**1227**	4,67
3137,3869	14,4486	3137	9,39	**1910,2987**	1623,0797	[redacted]		**1386,8026**	21,7506	**1387**	5,82	**1284,9287**	25,7985	**1285**	6,34
3165,397	14,8123	3165	9,51	**1926,9748**	1068,2782	**1927**	40,31	**1400,6772**	46,6062	**1401**	8,52	**1298,4588**	37,1542	**1298**	7,61
3167,7867	31,6143	3168	13,89	**1949,343**	207,0194	**1949**	17,75	**1411,5116**	40,2206	**1412**	7,92	**1331,7954**	92,9914	**1332**	12,04
3209,6604	6,6089	3210	6,35	**2022,0293**	296,773	**2022**	21,25	**1479,1286**	2,9033	**1479**	2,13	**1392,0039**	46,6673	**1392**	8,53
3217,9389	7,9877	3218	6,98	**3034,3337**	7,3939	**3034**	3,35	**1509,8385**	36,1978	**1510**	7,51	**1402,1649**	28,7552	**1402**	6,69
[redacted]				**3062,7863**	15,1026	**3063**	4,79	**1527,318**	34,3952	**1527**	7,32	**1410,0413**	22,4177	**1410**	5,91
				3066,7455	16,4511	**3067**	5	**1536,9149**	9,3371	**1537**	3,82	**1479,9482**	2,8986	**1480**	2,13
				3087,3169	5,6355	**3087**	2,93	**1554,769**	5,7761	**1555**	3	**1505,145**	41,2609	**1505**	8,02
				3125,2468	7,4757	**3125**	3,37	**1628,0841**	50,2868	**1628**	8,85	**1528,491**	38,199	**1528**	7,71
				3137,4041	14,0747	**3137**	4,63	**1652,3101**	245,6644	**1652**	19,57	**1536,1354**	8,538	**1536**	3,65
				3141,5298	17,9021	**3142**	5,22	**1666,7332**	137,588	**1667**	14,65	**1559,0703**	15,2244	**1559**	4,87
				3161,4184	21,3947	**3161**	5,7	**1908,9608**	1647,3312	**1909**	100	**1632,4983**	179,489	**1632**	16,72
				3170,5674	31,9025	**3171**	6,97	**1909,4271**	1560,6196	[redacted]		**1657,0196**	294,2858	**1657**	21,41
				3217,95	8,0059	**3218**	3,49	**1925,3909**	1104,9567	**1925**	41,5	**1666,8159**	48,9439	**1667**	8,73
								1950,7818	254,362	**1951**	19,91	**1906,7133**	1653,3649	**1907**	100
								2020,2447	531,3451	**2020**	28,78	**1906,9813**	1556,6315	[redacted]	
								3066,202	24,8913	**3066**	6,23	**1922,4193**	1131,2117	**1922**	41,98
								3157,9196	16,4928	**3158**	5,07	**1949,0708**	260,7093	**1949**	20,15
								3184,5314	24,1126	**3185**	6,13	**2019,0135**	508,6413	**2019**	28,15
								3200,0958	2,2931	**3200**	1,89	**3069,2599**	25,8055	**3069**	6,34
								3204,2476	0,2906	**3204**	0,67	**3161,1296**	15,5695	**3161**	4,93
								3206,5415	9,3101	**3207**	3,81	**3186,6584**	14,1041	**3187**	4,69
								3214,1208	3,2202	**3214**	2,24	**3205,4399**	10,1493	**3205**	3,98
								3219,3617	5,6938	**3219**	2,98	**3206,8805**	1,267	**3207**	1,4
								3224,1103	29,3307	**3224**	6,76	**3211,5263**	1,3781	**3212**	1,47
								3234,0272	29,2134	**3234**	6,75	**3218,9239**	13,0793	**3219**	4,51
								[redacted]				**3237,643**	19,5148	**3238**	5,51
												3258,2448	0,6522	**3258**	1,01
												3659,5153	44,8638	**3660**	8,36

Multisystem Systems Conservation

97

Methadone Cabinet Condensation
Kidney

Appendix -**2B(iii):**

Predicted IR of condensation products

Tungsten Condensation products

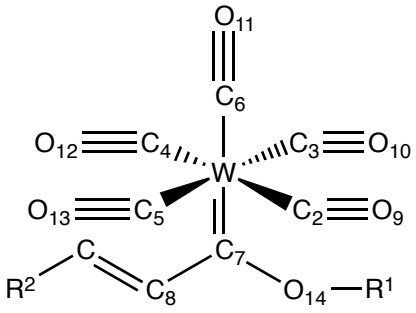

R^1 = Me, Et, Allyl
R^2 = Me, Et, Benz, Sali

Tungsten Carbene Condensation

R^1=Me

R^2=Me				R^2=Et				R^2=Benz				R^2=Sali			
Calculated (Original)		Calculated (IR Plotter)		Calculated (Original)		Calculated (IR Plotter)		Calculated (Original)		Calculated (IR Plotter)		Calculated (Original)		Calculated (IR Plotter)	
Frequency (1/cm)	IR Intensity (a.u.)	Frequency (1/cm)	IR Intensity (a.u.)	**Frequency (1/cm)**	IR Intensity (a.u.)	**Frequency (1/cm)**	IR Intensity (a.u.)	**Frequency (1/cm)**	IR Intensity (a.u.)	**Frequency (1/cm)**	IR Intensity (a.u.)	**Frequency (1/cm)**	IR Intensity (a.u.)	**Frequency (1/cm)**	IR Intensity (a.u.)
15,211	0,015	15	0,3					**14,7837**	0,1381	**15**	0,45	**14,6242**	0,007	**15**	0,1
42,1904	0,5371	42	1,77					**19,5895**	0,0238	**20**	0,19	**20,9702**	0,172	**21**	0,51
52,9379	1,1628	53	2,6					**42,7738**	0,0622	**43**	0,3	**42,7869**	0,1375	**43**	0,45
54,7839	0,9975	55	2,41					**47,4247**	1,1867	**47**	1,33	**48,7151**	1,4678	**49**	1,48
74,0329	0,1635	74	0,98					**56,8499**	0,1825	**57**	0,52	**57,0668**	0,085	**57**	0,36
80,6024	0,0772	81	0,67					**66,3556**	1,4075	**66**	1,45	**65,4814**	1,1751	**65**	1,32
82,1936	1,1189	82	2,56					**72,0714**	0,0201	**72**	0,17	**71,6444**	0,1412	**72**	0,46
84,2657	0,7111	84	2,04					**82,3678**	0,9441	**82**	1,19	**81,7286**	1,0002	**82**	1,22
88,6932	0,5574	89	1,8					**86,3291**	0,8985	**86**	1,16	**84,1369**	0,3895	**84**	0,76
90,7453	0,687	91	2					**87,1873**	0,1679	**87**	0,5	**85,7192**	0,6356	**86**	0,97
93,9567	0,6711	94	1,98					**90,3155**	0,3008	**90**	0,67	**89,4282**	0,2596	**89**	0,62
129,32	0,6594	129	1,96					**90,5179**	1,1771			**90,35**	1,0935	**90**	1,28
159,2568	2,296	159	3,66					**91,1444**	0,0815	**91**	1,67	**90,9162**	0,1279	**91**	0,44
179,7347	0,1568	180	0,96					**122,4619**	0,0001	**122**	0,01	**133,3647**	0,3001	**133**	0,67
193,0876	1,4301	193	2,89					**141,8383**	0,8301	**142**	1,11	**141,3301**	0,078	**141**	0,34
202,787	0,8468	203	2,22					**159,609**	3,024	**160**	2,12	**161,758**	2,663	**162**	1,99
239,745	1,3629	240	2,82					**197,1135**	4,8468	**197**	2,69	**190,5008**	4,2779	**191**	2,52
249,2282	17,3612	249	10,06					**233,134**	0,2105	**233**	0,56	**209,1229**	0,0395	**209**	0,24
364,3932	1,6153	364	3,07					**272,7104**	0,012	**273**	0,13	**249,8179**	0,275	**250**	0,64
365,2894	0,0581	365	0,58					**284,2587**	9,5849	**284**	3,78	**278,851**	11,4535	**279**	4,13
400,4703	7,8608	400	6,77					**365,9441**	0,0529	**366**	7,56	**307,8735**	5,8667	**308**	2,96
405,1622	30,9269	405	13,43					**366,4098**	35,538			**361,744**	38,6242	**362**	7,59
407,0535	37,9432	407	14,88					**400,7508**	9,9173	**401**	3,84	**365,9657**	0,0042	**366**	0,08
412,2737	5,2263	412	5,52					**406,256**	28,266	**406**	6,49	**394,6769**	0,279	**395**	0,64
426,0292	23,9153	426	11,81					**408,3177**	36,5836	**408**	7,38	**402,5062**	10,1929	**403**	3,9
437,6565	2,1164	438	3,51					**418,9509**	0,0489	**419**	0,27	**406,876**	22,9192	**407**	5,84
449,6243	2,4047	450	3,75					**425,1266**	14,2944	**425**	4,62	**408,5283**	35,7915	**409**	7,3
491,8893	5,2177	492	5,52					**428,0495**	13,924	**428**	4,56	**420,9913**	143,386	**421**	14,62
501,9441	2,1677	502	3,56					**438,2526**	1,9554	**438**	1,71	**423,9672**	5,3884	**424**	2,83
506,5992	10,1636	507	7,7					**439,6765**	1,5094	**440**	1,5	**431,0079**	18,2853	**431**	5,22
533,9988	5,7304	534	5,78					**452,1649**	1,5047	**452**	1,5	**438,5359**	3,0994	**439**	2,15
541,3315	0,2941	541	1,31					**486,8029**	2,1772	**487**	1,8	**450,9869**	2,5987	**451**	1,97
570,5778	25,6334	571	12,23					**493,2208**	2,3007	**493**	1,85	**476,7717**	0,8924	**477**	1,15
591,8975	48,9035	592	16,89					**508,7605**	5,5459	**509**	2,88	**477,5971**	6,4793	**478**	3,11
613,8399	96,0931	614	23,68					**534,6807**	7,6477	**535**	3,38	**493,8862**	1,5446	**494**	1,52
622,9198	50,7629	623	17,21					**542,6162**	0,0727	**543**	0,33	**507,3789**	2,9451	**507**	2,09
637,3164	24,4336	637	11,94					**575,7557**	46,3072	**576**	8,31	**535,3269**	7,6695	**535**	3,38
862,6721	6,2647	863	6,05					**591,1447**	55,5436	**591**	9,1	**542,8748**	0,0766	**543**	0,34
867,2532	6,9914	867	6,39					**614,192**	113,9726	**614**	13,03	**556,1464**	9,1357	**556**	3,69
976,3748	48,4146	976	16,81					**633,2846**	14,6475	**633**	4,67	**566,3848**	11,6625	**566**	4,17
1008,3239	20,7453	1008	11					**635,9347**	25,8355	**636**	6,21	**579,2511**	35,1635	**579**	7,24
1094,7831	300,9933	1095	41,91					**649,4371**	0,627	**649**	0,97	**591,9907**	52,2941	**592**	8,83
1106,7224	4,4174	1107	5,08					**677,5454**	29,2195	**678**	6,6	**614,9464**	117,7997	**615**	13,25
1133,3032	0,611	1133	1,89					**712,9596**	22,5588	**713**	5,8	**639,7925**	27,701	**640**	6,42
1166,4154	14,682	1166	9,26					**793,2954**	53,8203	**793**	8,96	**647,3347**	19,3513	**647**	5,37
1202,1477	215,3132	1202	35,44					**847,9721**	1,2134	**848**	1,34	**685,0865**	27,3537	**685**	6,38
1236,9278	180,0522	1237	32,41					**870,0271**	0,3483	**870**	0,72	**763,2743**	1,1973	**763**	1,34
1349,3495	19,2033	1349	10,59					**893,1366**	14,9104	**893**	4,71	**782,3089**	0,6928	**782**	1,02
1410,0162	32,4196	1410	13,75					**928,1791**	15,1405	**928**	4,75	**784,9934**	82,3581	**785**	11,08
1458,5353	15,3853	1459	9,47					**960,0525**	1,575	**960**	1,53	**865,1613**	0,7417	**865**	1,05
1482,1863	0,505	1482	1,72					**1005,743**	0,8415	**1006**	1,12	**881,3243**	0,1203	**881**	0,42
1515,5647	12,9218	1516	8,68					**1022,6426**	9,1319	**1023**	3,69	**919,5076**	49,1917	**920**	8,56
1523,214	60,3658	1523	18,77					**1035,1572**	10,7994	**1035**	4,01	**949,6368**	14,3414	**950**	4,62
1529,7432	2,3227	1530	3,68					**1044,4471**	0,7111	**1044**	1,03	**981,7053**	2,137	**982**	1,78
1538,939	8,9459	1539	7,22					**1064,423**	2,0821	**1064**	1,76	**1020,2436**	6,8752	**1020**	3,2
1685,8118	119,5545	1686	26,41					**1113,2141**	305,1252	**1113**	21,33	**1033,9086**	10,4158	**1034**	3,94
1908,9994	1700,0308	1909	99,6					**1130,7777**	18,225	**1131**	5,21	**1082,2539**	2,6142	**1082**	1,97
1911,139	1713,8598	1911	100					**1132,7814**	0,1955	**1133**	0,54	**1115,5657**	347,2735	**1116**	22,75
1927,2525	1096,441	1927	79,98					**1181,3235**	255,2399	**1181**	19,51	**1134,9608**	0,1341	**1135**	0,45
1951,9284	238,7215	1952	37,32					**1222,3071**	471,812	**1222**	26,52	**1136,2355**	45,4667	**1136**	8,23
2028,1284	332,4696	2028	44,04					**1227,1763**	40,5838	**1227**	7,78	**1182,6912**	237,1966	**1183**	18,8
3033,906	7,5431	3034	6,63					**1244,0104**	2,0138	**1244**	1,73	**1214,1278**	97,5781	**1214**	12,06
3069,7828	27,7027	3070	12,71					**1287,3217**	35,8103	**1287**	7,31	**1220,1**	456,7664	**1220**	26,09
3086,7839	5,7016	3087	5,77					**1344,2552**	14,1702	**1344**	4,6	**1226,9876**	14,1033	**1227**	4,58
3136,9189	14,9437	3137	9,34					**1386,7708**	24,5402	**1387**	6,05	**1287,3987**	29,9291	**1287**	6,68
3162,8043	14,9106	3163	9,33					**1401,2685**	51,2626	**1401**	8,74	**1297,9966**	36,1198	**1298**	7,34
3172,0378	29,6459	3172	13,15					**1413,3052**	38,2868	**1413**	7,55	**1332,0471**	90,4933	**1332**	11,61
3208,0465	6,6834	3208	6,24					**1480,9008**	1,9582	**1481**	1,71	**1392,2512**	48,6524	**1392**	8,51
3219,1524	8,6803	3219	7,12					**1509,9851**	35,1853	**1510**	7,24	**1402,4242**	26,0366	**1402**	6,23
[redacted]								**1528,5007**	34,199	**1529**	7,14	**1412,4741**	26,0843	**1412**	6,23
								1537,7322	9,2203	**1538**	3,71	**1482,0287**	1,8132	**1482**	1,64
								1554,8789	5,7447	**1555**	2,93	**1505,3878**	40,7218	**1505**	7,79
								1628,0263	51,0277	**1628**	8,72	**1529,9808**	37,9082	**1530**	7,51
								1651,6045	252,6338	**1652**	19,41	**1537,2647**	8,4115	**1537**	3,54
								1666,6222	130,8624	**1667**	13,97	**1559,0259**	15,4927	**1559**	4,8
								1908,0084	1722,2037	**1908**	100	**1632,2046**	187,4335	**1632**	16,71
								1908,2916	1632,4626			**1656,2182**	293,68	**1656**	20,92
				[redacted]				**1924,052**	1137,5109	**1924**	41,18	**1666,8644**	44,0162	**1667**	8,1
								1950,8201	247,036	**1951**	19,19	**1905,8011**	1729,3897	**1906**	100
								2024,8065	572,4687	**2025**	29,21	**1905,8707**	1627,5808	[redacted]	
								3064,7343	27,1053	**3065**	6,36	**1921,1109**	1164,0252	**1921**	41,64
								3155,4911	16,7318	**3155**	4,99	**1949,1022**	252,4555	**1949**	19,39
								3189,8928	22,1467	**3190**	5,75	**2023,5078**	550,8978	**2024**	28,65
								3200,1908	2,2059	**3200**	1,81	**3068,1663**	27,6067	**3068**	6,41
								3204,2636	1,5029	**3204**	1,5	**3159,1929**	15,7297	**3159**	4,84
								3205,3744	0,3533	**3205**	3,53	**3186,573**	14,4609	**3187**	4,64
								3214,2214	3,0758	**3214**	2,14	**3204,1198**	10,4035	**3204**	3,94
								3221,0774	5,353	**3221**	2,82	**3207,4908**	0,7589	**3207**	1,06
								3224,2491	30,8891	**3224**	6,79	**3212,5641**	1,6693	**3213**	1,58
								3234,0397	30,1024	**3234**	6,7	**3218,9957**	13,375	**3219**	4,46
												3237,6218	19,8611	**3238**	5,44
												3262,8035	0,5326	**3263**	0,89
												3659,5433	45,7624	**3660**	8,26

Tungsten Carbide Oxidation

[illegible]

[illegible]			
Calculated (Original)		Calculated (IR Plotter)	
Frequency (1/cm)	IR Intensity (a.u.)	Frequency (1/cm)	IR Intensity (a.u.)
37,063	0,3029	37	4,2
44,6154	4,0601	45	2,7
49,3308	0,7172	49	2,04
50,7177	0,6150	51	3,41
68,2537	0,0033	69	0,14
77,3254	0,3664	77	3,5
78,8036	4,173	79	0,84
84,0779	1,5505	84	5
90,2227	0,6255	88	3,02
90,5755	0,344	91	3,56
93,0707	0,8175	[redacted]	
116,2431	0,2075	116	5,3
125,2066	0,8522	125	1,62
138,1619	0,5179	139	1,35
141,5146	0,5554	142	1,64
184,2053	0,6011	184	1,87
212,4255	1,4035	213	2,85
248,4773	14,3349	244	9,65
248,8235	0,8625	249	2,24
315,1985	0,5540	319	1,75
354,0352	2,8615	354	4,07
365,6283	0,0454	366	0,51
402,1748	9,3125	402	7,35
406,2947	28,3985	406	12,83
407,6174	35,4985	408	14,55
415,3274	4,4565	415	5,05
427,323	29,2260	428	21,61
438,1172	2,1065	438	3,5
450,2646	2,9974	450	3,86
463,1375	3,2976	463	4,35
503,2218	7,2960	503	3,57
527,25	13,6377	527	5,91
542,2942	3,4785	542	4,27
542,6089	13,3893	543	7,76
573,3198	28,3593	573	11,96
594,9667	51,7501	595	17,37
615,1659	102,5611	615	24,44
624,5026	51,0631	625	17,2
650,5870	7,742	650	6,7
662,7671	11,6382	663	3,57
851,3892	9,4575	851	7,62
872,4634	1,5926	872	3,04
979,3924	49,1537	979	15,95
1008,4561	16,8278	1008	10,15
1022,4962	41,4003	1022	15,5
1103,018	355,6906	1103	45,52
1106,0607	12,5453	1107	3,53
1144,9064	4,4127	1145	5,02
1165,965	5,5182	1166	3,56
1195,5835	148,8977	1196	38
1233,2848	217,8276	1233	35,17
1313,0607	9,052	1313	9,43
1350,5358	27,5531	1351	12,67
1400,6319	2,8579	1401	4,67
1416,3504	35,7345	1416	14,2
1459,4711	14,5714	1459	9,23
1467,2458	35,4175	1467	9,36
1516,241	41,9622	1516	8,54
1525,417	42,7320	1525	15,75
1538,4569	12,5099	1538	5,55
1540,0387	7,322	1541	6,52
1550,5342	1,8427	1551	3,5
1684,2734	743,5475	1685	70,56
1900,4561	1717,8953	1900	99,87
1910,0127	1774,6455	1910	100
1925,3075	1099,7063	1925	78,38
1943,676	155,2481	1950	33,72
2026,954	473,9026	2027	47,48
3034,2429	7,8768	3034	6,2
3062,3451	45,2910	3062	5,42
3065,7493	17,7987	3066	17,16
3087,1278	5,7759	3087	5,75
3123,2146	8,2182	3123	6,51
3137,8448	14,4754	3137	9,16
3141,909	18,2208	3141	12,16
3161,3648	23,7557	3162	12,87
3174,2278	23,8171	3174	13,35
3218,3538	6,901	3218	7,09

[illegible]			
Calculated (Original)		Calculated (IR Plotter)	
Frequency (1/cm)	IR Intensity (a.u.)	Frequency (1/cm)	IR Intensity (a.u.)
16,6008	0,7488	17	0,74
23,0413	0,1746	23	0,87
42,0761	0,7000	42	2,02
50,1964	0,4378	51	1,69
55,7234	0,1434	55	0,92
76,3	0,2102	75	1,32
77,3414	0,3516	77	1,64
79,1766	1,2981	79	2,75
86,5066	1,3309	87	2,78
87,8764	0,5786	88	1,84
89,8875	0,4625	89	2,64
90,893	0,3189	91	1,4
98,3525	0,0556	98	0,57
121,2541	0,0308	121	0,92
128,3931	0,6027	129	1,67
147,4138	0,6954	147	2,02
178,2747	0,6573	178	1,94
213,8098	1,2041	214	5,54
247,4255	0,8835	247	2,51
250,8732	1,2149	251	2,66
308,9008	2,0047	309	3,41
319,6831	0,6015	320	1,87
365,5734	0,0318	366	0,85
394,7593	7,3804	366	6,54
405,344	28,7383	405	12,93
407,0532	36,4033	407	14,56
412,09	6,9236	412	6,9
420,5540	19,5124	420	10,56
433,5673	5,5096	432	5,68
437,7518	3,3146	438	3,67
445,8945	2,5216	450	3,85
498,944	3,5204	498	4,53
504,0826	2,5165	504	3,85
520,8439	15,4986	521	9,5
557,5442	9,608	558	7,06
561,8079	0,7387	542	2,16
575,9000	30,2040	578	13,69
594,0194	50,3616	594	17,63
614,3575	103,9816	614	24,62
636,4691	80,6508	636	15,39
674,2964	10,0414	674	7,66
802,6736	13,9656	802	9,02
816,0636	11,3784	820	8,14
856,6344	5,0464	857	6,63
907,4497	9,9936	907	7,59
940,4167	15,2474	940	9,35
1012,9048	19,6264	1013	10,68
1021,6470	41,7219	1022	15,59
1032,1113	50,4601	1032	17,65
1112,5517	197,9181	1113	41,65
1123,7762	150,8198	1124	30,52
1145,5324	5,2494	1145	5,56
1165,7606	5,6132	1166	5,72
1208,1294	161,5644	1208	30,72
1232,4866	111,5306	1233	35,3
1299,0561	8,5296	1299	7,05
1318,1385	0,0089	1318	0,92
1340,5848	20,0389	1341	10,8
1371,4067	42,0181	1371	8,37
1406,3674	0,9956	1407	2,61
1425,4074	52,0080	1421	17,81
1465,5248	3,8007	1462	4,7
1468,275	152,232	1468	9,72
1527,0574	10,2002	1527	7,03
1529,0273	32,4741	1529	8,52
1546,3235	9,122	1549	7,29
1542,0149	10,4767	1542	7,82
1548,0784	5,9847	1548	5,9
1550,1523	4,8008	1550	5,05
1678,5092	144,876	1679	29,05
1907,0254	1690,102	1907	99,71
1909,8657	1717,2197	1910	100
1925,2849	1015,748	1925	99,09
1948,5503	707,9778	1949	34,73
2018,4856	321,7316	2025	48,24
3021,2132	17,2090	3021	9,07
3055,0331	37,7655	3055	10,77
3062,5268	19,3648	3063	9,46
3066,9535	17,8204	3066	10,07
3081,791	13,6877	3082	8,93
3123,6275	7,953	3124	6,78
3134,7023	31,2621	3135	13,49
3135,3946	25,9139	3139	12,29
3141,936	28,0512	3142	12,23
3161,494	20,8067	3161	11,05
3172,2242	28,1896	3172	12,79
3209,4615	8,7194	3209	7,13

[illegible]			
Calculated (Original)		Calculated (IR Plotter)	
Frequency (1/cm)	IR Intensity (a.u.)	Frequency (1/cm)	IR Intensity (a.u.)
8,5410	0,0836	9	1,7
18,825	0,0142	19	0,32
34,939	0,241	35	2,18
41,5838	0,0595	42	0,59
54,4518	0,0179	54	0,35
61,057	1,0145	61	2,43
66,3087	0,3769	66	1,49
77,6543	0,2976	78	1,52
81,5656	0,4603	82	1,69
84,4712	1,6366	84	3,09
87,4438	0,3306	87	1,39
88,2826	0,4946	88	1,7
90,5908	0,8357	91	2,22
92,8441	0,0223	93	0,56
115,3054	0,0145	118	0,20
141,2164	0,9759	141	2,39
159,6154	2,318	160	3,84
160,5085	0,318	161	1,36
252,7686	0,7524	253	2,1
253,7503	6,9362	254	6,58
272,536	0,0659	273	0,63
291,6678	8,4157	292	7,01
356,3451	0,0377	356	0,58
390,8874	20,2733	391	23,03
401,1887	30,7728	401	7,94
407,158	25,442	407	12,43
409,6324	43,671	410	15,42
418,6491	0,0461	419	0,52
421,8463	36,9557	422	9,96
434,7323	4,314	435	5,29
438,6715	1,8958	439	3,33
451,6116	3,8356	452	4,74
462,5434	7,5358	463	6,64
486,8595	2,0362	487	3,40
493,6934	2,9307	494	3,95
509,2259	5,761	509	5,9
534,9951	9,1429	535	7,35
543,8056	0,0407	543	0,89
576,0367	40,4903	576	10,49
591,4641	58,8136	591	38,51
614,937	113,0518	615	35,6
635,7952	24,9309	636	12,08
645,3490	7,0329	646	5,41
649,3662	1,2702	649	2,74
691,1139	30,4975	691	33,39
712,4485	22,4434	715	31,46
792,9727	84,362	793	17,81
805,8003	7,6977	806	6,71
856,8528	3,3030	856	4,35
869,6762	0,1063	870	1,07
878,3461	18,445	878	10,66
928,2569	12,0445	928	5,40
960,648	2,177	960	2,62
1005,2851	0,6803	1005	1,89
1032,4779	99,1357	1032	35,33
1073,7985	8,5982	1074	7,09
1055,1457	30,8142	1055	7,95
1044,1275	0,6329	1044	2,18
1064,5292	3,6947	1064	3,55
1120,7201	477,8486	1121	40,31
1136,7436	150,8962	1137	30,57
1149,6124	119,4364	1150	36,43
1165,5123	4,6621	1166	5,2
1215,4252	641,7549	1216	21,20
1226,9296	36,7846	1227	9,76
1243,4093	1,1043	1243	2,54
1287,7604	40,3600	1288	35,30
1412,9579	0,0675	1413	0,77
1344,2812	30,0623	1344	10,82
1365,1135	23,318	1365	10,21
1396,3099	25,2157	1396	9,94
1409,9726	32,0873	1410	15,7
1415,1110	52,1800	1415	57,44
1465,7505	35,3246	1466	9,8
1510,1138	32,0764	1510	13,69
1525,0685	12,404	1525	9,54
1516,5850	17,8275	1541	8,68
1550,2306	9,1067	1550	5,96
1654,7696	4,6722	1655	5,22
1672,4556	59,4876	1672	17,6
1651,0185	244,4786	1652	37,81
1667,1045	173,5197	1667	28,97
1907,4757	1730,2715	1907	100
1907,5651	1561,9748	1908	98,58
1922,6911	1147,392	1923	81,93
1948,9383	207,1352	1949	38,8
2023,8537	635,5049	2024	58,86
3057,431	15,6868	3057	9,58
3063,8417	38,0959	3064	10,23
3116,3050	30,7326	3116	7,92
3141,2083	17,069	3141	10
3158,8636	30,2142	3160	10,87
3150,6021	29,1631	3151	11,64
3196,8028	4,3706	3250	2,83
3203,8949	0,3773	3204	1,49
3213,7435	3,2934	3214	4,39
3220,9775	4,5417	3221	5,28
3223,7251	32,5808	3224	13,8
3253,6673	30,6361	3254	13,39

[illegible]			
Calculated (Original)		Calculated (IR Plotter)	
Frequency (1/cm)	IR Intensity (a.u.)	Frequency (1/cm)	IR Intensity (a.u.)
13,7482	0,0810	14	0,06
21,6714	0,146	22	0,07
37,2653	0,0349	37	0,57
43,0721	0,424	43	0,43
56,2275	0	[redacted]	
62,0303	0,8857	62	1,15
64,5386	0,0395	64	0,17
77,2426	0,2884	77	0,65
81,7952	0,1009	[redacted]	
83,9168	3,996	84	1,95
87,4801	0,9738	[redacted]	
88,1271	0,5273	88	2,00
90,5627	0,8786	91	1,11
92,407	0,1025	92	0,98
114,8087	0,0212	115	0,18
142,3786	1,2458	142	1,3
152,0385	1,9039	152	1,51
174,2575	0,0093	174	0,12
220,8404	0,1189	221	0,42
250,4981	7,5847	251	5,31
253,1086	0,579	253	0,93
288,3403	8,9216	288	3,64
307,9350	5,8034	308	2,95
366,4088	0,0038	366	0,07
372,8384	20,4517	373	6,27
402,9900	11,12	403	4,06
404,1511	13,8461	404	4,53
407,8522	21,4662	408	5,64
412,1451	23,5867	412	5,91
421,2080	141,4138	421	14,49
430,4183	26,4878	430	6,26
438,9692	3,6825	439	2,14
449,0203	8,4763	449	3,51
454,3819	2,7595	454	2,02
473,298	6,5023	473	3,11
476,8979	0,9712	477	1,2
494,2057	1,2166	494	1,34
507,9666	3,2137	508	2,18
535,0138	9,028	536	3,73
543,5346	0,2213	544	0,41
556,1933	9,1713	556	3,69
572,9387	12,6050	573	4,34
579,5682	35,1040	580	7,21
592,0082	41,2064	592	8,79
615,8306	216,7358	616	13,16
638,5442	16,9859	640	6,53
654,0034	8,6399	653	3,58
694,2426	30,3096	694	6,77
763,1665	1,2047	763	1,34
784,6203	3,2176	785	13,19
784,8687	42,6868	[redacted]	
812,2245	6,0376	812	2,69
856,6243	3,1642	856	2,17
881,4031	0,2719	881	0,63
915,9627	13,4634	916	8,91
949,5699	11,9802	950	4,12
983,4277	2,6742	983	1,55
1020,2615	3,5203	1020	2,66
1023,8723	17,6772	1024	7,47
1055,0759	30,219	1055	10,60
1062,5611	3,2583	1063	2,15
1125,1313	468,1523	1125	16,36
1157,0826	37,5504	1157	7,95
1154,0297	58,6095	1154	9,34
1166,7856	14,6724	1167	7,62
1213,9562	455,5101	1213	11,19
1214,9776	70,1777	1215	18,2
1226,6895	17,5054	1227	5,1
1287,94	44,6109	1288	8,14
1298,2534	31,2546	1298	6,61
1315,3015	0	[redacted]	
1332,2412	105,9841	1332	12,54
1391,0371	36,3863	1391	7,35
1399,5524	70,9468	1400	5,57
1406,6094	19,7074	1407	5,41
1420,8148	14,7768	1421	7,13
1466,5971	15,6719	1467	4,61
1505,5062	18,0819	1506	7,51
1529,4815	11,0478	1529	4,31
1561,4191	11,7377	1561	8,17
1550,8212	5,3733	1551	2,82
1559,1269	14,4796	1559	4,64
1652,8273	182,8359	1653	16,47
1656,5762	290,9882	1657	20,79
1667,2367	16,6239	1667	9,17
1905,1332	3638,3191	1905	100
1903,1373	3734,1087	[redacted]	
1919,9544	3173,9086	1920	41,72
1947,1264	215,2432	1947	17,87
2023,6281	535,992	2023	17,68
3060,8031	16,0663	3061	6,92
3064,6455	17,2759	3065	5,06
3120,5368	8,5835	3121	3,69
3139,4658	28,612	3139	5,25
3156,9675	12,1032	3159	5,73
3186,471	14,3744	3186	4,62
3207,5735	0,6741	3208	1
3212,4637	1,7202	3213	1,6
3218,9847	15,5962	3219	4,49
3257,5984	20,7052	3258	6,5
3263,5491	0,6765	3264	1
3608,0117	44,5663	3580	8,13

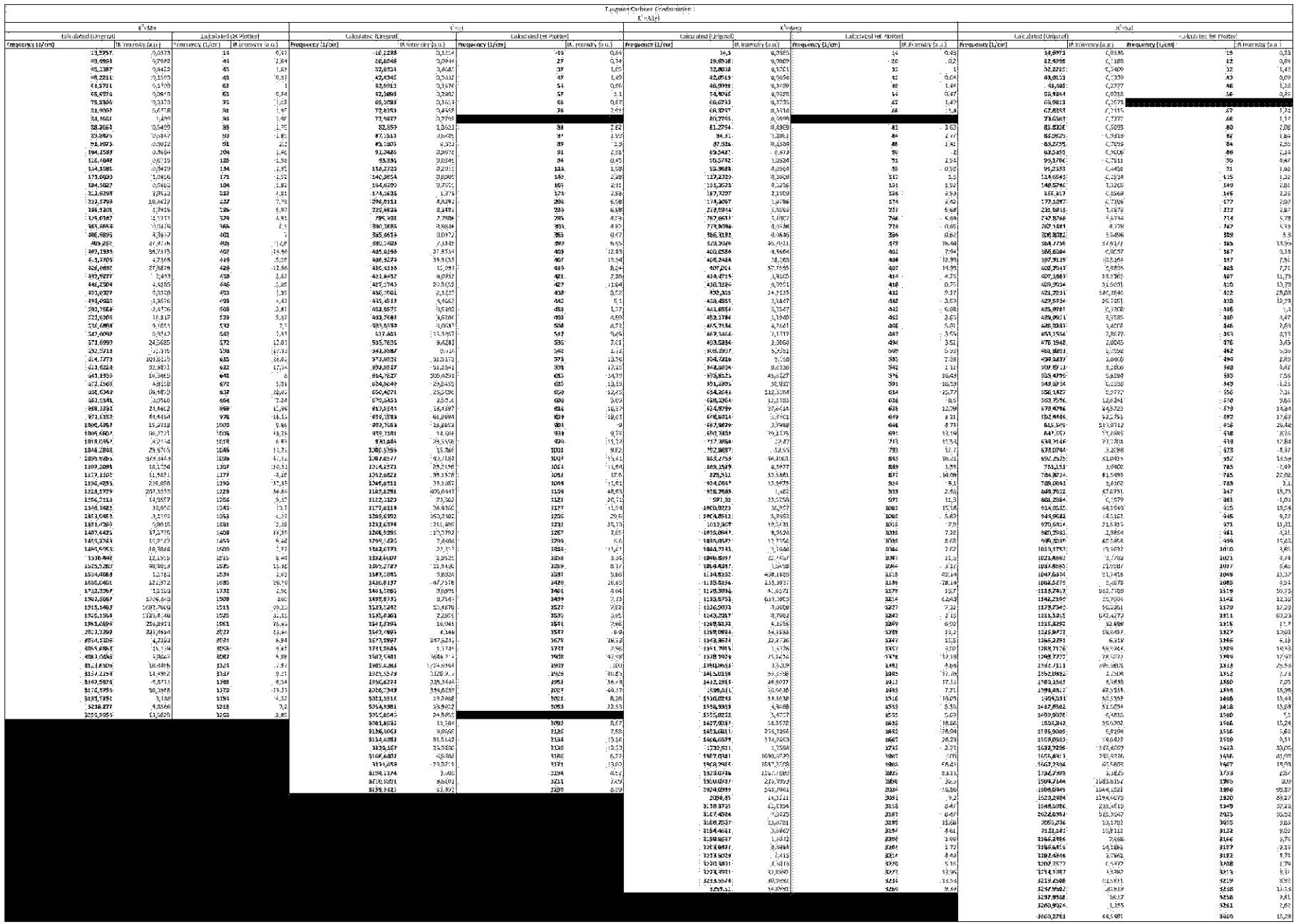
Tungsten Carbide Coordination
K²=Mn
K²=Ni
K²=Mn+Ni
Calculated (Original)
Calculated (GF Plotter)
Frequency (1/cm)
IR Intensity (a.u.)

Appendix -3A(i):

Optimized structures for Carbenes (Cr) (NBO)

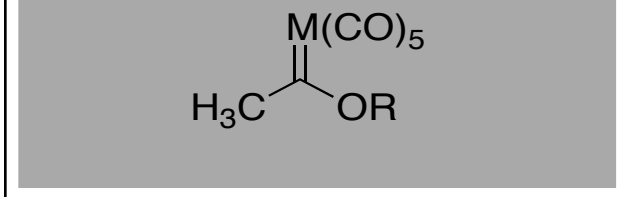

M	R
Cr	Me

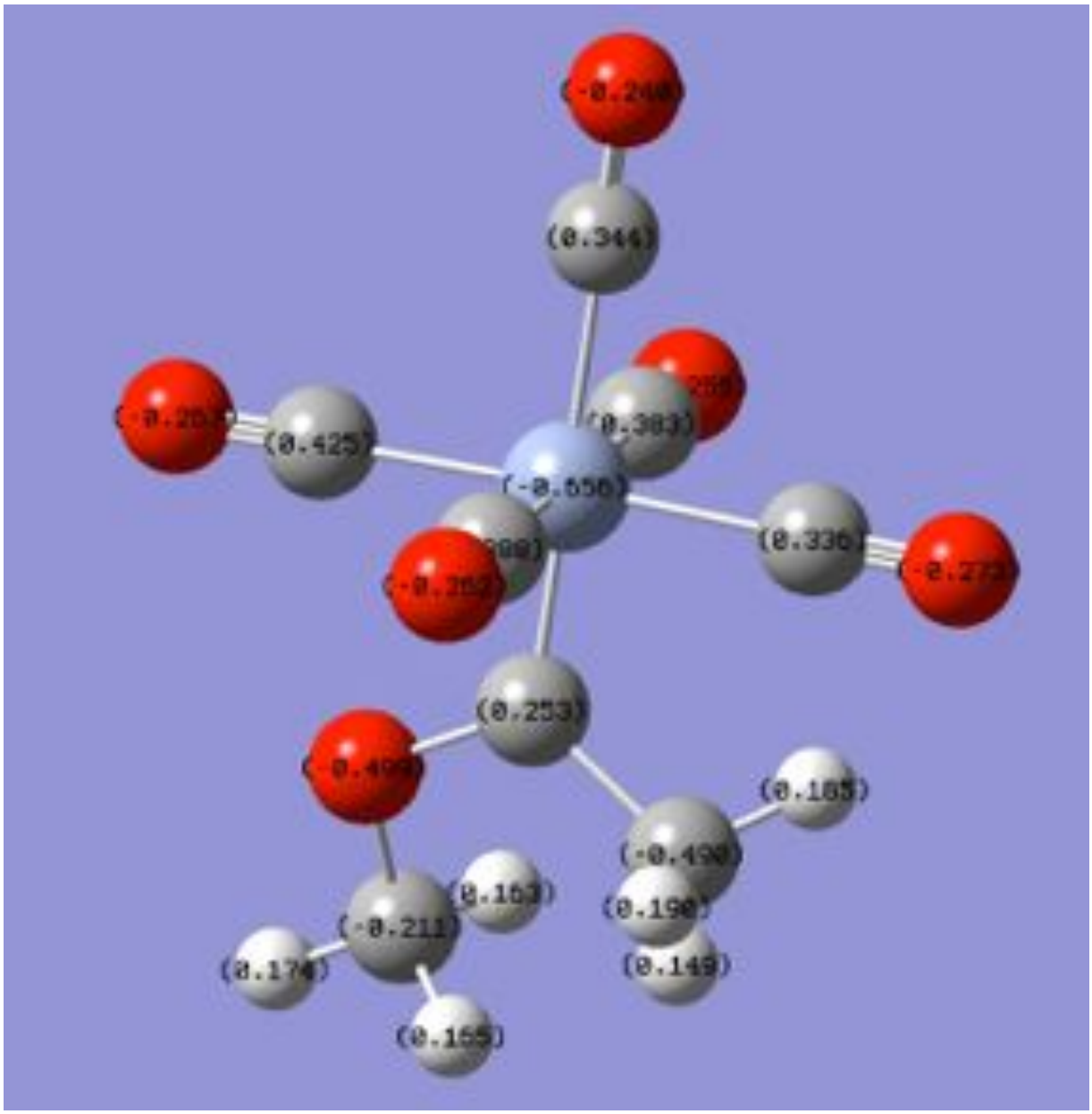

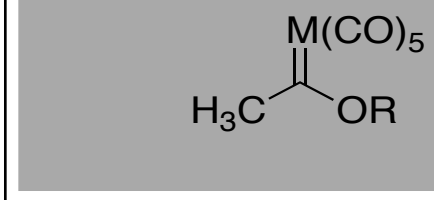

M	R
Cr	Et

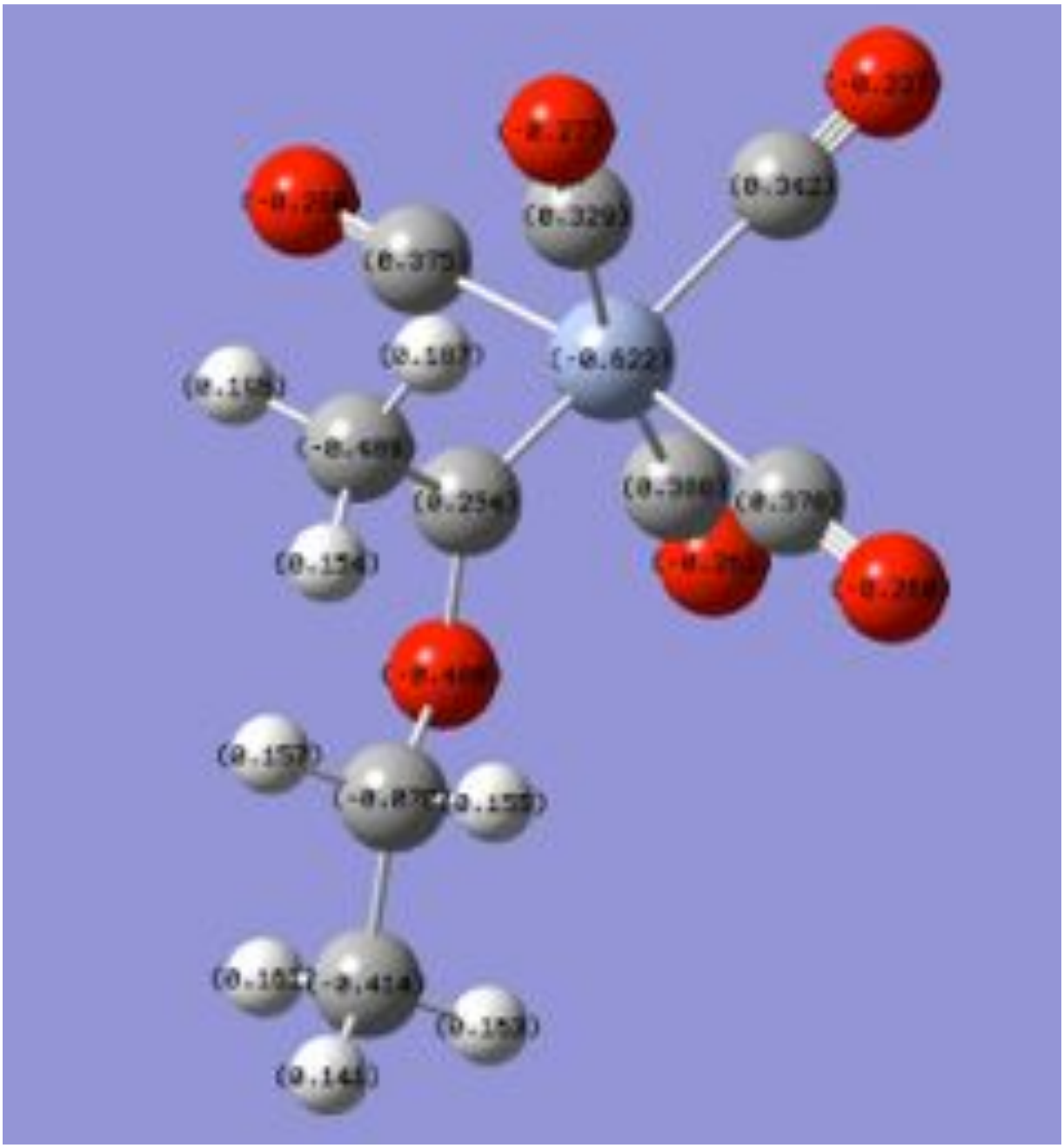

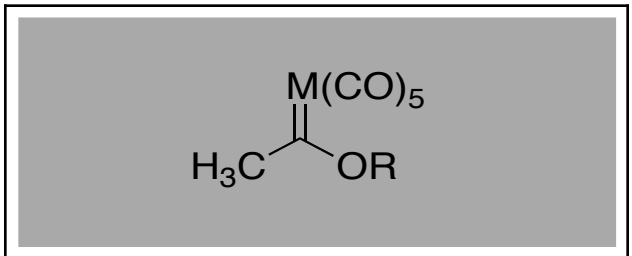

M	R
Cr	Allyl

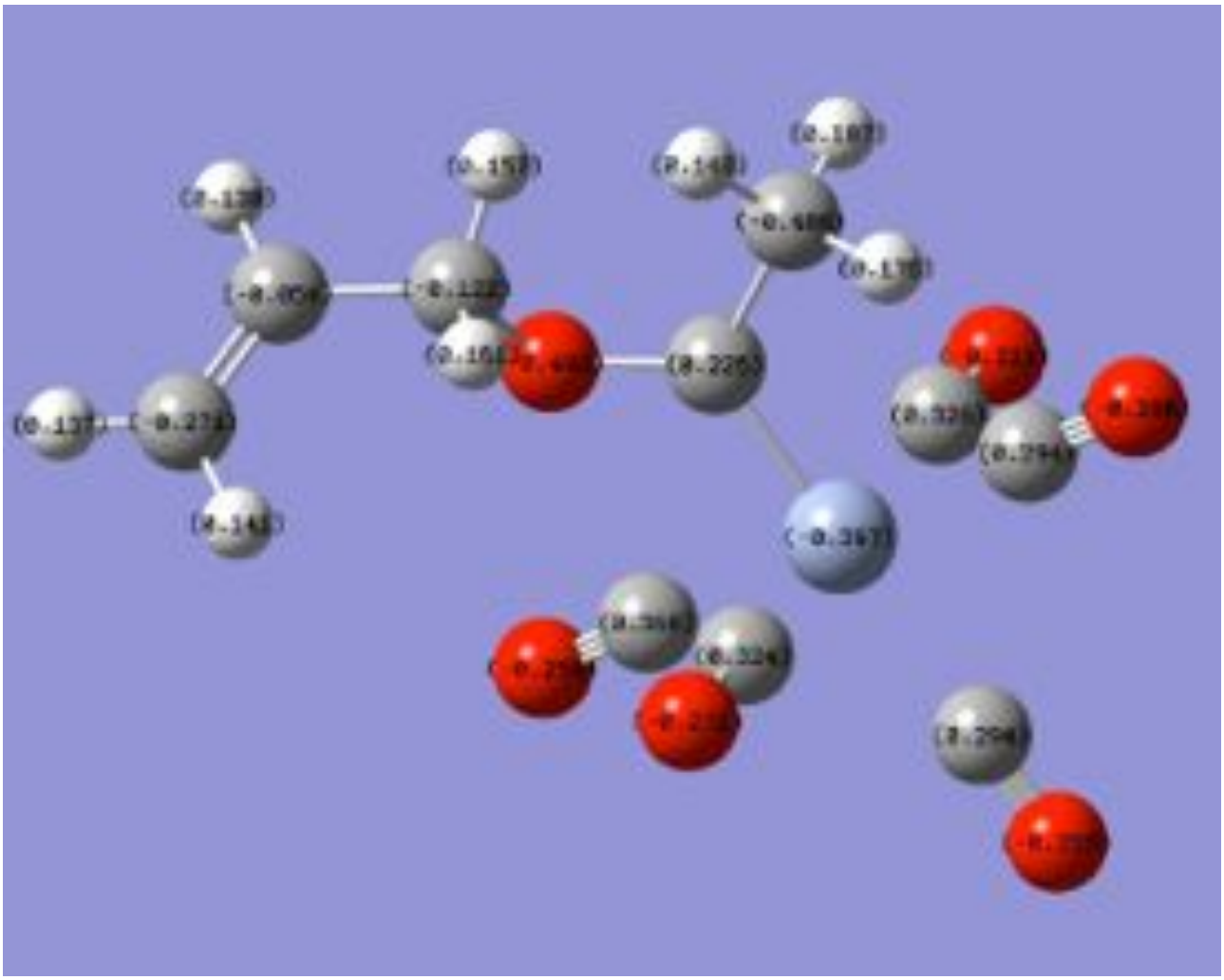

Appendix -3A(ii):

Optimized structures for Carbenes (Mo) (NBO)

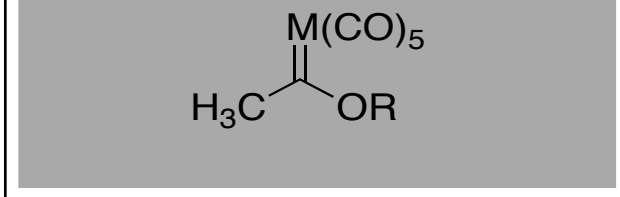

M	R
Mo	Me

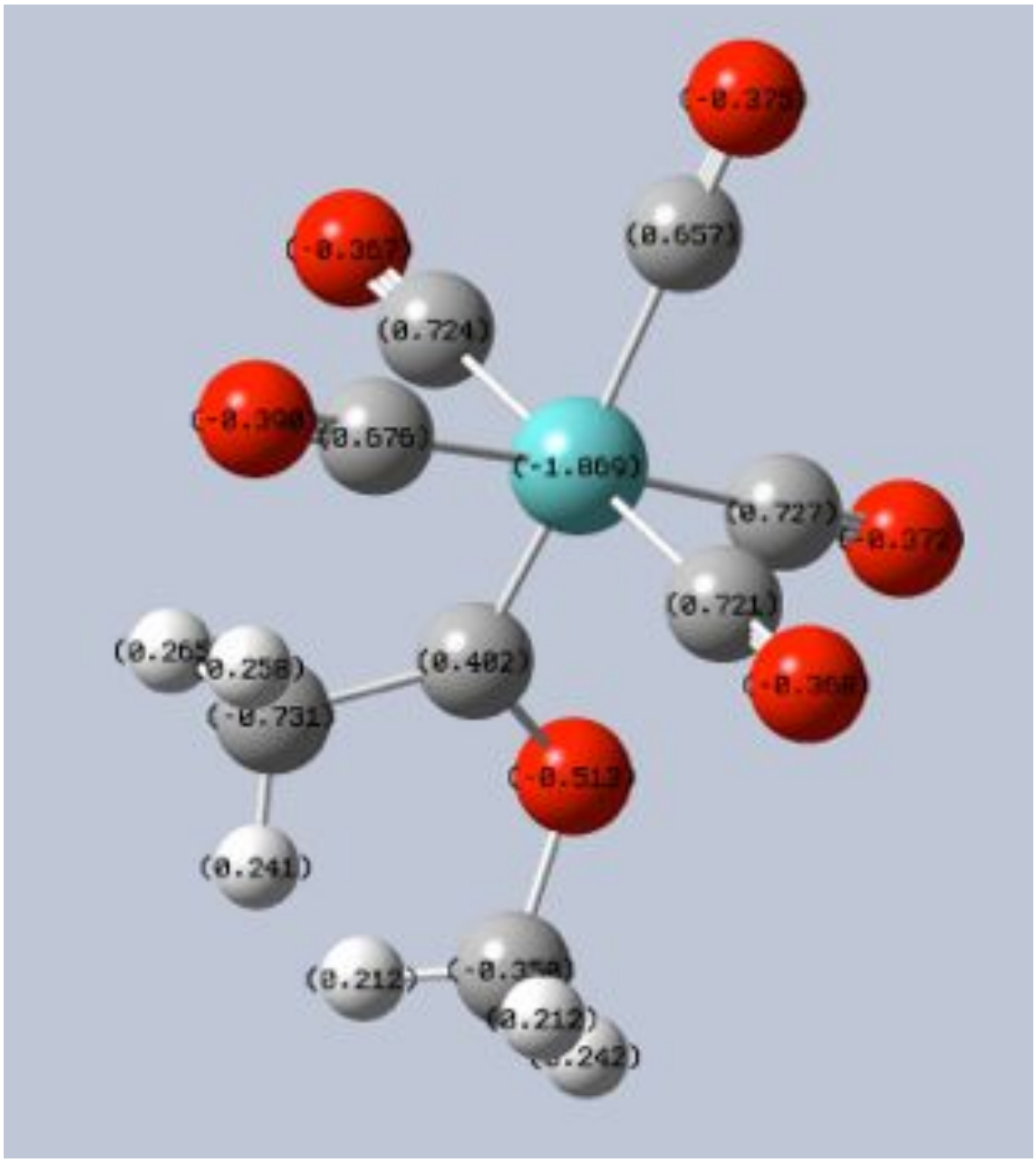

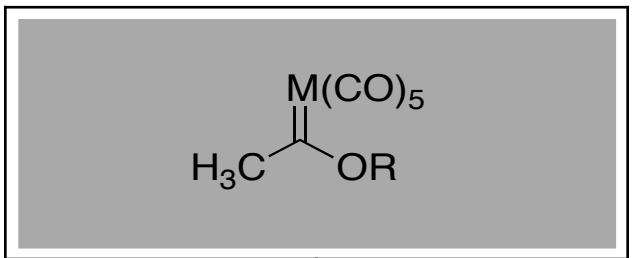

M	R
Mo	Et

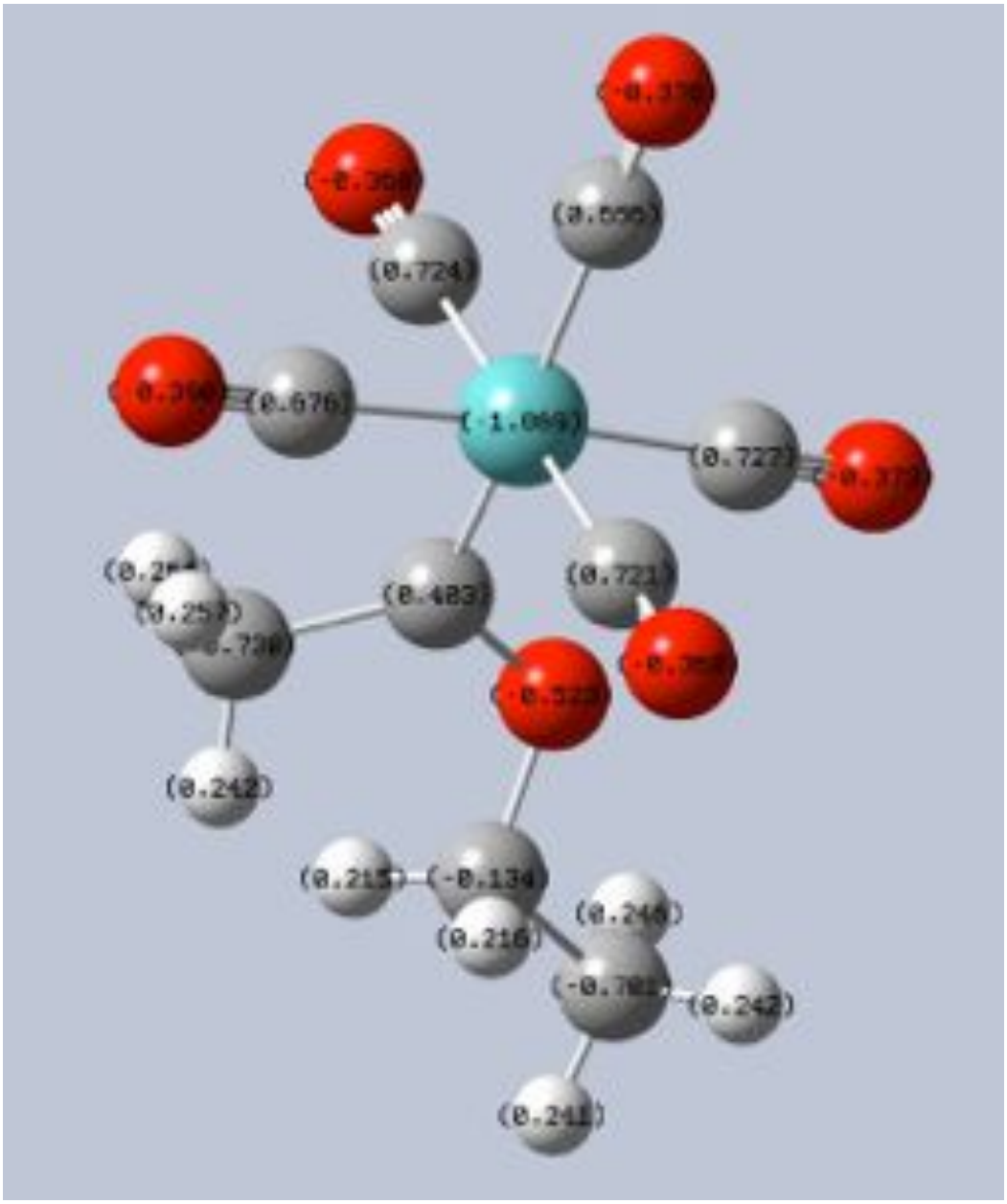

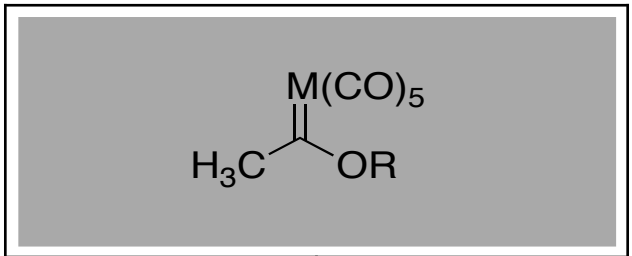

M	R
Mo	Allyl

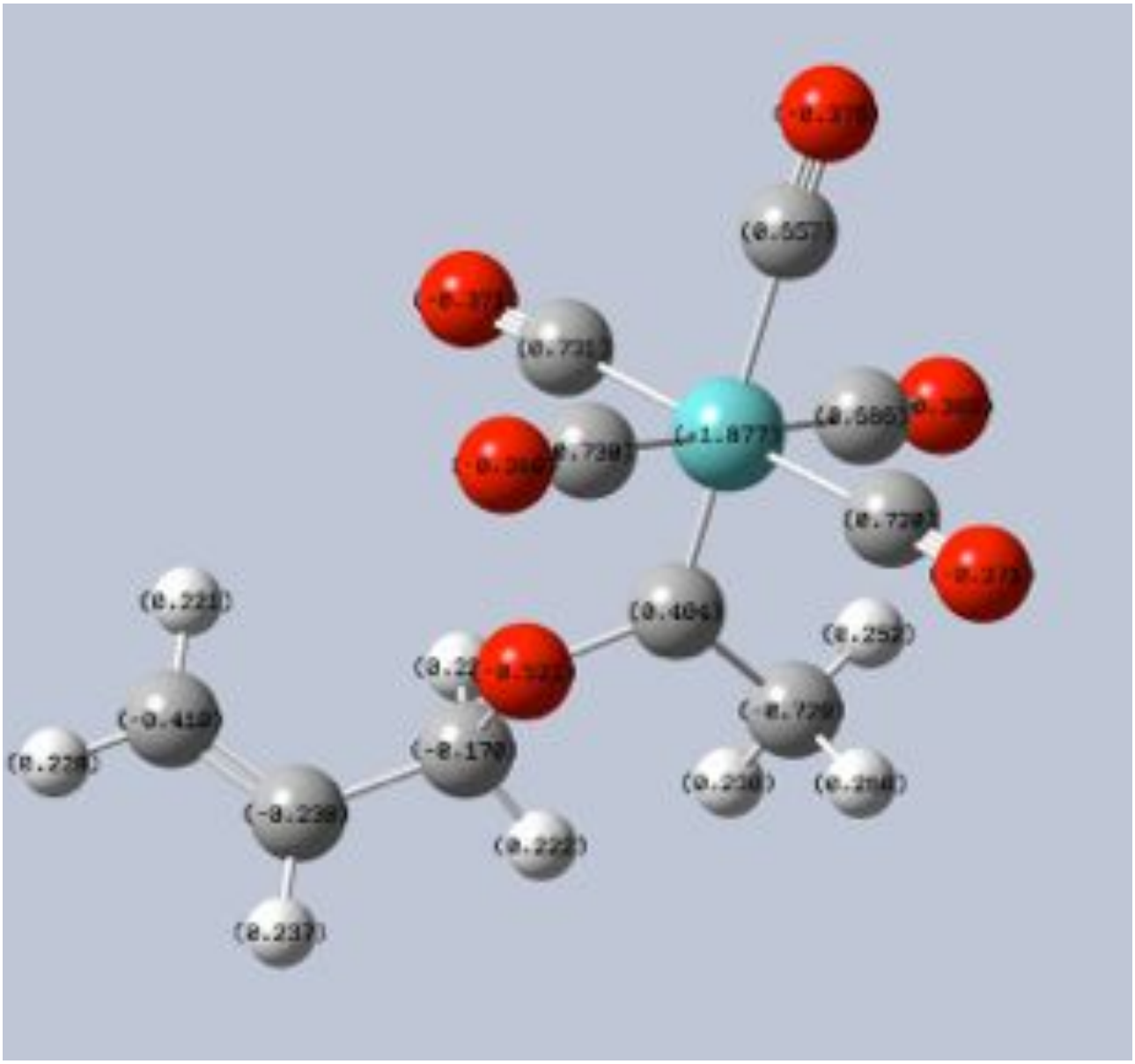

Appendix -3A(iii):

Optimized structures for Carbenes (W)(NBO)

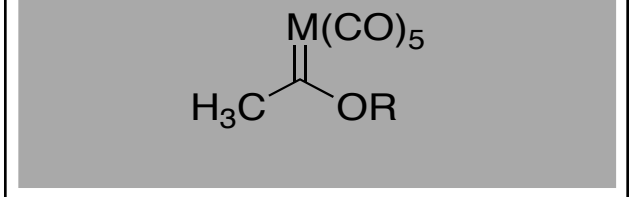

M	R
W	Me

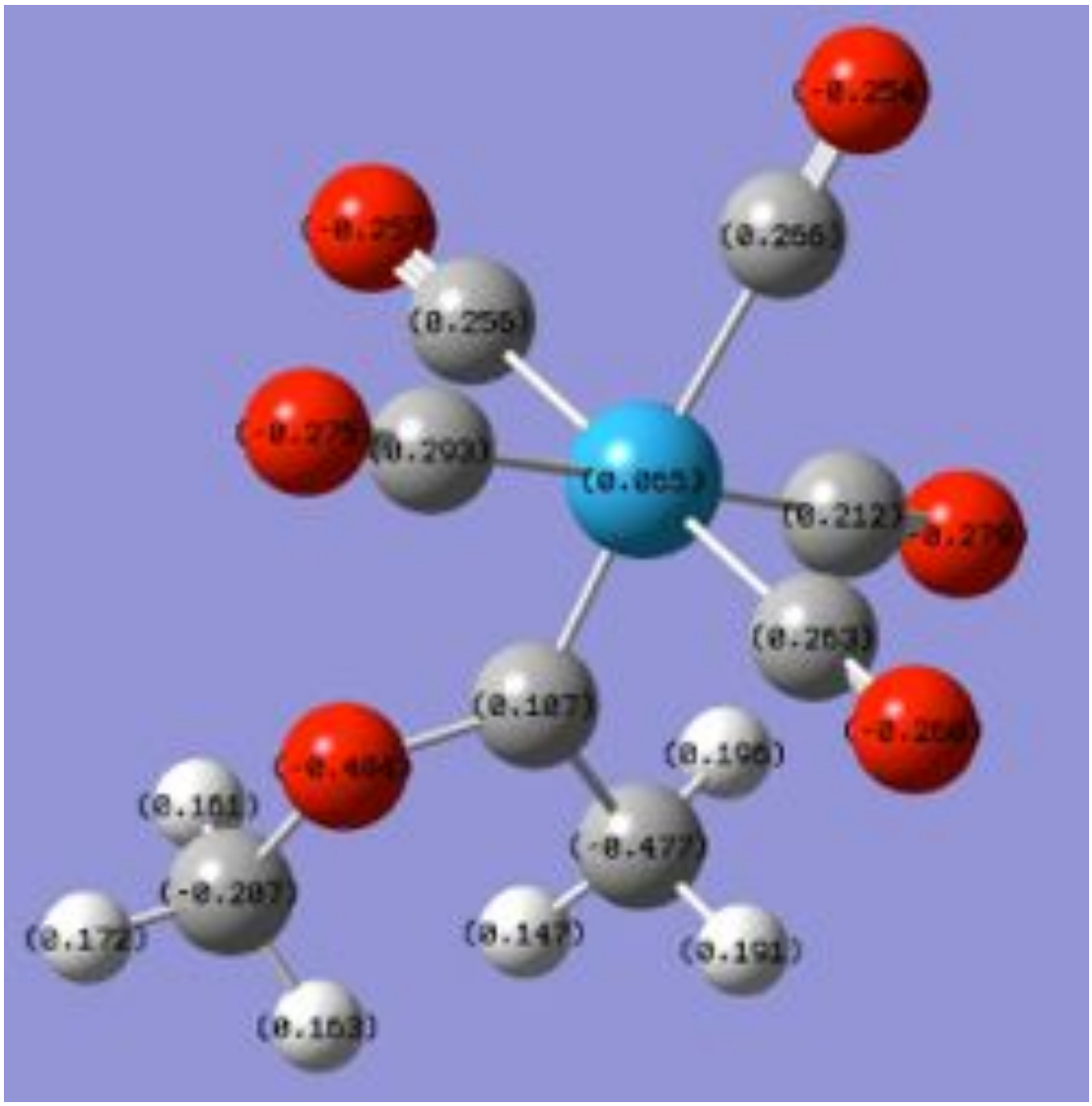

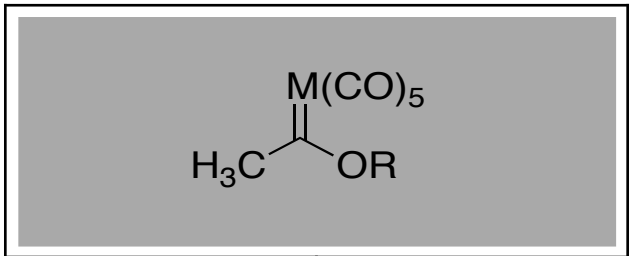

M	R
W	Et

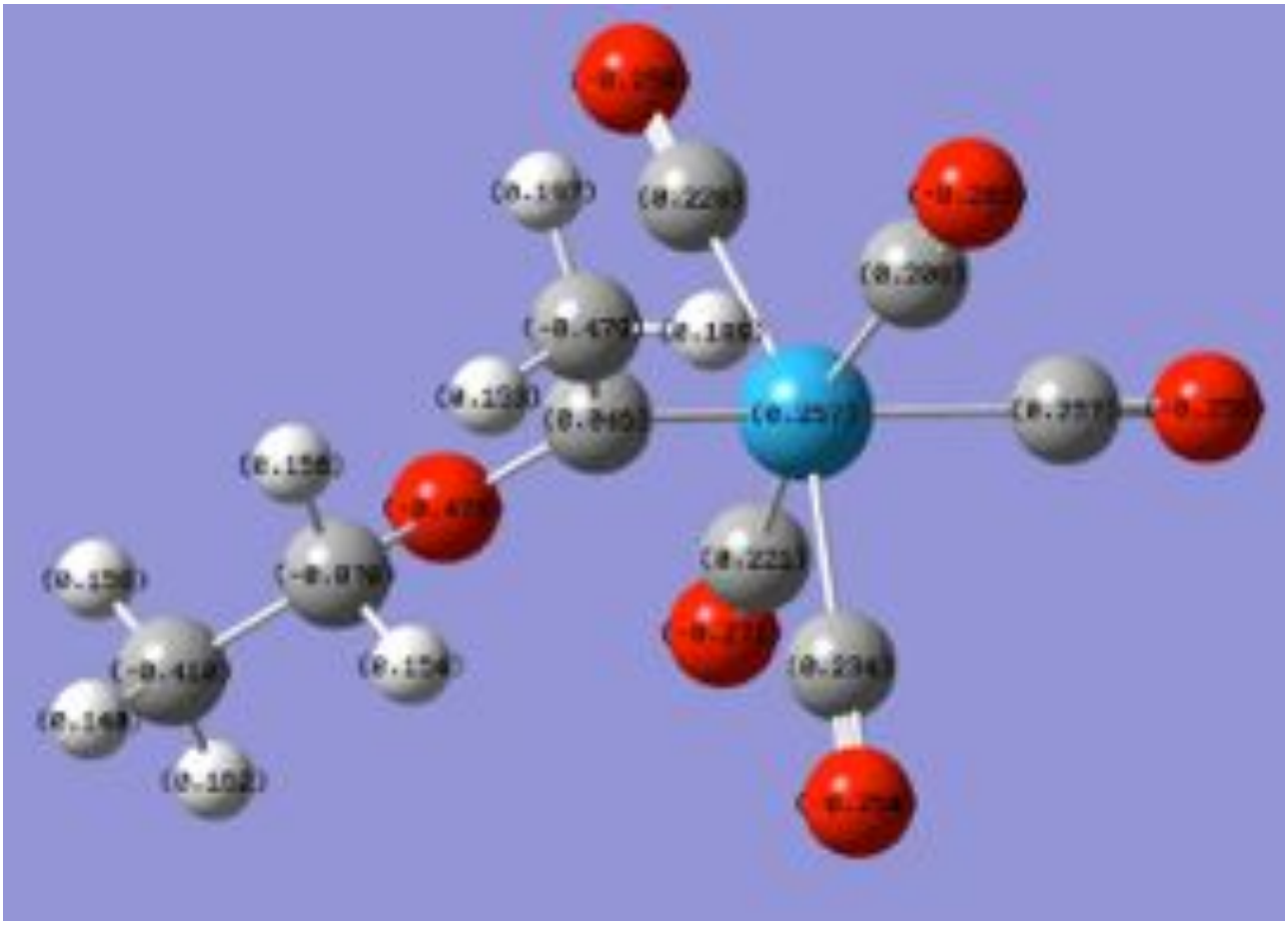

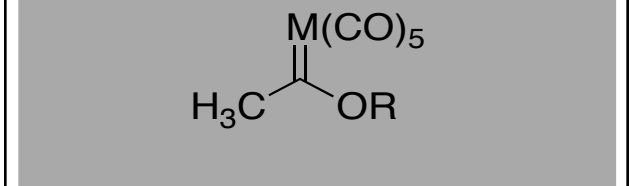

M	R
Cr	Me

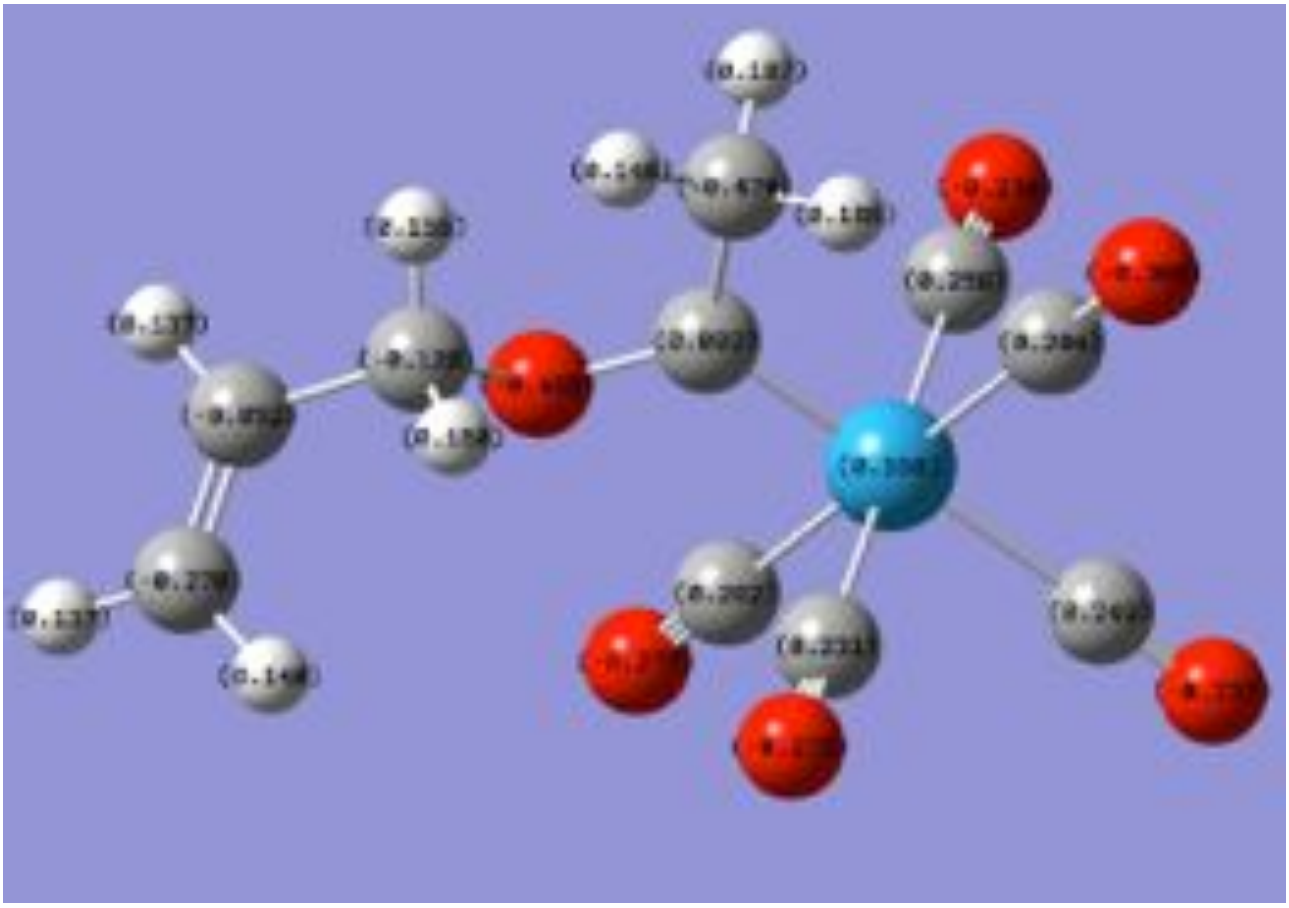

Appendix **-3B:**

Optimized structures for condensation products (Cr)(NBO)

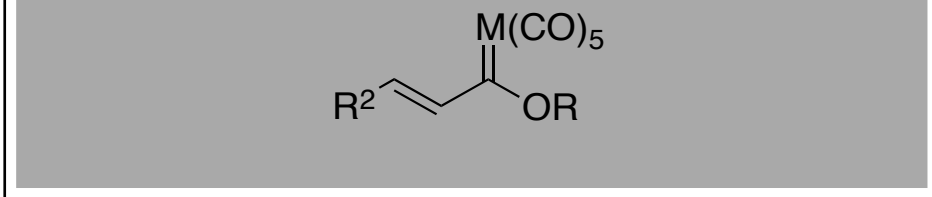

M	R	R²
Cr	Me	Me

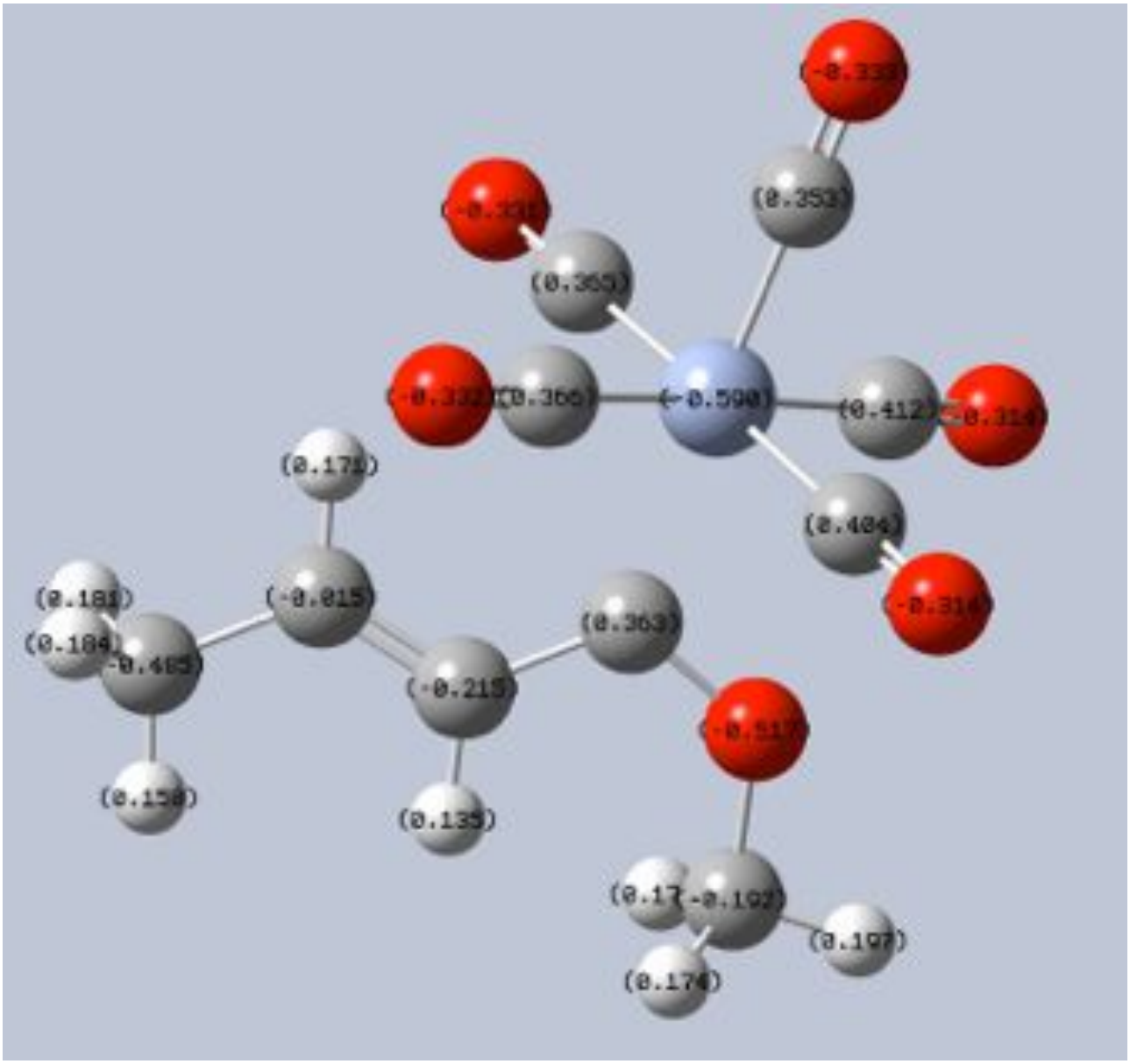

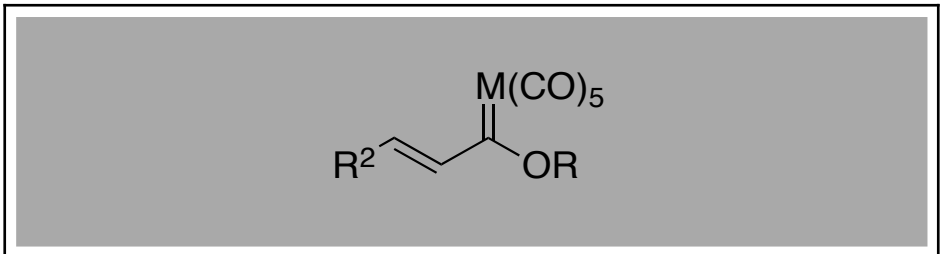

M	R	R²
Cr	Me	Phenyl

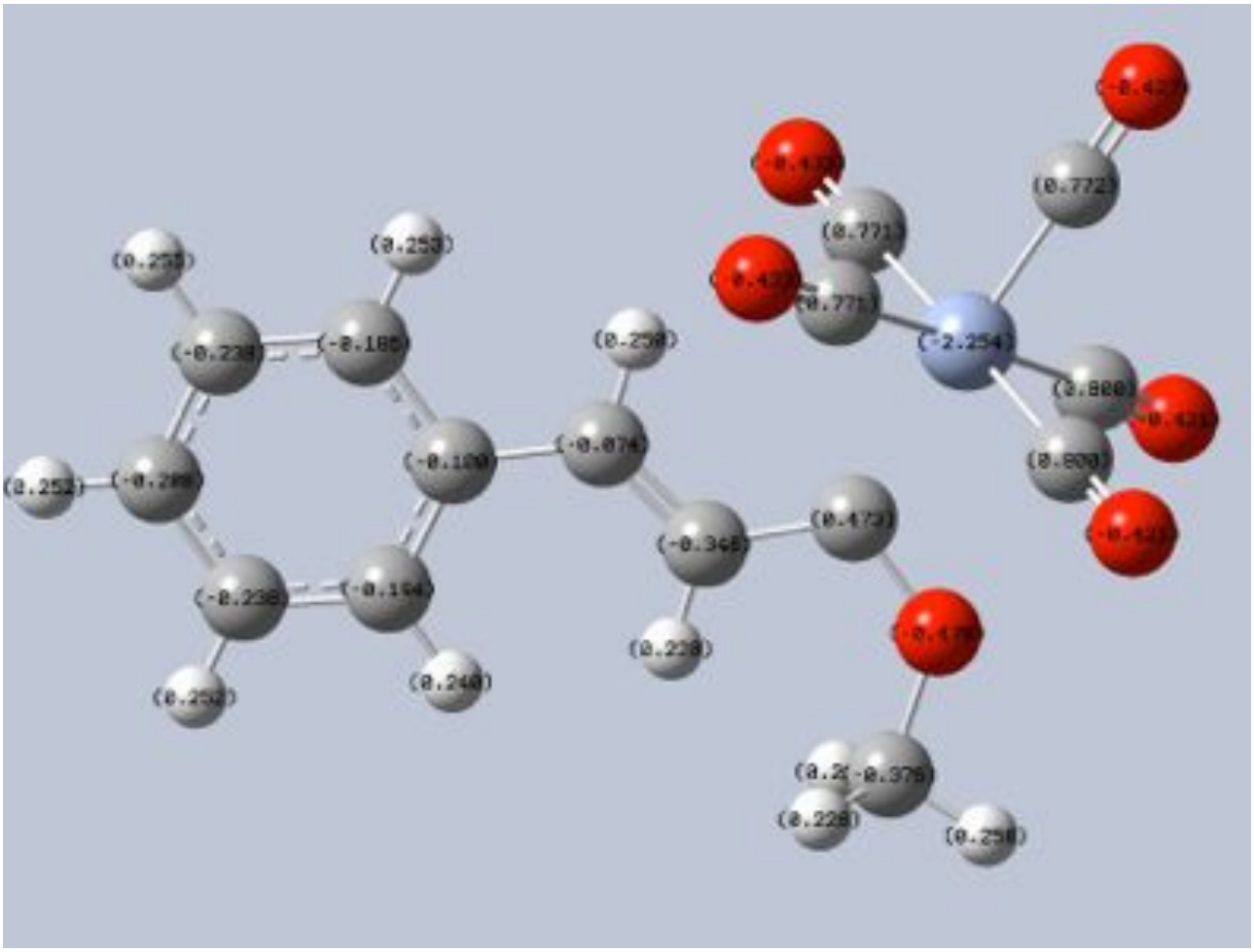

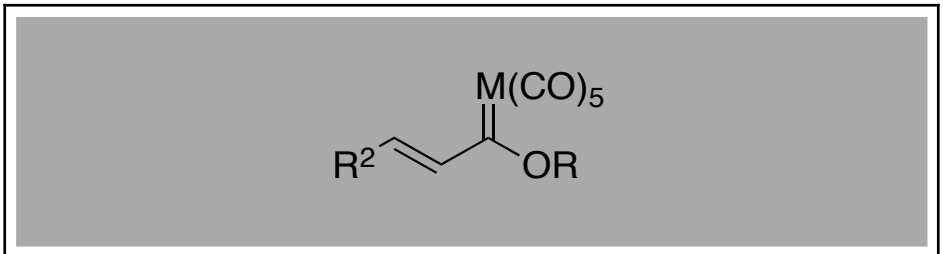

M	R	R²
Cr	Me	2-(HO)Ph

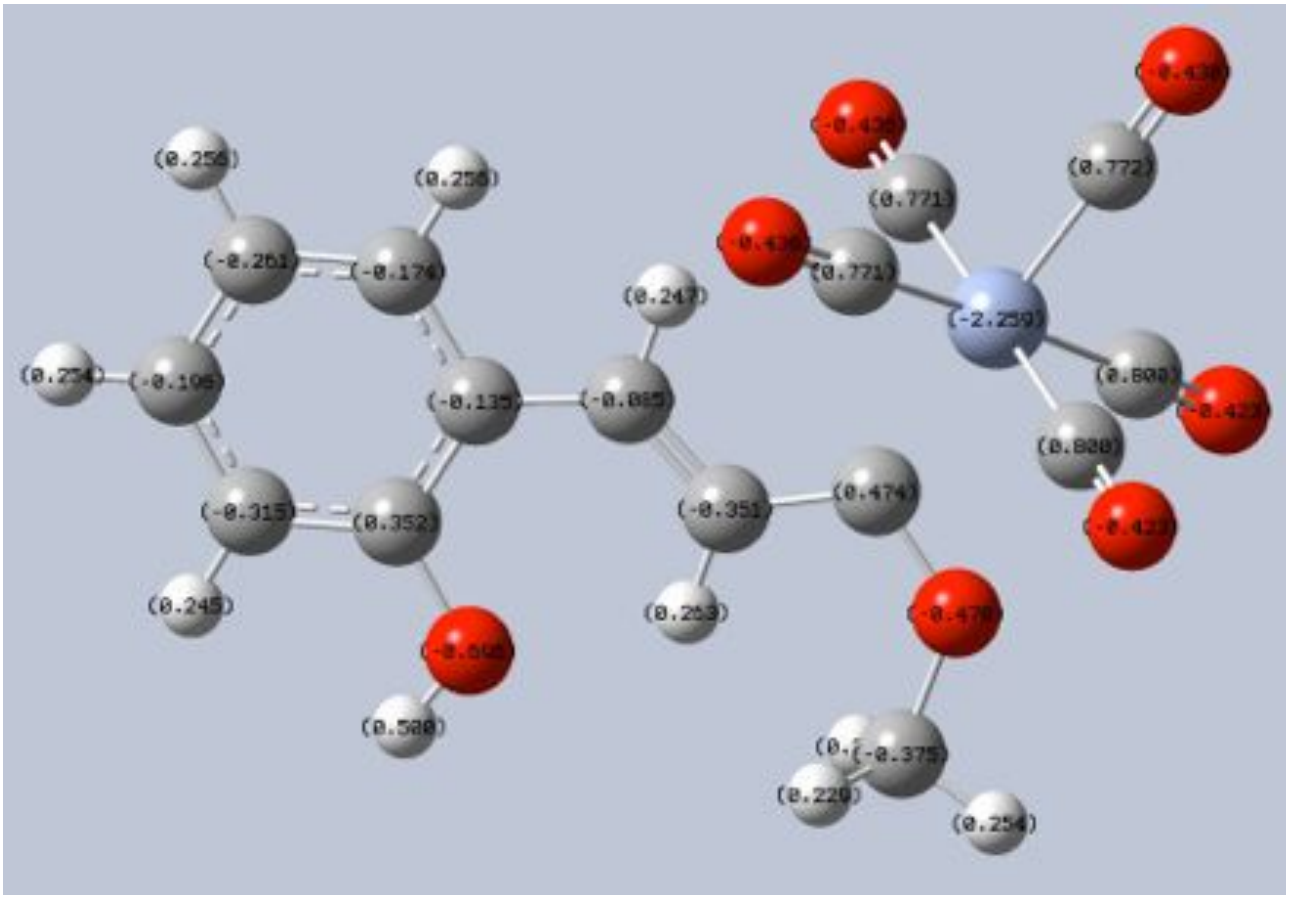

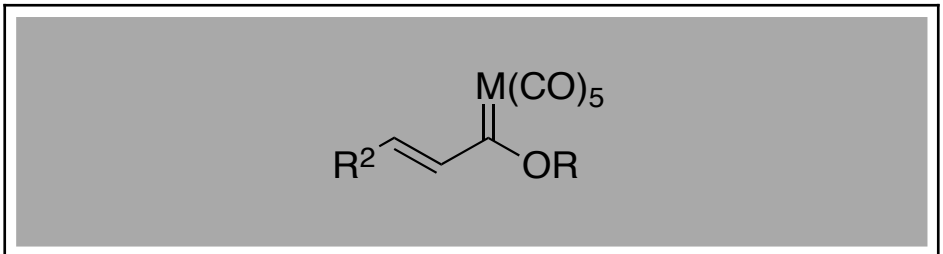
M(CO)5
R2
OR

M	R	R²
Cr	Et	Me

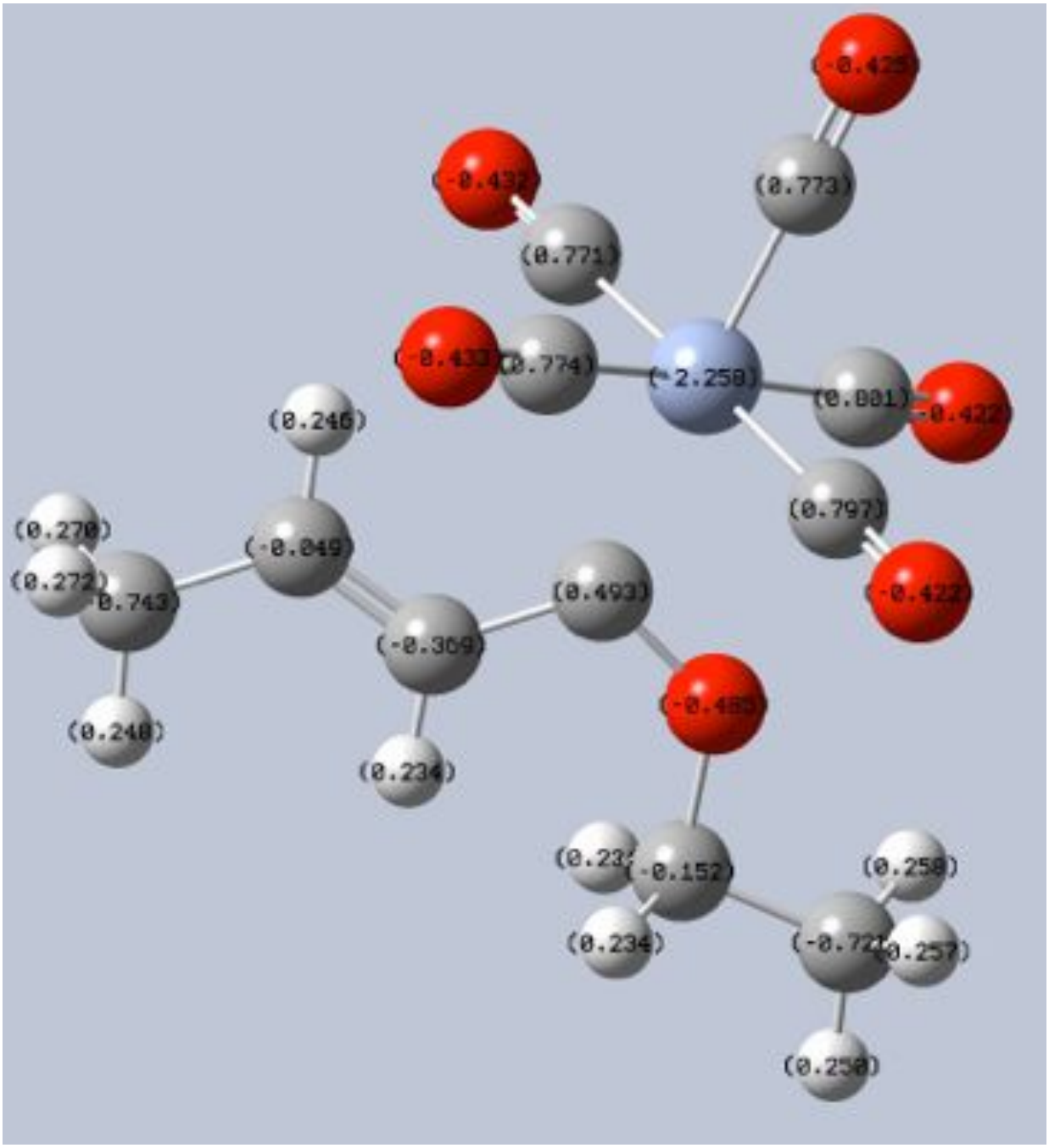
(0.773)
(0.771)
(0.774)
(-2.258)
(0.246)
(0.270)
(-0.049)
(0.272)
(0.743)
(0.493)
(-0.369)
(0.248)
(0.234)
(-0.152)
(0.258)
(0.234)
(0.257)

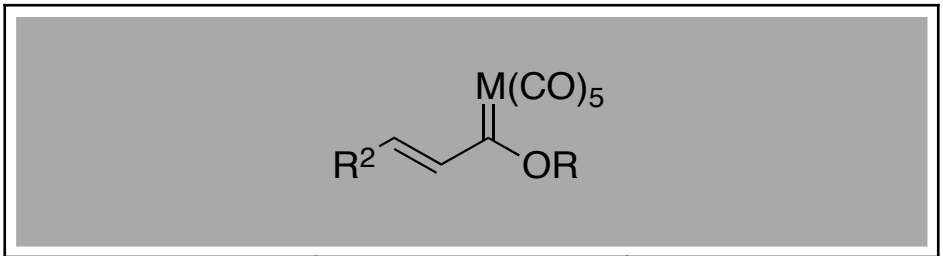
M(CO)5
R2
OR

M	R	R²
Cr	Et	Et

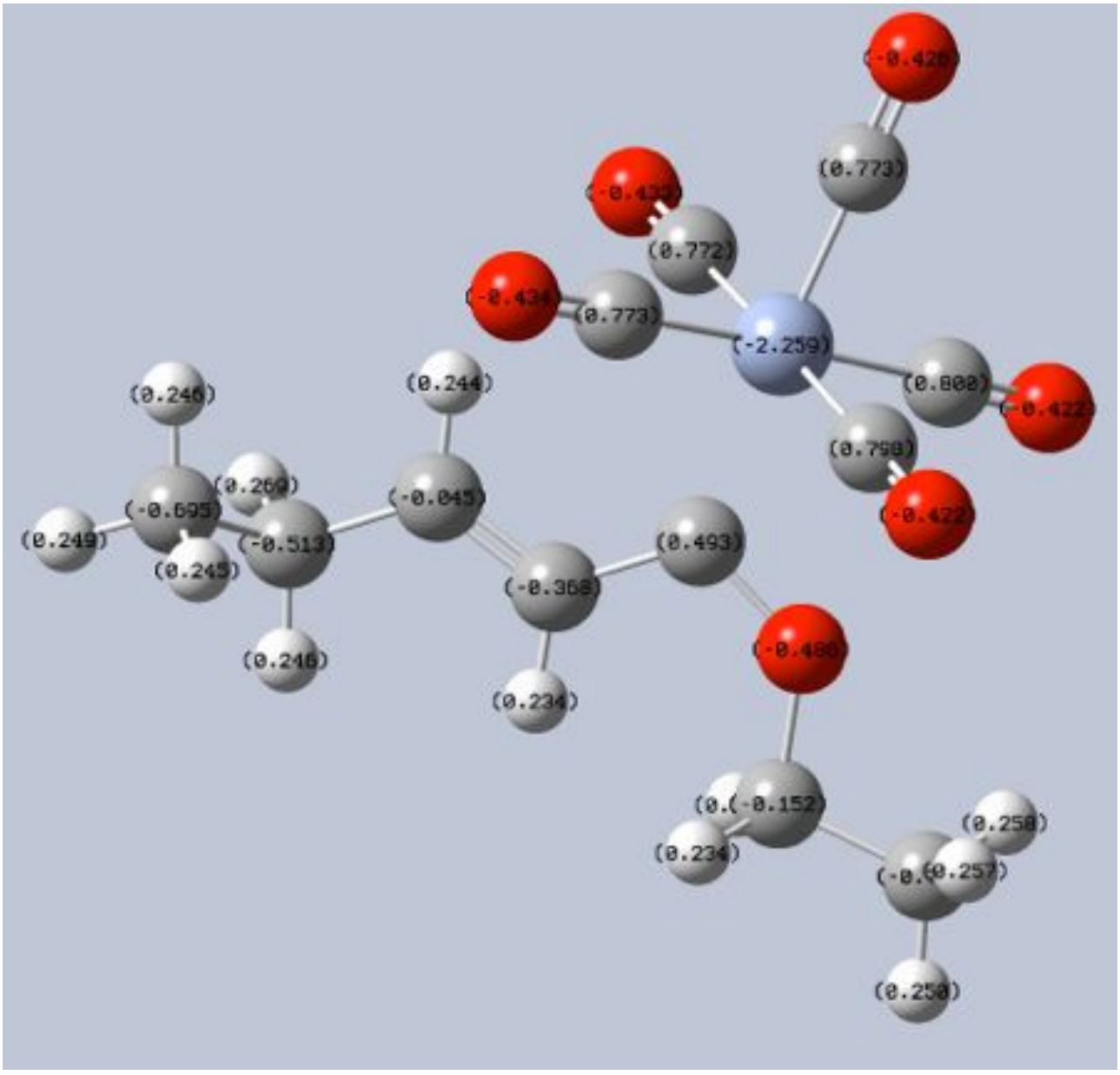
(-0.428)
(0.773)
(-0.428)
(0.772)
(-0.434)
(0.773)
(-2.259)
(0.808)
(-0.422)
(0.798)
(-0.422)
(0.244)
(0.246)
(0.260)
(-0.695)
(0.249)
(-0.513)
(-0.045)
(0.245)
(0.493)
(-0.368)
(0.246)
(-0.480)
(0.234)
(0.(-0.152)
(0.234)
(0.258)
(-0.(0.257)
(0.258)

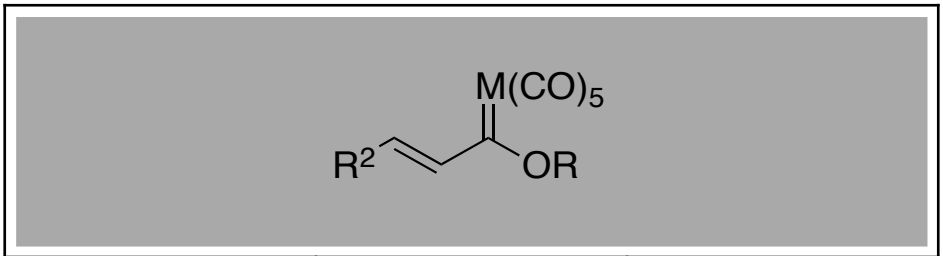

M	R	R²
Cr	Et	Phenyl

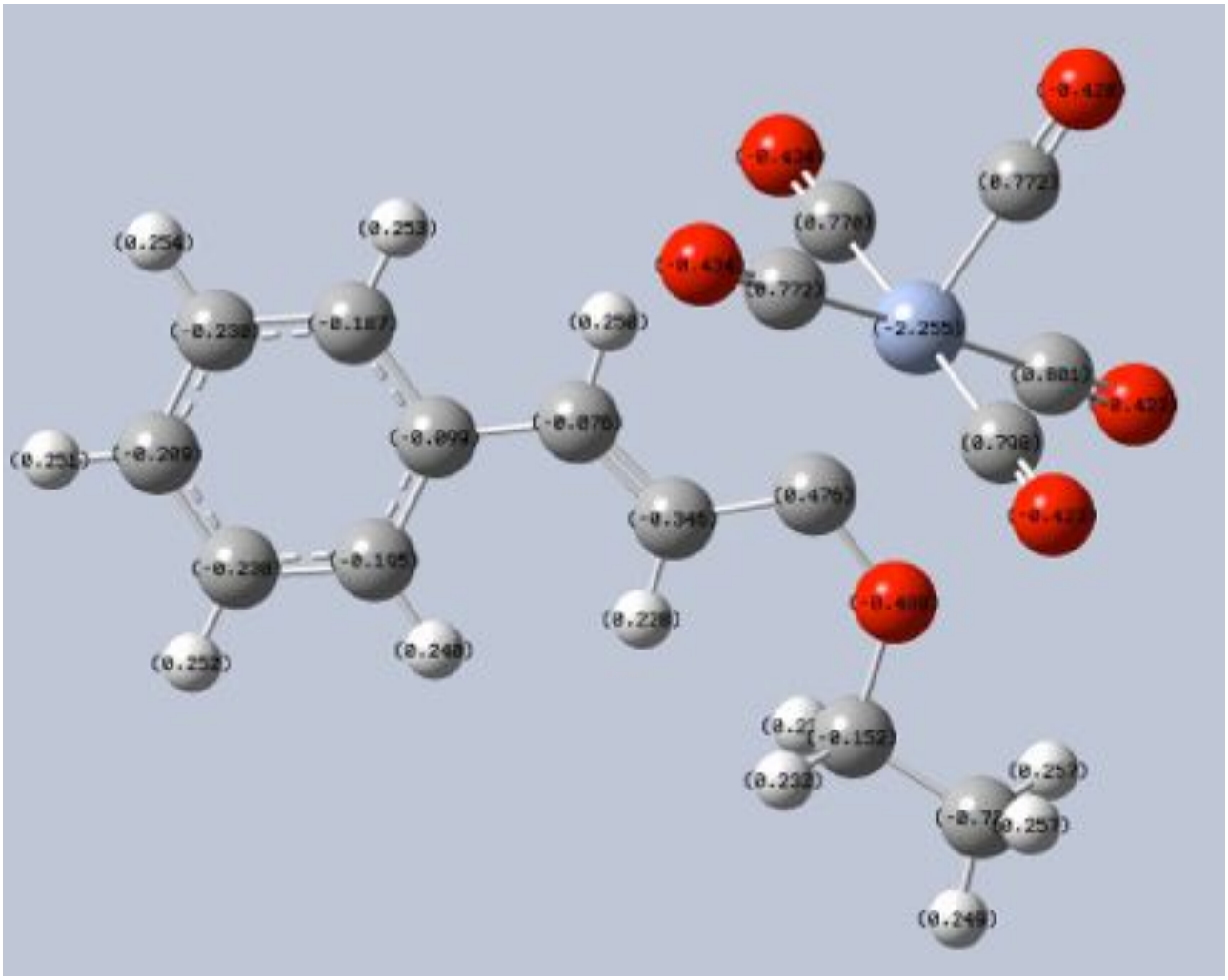

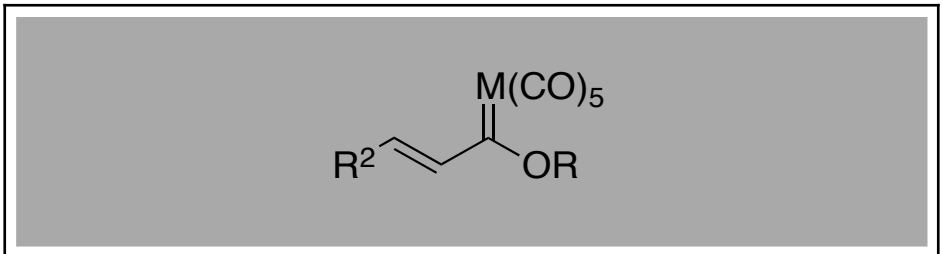

M	R	R²
Cr	Et	2-(HO)Ph

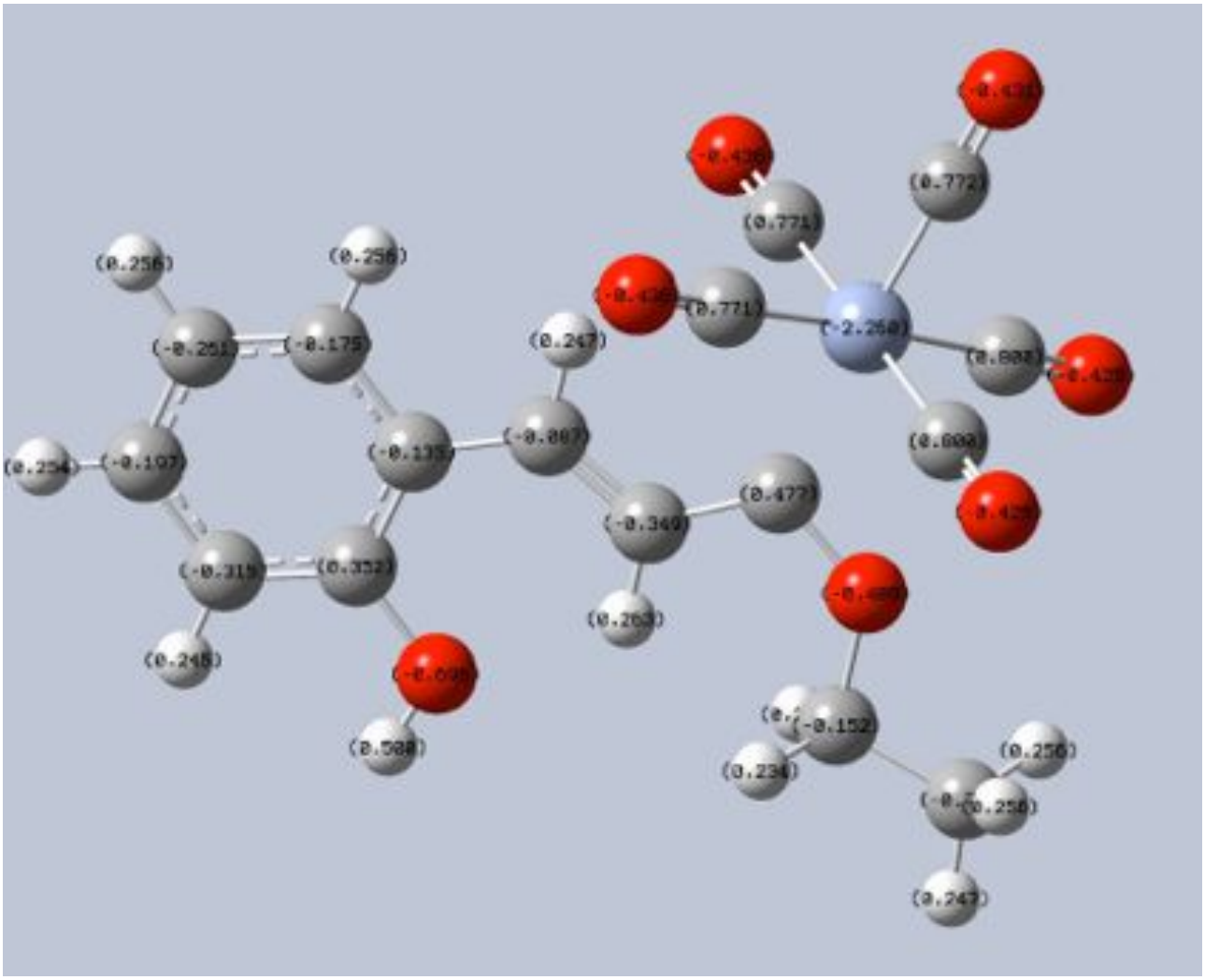

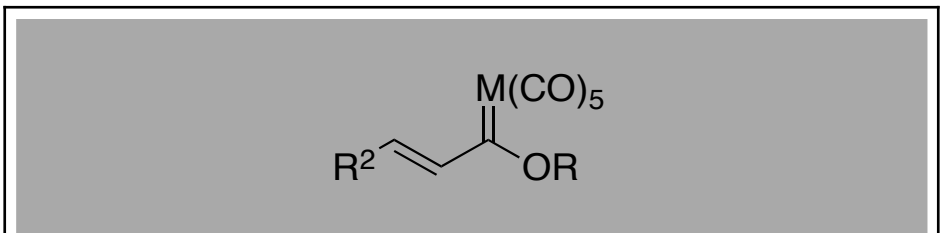

M	R	R²
Cr	Allyl	Me

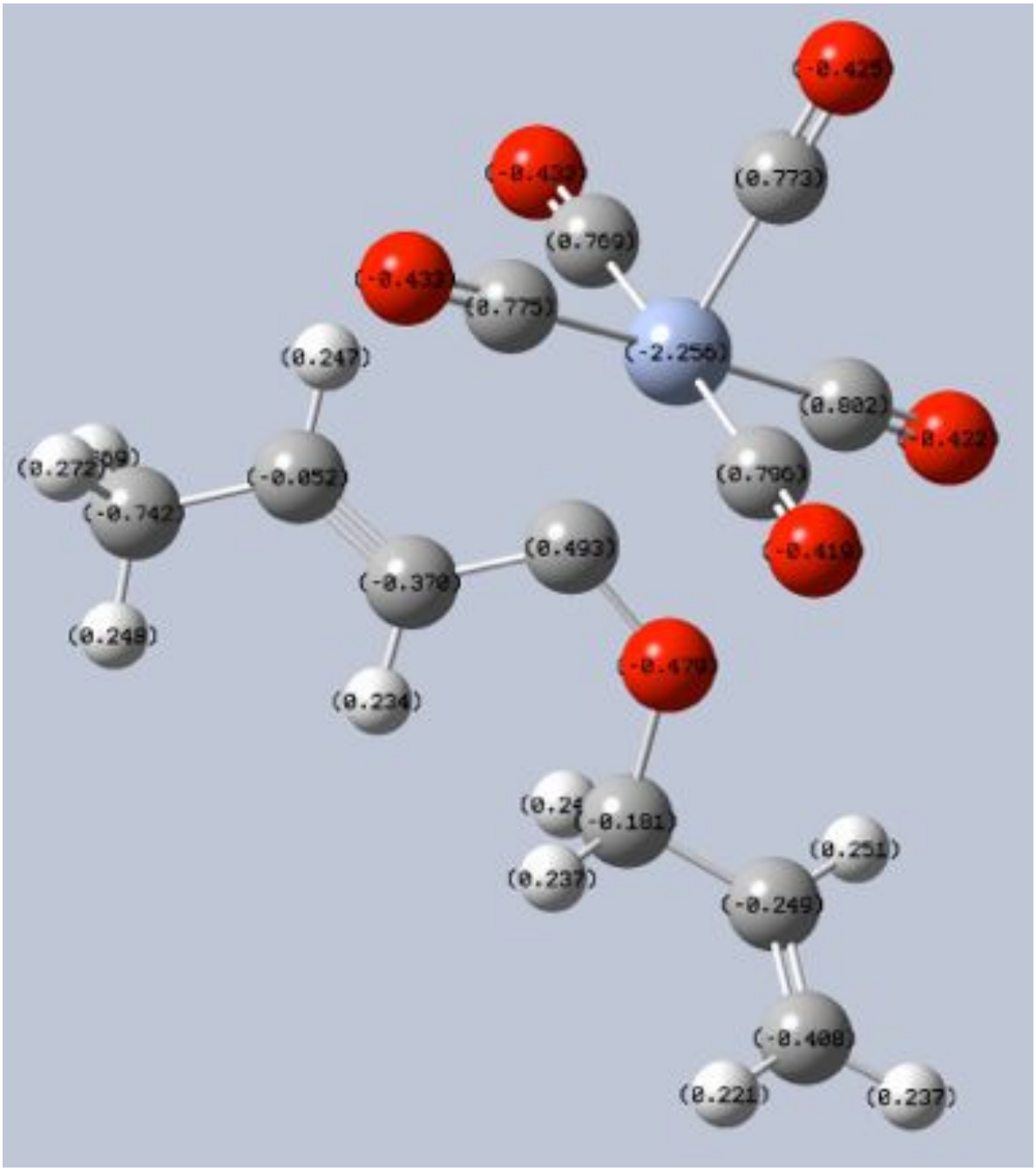

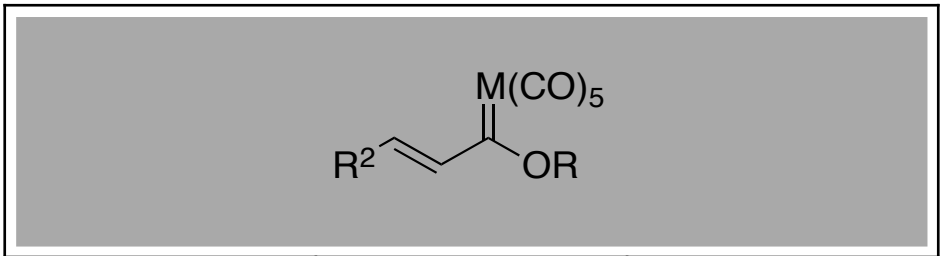

M	R	R²
Cr	Allyl	Et

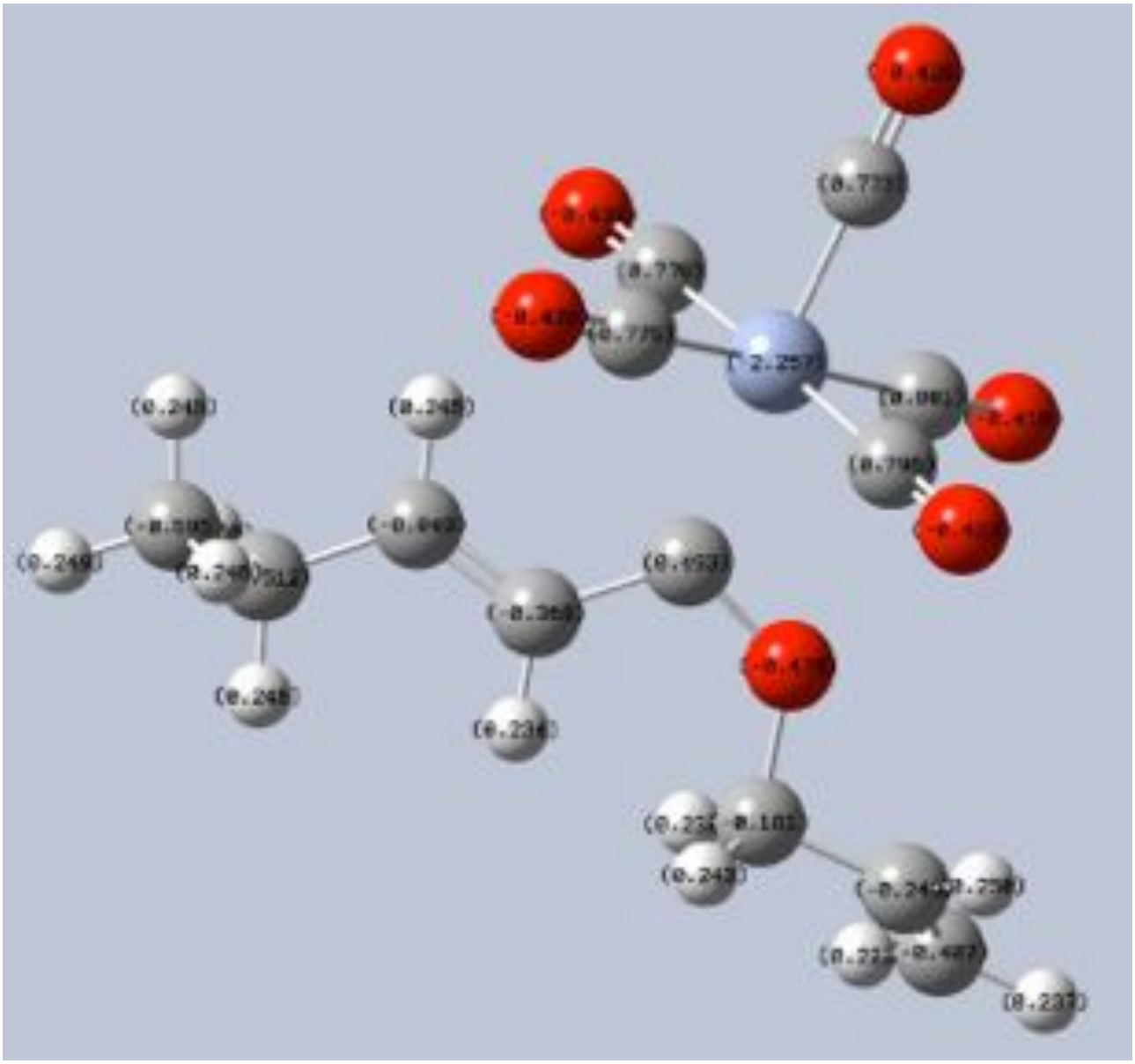

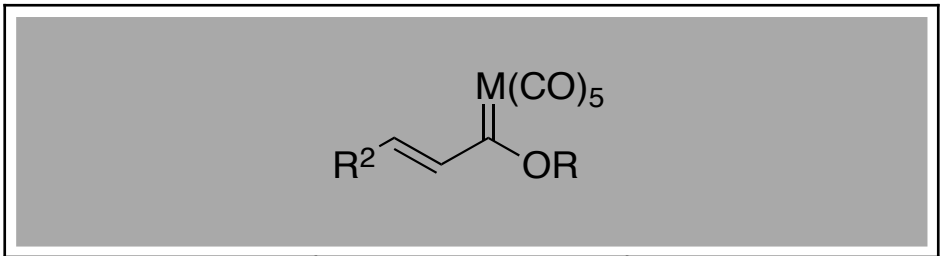

M	R	R²
Cr	Allyl	Phenyl

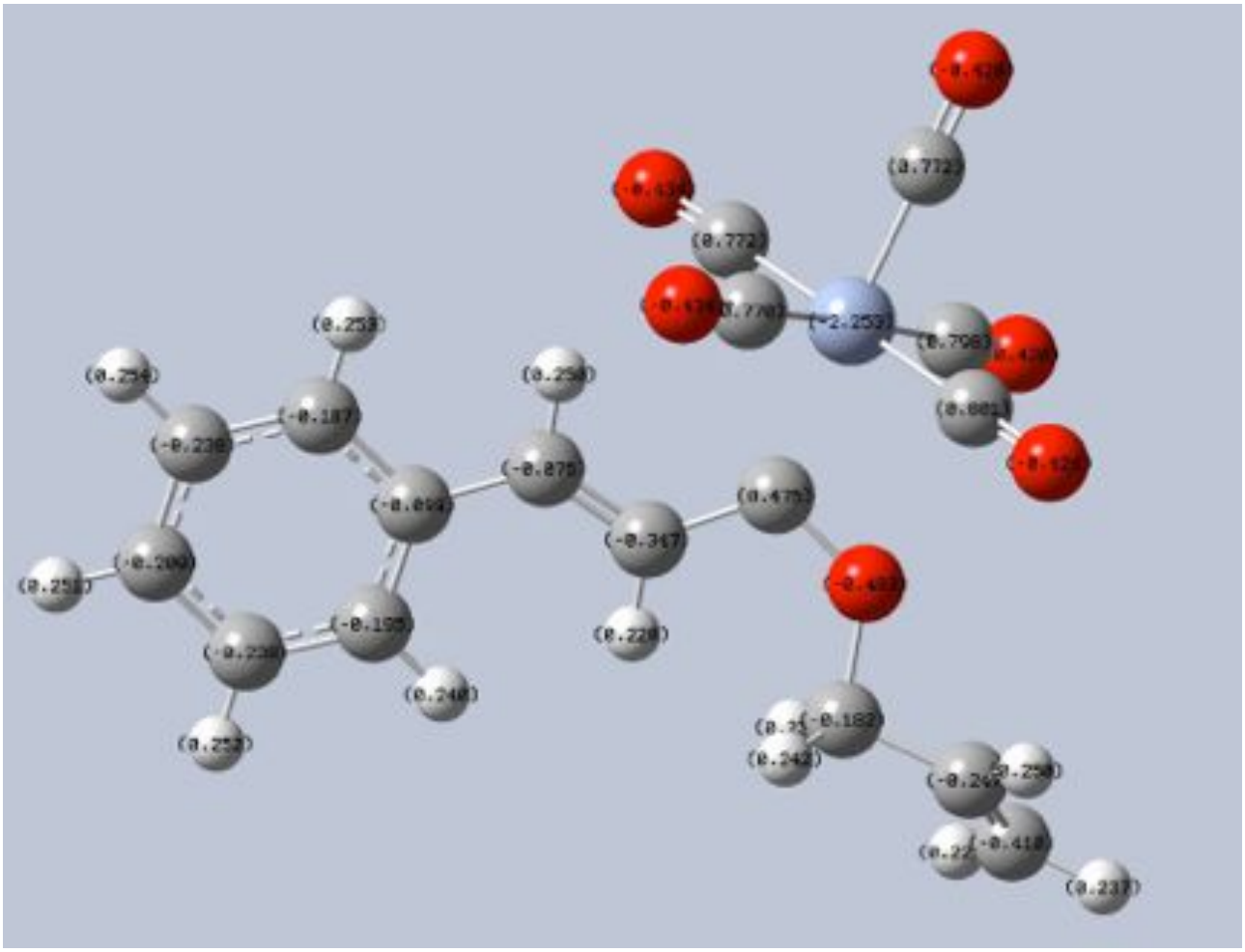

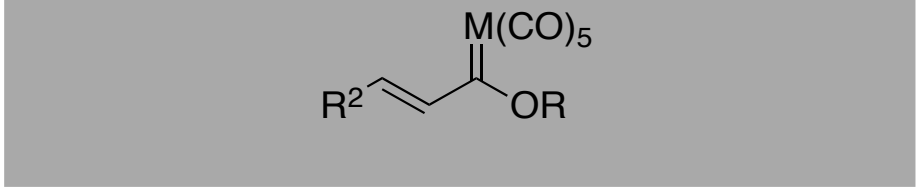

M	R	R²
Cr	Allyl	2-(HO)Ph

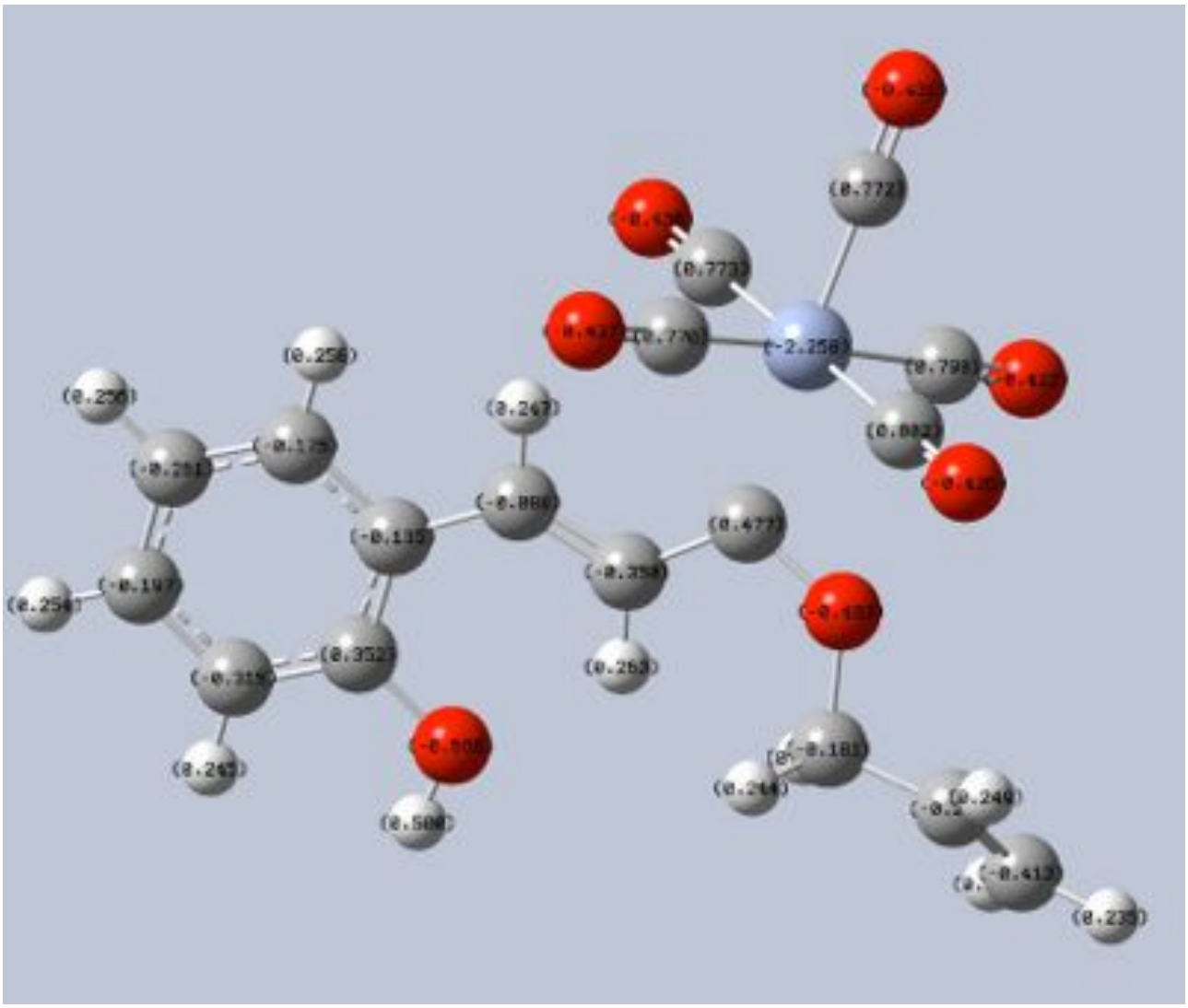

Appendix -3C(i):

Optimized structures of Baylis Hillman products (Cr)(NBO)

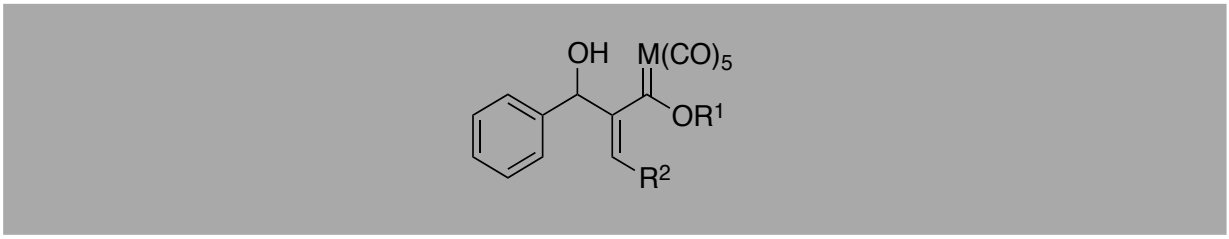

M	R	R^2	R^3
Cr	Allyl	Me	OH

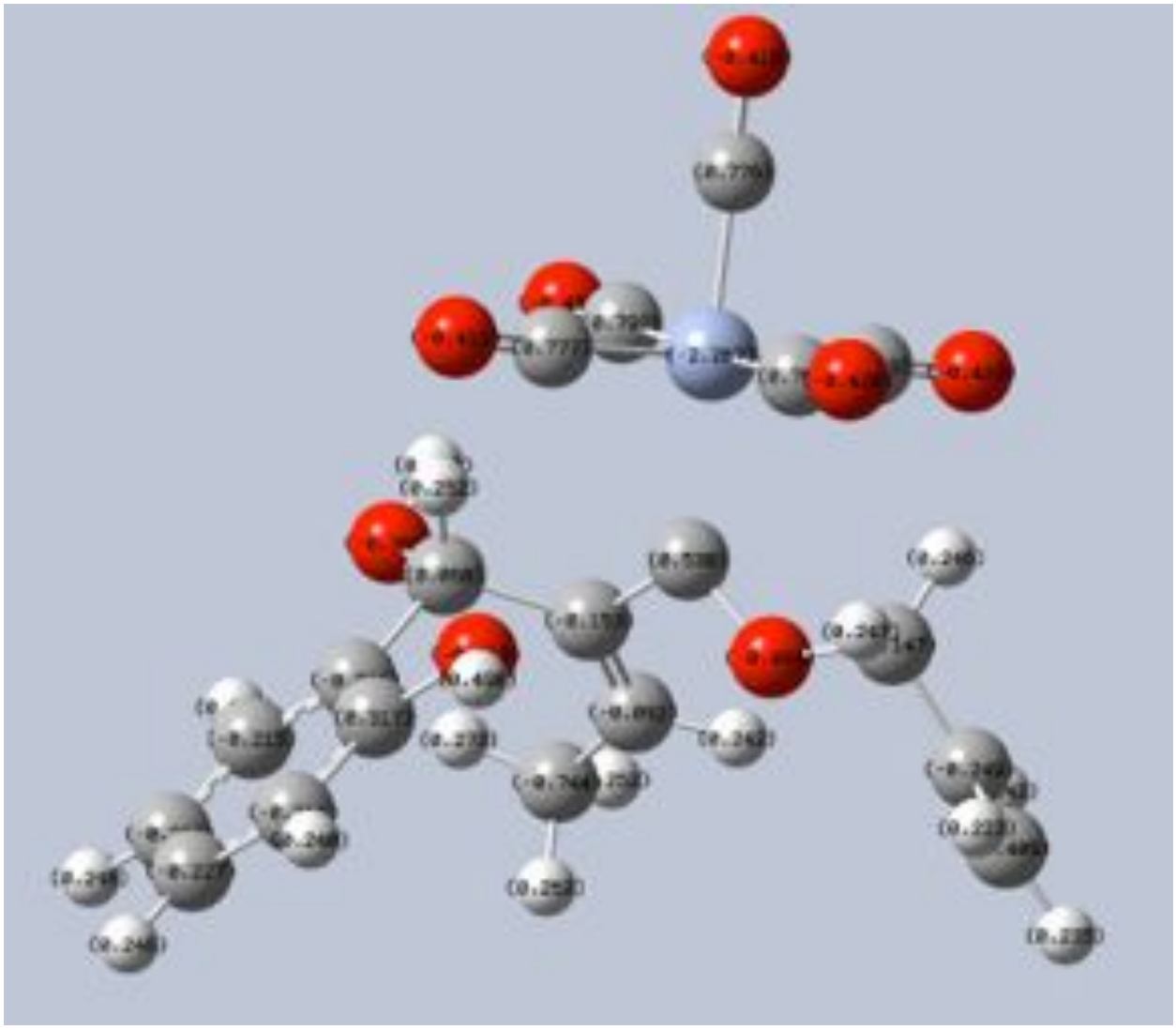

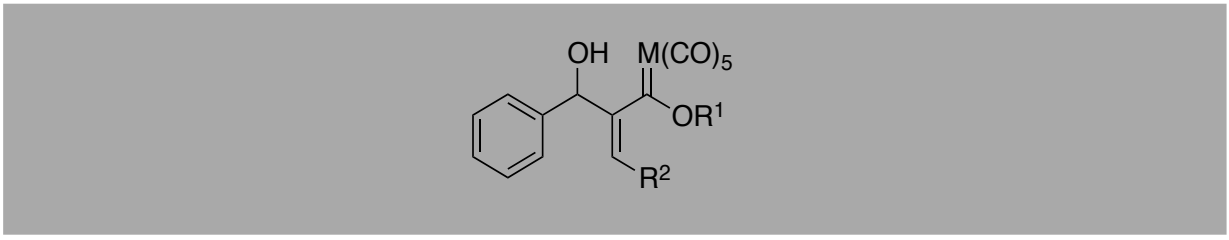

M	R	R²	R³
Cr	Me	Me	OH

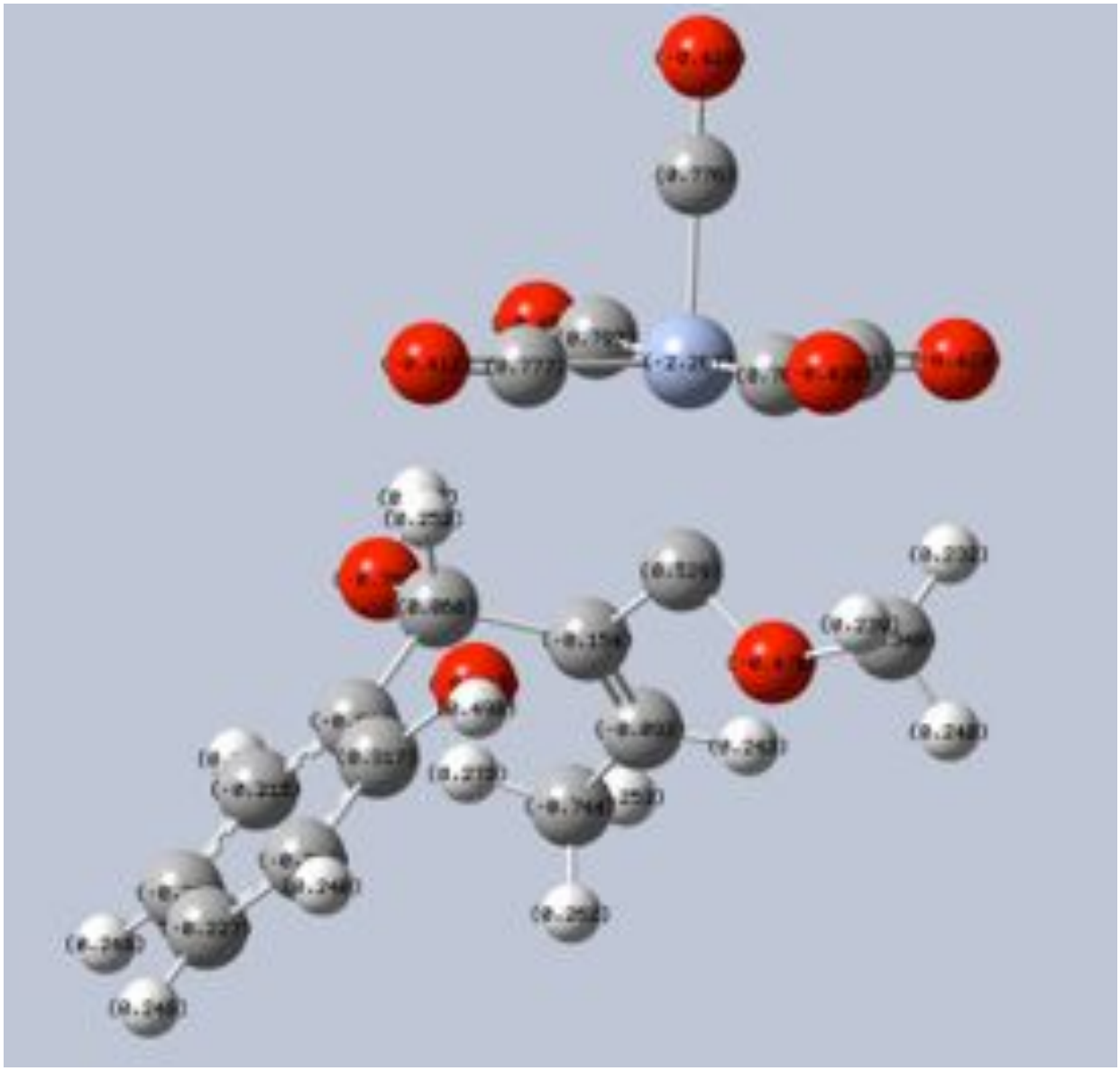

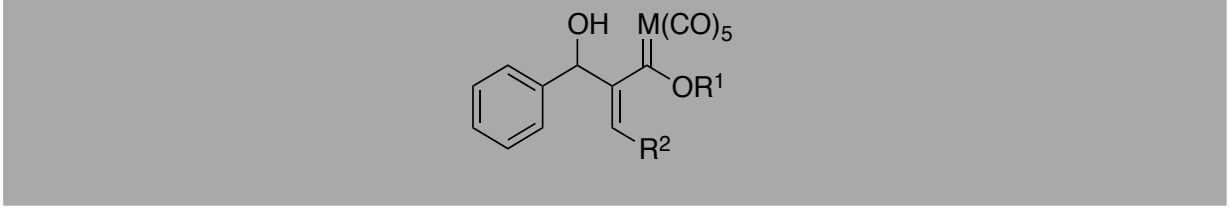

M	R	R^2	R^3
Cr	Allyl	Benzyl	OH

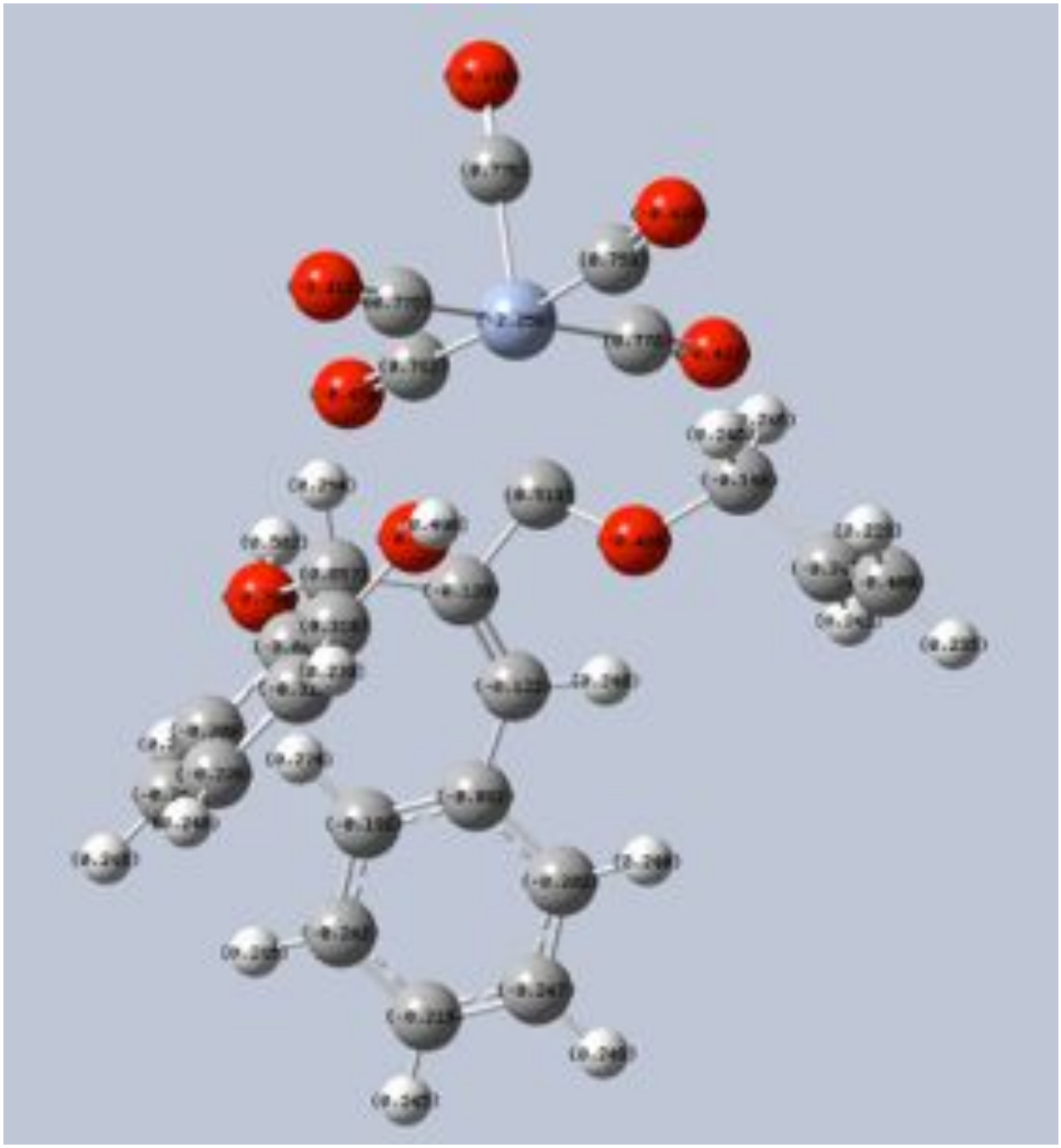

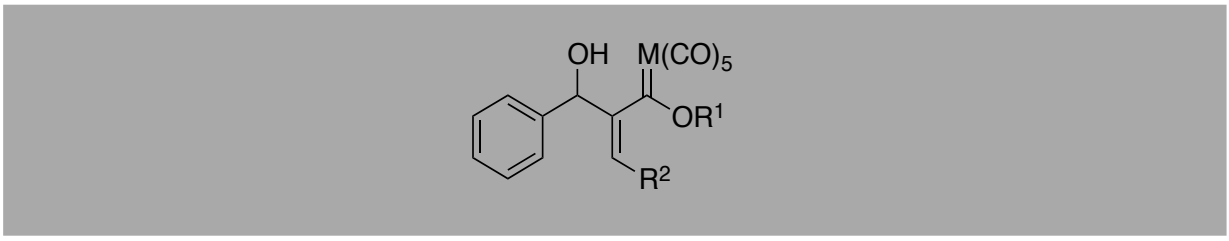

M	R	R^2	R^3
Cr	Et	Benzyl	OH

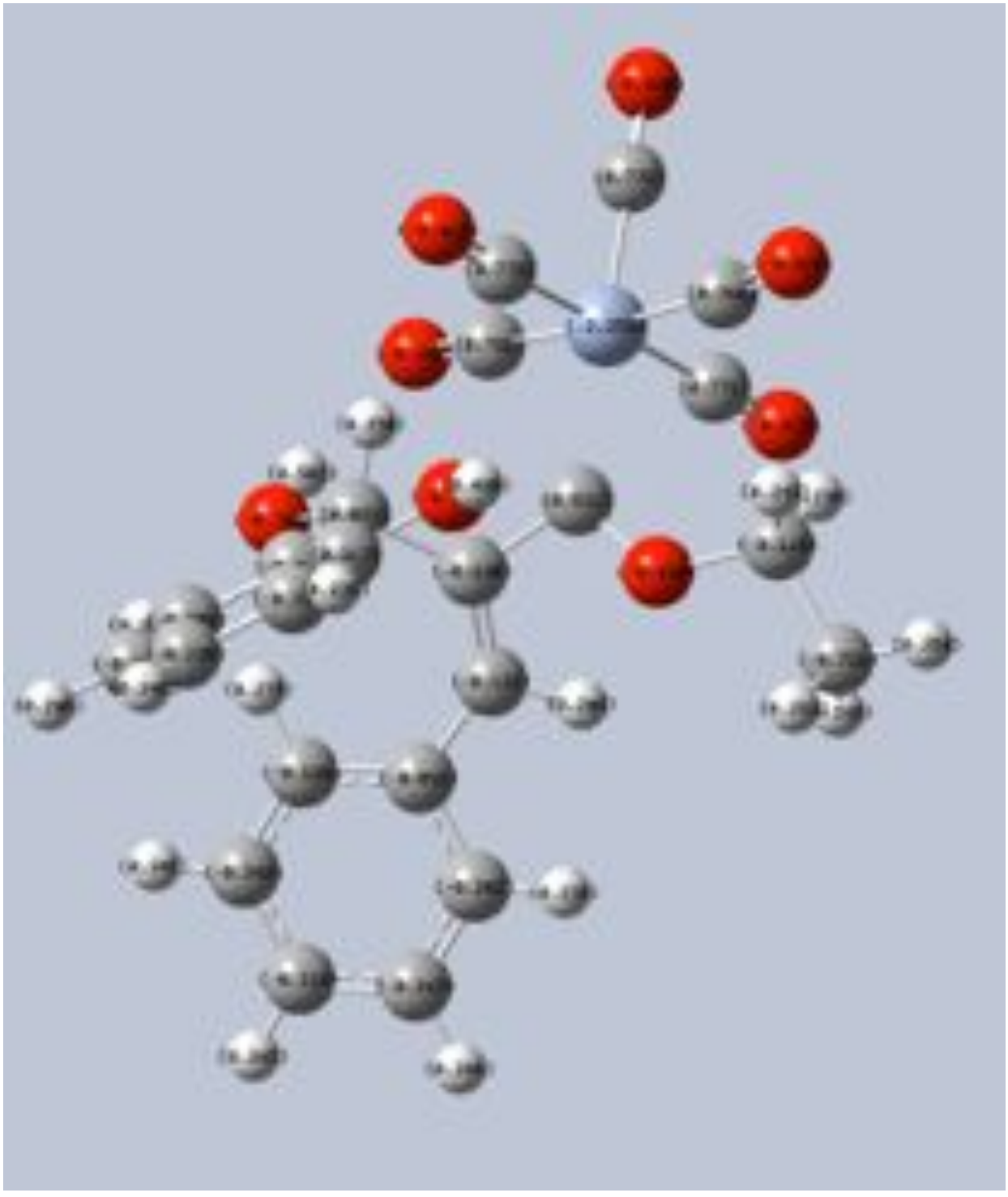

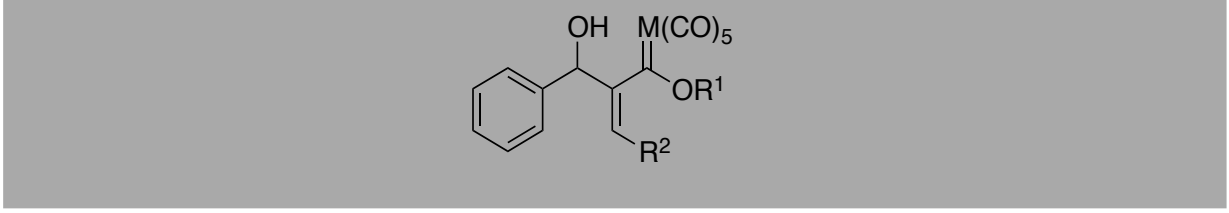

M	R	R^2	R^3
Cr	Me	Benzyl	OH

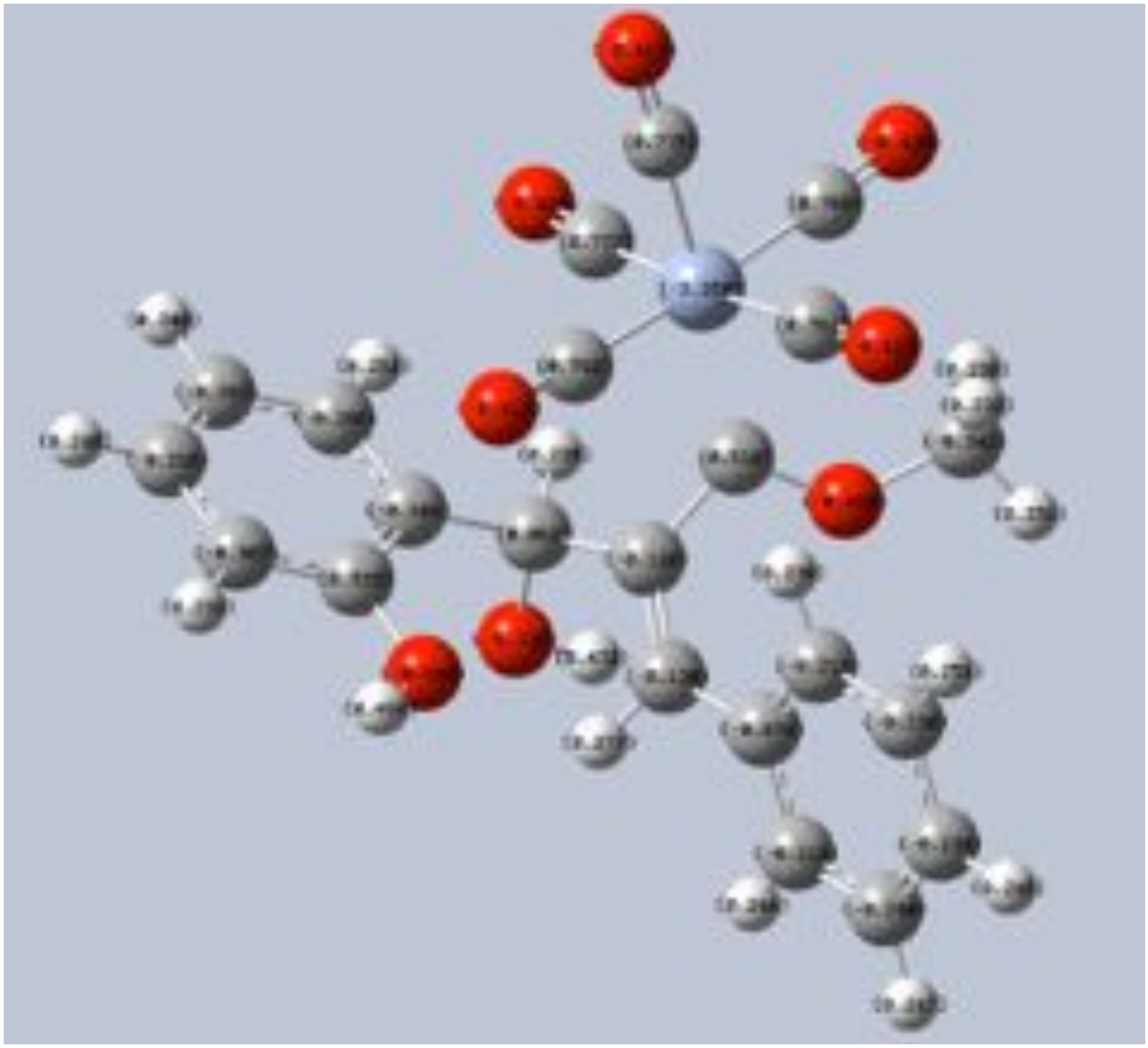

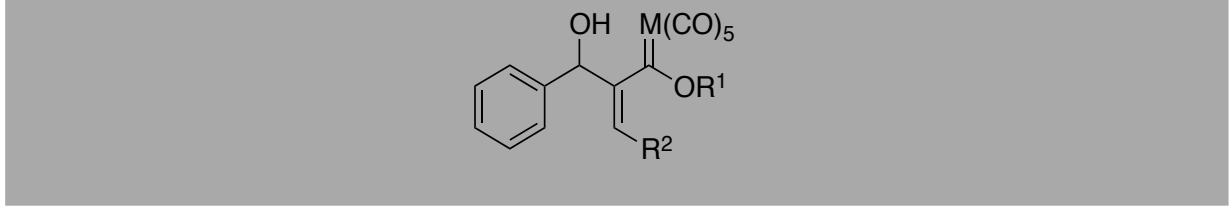

M	R	R²	R³
Cr	Allyl	Salicyl	Salicyl

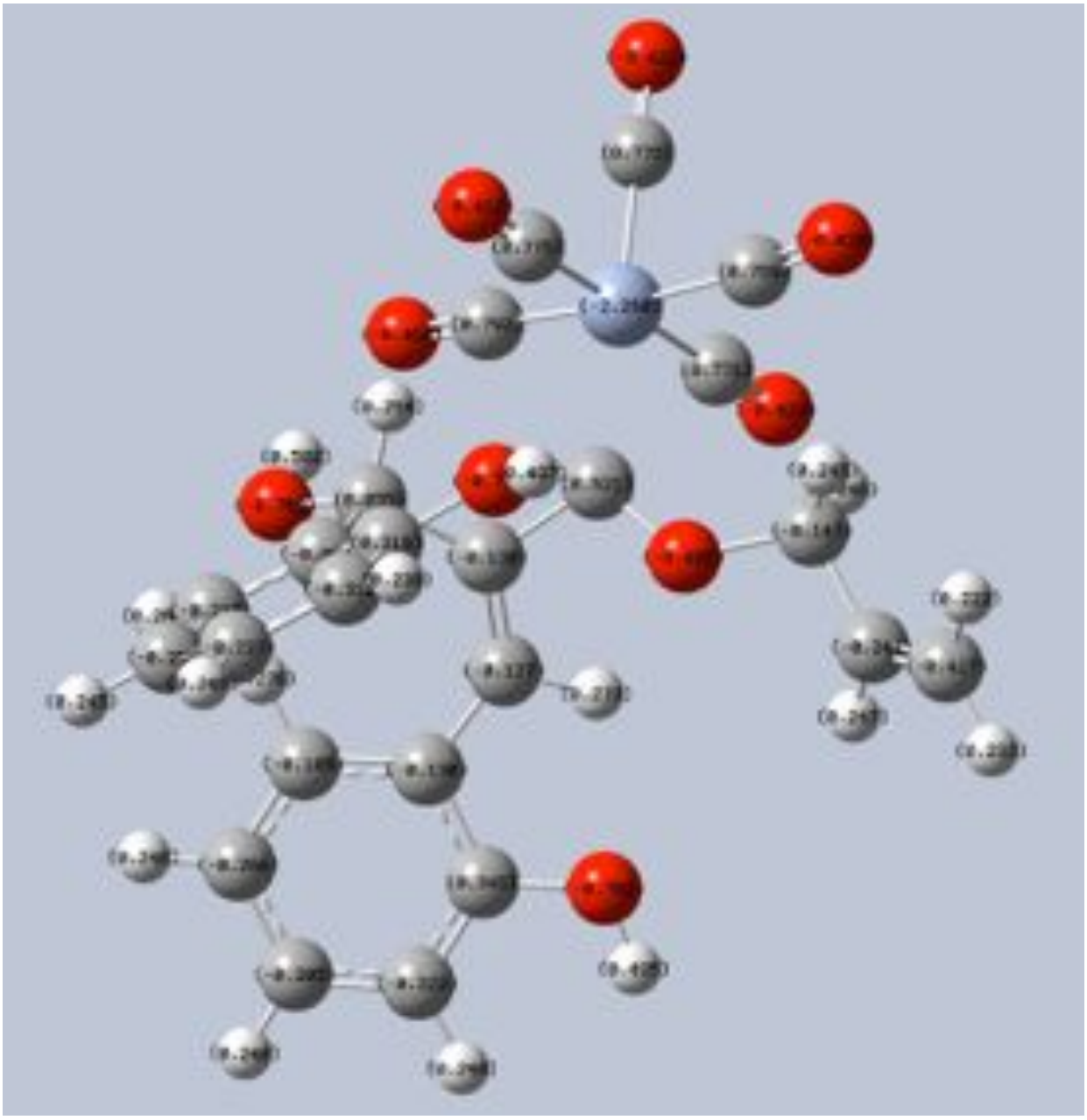

M	R	R^2	R^3
Cr	Et	Salicyl	Salicyl

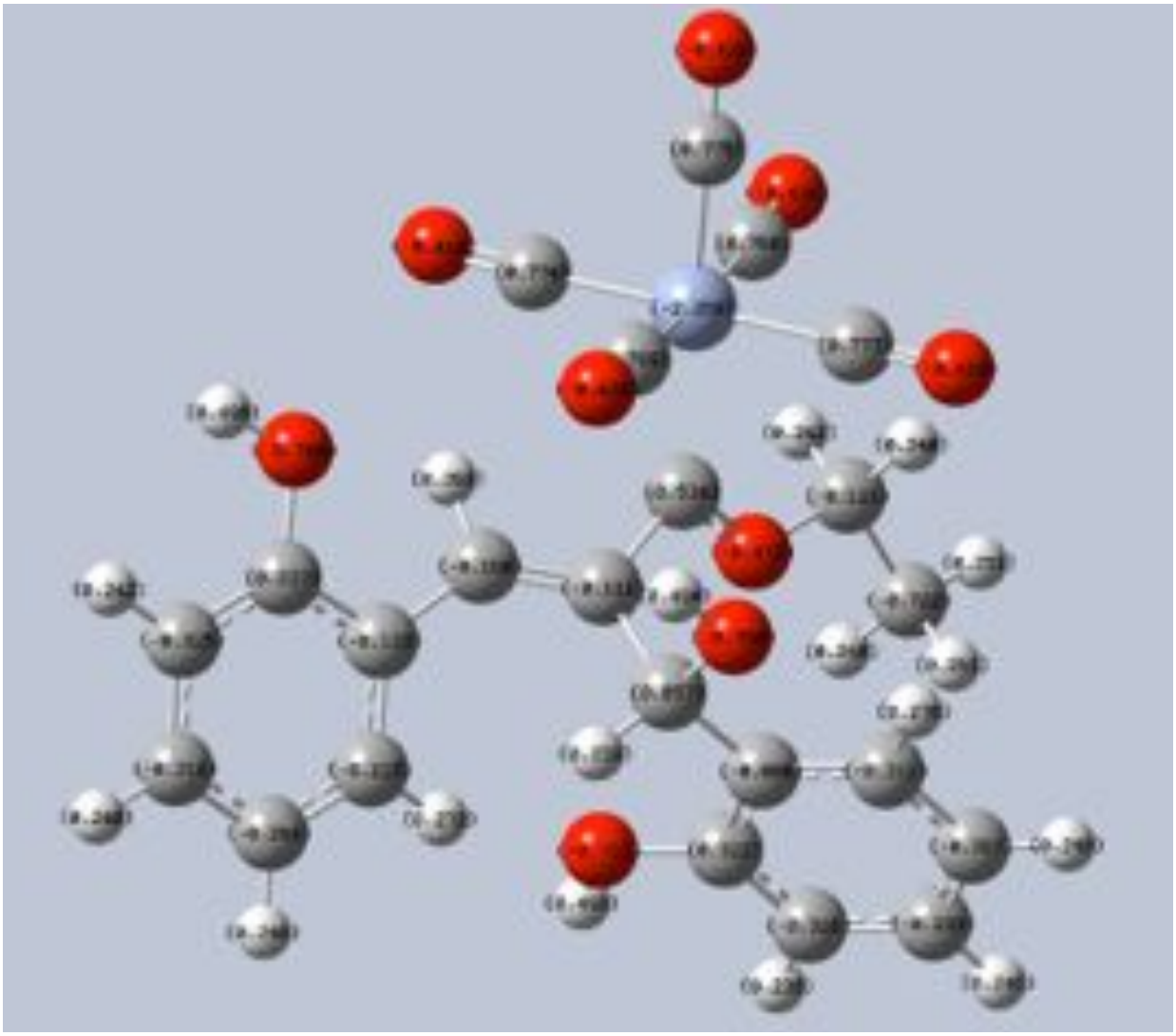

Appendix -**4A:**

Optimized structures of Benzannulated Products (NBO)

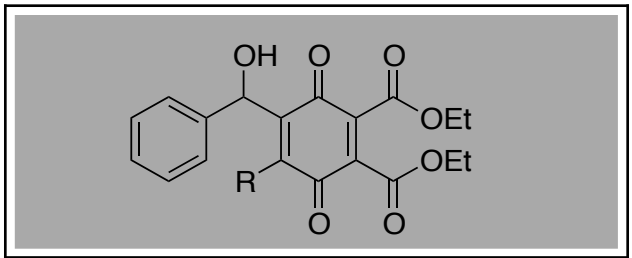

R
Me

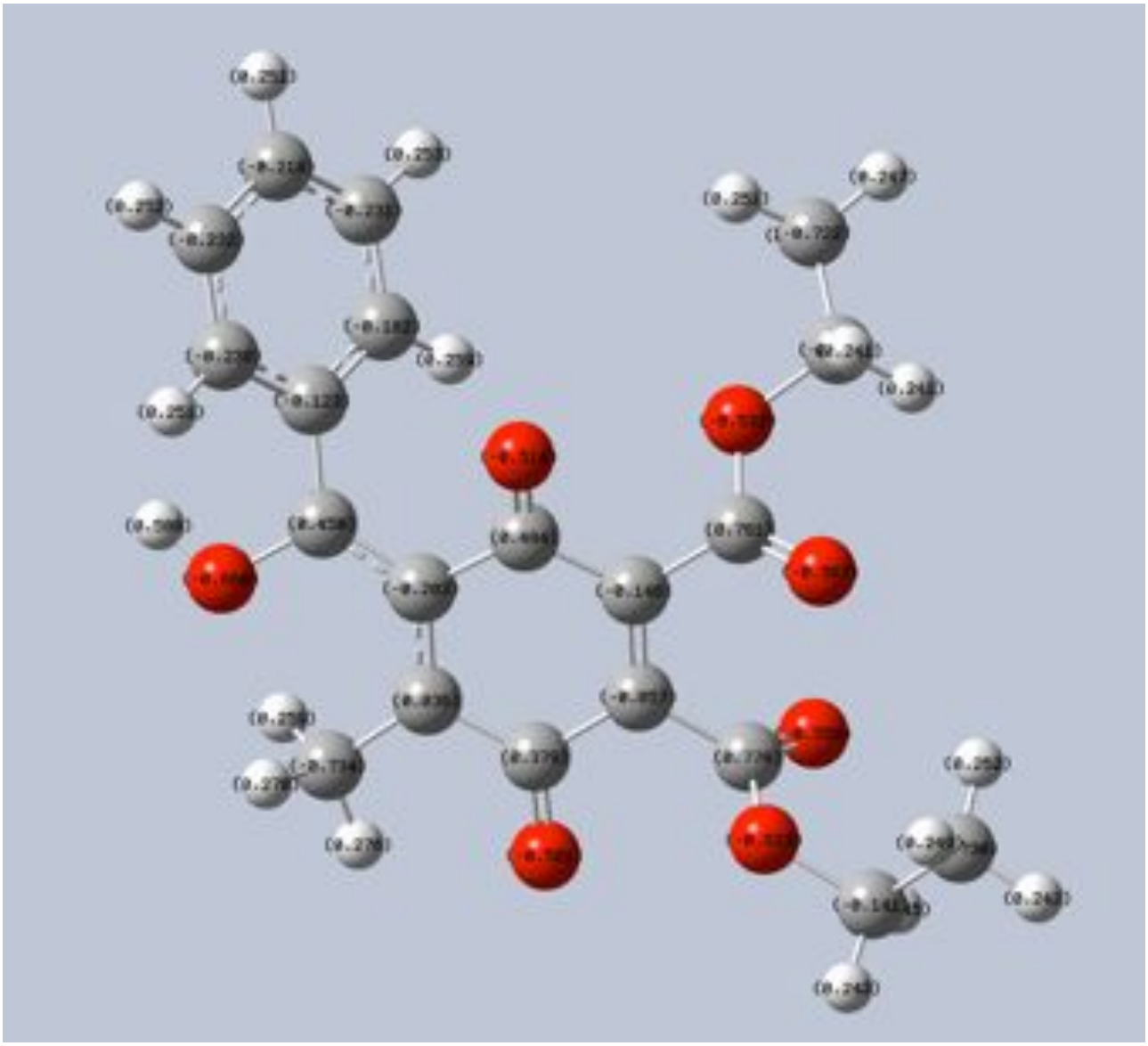

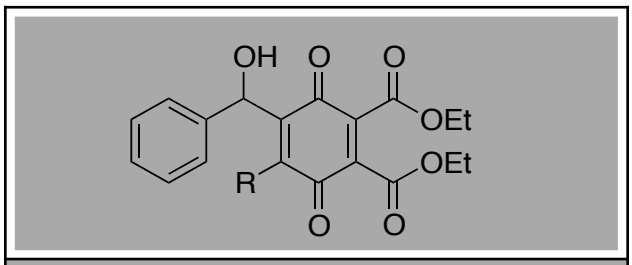

R
Ph

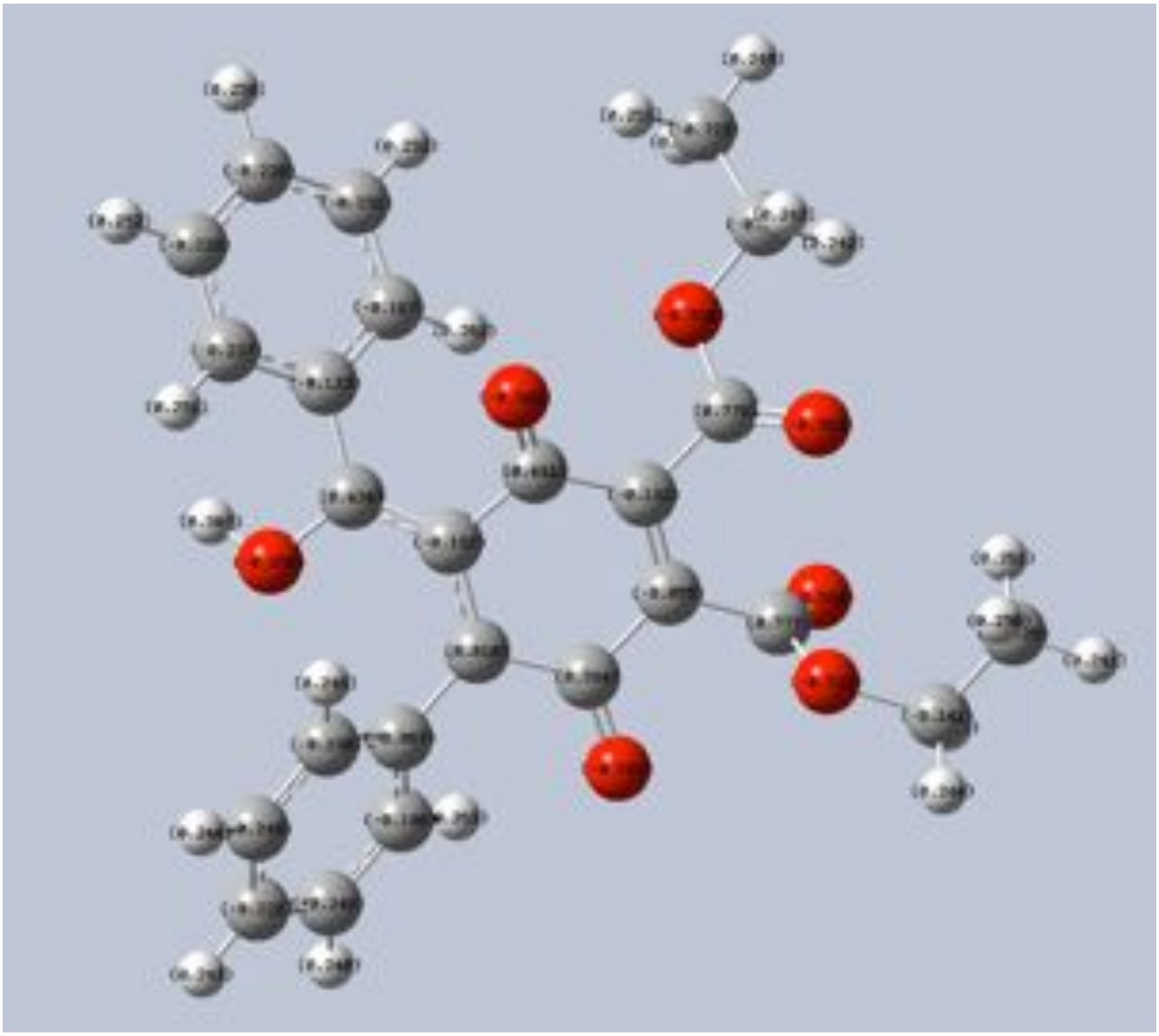

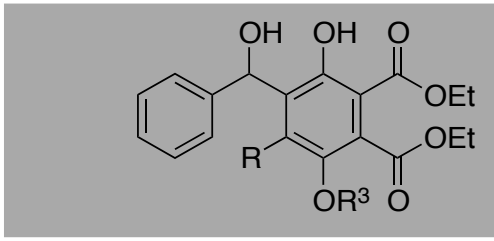

R	R^3
Me	Me

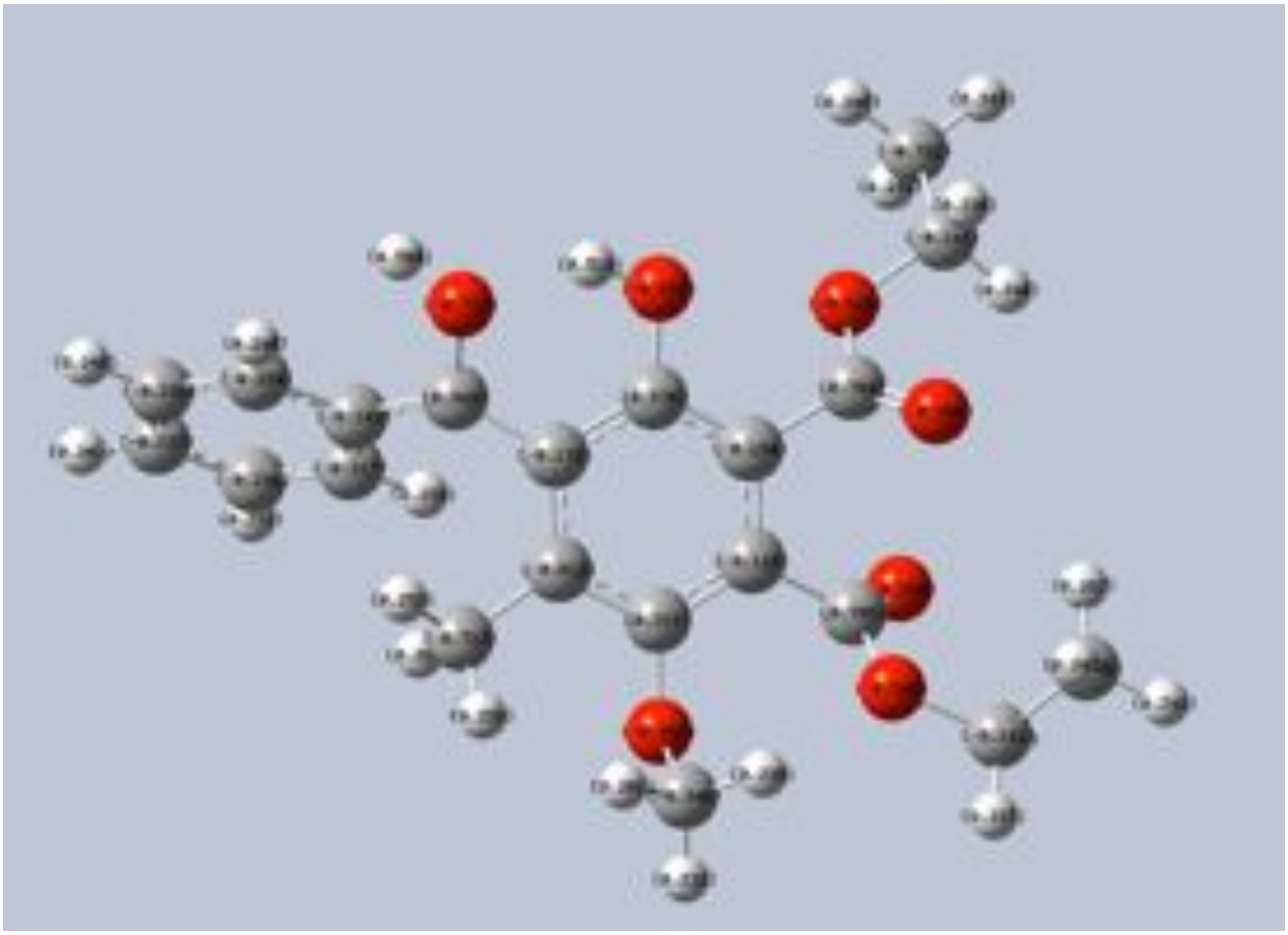

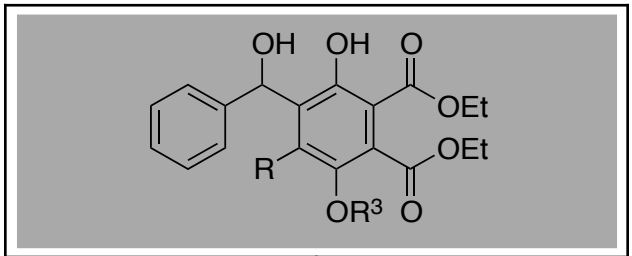

R	R^3
Ph	Me

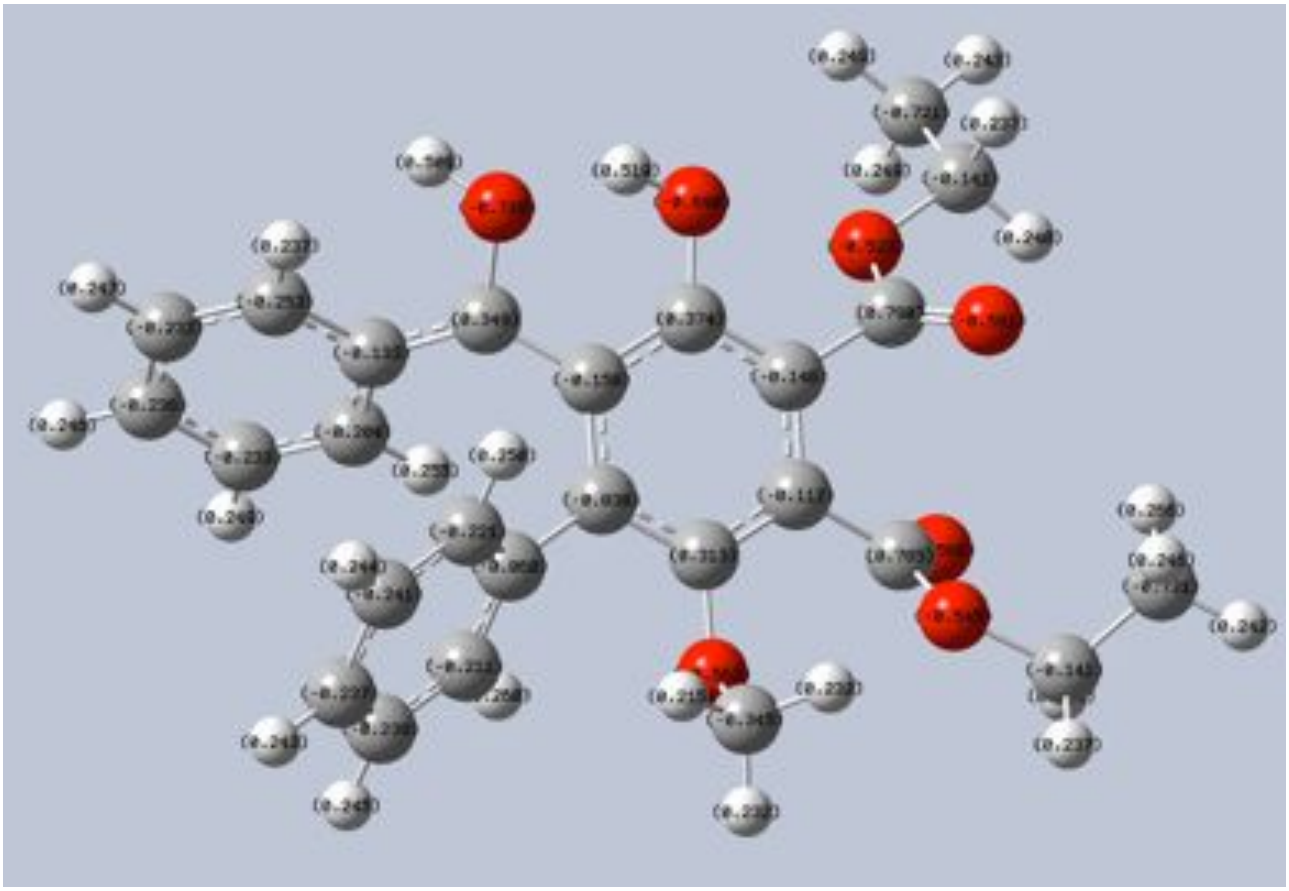

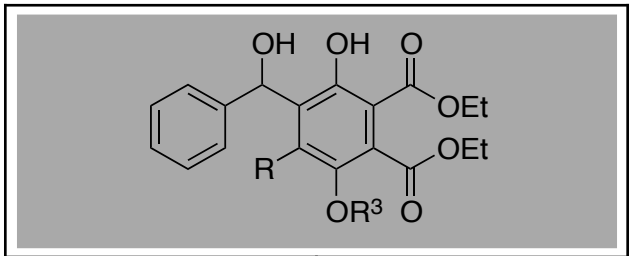

R	R^3
2-(HO)Ph	Me

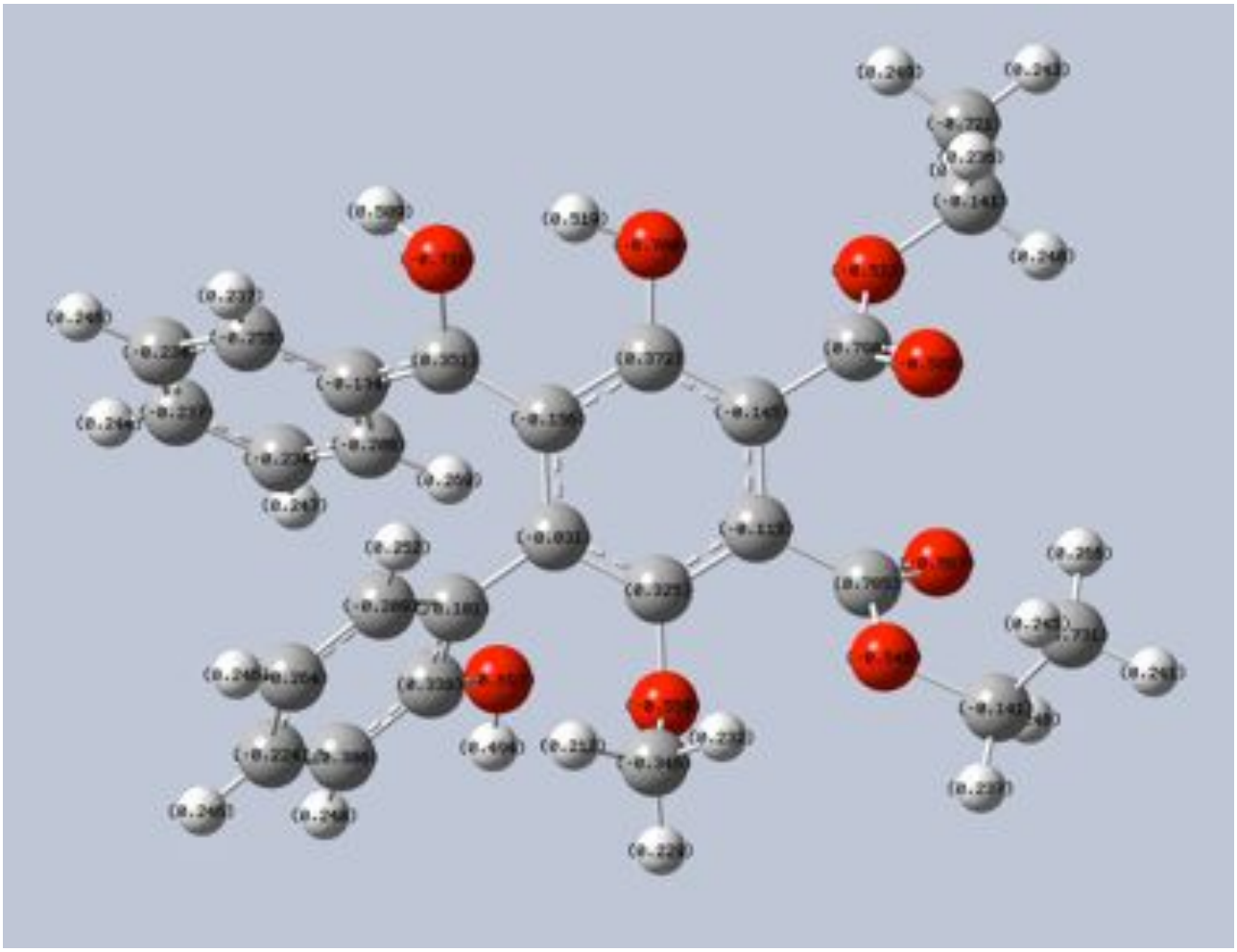

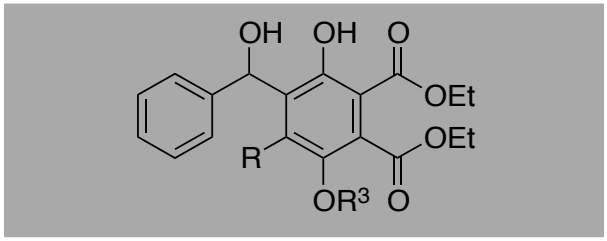

R	R^3
Me	Et

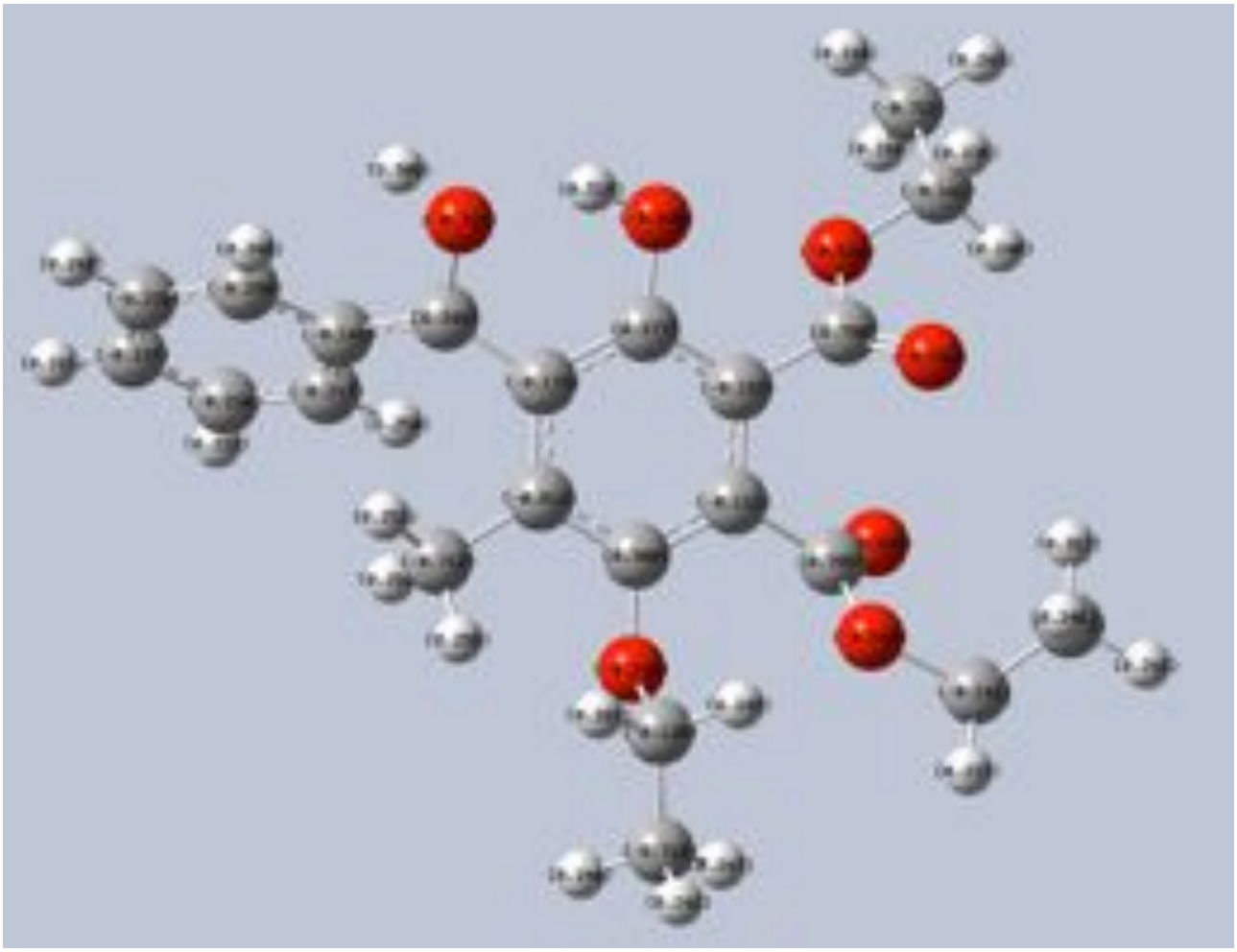

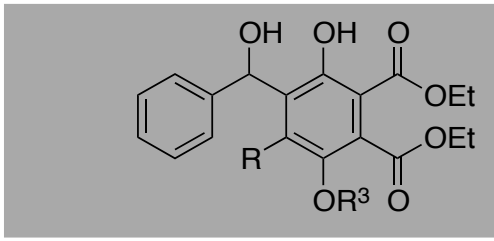

R	R^3
2-(HO)Ph	Et

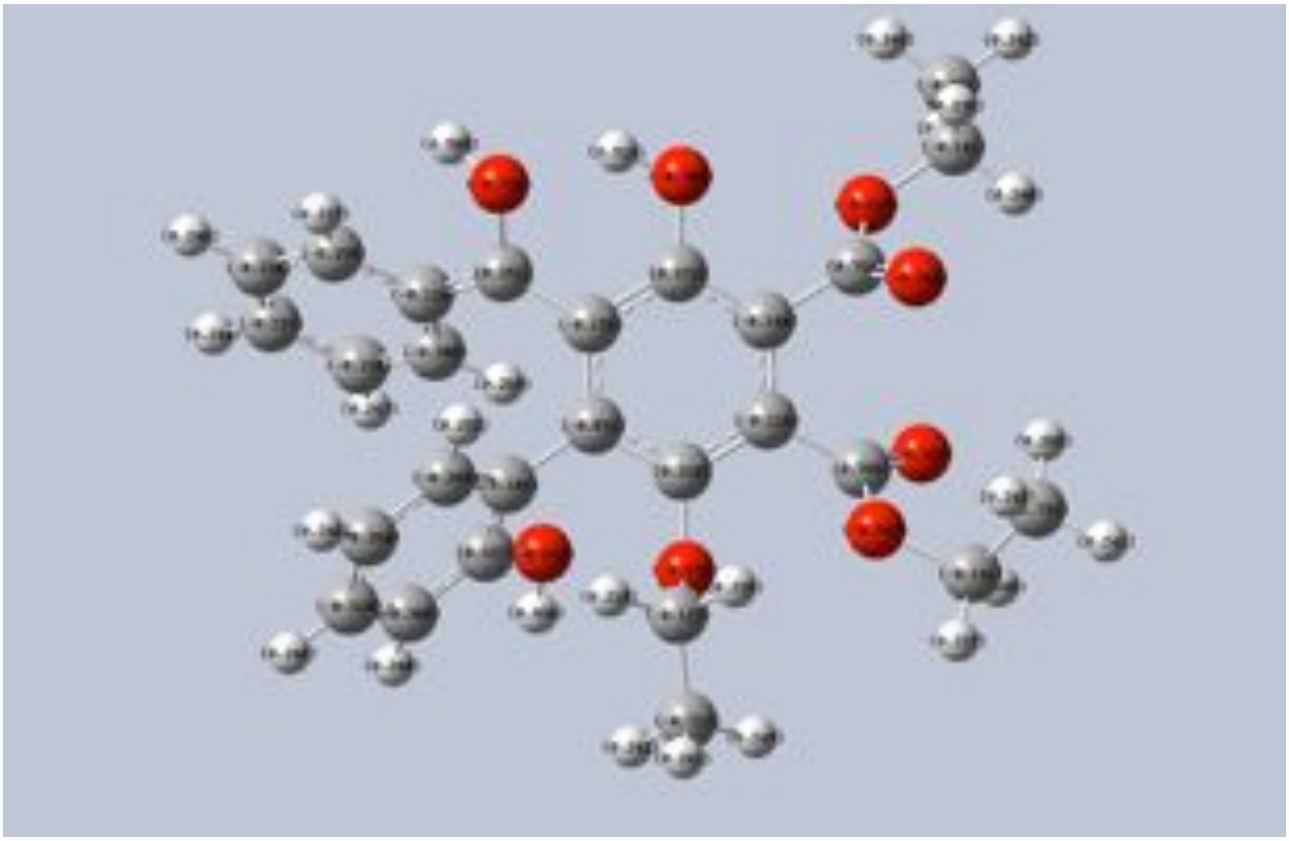

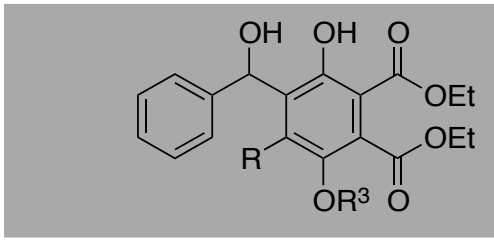

R	R³
2-(HO)Ph	Allyl

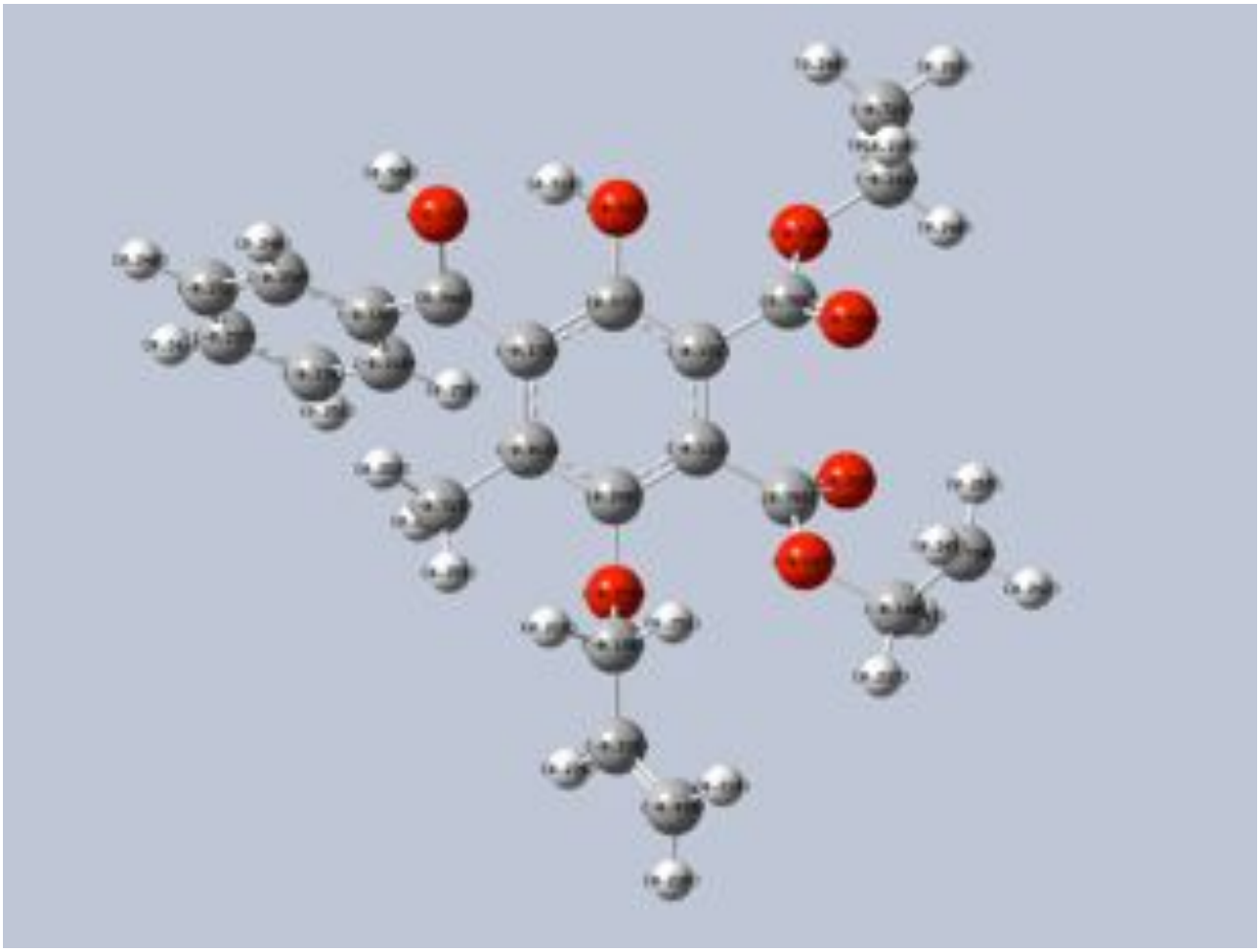

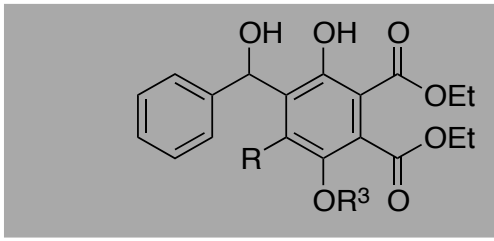

R	R^3
Ph	Allyl

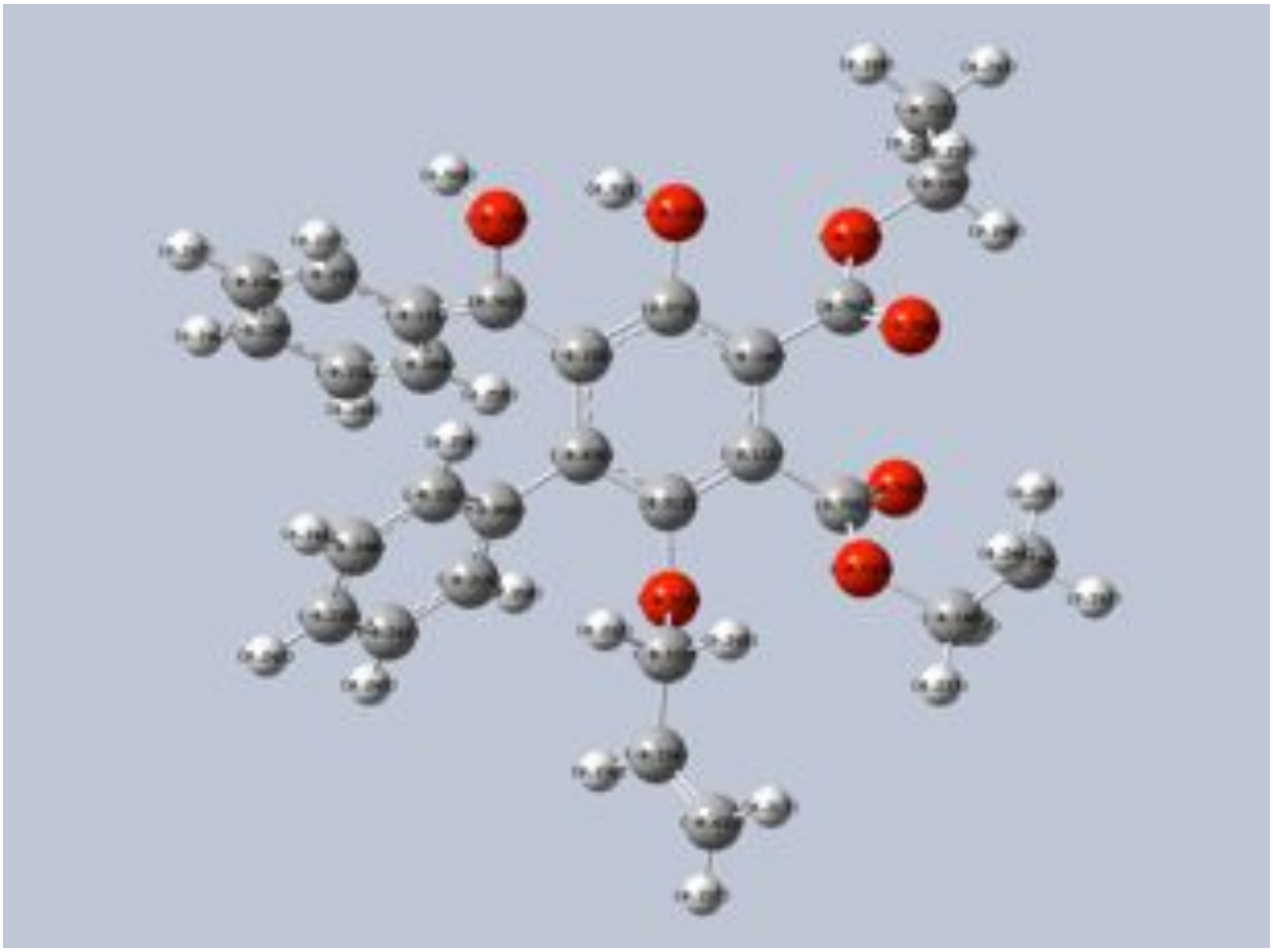

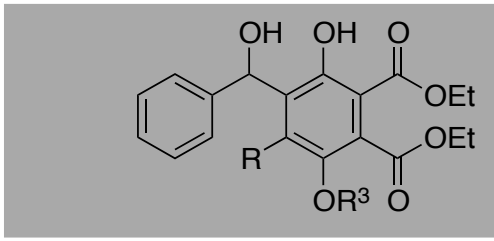

R	R³
2-(HO)Ph	Allyl